

HIGH RESOLUTION SPECTROSCOPY
OF THE LOW-LYING STATES OF
SrBr, YbF, YbCl AND YbBr RADICALS

by

Cameron S. Dickinson

Submitted in partial fulfillment of
the requirements for the degree of

Doctor of Philosophy

at

Dalhousie University

Halifax, Nova Scotia

July 2003

National Library
of Canada

Bibliothèque nationale
du Canada

Acquisitions and
Bibliographic Services

Acquisisitons et
services bibliographiques

395 Wellington Street
Ottawa ON K1A 0N4
Canada

395, rue Wellington
Ottawa ON K1A 0N4
Canada

Your file *Votre référence*

ISBN: 0-612-83704-1

Our file *Notre référence*

ISBN: 0-612-83704-1

The author has granted a non-exclusive licence allowing the National Library of Canada to reproduce, loan, distribute or sell copies of this thesis in microform, paper or electronic formats.

L'auteur a accordé une licence non exclusive permettant à la Bibliothèque nationale du Canada de reproduire, prêter, distribuer ou vendre des copies de cette thèse sous la forme de microfiche/film, de reproduction sur papier ou sur format électronique.

The author retains ownership of the copyright in this thesis. Neither the thesis nor substantial extracts from it may be printed or otherwise reproduced without the author's permission.

L'auteur conserve la propriété du droit d'auteur qui protège cette thèse. Ni la thèse ni des extraits substantiels de celle-ci ne doivent être imprimés ou autrement reproduits sans son autorisation.

Canada

DALHOUSIE UNIVERSITY
DEPARTMENT OF CHEMISTRY

The undersigned hereby certify that they have read and recommend to the Faculty of Graduate Studies for acceptance a thesis entitled "High Resolution Spectroscopy of the Low-Lying States of SrBr, YbF, YbCl and YbBr Radicals" by Cameron Dickinson in partial fulfillment for the degree of Doctor of Philosophy.

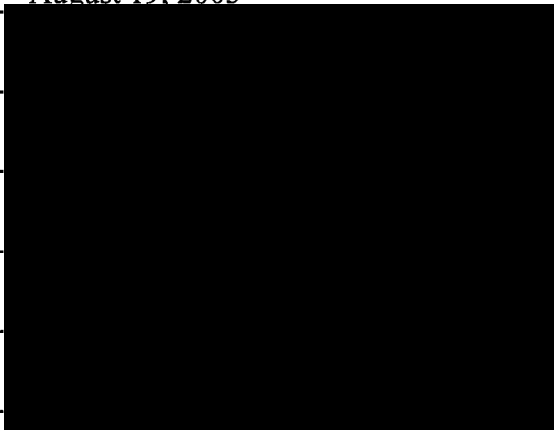
Dated: _____ August 19, 2003

External Examiner: _____

Research Supervisor: _____

Examining Committee: _____

Departmental Representative: _____



DALHOUSIE UNIVERSITY

DATE: August 19, 2003

AUTHOR: Cameron S. Dickinson

TITLE: High Resolution Spectroscopy of the Low-Lying States of
SrBr, YbF, YbCl and YbBr Radicals

DEPARTMENT OR SCHOOL: Chemistry

DEGREE: Ph.D. CONVOCATION: October YEAR: 2003

Permission is herewith granted to Dalhousie University to circulate and to have copied for non-commercial purposes, at its discretion, the above title upon the request of individuals or institutions.



Signature of Author

The author reserves other publication rights, and neither the thesis nor extensive extracts from it may be printed or otherwise reproduced without the author's written permission.

The author attests that permission has been obtained for the use of any copyrighted material appearing in the thesis (other than the brief excerpts requiring only proper acknowledgement in scholarly writing), and that all such use is clearly acknowledged.

Dedicated to the memory of my grandfathers,

Jack Dickinson and Donald Elfner

Table of Contents

	Page
Table of Contents	v
List of Figures	ix
List of Tables	x
Abstract	xii
List of Abbreviations and Symbols	xiii
Acknowledgements	xvi
Chapter 1 – Introduction	1
Chapter 2 – Theoretical Background	5
2.1 Introduction	5
2.2 Hund's Coupling Cases	6
2.2.1 Hund's Case (a)	6
2.2.2 Hund's Case (b)	8
2.2.3 Hund's Case ($b_{\beta J}$)	10
2.3 Parity	10
2.4 Selection Rules	13
2.5 Matrix Elements	13
2.6 Fitting of Parameters to Observed Transitions	21
2.7 Properties of the Molecular Parameters	25
Chapter 3 - Experimental Arrangement	29
3.1 Methods of Production	29
3.1.1 The Broida Oven	29

3.1.2	The Laser Ablation Source	31
3.2	Laser Spectroscopy	34
3.2.1	Laser System	34
3.2.2	PMT Arrangement	36
3.2.3	PMT Detection Techniques: Selective Detection	36
3.2.4	CCD Arrangement	39
3.2.5	CCD Detection Techniques: Resolved Fluorescence	39
3.3	Fourier Transform Microwave (FTMW) Spectroscopy	40
3.3.1	Microwave Cavity	40
3.3.2	Microwave Detection and Signal Processing	41
3.3.3	Fourier Transform and FTMW Spectral Characteristics	45
	Chapter 4 - The $A^2\Pi \sim B^2\Sigma^+$ Interaction in SrBr	48
4.1	Background	48
4.2	Theory	49
4.3	Experimental Arrangement	50
4.4	Results	51
4.5	Discussion	54
4.5.1	Extra Lines	54
4.5.2	Interactions Between the $A^2\Pi$ and $B^2\Sigma^+$ States	58
4.5.3	Ab initio Estimates of α_{AB} and b_{AB}	73
4.5.4	Interaction of the B ($\nu = 2$) and A ($\nu = 5$) Levels	74
4.6	Conclusions	77

Chapter 5 - A FTMW Study of the $X^2\Sigma^+$ States of YbF, YbCl and YbBr	78
5.1 Background	78
5.2 Experimental Arrangement	79
5.3 Results	80
5.3.1 YbF	80
5.3.2 YbCl	84
5.3.3 YbBr	88
5.4 Discussion	88
5.4.1 Hyperfine Parameters	88
5.4.2 Bond Lengths	95
5.5 Conclusions	100
Chapter 6 - The $B^2\Sigma \leftarrow X^2\Sigma^+$ System of YbBr	101
6.1 Background	101
6.2 Experimental Arrangement	102
6.3 Results	103
6.3.1 General Description of Spectra	103
6.3.2 Blended Spectral Lines	104
6.3.3 Rotational Assignment and Fitting Procedure	107
6.4 Discussion	111
6.4.1 Isotopic Electronic Energy Shifts in YbBr	111
6.4.2 Mass Shifts – “Born-Oppenheimer Breakdown”	117
6.4.3 Field Shifts	119
6.4.4 Effects of Field Shifts on Bond Length	120

6.5	Conclusions	123
Chapter 7 - The $A^2\Pi \leftarrow X^2\Sigma^+$ System of YbBr		124
7.1	Background	124
7.2	Experimental Arrangement	125
7.2.1	Dalhousie Arrangement	125
7.2.2	UNB Arrangement	125
7.3	Results	126
7.3.1	General Description of Spectra	126
7.3.2	The $A^2\Pi_{1/2} \leftarrow X^2\Sigma^+$ System	127
7.3.3	The $A^2\Pi_{3/2} \leftarrow X^2\Sigma^+$ System	130
7.3.4	Fits of the $A^2\Pi \leftarrow X^2\Sigma^+$ Data	130
7.4	Discussion	131
7.5	Conclusions	134
Appendix I – SrBr Laser Excitation Line Positions, and Overlap Integrals		135
Appendix II – YbF, YbCl and YbBr FTMW Line Positions		179
Appendix III – YbBr Laser Excitation Line Positions - $B^2\Sigma^+ \leftarrow X^2\Sigma^+$ System		184
Appendix IV – YbBr Laser Excitation Line Positions - $A^2\Pi \leftarrow X^2\Sigma^+$ System		219
References		238

List of Figures

Figure	Page
2.1 Coupling and precessional motion in Hund's case (a)	7
2.2 Coupling and precessional motion in Hund's case (b)	9
2.3 Schematic of ${}^2\Pi \leftrightarrow {}^2\Sigma^+$ manifold	22
2.4 Schematic of ${}^2\Sigma^+ \leftrightarrow {}^2\Sigma^-$ manifold	23
2.5 Schematic of energy level splittings in a ${}^2\Sigma^-$ state	24
3.1 Broida oven diagram	30
3.2 Diagram of pulsed ablation source	33
3.3 Arrangement of laser system, spectrometer, and CCD/PMT systems	35
3.4 Schematic diagram of Fourier transform microwave spectrometer	42
3.5 Pulse Sequence for FTMW arrangement	43
3.6 Diagram of microwave signal production and detection	44
3.7 Effect of Helmholtz coils on the FTMW spectra of ${}^{174}\text{Yb}{}^{35}\text{Cl}$	47
4.1 Fortrat Diagram of for an $A^2\Pi_{3/2} \leftarrow X^2\Sigma^+$ band in SrBr	52
4.2 RKR Curves for the $A^2\Pi_{1/2}$ and $B^2\Sigma^+$ states of SrBr	63
4.3 Rotational energy levels in the $A^2\Pi(\nu_A = 5)$ and $B^2\Sigma^+(\nu_B = 2)$ states	75
6.1 Portion of the 0 – 0 band in the $B \leftarrow X$ absorption Spectra of YbBr	105
7.1 Recorded spectra of Q ₂₁ and R ₂₂ lines in the 0 – 0 band of YbBr	128

List of Tables

Table	Page
2.1 Hamiltonian matrix elements for ${}^2\Pi$ and ${}^2\Sigma^+$ states	15
2.2 Hamiltonian matrix elements for a ${}^2\Pi \sim {}^2\Sigma^+$ Interaction	17
2.3 Hyperfine matrix elements for a ${}^2\Sigma^+$ state	19
2.4 Dependence of parameters for ${}^2\Sigma^+$ and ${}^2\Pi$ states on reduced mass	27
2.5 Dependence of hyperfine parameters in a ${}^2\Sigma^+$ state on nuclear moments	28
4.1 Fitted parameters for the $A^2\Pi \leftarrow X^2\Sigma^+$ and $B^2\Sigma^+ \leftarrow X^2\Sigma^+$ systems of ${}^{88}\text{Sr}{}^{79}\text{Br}$ and ${}^{88}\text{Sr}{}^{81}\text{Br}$	55
4.2 Calculated and observed extra lines in the spectra of SrBr	59
4.3 Overlap integrals for selected $A^2\Pi \sim B^2\Sigma^+$ interactions in ${}^{88}\text{Sr}{}^{79}\text{Br}$	65
4.4 Deperturbed parameters for ${}^{88}\text{Sr}{}^{79}\text{Br}$ and ${}^{88}\text{Sr}{}^{81}\text{Br}$	68
4.5 Correlation coefficients between the a_{AB} and b_{AB} parameters of ${}^{88}\text{Sr}{}^{81}\text{Br}$ and selected A , B and X state parameters	72
5.1 Molecular parameters for the $\nu = 0$ and 1 levels of ${}^{174}\text{YbF}$ ($X^2\Sigma^+$)	82
5.2 Fitted parameters for the $\nu = 0$ levels of ${}^{172}\text{Yb}{}^{35}\text{Cl}$ and ${}^{174}\text{Yb}{}^{37}\text{Cl}$, and the $\nu = 0$ and 1 levels of ${}^{174}\text{Yb}{}^{35}\text{Cl}$	85
5.3 Table of experimental and theoretical ratios for the fine and hyperfine parameters of YbCl	87
5.4 Fitted parameters for the $\nu = 0$ levels of ${}^{174}\text{Yb}{}^{79}\text{Br}$ and ${}^{174}\text{Yb}{}^{81}\text{Br}$	89
5.5 Experimental and theoretical ratios for the fine and hyperfine parameters of ${}^{174}\text{Yb}{}^{79}\text{Br}$ and ${}^{174}\text{Yb}{}^{81}\text{Br}$	90
5.6 Trends in unpaired halide spin density in the $X^2\Sigma^+$ ground states of YbF, YbCl and YbBr	92
5.7 Comparison of percentage ionic character for the $X^2\Sigma^+$ ground states of alkaline earth molecules and YbF, YbCl and YbBr	94

5.8	Bond lengths calculated for ^{174}YbF , $^{174}\text{Yb}^{35}\text{Cl}$, $^{174}\text{Yb}^{79}\text{Br}$ and $^{174}\text{Yb}^{81}\text{Br}$	99
6.1	Calculated and observed isotope shifts for bands in the $A - X$ and $B - X$ systems of YbCl	109
6.2	Determined parameters (cm^{-1}) from combined fits of the $0 - 0$, $0 - 1$, $1 - 0$ and $1 - 1$ bands for $^{174}\text{Yb}^{79}\text{Br}$, $^{174}\text{Yb}^{81}\text{Br}$, $^{172}\text{Yb}^{79}\text{Br}$ and $^{172}\text{Yb}^{81}\text{Br}$	112
6.3	Comparison of $\nu = 0$ parameters for the $X^2\Sigma^+$ state of YbBr	113
6.4	Calculated and observed isotope shifts for bands in the $B - X$ system of YbBr	114
6.5	Calculated vibrational constants for the B and X states of YbBr	116
7.1	Determined parameters from combined fits of the $A^2\Pi \leftarrow X^2\Sigma^+$ system $0 - 0$ and $1 - 0$ bands for $^{174}\text{Yb}^{79}\text{Br}$ and $^{174}\text{Yb}^{81}\text{Br}$	132

Abstract

High resolution laser excitation spectra of the 2 – 1, 3 – 2 and 4 – 3 bands of the $A^2\Pi \leftarrow X^2\Sigma^+$ system of $^{88}\text{Sr}^{79}\text{Br}$ and $^{88}\text{Sr}^{81}\text{Br}$ have been recorded. Observed perturbations in the $\nu_A = 3$ and 4 levels of the $A^2\Pi_{1/2}$ sub-state are confirmed to be caused by level crossings with the $\nu_B = 0$ and 1 levels of the $B^2\Sigma^+$ state. A least squares fit of all known electronic data of both the $A^2\Pi \leftarrow X^2\Sigma^+$ and $B^2\Sigma^+ \leftarrow X^2\Sigma^+$ systems was employed to simultaneously characterize the $\nu_A = \nu_B + 3$ level crossings, as well as the $^2\Pi \sim ^2\Sigma^+$ interactions, responsible for Λ -doubling in the $^2\Pi$ state and “spin-rotation” splitting in the $^2\Sigma^+$ state. An unobserved level crossing is predicted to occur between levels of e parity of $\nu_B = 2$ and $\nu_A = 5$.

The pure rotational spectra of low-lying $\nu = 0$ and 1 vibrational levels of the $^2\Sigma^+$ ground states of several isotopomers of YbF, YbCl and YbBr were recorded using a pulsed jet cavity Fourier transform microwave spectrometer. Through least squares fits, parameters describing rotational, fine and hyperfine effects (such as Fermi-contact, dipole-dipole coupling and nuclear spin-rotation coupling) are presented.

The $\nu = 0$ and 1 vibrational levels of the $B^2\Sigma^+$ state of YbBr were characterized for the first time through a high resolution laser investigation of rotational transitions in several bands of the $B^2\Sigma^+ \leftarrow X^2\Sigma^+$ system. The spectra were found to be highly congested, owing to the multitude of isotopomers with similar rotational B_ν values, which made assignment of rotational structure difficult. The effects of electronic *field shifts* were observed as small differences between calculated and observed isotope shifts of $^{174}\text{YbBr}$ and $^{172}\text{YbBr}$ isotopomers. This field shift has been observed in only a few heavy molecules, and its effect on electronic, vibrational and rotational parameters is discussed.

Finally, an absorption study of the $A^2\Pi \leftarrow X^2\Sigma^+$ system of YbBr has been made at high resolution using a laser arrangement. Similar to the $B - X$ study, spectra of the $A - X$ system were observed to be highly congested, making analysis challenging. Besides highly accurate estimates of the A state equilibrium bond length, comparisons with the analogous YbF and YbCl molecules are discussed.

List of Abbreviations and Symbols

a_{AB}	Homogenous Electronic Interaction Parameter; also given as $a_{AB}(R)$.
α	Homogenous Interaction Parameter; also given as $\alpha_{v'v''}$
α_p^v	First order Vibrational Dependence of Parameter P
A	Spin-Orbit Coupling Parameter
b_{AB}	Heterogeneous Electronic Interaction Parameter; also given as $b_{AB}(R)$
b_F	Fermi Contact Parameter
β	Heterogeneous Interaction Parameter; also given as $\beta_{v'v''}$
B	Rotational Parameter, also given as $B(R)$
c	Dipole-Dipole Interaction Parameter
C_I	Nuclear Spin-Rotation Parameter
CCD	Charge Coupled Device
CW	Continuous Wave
$\delta\Delta\nu$	Electronic Isotope Shift
D	Centrifugal Distortion Parameter
eQq	Nuclear Quadrupole Coupling Constant
F	Total Angular Momentum Quantum Number (including nuclear spin)
\vec{F}	Total Angular Momentum Vector
$F_{1,2}$	Spin Components
FID	Free Induction Decay
FTMW	Fourier Transform Microwave

γ	Spin-Rotation Parameter
γ_p^v	Second Order Vibrational Dependence of Parameter P
I	Nuclear Spin Quantum Number
\vec{I}	Nuclear Spin Angular Momentum Vector
\hat{I}	Nuclear Spin Angular Momentum Operator
\hat{I}_z	Operator for z-Component of Nuclear Spin Angular Momentum
J	Total Angular Momentum Quantum Number (excluding nuclear spin)
\vec{J}	Total Angular Momentum Vector (excluding nuclear spin)
\vec{L}	Total Orbital Angular Momentum Vector
$\vec{\Lambda}$	Projection of \vec{L} onto Internuclear Axis
MWFT	Microwave Fourier Transform
n	Principal Quantum Number
N	Total Angular Momentum Quantum Number (excluding electron & nuclear spin)
\vec{N}	Total Angular Momentum Vector (excluding electron & nuclear spin)
\hat{N}	Total Angular Momentum Operator (excluding electron spin)
$\vec{\Omega}$	Vector Sum of $\vec{\Lambda} + \vec{\Sigma}$
p	Λ -Doubling Parameter
PMT	Photomultiplier Tube
q	Λ -Doubling Parameter
Q	Quadrupole Moment
\hat{Q}	Quadruple Moment Operator
r	Electron-Nucleus Distance

R	Internuclear Distance
\bar{R}	Quantized Rotational Motion Angular Momentum Vector
$\bar{R}_{v'v''}$	R-Centroid
R_{NC}	Nuclear Charge Radius
S	Electron Spin Quantum Number
\bar{S}	Total Electron Spin Vector
\hat{S}	Electron Spin Angular Momentum Operator
\hat{S}_z	Operator for z-Component of Electron Spin Angular Momentum
$\bar{\Sigma}$	Projection of \bar{S} onto Internuclear Axis

Subscripts:

	X_e Value of Parameter X at Equilibrium
	X_D Centrifugal Distortion of Parameter X
	X_v Value of Parameter X at Vibrational Level v .
v	Vibrational Quantum Number
x,y	Atomic Labels
Y_{kl}	Dunham Parameter for Vibration (k) and Rotation (l).

Acknowledgements

I wish to thank my supervisor, Dr. John Coxon, for his support and direction during my course of study at Dalhousie University. I have greatly been enriched, both professionally and personally, by working with such a gifted experimentalist and teacher, and I will greatly miss our afternoon discussions about politics, economics and life in general.

I am deeply indebted to both my fiancée Sarah and my family (in the many different forms that my “family” comes in) for their unfailing emotional (and financial) support throughout my thesis.

I wish to thank my colleagues Dr. Todd Melville, Dr. Minguang Li, Kevin Noonan and Andrew MacDonald, and I also greatly appreciate the contributions made by Rick Conrad, Brian Miller, Jürgen Muller, Paul Ragogna and Ross Shortt.

Special thanks to Dr. Colan Linton of the University of New Brunswick, and Dr. Michael Gerry of the University of British Columbia for their respective invitations to work in their labs.

I am also grateful to Tony and Danny Tam for their years of instruction as my karate senseis. 押

Both the Natural Sciences and Engineering Research Council of Canada and Dalhousie University are thanked for their financial contributions over the years.

Finally, I wish to thank my friends from New Brunswick, who always encouraged the pursuit of excellence.

Chapter 1

Introduction

The development of the single-frequency laser has provided molecular spectroscopists with a tool to analyze previously intractable systems. Owing to its small spectral bandwidth (20 MHz), the single-frequency laser is able to probe molecules that exhibit highly congested spectra, and techniques such as selective detection, and resolved (laser induced) fluorescence provided further aid in characterizing these complicated systems.

Many of the molecules initially studied using such techniques were the diatomic alkaline earth metal halides. The visible transitions observed in these molecules, along with their ease of production in a simple oven arrangement, allowed pioneering work to be undertaken using a laser as an excitation source [1].

The present work on the $A - X$ system of SrBr extends previous studies of alkaline earth metal-containing molecules, MX ($M \equiv \text{Ca, Sr and Ba}$; $X \equiv \text{F, Cl, Br and I}$) and also includes some detailed study of analogous ytterbium ($M \equiv \text{Yb}$) containing species. Ytterbium is unique among the lanthanide elements, as the ground state electronic configuration, $[\text{Xe}]4f^{14}6s^2$, is very similar to the $[\text{Rg}]ns^2$ ground state electronic configurations of the alkaline earth metals. Thus, comparisons between ytterbium and alkaline earth metal-containing diatomic molecules will be made throughout this thesis. There are seven naturally occurring isotopes of Yb, with three isotopes having abundances between 13 and 32% (and zero nuclear spin), as compared to the alkaline earth metals, where each metal has a single isotope with an abundance above 70%. This

difference leads to more congested, and therefore more complicated, spectra for ytterbium halide molecules when compared with the alkaline earth metal halides.

The theoretical background necessary for discussion of the various projects presented in this thesis is given in the following chapter. The properties of electronic states having $^2\Sigma^+$ and $^2\Pi$ symmetry are given, with particular attention to modeling the mechanical, and electronic properties of both $^2\Sigma^+$ and $^2\Pi$ states, as well as modeling of nuclear-electron interactions in $^2\Sigma^+$ states. These nuclear-electron, or *hyperfine* interactions are present in molecules containing a nucleus with non-zero spin ($I > 0$), such as F ($I = \frac{1}{2}$), Cl ($I = \frac{3}{2}$), or Br ($I = \frac{3}{2}$). Hyperfine parameters that model such interactions can provide insight into the percent ionic character of the molecule, or the percent orbital occupations for the $I > 0$ nucleus. Chapter 2 also describes the nature of interactions that can be observed between $^2\Sigma^+$ and $^2\Pi$ states, in particular, *local* level crossings and *global* interactions (The latter effect causes Λ -doubling in $^2\Pi$ states, and “spin-rotation” in $^2\Sigma^+$ states).

Chapter 3 outlines the experimental details for the different projects covered in the present work. Features of the different types of apparatus used in obtaining continuous wave (CW) laser excitation and resolved laser fluorescence spectra will be discussed, most notably the use of phase sensitive photoelectric techniques, and charge coupled devices (CCD), respectively. Two different molecular production methods used in this work (the Broida oven and the pulsed laser ablation source) will be described, and a brief comparison will be given.

The details of a Fourier transform microwave spectrometer are also given in chapter 3. This arrangement employs laser ablation techniques in the production of gas-

phase molecules, which are subsequently probed with a pulsed microwave source. Molecular spectra are initially recorded as a time domain signal, subsequently transformed, using Fourier's algorithm, into the frequency domain for the purposes of analysis.

The previously observed level crossings in SrBr [2,3] are examined in more detail and are discussed in chapter 4. In the present work, a previous study [4] of the 0 – 0 and 1 – 0 bands in the red $A^2\Pi \leftarrow X^2\Sigma^+$ system has been extended to include data on the 2 – 1, 3 – 2, and 4 – 3 bands for the $^{88}\text{Sr}^{79}\text{Br}$ and $^{88}\text{Sr}^{81}\text{Br}$ isotopomers. The latter two bands exhibit perturbations between the A and B states in the form of *local* level crossings at $\nu_A = \nu_B + 3$. *Local* level crossings for these bands, and *global* interactions between these two states (described by the parameters a_{AB} and b_{AB}) are considered in a simultaneous treatment of the A and B states together. As far as can be determined, this represents the first effort to characterize both *local* and *global* interactions concurrently. This simultaneous treatment of the A and B states yields estimated rotational and electronic parameters that should be closer to their respective “true” mechanical and electronic definitions [5], rather than “effective” parameters that correctly model the data, but which are composed of a mixture of electronic and mechanical effects. The electronic interaction parameters a_{AB} and b_{AB} are also estimated from *ab initio* results [6], and a comparison with the experimentally fitted values is given.

In chapter 5, a study of the microwave spectra of YbF, YbCl and YbBr is described. This work recorded the first pure rotational spectra for any of the lanthanide halides, and is only the second study on lanthanide-containing diatomic molecules after LaO [7]. Rotational transitions in the $\nu = 0$ and 1 levels of ^{174}YbF and $^{174}\text{Yb}^{35}\text{Cl}$, and the

$\nu = 0$ levels of $^{174}\text{Yb}^{37}\text{Cl}$, $^{172}\text{Yb}^{35}\text{Cl}$, $^{174}\text{Yb}^{79}\text{Br}$ and $^{174}\text{Yb}^{81}\text{Br}$ have been observed. In addition to accurate rotational constants, the hyperfine structures of ytterbium-containing diatomic molecules were characterized for the first time. From the rotational constants, extremely accurate bond lengths have been calculated, and from the hyperfine parameters, estimates of electronic properties, such as percent ionic character and electron distribution, are estimated. Finally, a comparison of the $^2\Sigma^+$ ground states is made between YbX molecules and similar alkaline earth metal halide species [8-11].

A study of the green $B^2\Sigma^+ \leftarrow X^2\Sigma^+$ system of YbBr is presented in Chapter 6. Characterizations of the 0 – 0, 0 – 1, 1 – 0 and 1 – 1 bands for the $^{174}\text{Yb}^{79}\text{Br}$, $^{174}\text{Yb}^{81}\text{Br}$, $^{172}\text{Yb}^{79}\text{Br}$ and $^{172}\text{Yb}^{81}\text{Br}$ isotopomers are discussed, with particular attention to the challenges of rotational assignment in molecules with extreme spectral congestion. The observation of minute field shifts in the spectra of YbCl and YbBr are also described, with particular attention to the effect that such shifts have on the electronic energy and bond lengths in “heavy” atom containing molecules. Owing to a lack of high resolution data on multiple bands and multiple isotopomers for heavy atom diatomic molecules, field shifts have been observed for sparingly few molecules, with PbCh (Ch \equiv O, S, Se, Te) [12-14], TlX (X \equiv F, Cl, Br, Br) [12], and Cu₂ [15] being a few notable examples.

Finally, work on the yellow-green $A^2\Pi \leftarrow X^2\Sigma^+$ system of YbBr is presented in chapter 7. This study of the $^{174}\text{Yb}^{79}\text{Br}$ and $^{174}\text{Yb}^{81}\text{Br}$ isotopomers makes use of the constants determined in the preceding chapters to aid in the analysis of the 1 – 0 and 0 – 0 bands of the $A^2\Pi$ state. Challenges such as the extreme spectral congestion, and the equal abundance of bromine isotopes, are discussed in reference to the analysis of the YbBr spectra.

Chapter 2

Theoretical Background

2.1 Introduction

The background material for this chapter was obtained from Refs [16-18], except where otherwise indicated.

The characterizations of the different mechanical and magnetic interactions within a diatomic molecule are generally based on the choice of a suitable Hamiltonian. For a particular system, the model Hamiltonian describes the potential and kinetic energy of the electrons (**Elec**), vibrational and rotational motions (**Vib** and **Rot**), and magnetic effects (fine and hyperfine structure, **FS** and **HFS**). The total Hamiltonian (**Tot**) can be expressed as a sum of the separate components:

$$\hat{\mathcal{H}}_{\text{Tot}} = \hat{\mathcal{H}}_{\text{Elec}} + \hat{\mathcal{H}}_{\text{Vib}} + \hat{\mathcal{H}}_{\text{Rot}} + \hat{\mathcal{H}}_{\text{FS}} + \hat{\mathcal{H}}_{\text{HFS}}. \quad 2.1$$

The stationary state energies, E , are given as solutions of the Schrödinger equation,

$$\hat{\mathcal{H}}_{\text{Tot}} \Psi_{\text{Tot}} = E \Psi_{\text{Tot}}, \quad 2.2$$

where Ψ_{Tot} is the total wavefunction for the particular state.

In practice, the method of solving the Schrödinger equation directly is not often employed, and instead an equivalent method called *matrix mechanics* is used. In matrix mechanics, the total wavefunction is given as a linear combination of orthonormal *basis functions* ($\Psi_{\mathbf{B}}$) known as a *basis set*. The choice of basis set is determined by the type(s) of angular momentum coupling present in a given state, and, as described in Herzberg [16], different coupling schemes are labeled as *Hund's coupling cases*. The details of two of these coupling cases, case (a) and case (b), will be presented here.

2.2 Hund's Coupling Cases

2.2.1 Hund's Case (a)

An electronic state having a weak electronic and rotational interaction is classified as Hund's case (a). In this case, the total orbital angular momentum vector, \vec{L} , is coupled to the strong electric field generated between the two nuclei. The vector \vec{L} thus precesses about the internuclear axis with a projection labeled $\bar{\Lambda}$. This precession generates a magnetic moment along this axis (Figure 2.1a) and in turn, this leads to a coupling of the total electron spin angular momentum, such that the vector \vec{S} also precesses about the internuclear axis. The projection of \vec{S} onto the internuclear axis is labeled as $\bar{\Sigma}$, and the absolute value of the sum of $\bar{\Lambda}$ and $\bar{\Sigma}$ is termed $\bar{\Omega}$. An important feature of the coupling between the spin and orbital angular momenta, known as spin-orbit coupling, is the removal of the $2S+1$ spin degeneracy¹, such that spin-orbit components of different Ω -values have different energies, as defined by the spin-orbit coupling parameter A .

Each spin-orbit component has an inherent two-fold degeneracy due to the different combinations of $\bar{\Sigma}$ and $\bar{\Lambda}$ for a given value of Ω . For example, if one considers a $^2\Pi$ state for which $\Lambda = \pm 1$ and $\Sigma = \pm \frac{1}{2}$, the two possible values of Ω are $\frac{1}{2}$ and $\frac{3}{2}$, with each component being doubly degenerate owing to the possible vector additions, as shown in figure 2.1b.

¹ Here S is the quantum number associated with the vector \vec{S} . This association is inferred for other vectors (denoted with the arrow) and quantum numbers (italicized or in capital Greek letters) used herein.

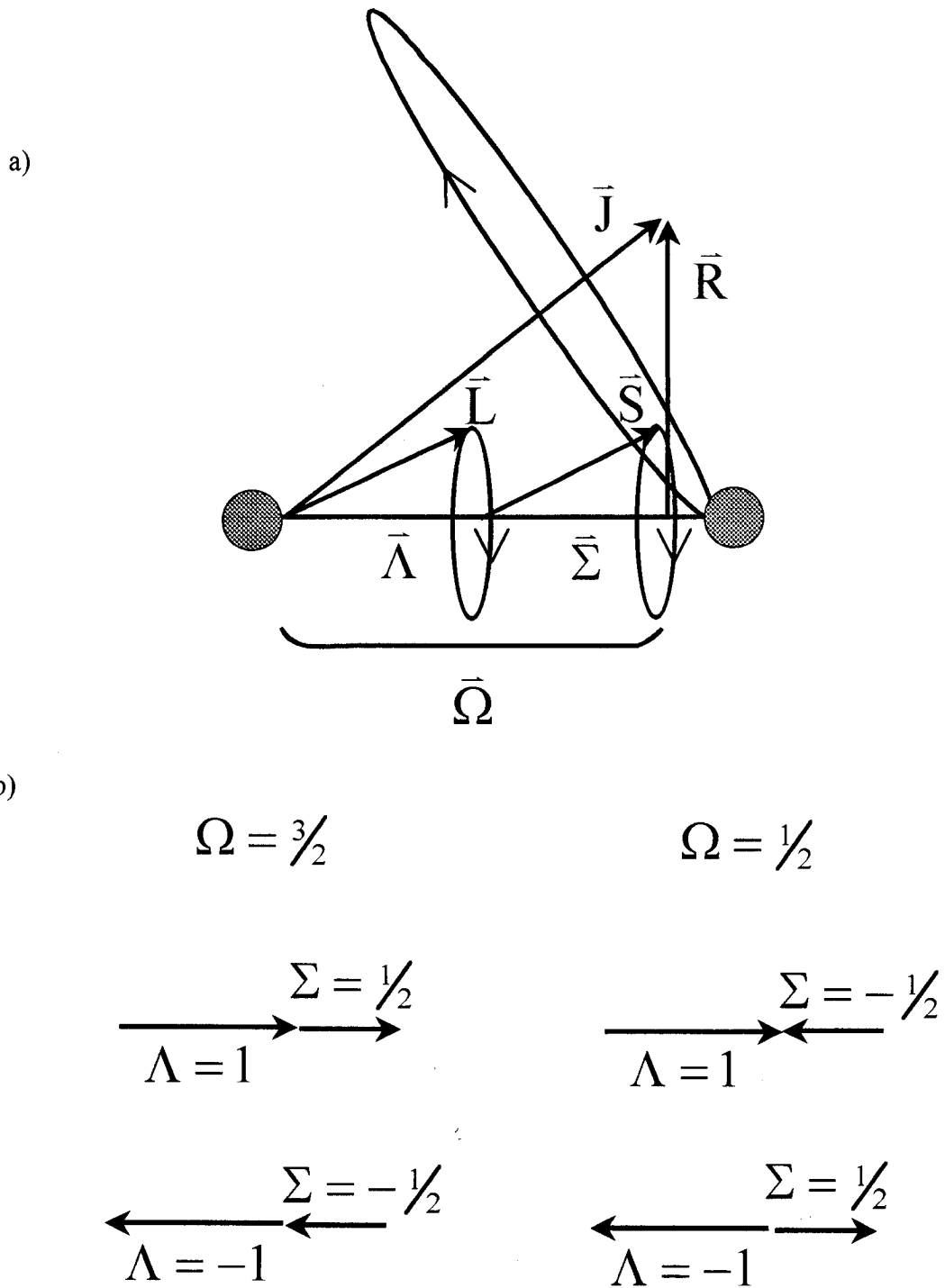


Figure 2.1 a) Coupling and precessional motion in Hund's case (a) [16].
 b) Different possible coupling arrangements for a ${}^2\Pi$ state.

In Hund's case (a), the vector $\vec{\Omega}$ couples to the nuclear rotation vector \vec{R} , to form the total angular momentum vector \vec{J} . Since \vec{J} is the sum of $\vec{\Omega}$ and \vec{R} , the possible values of the quantum number J are $\Omega, \Omega+1, \Omega+2, \dots$

The Hund's case (a) basis set is given in *ket* notation as $|n\nu J\Omega S\Lambda\Sigma\rangle$; this notation specifies the quantum numbers that are well defined (n and ν are the principal and vibrational quantum numbers, and all remaining quantum numbers are defined by the respective angular momentum vectors, as described in Footnote 1). There are four basis functions for each value of $J \geq \frac{1}{2}$ in a ${}^2\Pi$ state, and thus four different rotational energy levels, i.e. two for each value of Ω . These two sub-states are often given the labels of F_1 and F_2 corresponding to $\Omega = \frac{1}{2}$ and $\Omega = \frac{3}{2}$, respectively.

2.2.2 Hund's Case (b)

If the orbital angular momentum vector, \vec{L} , is not strongly coupled to the internuclear axis, or is perpendicular to the internuclear axis (as is the case of Σ states with $\Lambda = 0$), the spin angular momentum does not couple along the internuclear axis. Thus, the quantum number Ω is no longer defined. The result is that the vector $\vec{\Lambda}$ couples directly to the rotational vector \vec{R} , to form a resultant vector \vec{N} , where \vec{N} is defined as the total angular momentum apart from spin, as shown in Figure 2.2. Thus the quantum number N can have values of $\Lambda, \Lambda+1, \Lambda+2, \dots$. The vector \vec{N} may in turn couple weakly to the spin angular momentum vector \vec{S} to form the total angular momentum vector \vec{J} . This vector has the same meaning as that described in case (a), but is a result of a different mechanism.

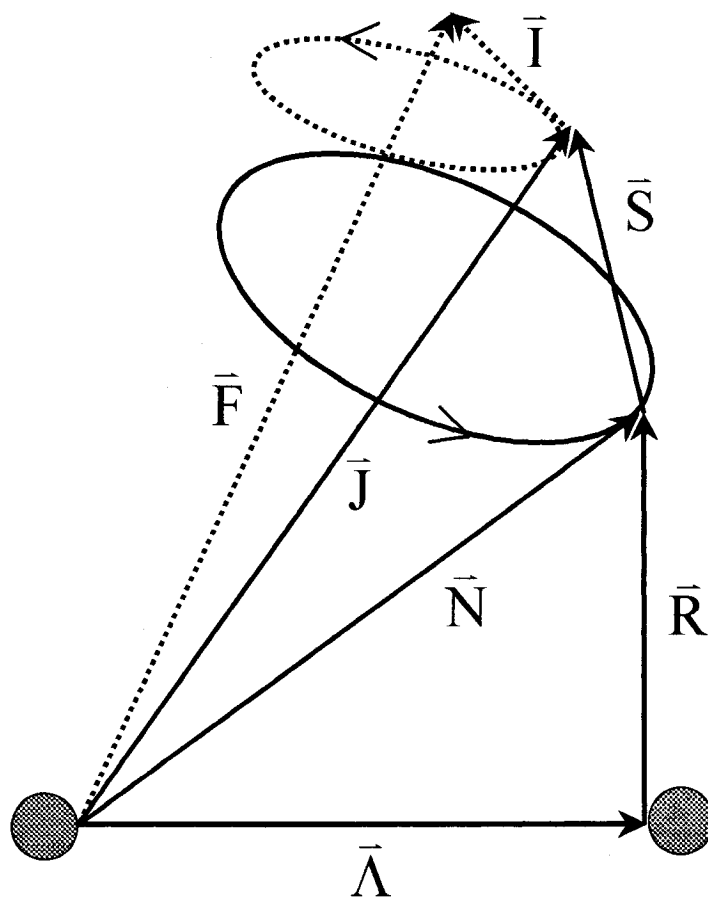


Figure 2.2 Coupling and precessional motion in Hund's case (b) [16]; the dotted lines indicate the sub case b_{β} . For a $^2\Sigma^+$ state, $\Lambda = 0$, and $N \equiv R$.

The Hund's case (b) basis set can also be described in *ket* notation, and is given as $|mNSJ\rangle$. For a $^2\Sigma^+$ state, there are two basis functions, and thus two rotational energy levels, for each value of N , labeled as F_1 and F_2 for $J = N + \frac{1}{2}$ and $J = N - \frac{1}{2}$.

2.2.3 Hund's Case (b_{β})

In molecules containing a nucleus with non-zero nuclear spin (I), states that are $^2\Sigma^+$ in nature have the property that the spectral lines are split into $2I + 1$ components [19]. In Doppler limited electronic spectra, this *hyperfine* splitting is often not resolved (if the splitting is small), or the transitions are not observed (due to a decrease in intensity). In microwave spectroscopy, however, the extremely high resolution and sensitivity allows for characterization of this effect, and it thus becomes essential to account for this interaction in the Hund's case (b) basis set. As seen in Figure 2.2, the coupling of the nuclear spin vector, \vec{I} , with the total angular momentum vector, \vec{J} , yields a resultant vector \vec{F} . This sub-case is known as case (b_{β}), the basis set of which is given as $|mNSJIF\rangle$ in *ket* notation.

2.3 Parity

Since the rotational levels of a diatomic molecule have either even (+) or odd (−) parity, the matrix approach is simplified by choosing basis functions of defined parity. Parity is a symmetry property that depends on the behavior of the total wavefunction with respect to the operation \hat{i}_{sp} , namely the inversion of the coordinates of the nuclei and all

electrons through the origin (i.e. $x_i, y_i, z_i \rightarrow -x_i, -y_i, -z_i$). The use of parity for a ${}^2\Pi$ state using a case (a) basis set will now be considered as an example².

As mentioned above, for a ${}^2\Pi$ state there are four basis functions for each set of n , ν , and J , leading to a 4×4 Hamiltonian matrix for the (n, ν, J) block; each row and column of the matrix is associated with one of the $|m_J \Omega S \Lambda \Sigma\rangle$ basis functions. (Each element of this matrix contains mathematical expressions, given in a following section, that are used to obtain the energy levels by matrix diagonalization: diagonal elements describe the energy associated with a single basis function, and off-diagonal matrix elements take account of *mixing* between the respective basis functions.)

Although it is possible to solve for the energy levels by diagonalizing the full 4×4 matrix, transforming the $|m_J \Omega S \Lambda \Sigma\rangle$ basis set into a new basis set of defined *parity* leads to two simpler 2×2 block diagonal matrices. (Similarly, the 2×2 matrix required for a ${}^2\Sigma^+$ state is reduced to two block diagonal 1×1 matrices using a case (b) basis set of defined parity).

As outlined in Zare *et al.* [20], the effect of the parity operator \hat{i}_{sp} on the Hund's case (a) basis set is found to be

$$\hat{i}_{sp} |m_J \Omega S \Lambda \Sigma\rangle = (-1)^{J+S} |m_J, -\Omega S, -\Lambda, -\Sigma\rangle. \quad 2.3$$

It can be seen from Eq. 2.3 that the wavefunction is changed to another member of the basis set by the operation of \hat{i}_{sp} . In this situation, it is appropriate to consider new basis functions defined as linear combination of Eq. 2.3 case (a) basis functions, namely

² A similar treatment can be derived for Hund's case (b), but is not given here for brevity.

$$\Psi_{\mathbf{B}} = |n^{2S+1}\Lambda_{\Omega}\nu Jp^{\pm}\rangle = \frac{1}{\sqrt{2}} \left[|m\nu J\Omega S\Lambda\Sigma\rangle \pm |m\nu J, -\Omega S, -\Lambda, -\Sigma\rangle \right]. \quad 2.4$$

The Hund's case (a) symmetry label $^{2S+1}\Lambda_{\Omega}$ is thus defined in this step; in addition the new basis functions have a defined parity ($p^{\pm} = \pm(-1)^{J+S}$). The operation of \hat{i}_{sp} on this new parity basis function is

$$\hat{i}_{sp}\Psi_{\mathbf{B}} = \hat{i}_{sp}|n^{2S+1}\Lambda_{\Omega}\nu Jp^{\pm}\rangle = \pm|n^{2S+1}\Lambda_{\Omega}\nu Jp^{\pm}\rangle = \pm\Psi_{\mathbf{B}}, \quad 2.5$$

and it can be seen that although the basis function does not change with this operation, the *sign* of the basis function can change, thus allowing labels of even (+) or odd (−) parity to be applied to the new basis functions of Eq. 2.4. It follows then that the rotational energy states (eigenvalues) determined from each 2×2 matrix have a defined parity that alternates with consecutive values of J .

An alternate, and possibly more useful, parity label is known as rotationless, or residual parity. It can be shown that the J -dependent portion of the wavefunction can be factored out, such that levels of half integer J that follow

$$\hat{i}_{sp}\Psi_{\mathbf{B}} = +(-1)^{J-\frac{1}{2}}\Psi_{\mathbf{B}} \quad 2.6$$

are labeled as e , and similarly levels that follow

$$\hat{i}_{sp}\Psi_{\mathbf{B}} = -(-1)^{J-\frac{1}{2}}\Psi_{\mathbf{B}} \quad 2.7$$

are labeled as f .

2.4 Selection rules

The new basis functions derived in the previous section are also useful in the determination of selection rules. For case (a) basis functions, consideration of the matrix elements of the dipole moment operator,

$$\langle n' 2S'+1 \Lambda'_{\Omega'} \nu' J' p^{\pm} | \hat{\mu} | n'' 2S''+1 \Lambda''_{\Omega''} \nu'' J'' p^{\pm} \rangle, \quad 2.8$$

leads to the $+ \leftrightarrow -$ and the $\Delta J = 0^3, \pm 1$ selection rules. These selection rules give rise to the three possible branches, labeled as P, Q and R, for transitions of $\Delta J = -1, 0$ and $+1$, respectively. It can thus be shown that P and R branches correspond to $e \leftrightarrow e$ or $f \leftrightarrow f$ transitions, and Q branches correspond to $e \leftrightarrow f$ transitions.

2.5 Matrix Elements

Once the choice of basis function is made, the matrix elements, given as:

$$\langle \Psi_{B_i} | \hat{\mathcal{H}}_{\text{Tot}} | \Psi_{B_j} \rangle = H_{ij} \quad 2.9$$

must be determined, allowing for the rotational energy states (E) to be found by solving for the n roots of the secular equation:

$$\begin{bmatrix} H_{11} - E_1 & \cdots & H_{1n} \\ \cdots & \cdots & \cdots \\ H_{n1} & \cdots & H_{nn} - E_n \end{bmatrix} = 0. \quad 2.10$$

Zare *et al.* [20] have determined expressions for the various elements (H_{ij}) in a case (a) basis set, from which the full Hamiltonian matrix can be determined. The evaluation of such matrix elements does not require that the form of the basis functions be known, but instead provides the results of their evaluation. (In mathematical terms, the problem of

³ $\Delta J = 0$ transitions do not occur when both states are $\Omega = 0$.

determining wavefunctions has been replaced with a set of simultaneous equations, one for each value of n , ν , J and parity; i.e. two blocks of 2×2 matrices for ${}^2\Pi$ states (Table 2.1(a) and two blocks of 1×1 matrices for ${}^2\Sigma^+$ states (Table 2.1 (b)).

The expressions within these matrix elements describe the effects of rotation and spin-rotation (the direct coupling of the \bar{S} and \bar{R} vectors), and associated with each expression is a parameter that describes the magnitude of the effect, in this case B and γ^{SR} , respectively. Purely electronic effects, such as the energy separation between two electronic states⁴, or spin-orbit coupling, are described using expressions containing the parameters T_e and A_e , respectively.

Although there are no interactions between basis functions of the same J but different parity, weak interactions are usually present between functions with $\Delta\nu \neq 0$ or $\Delta\Lambda \neq 0$. Such off-diagonal interactions are often treated in an approximate, but still satisfactory, fashion by means of the Van Vleck transformation [20]. Essentially, the off diagonal matrix elements are *folded* into the elements of the diagonal block being considered. The Van Vleck transformation is discussed in detail in the work of Zare *et al.* [20]; a series of expressions was obtained for increasing order (λ), such that as $\lambda \rightarrow \infty$, the corrections for basis function mixing becomes more reliable. Such expressions were derived using a method similar to 2nd order perturbation theory. In the work presented herein, it was only necessary to include those with $\lambda \leq 2$.

Off-diagonal elements that describe mixing between basis functions of different

⁴ The energy separation between the vibrational levels of two different electronic states is labeled as the band origin, $\nu_{\nu'\nu''}$, and may be substituted for the parameter T_e if data for only a single band was obtained.

Table 2.1

Hamiltonian matrix elements^a for a ${}^2\Pi$ state (a) and a ${}^2\Sigma^+$ state (b).

(a)

	$A^2\Pi_{3/2}$	$A^2\Pi_{1/2}$
$A^2\Pi_{3/2}$	$\nu_0^\Pi + \frac{1}{2}A_\Pi + (B_\Pi + A_D)(x^2 - 2)$ $-D_\Pi((x^2 - 2)^2 + x^2 - 1)$ $+ \frac{1}{2}(q + q_D(x^2 - \frac{1}{4}))(x^2 - 1)$	$-B_\Pi(x^2 - 1)^{1/2} + 2D_\Pi(x^2 - 1)^{3/2}$ $-\frac{1}{4}(p + p_D(x^2 - \frac{1}{4}))(x^2 - 1)^{1/2}$ $-\frac{1}{2}(q + q_D(x^2 - \frac{1}{4}))(1 \mp x)(x^2 - 1)^{1/2}$
$A^2\Pi_{1/2}$	$-B_\Pi(x^2 - 1)^{1/2} + 2D_\Pi(x^2 - 1)^{3/2}$ $-\frac{1}{4}(p + p_D(x^2 - \frac{1}{4}))(x^2 - 1)^{1/2}$ $-\frac{1}{2}(q + q_D(x^2 - \frac{1}{4}))(1 \mp x)(x^2 - 1)^{1/2}$	$\nu_0^\Pi - \frac{1}{2}A_\Pi + (B_\Pi - A_D)x^2$ $-D_\Pi(x^4 + x^2 - 1)$ $+ \frac{1}{2}(p + p_D(x^2 - \frac{1}{4}))(1 \mp x)$ $+ \frac{1}{2}(q + q_D(x^2 - \frac{1}{4}))(1 \mp x)^2$

(b)

	$B^2\Sigma^+$
$B^2\Sigma^+$	$\nu_0^\Sigma + B_\Sigma x(x \mp 1) - D_\Sigma x^2(x \mp 1)^2$ $-\frac{1}{2}(\gamma + \gamma_D(x^2 - \frac{1}{4}))(1 \mp x)$

^aThe “ \mp ” denotes e/f parity, given as e over f , $x = J + \frac{1}{2}$.

ν , are thus approximated by centrifugal distortion expressions, and parameters associated with these expressions are typically labeled with the subscript D or H (known as *radially* dependent parameters). Other off-diagonal interactions include the effects of Λ -doubling in ${}^2\Pi$ states, and “spin-rotation⁵” in ${}^2\Sigma^+$ states. These effects are off-diagonal in Λ and are represented by the parameters p_ν and q_ν for a ${}^2\Pi$ state, and γ_ν in a ${}^2\Sigma^+$ state. (In practice, expressions containing the parameters p_ν and q_ν describe the energetic “splitting” of rotational states of different parity within a ${}^2\Pi$ state. Physically, this splitting arises when the vector \bar{L} uncouples from the internuclear axis, and is caused by a slight mixing of electronic ${}^2\Pi$ states with ${}^2\Sigma^+$ states. This mixing is also apparent in ${}^2\Sigma^+$ states, where a similar splitting can be described using expressions containing the parameter⁵ γ_ν .)

For strong interactions between two different basis functions, i.e. large off diagonal matrix elements, the Van Vleck approximation is no longer reliable. This is the case for ${}^2\Pi$ states, where the interaction between $\Omega = 1/2$ and $\Omega = 3/2$ levels cannot be approximated, and thus the two 2×2 matrices, one for each parity, cannot be reduced in size any further.

The Van Vleck approximation also breaks down when the two interacting electronic states have levels that are nearly degenerate in energy, as is the case for levels in the $A^2\Pi$ and $B^2\Sigma^+$ states of SrBr. In order to describe these *locally perturbed* levels,

⁵ The experimental parameter γ describes both the small effects of pure spin rotation (γ^{SR}) and the splitting that arises from mixing of ${}^2\Pi$ basis functions [16].

Table 2.2

Hamiltonian matrix elements for a ${}^2\Pi \sim {}^2\Sigma^+$ Interaction. The 2×2 elements of a ${}^2\Pi$ state and the 1×1 elements of a ${}^2\Sigma^+$ are given for each parity, where the “ \mp ” denotes e/f parity, given as e over f . The off-diagonal elements involving the parameters α and β explicitly describe interactions between levels of the ${}^2\Pi$ and ${}^2\Sigma^+$ states. Expressions containing the parameter γ^{SR} have been omitted owing to the high correlation with expressions containing the parameter A_{D} .
 $x = J + \frac{1}{2}$

$B^2\Sigma^+$	$A^2\Pi_{3/2}$	$A^2\Pi_{1/2}$
$v_0^{\Sigma} + B_{\Sigma}x(x \mp 1) - D_{\Sigma}x^2(x \mp 1)^2$	$-\beta(x^2 - 1)^{1/2}$	$\alpha + \beta(1 \mp x)$
$-\frac{1}{2}(\gamma + \gamma_{\text{D}}(x^2 - \frac{1}{4}))(1 \mp x)$	$v_0^{\Pi} + \frac{1}{2}A_{\Pi} + (B_{\Pi} + A_{\text{D}})(x^2 - 2)$	$-B_{\Pi}(x^2 - 1)^{1/2} + 2D_{\Pi}(x^2 - 1)^{3/2}$
	$-D_{\Pi}((x^2 - 2)^2 + x^2 - 1)$	$-\frac{1}{4}(p + p_{\text{D}}(x^2 - \frac{1}{4}))(x^2 - 1)^{1/2}$
	$+\frac{1}{2}(q + q_{\text{D}}(x^2 - \frac{1}{4}))(x^2 - 1)$	$-\frac{1}{2}(q + q_{\text{D}}(x^2 - \frac{1}{4}))(1 \mp x)(x^2 - 1)^{1/2}$
		$v_0^{\Pi} - \frac{1}{2}A_{\Pi} + (B_{\Pi} - A_{\text{D}})x^2$
		$-D_{\Pi}(x^4 + x^2 - 1)$
		$+\frac{1}{2}(p + p_{\text{D}}(x^2 - \frac{1}{4}))(1 \mp x)$
		$+\frac{1}{2}(q + q_{\text{D}}(x^2 - \frac{1}{4}))(1 \mp x)^2$

coupling of the single 2×2 block (for a ${}^2\Pi$ state) with the 1×1 block (for a ${}^2\Sigma^+$ state) leads to a 3×3 matrix for the interacting levels of the same n , ν , J and parity. Expressions that describe the interaction between basis functions of these two states occur in the off-diagonal positions. The interaction between the basis functions of these two states is thus described explicitly, and is not approximated. The complete 3×3 matrix is shown in Table 2.2, and a more detailed description is given in chapter 4.

Additional matrix elements describing hyperfine coupling in ${}^2\Sigma^+$ states were also derived. Applying the $|n\nu NSJIF\rangle$ basis set to the hyperfine structure Hamiltonian ($\hat{\mathcal{H}}_{\text{HFS}}$) of Frosch and Foley [21], where:

$$\hat{\mathcal{H}}_{\text{HFS}} = b_{\text{F}} \hat{\mathbf{I}} \cdot \hat{\mathbf{S}} + \frac{c}{3} (3\hat{\mathbf{I}}_{\text{z}} \cdot \hat{\mathbf{S}}_{\text{z}} - \hat{\mathbf{I}} \cdot \hat{\mathbf{S}}) + T^2 (\nabla \hat{\mathbf{E}}) \cdot T^2 (\hat{\mathbf{Q}}) + C_1 \hat{\mathbf{I}} \cdot \hat{\mathbf{N}}, \quad 2.11$$

yields Hamiltonian matrix elements that describe the effects of hyperfine interactions. As noted by Radford [22], finite matrix elements of $\hat{\mathcal{H}}_{\text{HFS}}$ occur in general for $\Delta N = 0, \pm 1, \pm 2$; in the case of a ${}^2\Sigma$ state however, the only finite matrix elements off-diagonal in N are the spin-dipolar and electric quadrupole terms with $\Delta N = \pm 2$. The matrix elements were derived from the general expressions given by Dixon and Woods [23], and are listed in Table 2.3. The 9- j symbols can be evaluated using the computer code written by Zare [24]. Several additional parameters are required to account for interactions associated with $I > 0$ nuclei. The hyperfine parameter, b_{F} , is the Fermi contact parameter; the effect of dipole-dipole interactions is characterized by the parameter c ; the nuclear spin-rotation parameter is C_1 . Electric quadrupole interactions are described as a product of the electric field gradient tensor, $T^2(\nabla \mathbf{E})$, with the quadrupole moment tensor, $T^2(\mathbf{Q})$; evaluation of this operator involves the nuclear quadrupole coupling parameter, eQq .

Table 2.3

Matrix elements describing rotational, fine and hyperfine effects for a $^2\Sigma^+$ state, of the form $\langle n\nu NSJIF | \hat{\mathcal{H}}_{\text{HFS}} | n\nu N'SJ'IF \rangle$.

Rotation:

$$\langle J = N \pm \frac{1}{2} | B \hat{\mathbf{N}}^2 | J' = N \pm \frac{1}{2} \rangle = B[N(N+1)]$$

Spin-rotation:

$$\langle J = N \pm \frac{1}{2} | \gamma \hat{\mathbf{N}} \cdot \hat{\mathbf{S}} | J' = N \pm \frac{1}{2} \rangle = \frac{\gamma}{2} [J(J+1) - N(N+1) - S(S+1)]$$

Electric Quadrupole:

$$\langle J = N \pm \frac{1}{2} | T^2(\nabla \hat{\mathbf{E}}) \cdot T^2(\hat{\mathbf{Q}}) | J' = N \pm \frac{1}{2} \rangle = -eQq \frac{[\frac{3}{4}(C(C+1)) - I(I+1)(J)(J+1)]}{2I(2I-1)(J)(J+1)}$$

$$\langle J = N - \frac{1}{2} | T^2(\nabla \hat{\mathbf{E}}) \cdot T^2(\hat{\mathbf{Q}}) | J = N + \frac{1}{2} \rangle = eQq \frac{3D(N)E(N)}{4I(2I-1)(2N+3)(2N-1)(2N+1)}$$

$$\langle N, J = N + \frac{1}{2} | T^2(\nabla \hat{\mathbf{E}}) \cdot T^2(\hat{\mathbf{Q}}) | N + 2, J' = N + \frac{5}{2} \rangle = eQq \frac{3E(N+1)E(N+2)}{16I(2I-1)(2N+3)(2N+5)}$$

$$\begin{aligned} \langle N, J = N + \frac{1}{2} | T^2(\nabla \hat{\mathbf{E}}) \cdot T^2(\hat{\mathbf{Q}}) | N + 2, J' = N + \frac{3}{2} \rangle \\ = eQq \frac{3D(N+1)E(N+1)}{4I(2I-1)(2N+1)(2N+3)(2N+5)} \end{aligned}$$

$$\langle N, J = N - \frac{1}{2} | T^2(\nabla \hat{\mathbf{E}}) \cdot T^2(\hat{\mathbf{Q}}) | N + 2, J' = N + \frac{3}{2} \rangle = eQq \frac{3E(N)E(N+1)}{16I(2I-1)(2N+3)(2N+1)}$$

Fermi-Contact:

$$\langle J = N \pm \frac{1}{2} | b_F \hat{\mathbf{I}} \cdot \hat{\mathbf{S}} | J' = N \pm \frac{1}{2} \rangle = \pm b_F \frac{C}{2(2N+1)}$$

$$\langle J = N + \frac{1}{2} | b_F \hat{\mathbf{I}} \cdot \hat{\mathbf{S}} | J' = N - \frac{1}{2} \rangle = b_F \frac{E(N)}{2(2N+1)}$$

Table 2.3 (con't)

Nuclear Spin-rotation:

$$\langle J = N + \frac{1}{2} | C_1 \hat{\mathbf{I}} \cdot \hat{\mathbf{N}} | J' = N + \frac{1}{2} \rangle = C_1 C \frac{N}{(2N+1)}$$

$$\langle J = N - \frac{1}{2} | C_1 \hat{\mathbf{I}} \cdot \hat{\mathbf{N}} | J' = N - \frac{1}{2} \rangle = C_1 C \frac{(N+1)}{(2N+1)}$$

$$\langle J = N + \frac{1}{2} | C_1 \hat{\mathbf{I}} \cdot \hat{\mathbf{N}} | J' = N - \frac{1}{2} \rangle = -C_1 \frac{E(N)}{2(2N+1)}$$

Spin dipolar:

$$\langle J = N \pm \frac{1}{2} | c \hat{\mathbf{I}}_z \cdot \hat{\mathbf{S}}_z | J' = N \pm \frac{1}{2} \rangle = c \sqrt{\frac{5}{4}} C \left[\frac{N(N+1)(J+\frac{1}{2})}{(N-\frac{1}{2})(N+\frac{3}{2})(J+1)} \right]^{\frac{1}{2}} \begin{Bmatrix} \frac{1}{2} & \frac{1}{2} & 1 \\ N & N & 2 \\ J & J & 1 \end{Bmatrix}$$

$$\langle J = N - \frac{1}{2} | c \hat{\mathbf{I}}_z \cdot \hat{\mathbf{S}}_z | J' = N + \frac{1}{2} \rangle = c E(N) \sqrt{\frac{5}{2}} \left[\frac{N(N+1)}{(2N-1)(2N+3)} \right]^{\frac{1}{2}} \begin{Bmatrix} \frac{1}{2} & \frac{1}{2} & 1 \\ N & N & 2 \\ N - \frac{1}{2} & N + \frac{1}{2} & 1 \end{Bmatrix}$$

$$\begin{aligned} \langle N, J = N + \frac{1}{2} | c \hat{\mathbf{I}}_z \cdot \hat{\mathbf{S}}_z | N + 2, J' = N + \frac{3}{2} \rangle \\ = c E(N+1) \frac{[15 (N+1)(N+2)]^{\frac{1}{2}}}{2 (2N+3)} \begin{Bmatrix} \frac{1}{2} & \frac{1}{2} & 1 \\ N & N+2 & 2 \\ N + \frac{1}{2} & N + \frac{3}{2} & 1 \end{Bmatrix} \end{aligned}$$

where

$$C = F(F+1) - I(I+1) - J(J+1),$$

$$D(N) = F(F+1) - I(I+1) - (N - \frac{1}{2})(N + \frac{3}{2}),$$

$$E(N) = [(F + N - I + \frac{1}{2})(F + I - N + \frac{1}{2})(F + I + N + \frac{3}{2})(N + I - F + \frac{1}{2})]^{\frac{1}{2}},$$

$J = N + \frac{1}{2}$ denotes the F_1 level and $J = N - \frac{1}{2}$ denotes the F_2 level.

2.6 Fitting of Parameters to Observed Transitions

Once the Hamiltonian matrix elements have been determined for the state(s) of interest, an established procedure was used for reducing the observed transition frequencies to a set of molecular parameters.

There are two main steps in this procedure, the first being the identification and assignments of spectral lines. In Figures 2.3 and 2.4, the branch structures for electronic ${}^2\Pi - {}^2\Sigma^+$ and ${}^2\Sigma^+ - {}^2\Sigma^+$ transitions, respectively, are given. Similarly, pure rotational transitions of the sort observed in a ${}^2\Sigma^+$ state can be determined from the selection rules: $\Delta N = \pm 1$, $\Delta J = \pm 1$, $\Delta F = 0, \pm 1$ and $\Delta M_F = 0, \pm 1$, and from Figure 2.5. Once the identification of the type of transition and its assignment has been made (see chapter 3 for experimental assignment methods), parameters are determined that reproduce the measured lines positions.

For simple systems, such as a ${}^2\Sigma^+ - {}^2\Sigma^+$ transition, expressions are employed for each state *and* each parity separately. For each state, and for a each value of J and parity, a 1×1 matrix was constructed containing the expression of Table 2.1(b), and thus the solution of Eq. 2.10 reduces to a linear expression. The parameters were thus determined in a single step by solving for the roots of the secular equation.

For situations with off-diagonal matrix elements, such as a ${}^2\Pi$ state, the characterization of ${}^2\Pi \sim {}^2\Sigma^+$ interactions, or the fitting of parameters to microwave transitions within a ${}^2\Sigma^+$ state, a non-linear least squares fitting routine must be employed.

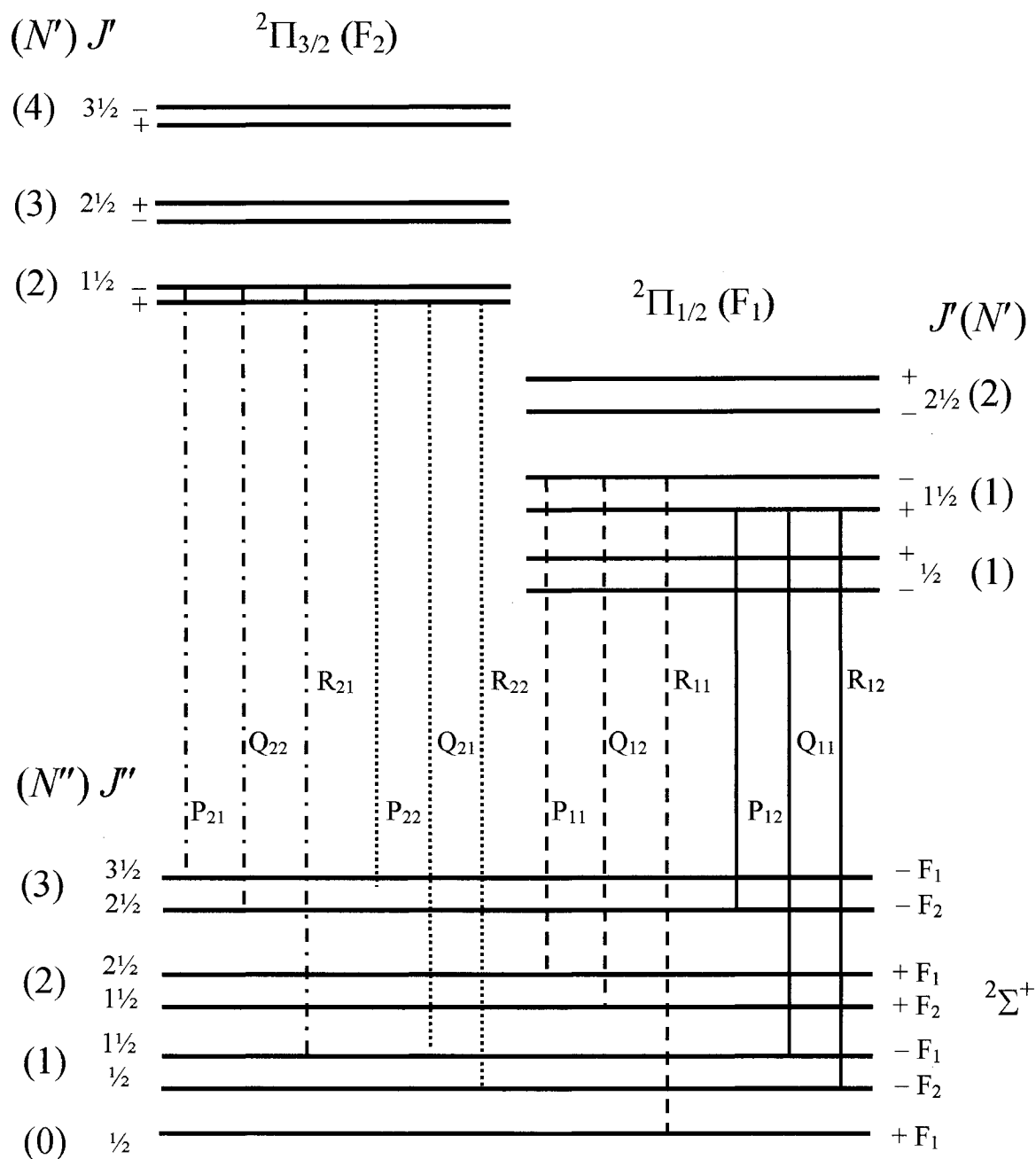


Figure 2.3 Schematic of ${}^2\Pi \leftrightarrow {}^2\Sigma^+$ manifold showing all possible branches [16]. Branches sharing the same upper component are distinguished from other branches in the same band.

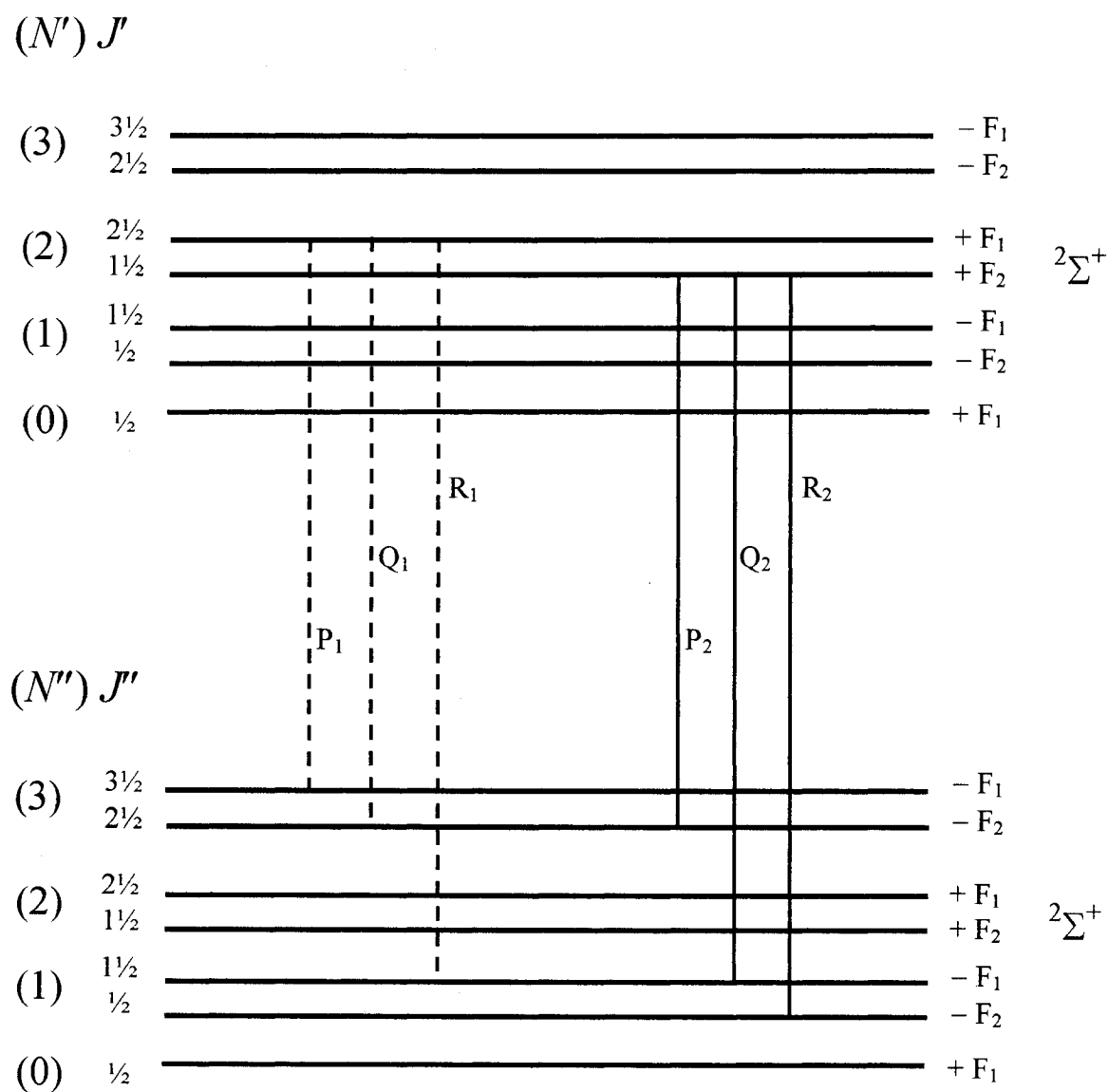


Figure 2.4 Schematic of $2\Sigma^+ \leftrightarrow 2\Sigma^+$ manifold showing all possible branches [16]. Branches sharing the same upper component are distinguished from other branches in the same band.

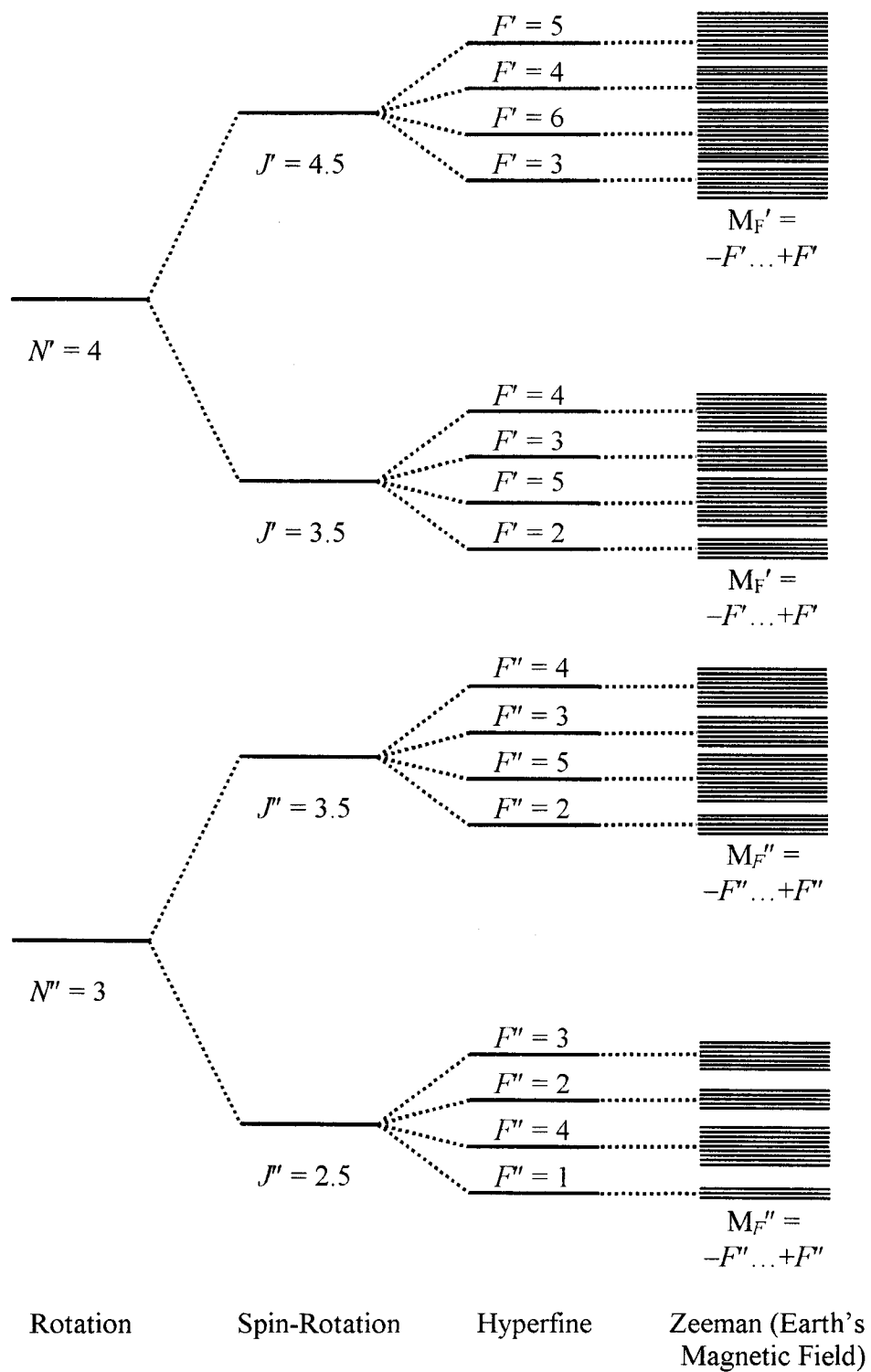


Figure 2.5 Schematic of energy level splittings due to spin-rotation, hyperfine and Zeeman effects in a $^2\Sigma^+$ state (energy separations not to scale). The selection rules are: $\Delta N = \pm 1$, $\Delta J = \pm 1$, $\Delta F = 0, \pm 1$ and $\Delta M_F = 0, \pm 1$.

As an example, modeling of the transitions between hyperfine levels of a $^2\Sigma^+$ state will be described further⁶. Energies of the hyperfine levels were first estimated by diagonalization of the full Hamiltonian matrix (of the form of Eq. 2.10) using trial values of the parameter set. The differences between relevant calculated energy levels were compared with experimental transition frequencies, and a sum of squares for all the data was determined. The value of each parameter is changed slightly, and the process was repeated until a convergence criterion was met, in this case, when the difference in the sum of squares was smaller than a set value.

All parameters given in this thesis will be accompanied by their respective 1σ uncertainties, determined using standard numerical methods outlined in Ref. [25].

2.7 Properties of the Molecular Parameters

If data are available for two or more vibrational levels of the same state, equilibrium parameters can be determined from

$$P_v = P_e + \alpha_p^v(v + \frac{1}{2}) + \gamma_p^v(v + \frac{1}{2})^2 + \dots \quad 2.12$$

where P_v and P_e are the vibrational (v), and equilibrium parameters (respectively), and α_p^v and γ_p^v describe⁷ the first and second order equilibrium vibrational dependence of parameter P , respectively. Equilibrium parameters for each individual state (including

⁶ Although the treatment of this matrix is similar to that employed in the characterization of $^2\Pi$ states or $^2\Pi \sim ^2\Sigma^+$ interactions, the actual matrix elements characterizing the hyperfine structure were diagonal in F and not J (as outlined in this chapter). Thus, the major difference will be that the Hamiltonian matrix in this case has n, v, F blocks (rather than n, v, J) and interactions between levels of different J are possible.

⁷ Also given as α_e^v and γ_e^v for the rotational parameter B .

the vibrational parameters ω_e and $\omega_e x_e$, not derived here) are dependent on physical attributes specific to the molecule and/or state. For example, the rotational parameter B_e is dependent on both internuclear distance⁸ (R_e) and the reduced mass (μ) of the diatomic molecule

$$B_e / \text{cm}^{-1} = \frac{h}{8\pi^2 c \mu R_e^2} \times 10^{-2}, \quad 2.13$$

where h is Planck's constant, and c is the speed of light in m/s.

A list of equilibrium parameters, and their associated mass relationships, is given in Table 2.4, while Table 2.5 shows the relationships between the hyperfine parameters and nuclear moments associated with the various isotopes [26].

Besides bond length (R_e), other useful properties can be derived from molecular parameters, such as the vibrational force constant (k_e) from the parameter ω_e , quantification of the ionic/covalent bond character from the parameter eQq , and the amounts of s and p orbital occupation at an $I > 0$ nucleus from the parameters b_F and c , respectively. It is this kind of determination of molecular properties that makes spectroscopy such an invaluable tool in understanding physical conditions at the molecular level.

⁸An equation analogous to 2.13 but using a B_v value leads to an effective R_v value for the vibrational level v .

Table 2.4

Dependence of parameters^a for ${}^2\Sigma^+$ and ${}^2\Pi$ states on reduced mass [26].

State symmetry	Parameter	Description	Mass dependence
${}^2\Pi$ & ${}^2\Sigma^+$	T_e	Electronic energy	
	ω_e	Vibrational energy	$\mu^{-1/2}$
	$\omega_e x_e$		μ^{-1}
	B_e $-\alpha_e$	Rotational energy	μ^{-1}
			$\mu^{-3/2}$
	D_e β_e or α_D	Centrifugal distortion	μ^{-2}
$\mu^{-5/2}$			
${}^2\Sigma^+$	γ_e	Spin-rotation	μ^{-1}
	α_γ		$\mu^{-3/2}$
	γ_D	Centrifugal distortion of spin rotation	μ^{-2}
	α_{γ_D}		$\mu^{-5/2}$
${}^2\Pi$	p_e	Λ -doubling	μ^{-1}
	α_p		$\mu^{-3/2}$
	q_e		μ^{-2}
	α_q		$\mu^{-5/2}$
	p_D	Centrifugal distortion of Λ -doubling	μ^{-2}
	α_{p_D}		$\mu^{-5/2}$
	q_D		μ^{-3}
	α_{q_D}		$\mu^{-7/2}$
	A_e α_A A_D α_{A_D}	Spin-orbit	$\mu^{-1/2}$
			μ^{-1}
Centrifugal Distortion of spin-orbit		μ^{-1}	
		$\mu^{-3/2}$	

^aAll α parameters defined as $X_v = X_e + \alpha_x(v + \frac{1}{2})$.

Table 2.5

Dependence of hyperfine parameters in a ${}^2\Sigma^+$ state on nuclear moments for nuclei with $I > 0$ [26].

State symmetry	Parameter	Description	Isotope Dependence
${}^2\Sigma^+$	b_F	Fermi contact	g_N
	c	Dipole-dipole	g_N
	C_I	Nuclear spin-rot.	$g_N \cdot \mu^{-1}$
	eQq	Quadrupolar coupling	Q

^aThe nuclear g -factor, g_N , is the ratio of the magnetic moment to the nuclear magneton; the quadrupole moment is given as **Q**.

Chapter 3

Experimental Arrangement

Three major components are used in the present experimental arrangements: a source of electromagnetic radiation, a source of radical molecule production in the gas phase; and a method of detection. The light sources used in the present work are either a single frequency ring dye laser, or a pulsed microwave source. Production methods include a low pressure Broida style oven or a pulsed laser ablation source. The detected electromagnetic radiation was converted to an electronic signal by employing either a spectrometer/photomultiplier tube (PMT) arrangement, a spectrometer/CCD array detector, or directly, from a microwave antenna in a Fourier transform arrangement. These systems proved extremely versatile for the present rotational studies, and will be discussed in some detail.

3.1 Methods of Production

3.1.1 The Broida Oven

West and co-workers developed a simple method of producing metal-containing gas phase molecules [27]. The apparatus was named after Broida, who proposed the original concept, and the general arrangement is shown in Figure 3.1.

The basic concept of the Broida oven is the reaction of an oxidant gas with a flow of metal vapour to produce the desired molecule. For example, when strontium is vaporized in a resistively heated alumina crucible (see Figure 3.1(i)), the metal is then

- a) Brewster Window
- b) Baffles
- c) Vacuum port
- d) Observation window
- e) Production/ observation area

- f) Oxidant inlet ring
- g) Chimney
- h) Argon carrier gas inlet ring
- i) Alumina crucible/ tungsten basket

- j) Inner jacket
- k) Outer jacket

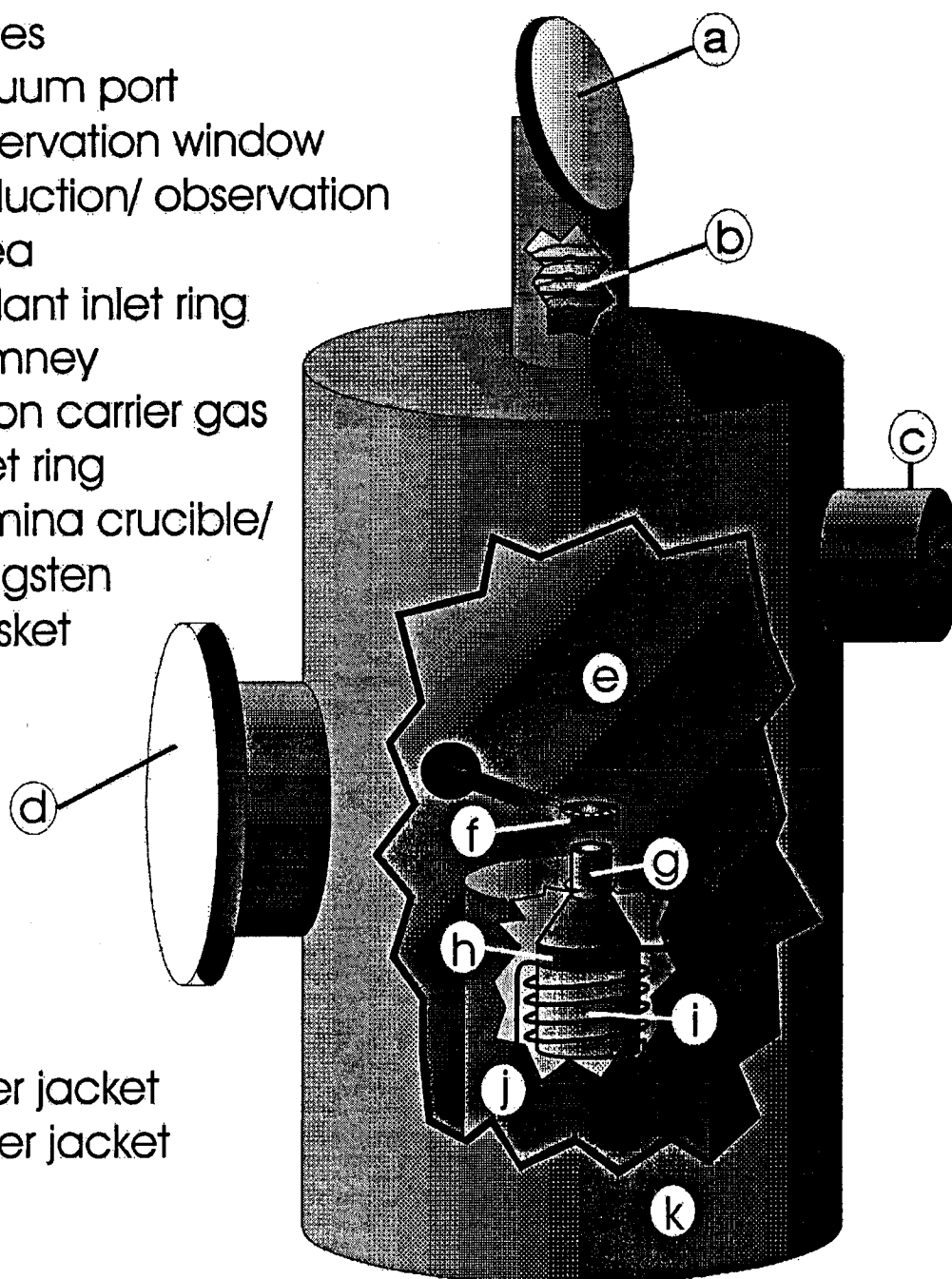


Figure 3.1 Diagram of a Broida oven.

entrained in a flow of argon gas and delivered to the observation chamber (see Figure 3.1 (e)), and reacted with methyl bromide to produce the desired molecule, in this case, SrBr.

The gas phase molecules can also be produced from a solid-state reaction of the metal with an appropriate salt. As was used herein for some of the YbBr work, a mixture of ytterbium metal and aluminum tribromide was heated inside the alumina crucible, and the desired diatomic was then entrained in an argon gas flow and carried into the observation area.

The reaction chamber of the oven is kept at pressures of 2-4 torr through the use of a mechanical pump. Employing such low-pressure flow systems reduces the contribution of pressure broadening to spectral line widths.

The laser beam is directed into the Broida oven through a Brewster window, and passes through a set of light baffles (see Figure 3.1 (a) and (b) respectively). Such baffles reduce the amount of scattered laser light within the observation area, thus reducing the background signal. The beam is focused into the centre of the observation chamber where laser induced fluorescence is detected perpendicular to the incident beam.

3.1.2 The Laser Ablation Source

Laser ablation in a supersonic jet is an effective way to produce neutral gas phase species. Two separate ablation sources were employed in the present work, one for the FTMW study of chapter 5, and one for the laser study of chapter 7. For the purposes of brevity, only the details of the FTMW ablation source are given, with the understanding that the other source will be nearly identical in design and function. All information

pertaining to this section, and the section concerning the FTMW spectrometer, were taken from the thesis of Dr. Kaley Walker [28].

A stainless steel chamber is mounted atop a differential pumping system to achieve a high vacuum of approximately 1×10^{-8} torr. As shown in Figure 3.2, a pulsed nozzle is mounted inside the chamber, and attached to a gas line containing argon at pressures of 5-6 atmospheres mixed with the appropriate oxidant (SF_6 , Cl_2 , and Br_2 or CH_3Br) in 0.05 % - 0.15 % quantities. A stainless steel housing is attached ~ 5 mm from the orifice of the pulsed nozzle. This guides a target metal rod (5mm ytterbium rod, *Goodfellow*, 99.9%) that is both translated and rotated so as to produce a fresh surface for each ablation laser pulse. The ablation is accomplished by directing the output from a Q-switched Nd:YAG laser system (*Continuum* Surelite I-10), operating at the second harmonic (532 nm), onto the rod through a quartz window on the chamber.

A time delay system is employed whereby the nozzle valve is triggered microseconds before the ablation pulse. This timing is adjusted to maximize the production of the desired molecule, and thus the signal.

There are both advantages and disadvantages to this method of production:

Doppler and pressure broadening in a supersonic expansion. Owing to the large difference between the backing pressure (~ 4500 torr) and the chamber pressure ($\sim 1 \times 10^{-8}$ torr), the molecules travel both supersonically and nearly uniformly in velocity. When probed perpendicular to the motion of travel, the molecular velocity towards and away from the detector is essentially zero, eliminating Doppler broadening. When probed parallel to the direction of travel in a microwave cavity, however, splitting of rotational

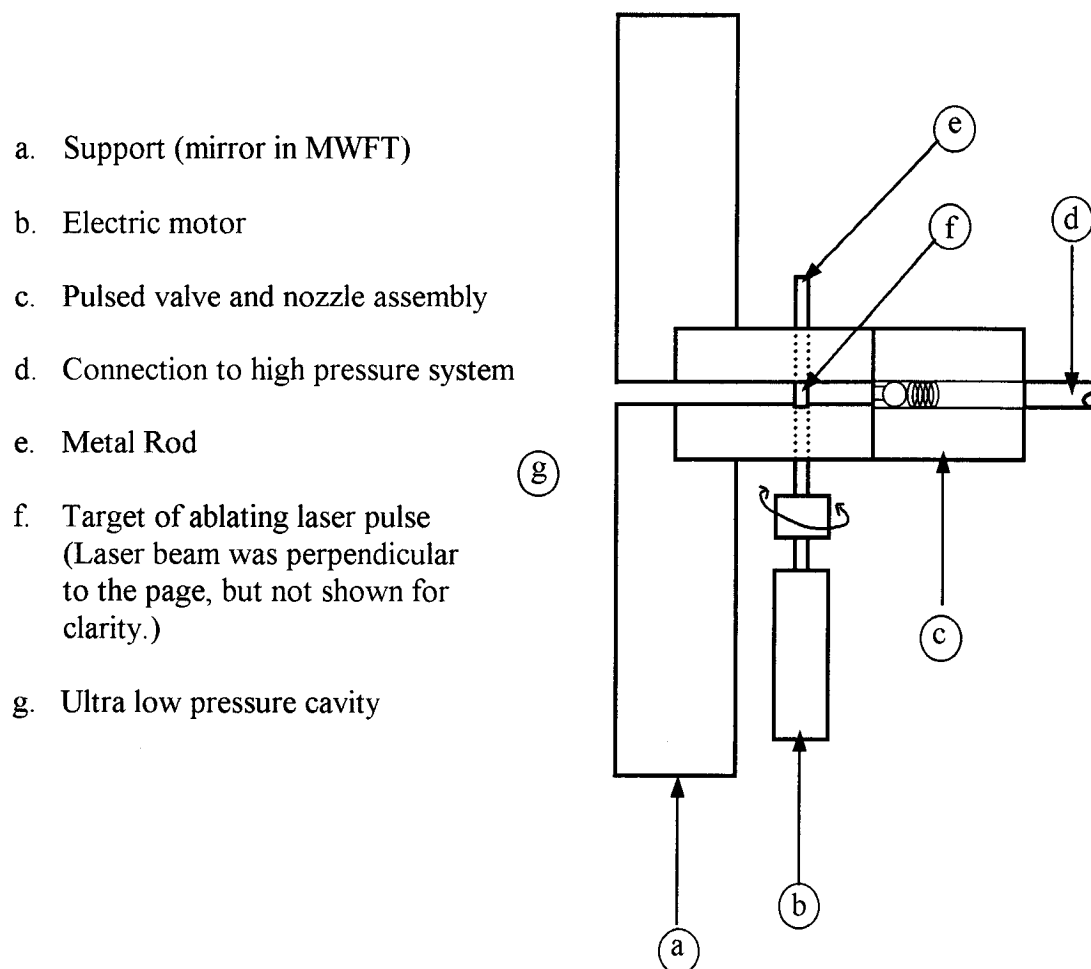


Figure 3.2 Diagram of pulsed ablation source, shown side-on, in a cut away view.

lines can be observed. This splitting arises from the molecular signal being detected both directly, and from reflection off of the opposing mirror. The low pressures inside the observation chamber eliminate most of the effects of pressure broadening. The reduction of line broadening effects is always advantageous in high-resolution studies.

Cooling of molecules in a supersonic expansion. The supersonic expansion creates a very low molecular temperature, which simplifies the spectra obtained using laser techniques. Conversely, when used in microwave spectroscopy, this effect serves as a hindrance to studying rotational motion in vibrational levels with $v > 0$. (Typical effective rotational and vibrational temperatures in the FTMW experiments are ~ 1 K and ~ 100 K respectively).

3.2 Laser Spectroscopy

3.2.1 Laser System

The source of continuous-wave laser light that is used in the present work is an argon ion (Ar^+) pumped ring dye laser [29]. The Ar^+ pump laser is a *Coherent Innova Sabre* (or an older *Innova 100*) which produces 6-8 W at 514 nm. This laser beam is directed into a *Coherent 699-29* ring dye laser. The ring configuration provides stability, and more importantly, the ability to scan the dye region (thus providing a continuous wavelength range of laser radiation). The scanning ability is obtained through the use of birefringent filters, as well as etalon type assemblies that ensure a bandwidth for the 699-29 laser of ~ 20 MHz. Typical single-frequency output power ranged from 30-400 mW, depending on the type of dye used, and the region being scanned. The general arrangement of the laser system is given in Figure 3.3.

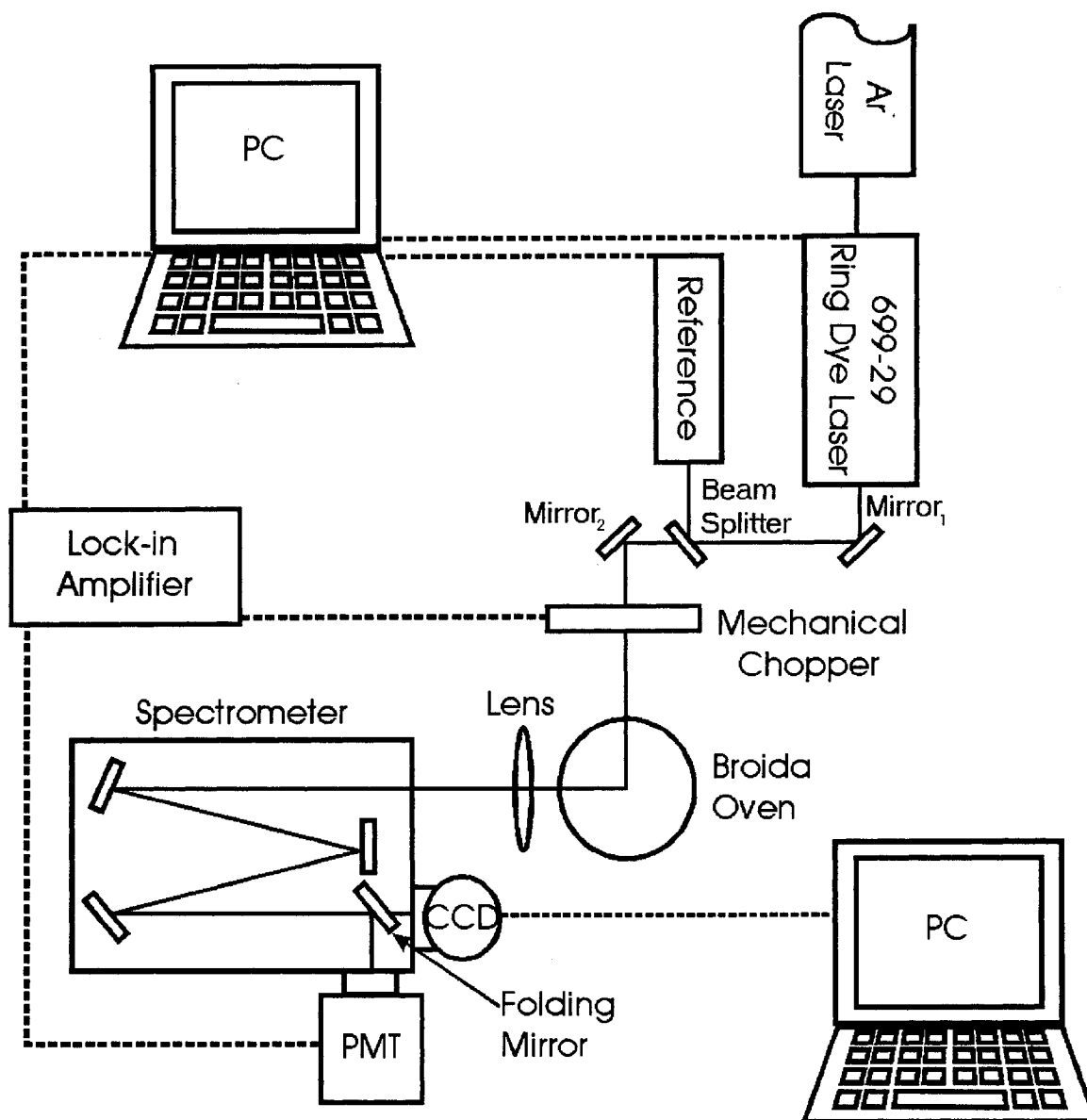


Figure 3.3 Arrangement of laser system, spectrometer, and CCD/PMT systems.

3.2.2 PMT Arrangement

Laser induced fluorescence dispersed with a SPEX 1.26 m spectrometer was detected using a GaAs photomultiplier tube detector (*RCA C31034A-02*) cooled to -20°C . By mechanically chopping the incident laser beam, background radiation was discriminated using a phase sensitive lock-in amplifier, and a reduction in the detection of unwanted chemiluminescence and ambient light was achieved. A desktop computer was used to control scanning of the ring dye laser system while recording three separate signals from the lock-in amplifier, an iodine reference cell, and an internal etalon. The iodine reference signal was produced by diverting $\sim 5\%$ of the incident laser beam into an iodine cell equipped with a second PMT. Although the *Coherent 699-29* ring dye laser has an internal wavelength meter, the iodine reference signal provided unequivocal wavelength assignments when compared with a standard iodine atlas [30]; the recommended offset [31] of -0.0056 cm^{-1} was applied.

3.2.3 PMT Detection Techniques: Selective Detection

Although the Broida oven greatly limits the variety of species produced within the reaction chamber, spectral density, or overlapping lines, can greatly complicate spectra. The selective detection method [32] utilizes the PMT arrangement described above, and is a technique designed to obtain a simplified spectrum. A common problem lies in the fact that in absorption experiments, more than one transition may come into resonance for a given frequency of laser light. The selective detection technique uses laser-induced fluorescence (LIF) as an indication that a particular absorbing transition is in resonance. That is, this technique utilizes the fact that absorption occurs at a given probe frequency,

while fluorescence occurs at a different frequency that is specific to the rotational and/or vibrational structure of the molecule. This eliminates detection of transitions between different states, or from different molecules. Two examples of the use of this method are as follows:

Selective Detection of an Individual Band

When using absorption techniques, there is often interference from either other molecules produced in the oven or ablation source, or from other absorptions within the desired molecule, but not from the system of interest. It is thus advantageous to spectrally discriminate against all other absorptions that may be detected simultaneously.

To facilitate this, the structure of an entire band is isolated when fluorescence is observed for an alternate band that shares the same upper vibrational level. For example, by probing the 0 – 0 band, and observing the fluorescence of the 0 - 1 band, all branches can be recorded with minimal obstructions. Although there are no selection rules for electronic-vibration transitions, the strength of the fluorescence transition, governed by the associated Franck-Condon factor [16], must be considered.

This technique allows for accurate measurements of bandheads, which can be invaluable in later rotational selective detection studies. Typically the slit width in this type of experiment is 500-800 μm , allowing for the detection of fluorescence across the entire band.

Selective Detection of Individual Branches

The detection of individual branches can be accomplished by the observation of a branch that shares the same upper rotational level as the excitation branch, but is in a

different spectral region. This different spectral region can either be within the same band or between bands.

The selection rules for rotational transitions between electronic transitions are $\Delta J = 0^1, \pm 1$. As Figures 2.3 and 2.4 illustrate, branches can be categorized into “groups” that share the same upper parity level. For example, it can be seen that P₁₁, R₁₁ and Q₁₂ branches in the $^2\Pi_{1/2} - ^2\Sigma^+$ system share the same upper level for a particular value of J' , but have different values of J'' in the lower state. By probing the R₁₁ branch, LIF can be detected in the corresponding P₁₁ branch, which is in a different spectral region. Care must be exercised, however, to maintain a spectral separation between the observation and excitation wavelengths so as not to observe scattered laser light.

The use of selective detection between bands gives very similar results, with two notable differences. First, there will be an isotope shift between bands that must be considered. This will cause a change in the intensity of the different isotopomers across the band, which, as described in Chapter 6, can aid in the assignment of rotational structure. Second, it is possible to observe both probe and detection branches within a given scan. For example, if the R₁ branch of the previous case were detected in the 0 – 1 band, both the P₁ and R₁ branches probed in the 0 – 0 band would be detected, as well as any other pair of branches that may be in the same spectral region. This second consideration can both aid and hinder the analysis in that the intensities of the two branches will reach a maximum at the same J' value making assignment of the branch structure easier, but if other branches are also detected, the spectra will be further

¹ $\Delta J = 0$ transitions do not occur when both states are $\Omega = 0$.

complicated. The measurement uncertainty of both selective detection techniques is estimated to be $\pm 0.004 \text{ cm}^{-1}$.

3.2.4 CCD Arrangement

A CCD array detector (*S.A. CCD-2000*, $15 \mu\text{m}$ pixel size) was cooled to -140°C , and the collected signal was sent to a computer station equipped with *Spectramax* data acquisition software. The array detector signal was integrated over times ranging from 5-300 seconds, depending on the intensity of the signal. The slit width was kept at $17 \mu\text{m}$ for all experiments of this nature, and the observed range of wavelengths is approximately 8 nm.

For calibration, a uranium spectrum is observed, and the wavelengths of measured lines are compared with those of the standard uranium atlas [33]. A second order fit of the measured versus known uranium line wavelengths is made, and applied to lines measured from the experimental spectra. From measurements of known spectra, an uncertainty of $\pm 0.02 \text{ cm}^{-1}$ is estimated.

3.2.5 CCD Detection Techniques: Resolved Fluorescence

Resolved fluorescence techniques involve maintaining the laser wavelength at a fixed value, while simultaneously utilizing the CCD array detector to observe fluorescence over an 8 nm range of wavelengths. Observation of both the excitation wavelength and the LIF is achieved concurrently, and is invaluable in the assignment of rotational numberings to the observed absorption transitions. As outlined in the work of Herzberg (16), if the energies (cm^{-1}) of two transitions sharing the same upper level are measured, the combination difference can be used to make a rotational assignment,

provided a fairly accurate value for B'' is known. Illustrated in Figures 2.3 and 2.4, and described using Table 2.1b, the separation between the R ($J' = J'' + 1$), and P ($J' = J'' - 1$) transitions will be approximately $4B''(J)$ (or $4B''(J + 1)$, depending on which parity levels are examined). In the absence of well-known B'' values, a plot of $\Delta\nu$ vs. J'' will produce a slope of $\sim 4B''$, and if the assignments of J'' are correct, an intercept close to zero.

There are two limitations to this technique, both of which stem from a lack of selectivity in fluorescence detection. The first drawback is the detection of unwanted background radiation, which includes ambient light and cosmic rays. Detection of the cosmic rays produces spikes, which increase in number with increased integration time. The second limitation is due to spectral overlap in the region under investigation. If several transitions are excited simultaneously, a multitude of overlapping fluorescence signals can be observed, as was evident in the study of the $A - X$ system of YbBr, and is discussed in more detail in Chapter 7.

Owing to the larger measurement uncertainty of this technique compared with laser excitation, the more accurate data from absorption spectra were used in least squares fits, and the less accurate resolved fluorescence data were only used to facilitate assignments.

3.3 Fourier Transform Microwave (FTMW) Spectroscopy

3.3.1 Microwave Cavity

The background information contained in this section can be found in Ref. [28]. A Fabry-Perot microwave cavity was located inside of a differentially pumped stainless

steel chamber. As shown in Figure 3.4, two aluminum mirrors (curvature: 38.4 cm, diameter: 28 cm) placed approximately 30 cm apart serve as the cavity, with one mirror manually adjusted to facilitate fine-tuning of the cavity length to a given microwave frequency. The microwave radiation was generated from a Hewlett-Packard 8340A synthesizer referenced to a continuous 10 MHz (Loran C) signal, accurate to 1 part in 10^{12} . This allowed the spectrometer to operate in the 4 to 26 GHz range. The ablation nozzle was mounted 2-3 cm off center of the stationary mirror, while the antenna was mounted in the center of the movable mirror. With a “parallel” configuration, such that the molecules and radiation are both moving in the same direction, each line appears as a doublet due to the antenna detecting both the forward and reflected Doppler shifted signals. The present configuration allows for a maximum observable spectral range of 1 MHz, which thus determines the *step-size* or searchable range. It can be seen from comparison of the step-size with the total range that good initial estimates of the line positions serve to greatly shorten the time taken to perform an experiment.

3.3.2 Microwave Detection and Signal Processing

A pulse generator connected to the various component systems controls the experimental sequence. As shown in Figure 3.5, this sequence involves initial sampling of the empty microwave cavity, followed by sampling after a molecular pulse. As indicated in Figure 3.6, a microwave signal is generated at a frequency of $\nu_{\text{MW}} + 20$ MHz. This signal is divided, with half used to generate the cavity pulse, and half used to modify the detected microwave signal into a radio frequency (r.f.) signal. The 20 MHz reference

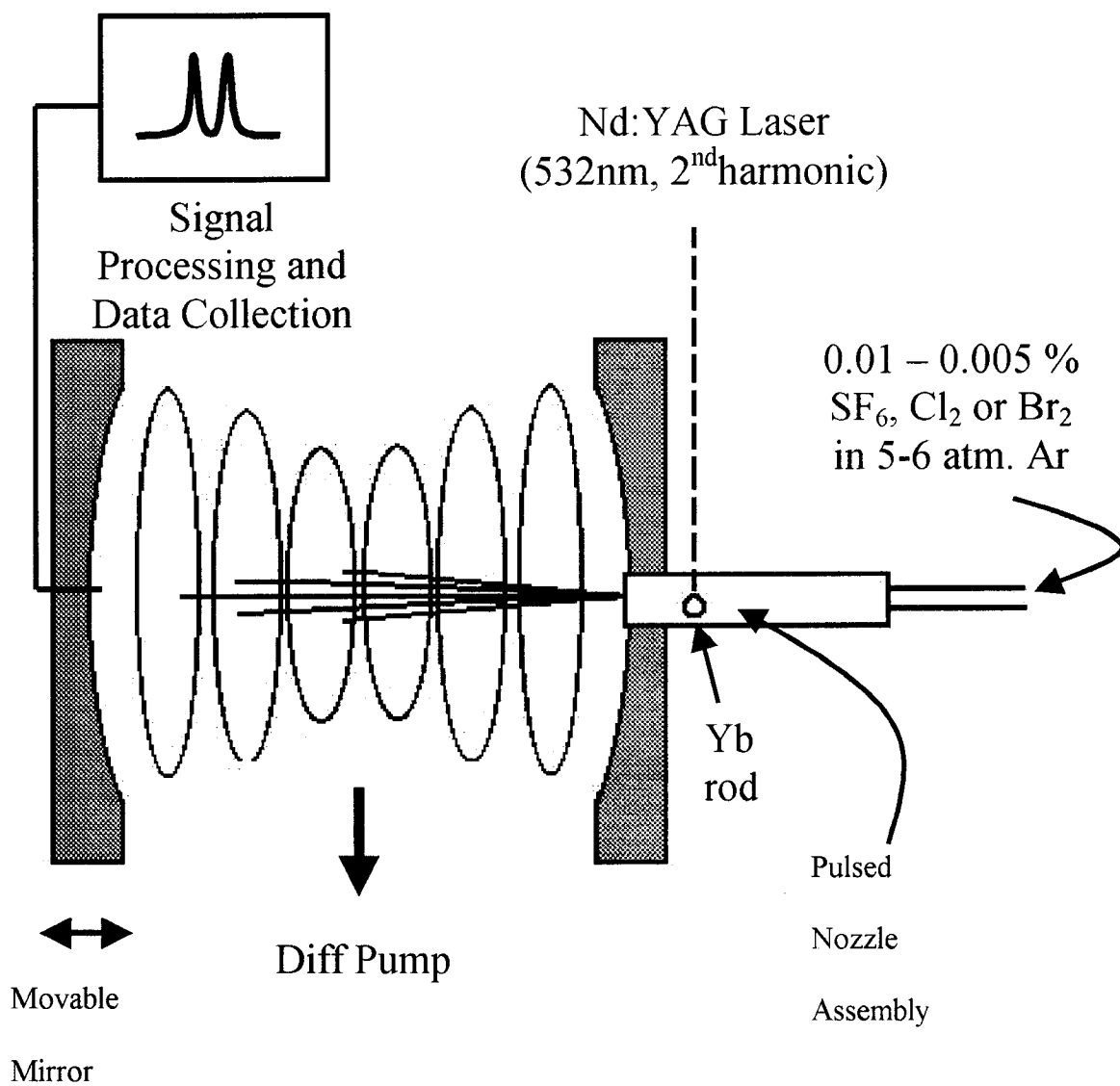


Figure 3.4 Schematic diagram of Fourier transform microwave spectrometer.

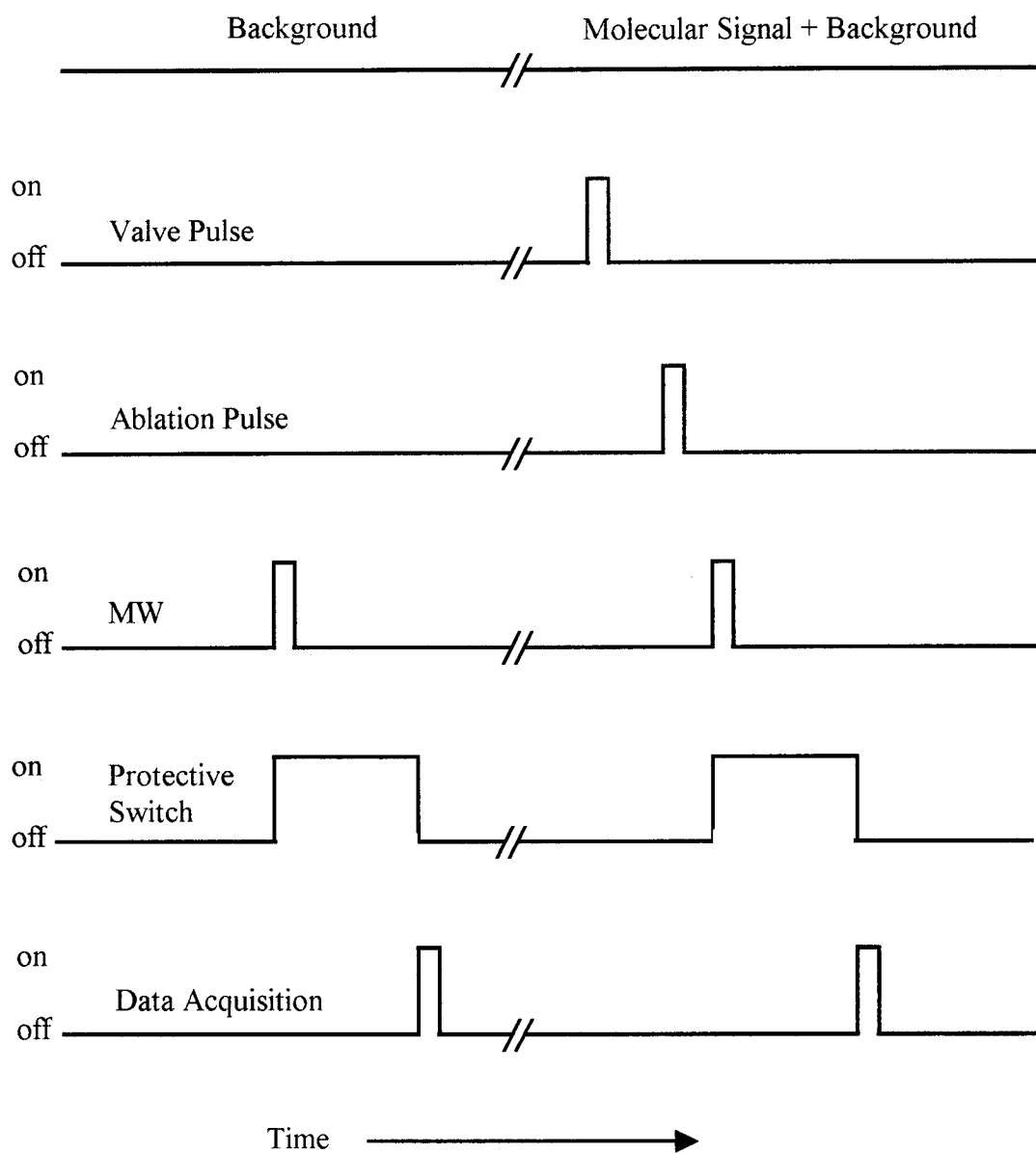


Figure 3.5 Pulse Sequence for FTMW arrangement [28].

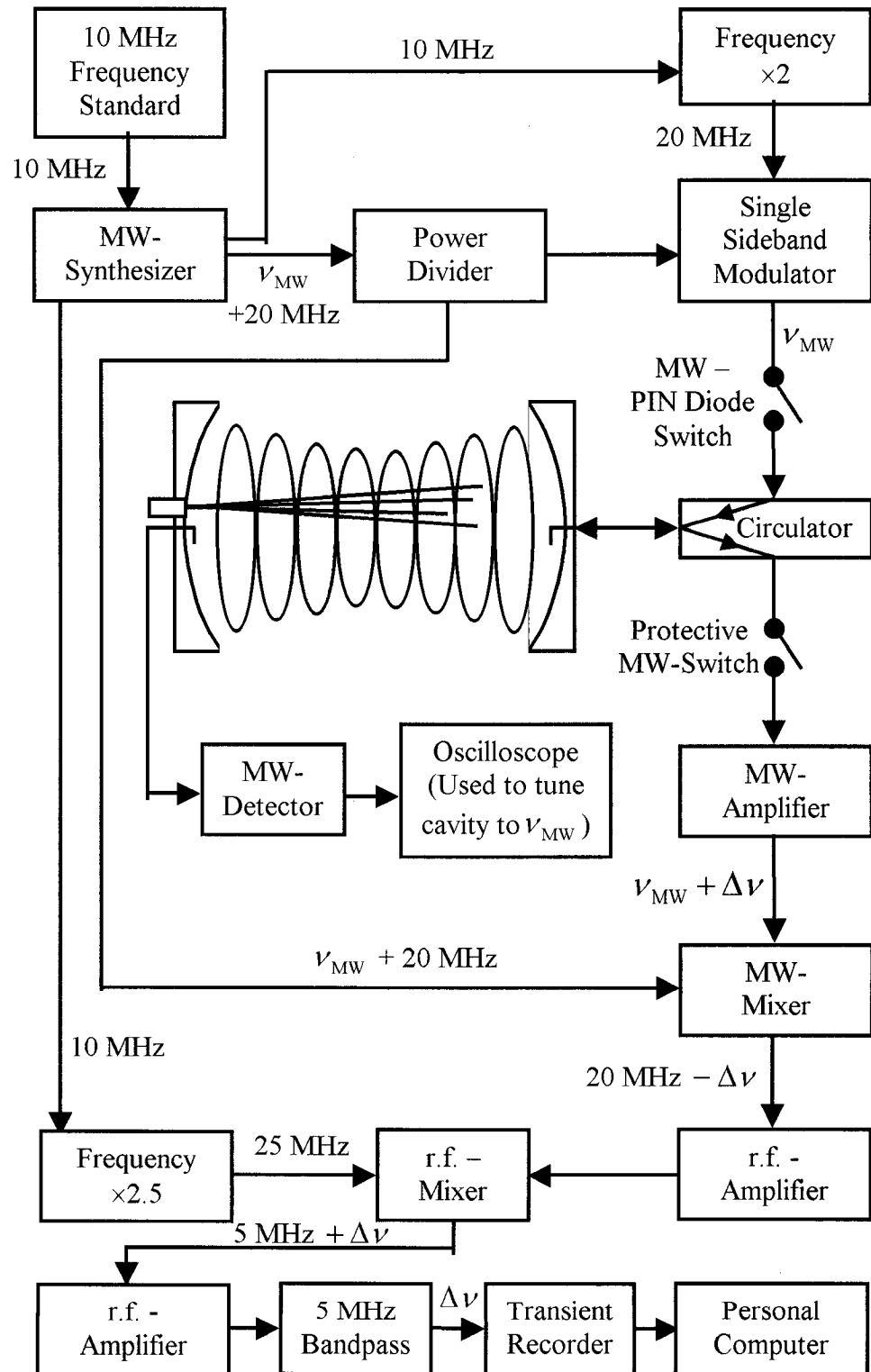


Figure 3.6 Diagram of microwave signal production and detection.

signal is subtracted from the pulse signal through the use of a single sideband modulator. This returns the pulse signal to the desired MW frequency in resonance with the cavity, and aids in the absolute frequency calibration. The detection antenna and amplifier is protected from being overloaded while the cavity is pulsed (shown in Fig. 3.5), and after a short period of time, the resonating free induction decay (FID) signal ($\nu_{\text{MW}} + \Delta\nu$) is collected and amplified (here, $\Delta\nu$ is the difference between the molecular resonance frequency and the pulse signal frequency). Through the use of a mixer, the $\nu_{\text{MW}} + 20$ MHz and $\nu_{\text{MW}} + \Delta\nu$ signals are subtracted, leaving only the r.f. $20 \text{ MHz} - \Delta\nu$ component. This is then amplified and mixed, as shown in Figure 3.6, to produce a signal that is $5 \text{ MHz} + \Delta\nu$. A 5 MHz r.f.-bandpass filter is used to produce the desired $\Delta\nu$ signal, and eliminate the spectral observation of higher frequency lines shifted to lower frequency, known as aliasing. The $\Delta\nu$ signal is sampled at a rate of 25 MHz using a transient recorder to produce 4000 data points per pulse. After the background is subtracted, FIDs from each pulse are co-added, to produce the time dependent spectrum.

3.3.3 Fourier Transform and FTMW Spectral Characteristics

The collected time-dependent signal is transformed to the frequency domain using the Fourier algorithm:

$$F(\nu) = \sum_{n=0}^{N-1} f(n\Delta t) e^{-i2\pi\nu n\Delta t},$$

where $f(n\Delta t)$ is the time domain signal, n is the number of data points sampled at intervals of Δt , and ν is the signal ($\nu_{\text{MW}} + \Delta\nu$). The resultant power spectrum is obtained by summing the squares of the real and imaginary parts of the Fourier

transform. This spectrum, as shown in Figure 3.7, consists of the two Doppler components with line widths of the order of 7-10 kHz. It can also be shown that the resolution of the frequency dependent signal is directly proportional to the acquisition time. In the place of longer acquisition times, a technique called “zero-filling,” whereby zeros are added to the end of the time-dependent FID, was employed in the present experiments, which artificially enhanced the digital resolution [34].

Owing to both the paramagnetic character of the molecules under study, and the high resolution of the technique, first order Zeeman splittings due to the earth’s magnetic field were observed for several of the spectra. Fig. 3.7a illustrates the effect that Helmholtz coils had in reducing these splittings, while Fig. 3.7b shows the same transition, but with the effects of Zeeman splitting present for this parallel $\Delta M_F = 0$ transition. The Helmholtz coils consisted of three mutually perpendicular coils surrounding the pumping chamber. A current is passed through the coils, and through careful physical alignment, the magnetic fields produced by the coils negate the effects of the earth’s magnetic field. This causes the components to collapse to the field-free position, although slight imperfections in the coils allow several magnetic components to be seen in the line profile. Several transitions were subject to a perpendicular ($\Delta M_F = \pm 1$) Zeeman effect, which caused their components to be shifted from their field-free position more than the cavity width. Accordingly, the transition frequencies were all obtained with the Helmholtz coils turned on. The outer horns of the resulting profile were typically separated in frequency by the Doppler splitting, and thus the unsplit line frequency was taken as the average of the horn frequencies. The uncertainty of line measurements is estimated as ± 5 kHz.

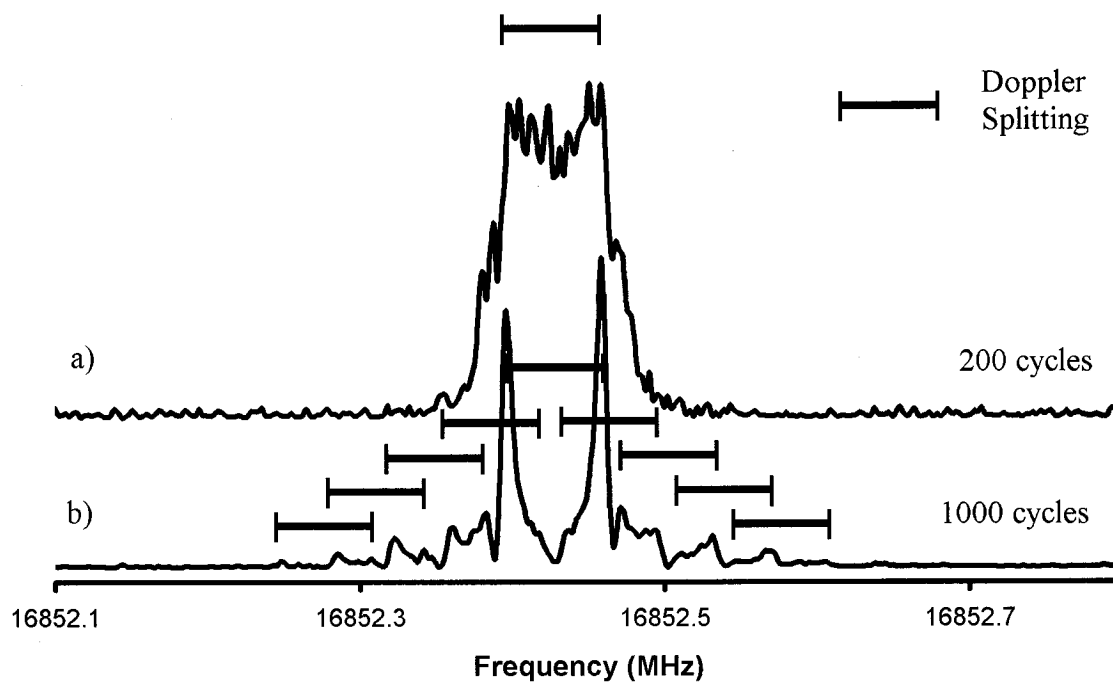


Figure 3.7 Overlaid spectra of the $N = 3 \leftarrow 2$, $J = \frac{7}{2} \leftarrow \frac{5}{2}$, $F = 5 \leftarrow 4$ transition of $^{174}\text{Yb}^{35}\text{Cl}$. The upper spectrum is with the Helmholtz coils on showing the magnetic components collapsed, while the lower spectrum has the coils off, showing splitting into $2F+1$ components in the presence of the earth's magnetic field. (0.01% Cl_2 in 5-6atm of Ar).

Chapter 4

The $A^2\Pi \sim B^2\Sigma^+$ Interaction in SrBr

4.1 Background

The low-lying electronic states of the alkaline earth metal halides (MX) have been the focus of numerous spectroscopic studies in recent years, with the work of Refs. 2-5,32,35,36 being a few relevant examples. In many cases, the MX species were created in the gas phase using an oven arrangement, and by taking advantage of their strong visible absorptions, they were usually probed with the output of a CW dye laser.

The first spectroscopic study of strontium bromide was a vibrational analysis of the $A - X$ system in 1931 by Hedfeld [37]. A later study by Harrington [38] showed that the $A^2\Pi_{3/2}$ sub-state assigned in Hedfeld's work was in fact the $B^2\Sigma^+$ state. As summarized in Herzberg and Huber [39], analyses of vibrational transitions in several systems ($\Theta - X$, where $\Theta \equiv A, B, C, D$ and E) have been carried out using both emission and absorption techniques. In 1985 Törring *et al.* [40] analyzed the pure rotational spectra of vibrational levels with $\nu \leq 3$ in the $X^2\Sigma^+$ state, while concurrently, Schröder and Ernst [2] vibrationally analyzed several bands of the $B - X$ system, and rotationally characterized the $0 - 0$, $1 - 1$, and $2 - 2$ bands. Perturbations observed in the $B^2\Sigma^+$ state were noted in Ref. [2], and when analyzed one year later [3], were believed to occur as a result of level crossings with $\nu_A = \nu_B + 3$ vibrational levels of the $A^2\Pi_{1/2}$ sub-state. In 1998, the first rotational analysis of the $0 - 0$ and $1 - 0$ bands of the $A - X$ system was reported [4].

The aim of the study presented in this chapter was to extend the $A - X$ data reported previously [4] to include levels with $v_A \geq 2$, and to describe in more detail the perturbing interactions between the A and B states. SrBr is particularly interesting in that transitions from both levels involved in a crossing can be sampled directly. A model Hamiltonian describing perturbing interactions between levels of the $A^2\Pi$ and $B^2\Sigma^+$ states was employed in order to describe the level crossings between these states. Characterizations of such interactions have been successfully undertaken for numerous other species, such as that for the CN radical [41].

4.2 Theory

A procedure for determining the matrix elements required to model such level crossings has been described previously by Zare et al. [20]. Distant 2nd order interactions between $^2\Pi$ and $^2\Sigma^+$ states can usually be treated adequately using the Van Vleck transformation. The block diagonal¹ matrix elements contain the parameters p_v , q_v and γ_v , and, employing the Hund's case (a) basis set, they are defined as [20]:

$$p_v^{n^2\Pi} = 4 \sum_{n'v'} \frac{\langle n^2\Pi vJ | \frac{1}{2} A(r) L_+ | n'^2\Sigma^+ v'J \rangle \langle n^2\Pi vJ | B(r) L_+ | n'^2\Sigma^+ v'J \rangle}{E_{nvJ} - E_{n'v'J}}, \quad 4.1$$

$$q_v^{n^2\Pi} = 2 \sum_{n'v'} \frac{\langle n^2\Pi vJ | B(r) L_+ | n'^2\Sigma^+ v'J \rangle^2}{E_{nvJ} - E_{n'v'J}}, \quad 4.2$$

and
$$\gamma_v^{n^2\Sigma^+} = 4 \sum_{n'v'} \frac{\langle n'^2\Pi v'J | \frac{1}{2} A(r) L_+ | n^2\Sigma^+ vJ \rangle \langle n'^2\Pi v'J | B(r) L_+ | n^2\Sigma^+ vJ \rangle}{E_{nvJ} - E_{n'v'J}}. \quad 4.3$$

¹ i.e. elements that are diagonal in n and v .

When levels of the ${}^2\Pi$ and ${}^2\Sigma^+$ states are nearly degenerate (or cross), the perturbation theory proposed by Van Vleck breaks down, and the energy difference, $E_{n'v'} - E_{n''v''}$, approaches zero. In order to describe a situation where *local* level crossings exist, the interaction between the two levels must be characterized by directly employing matrix elements off-diagonal in n' and v' . The effects of a single n' , v' term are expressed in terms of the two parameters², α and β , and are thus not folded into the p_v , q_v and γ_v parameters. This changes the definition of the parameters p_v , q_v and γ_v slightly, as the effect of the crossing n' v' term is removed from the summation. As illustrated in Table 2.2, a 3×3 matrix for each parity component is required to accurately characterize a single level crossing.

As discussed in more detail later in this chapter, this treatment can be extended to include a *global* characterization of the interactions between distant non-crossing levels, as was performed previously [5].

4.3 Experimental Arrangement

As outlined in chapter 3, SrBr molecules were produced in a Broida oven, using methyl bromide as the oxidant, and argon as the carrier gas of strontium vapour. Oven pressures were typically 3-5 torr, and both chemiluminescence, and strong laser induced fluorescence were observed. A *Coherent 699-29* ring dye laser using DCM dye, and pumped by a *Coherent Innova Sabre* argon ion laser, was used to probe the molecules.

Resolved fluorescence spectra were recorded using the CCD arrangement, also described in chapter 3, and integration times were typically between 30 and 300 seconds.

²Also labeled as $\alpha_{v_a-v_b}$ or $\beta_{v_a-v_b}$, in accordance with the particular interaction.

The use of resolved fluorescence spectra was essential in providing unequivocal assignment of the spectral lines, particularly those closest to the level crossings.

4.4 Results

Line positions in the 2 – 1, 3 – 2 and 4 – 3 bands of the $A \leftarrow X$ system were obtained for both the $^{88}\text{Sr}^{79}\text{Br}$ and $^{88}\text{Sr}^{81}\text{Br}$ isotopomers. All line positions, and their associated least squares fit residuals, are available in Appendix I. Owing to the small values of the rotational parameters B_v , lines were observed over a wide range of J -values ($J \leq 100$), though the majority of fitted line positions were in the range of $J = 30 - 80$. Attempts were made to record spectra for bands in the $\Delta v = 0$ and 2 sequences. Unfortunately low laser power for the $\Delta v = 0$ sequences, and overlap of the $\Delta v = 2$ sequences with the more Franck-Condon favored $B - X \Delta v = -1$ sequences, precluded any success in these attempts.

As shown in the Fortrat diagram in Figure 4.1, extensive spectral overlap occurs for all six branches in the $A^2\Pi_{3/2} \leftarrow X^2\Sigma^+$ sub-bands, with similar congestion existing in the $A^2\Pi_{1/2} \leftarrow X^2\Sigma^+$ sub-bands. The use of selective detection often made possible simplification of the spectra by removing both unwanted branch and band structures, and was frequently successful in discriminating between the two isotopes of bromine, despite band origin differences of only $\approx 1.5 \text{ cm}^{-1}$. This technique, however, was not completely successful, and blended lines with residuals greater than 0.012 cm^{-1} ($\approx 3\sigma$) were excluded from the final fits.

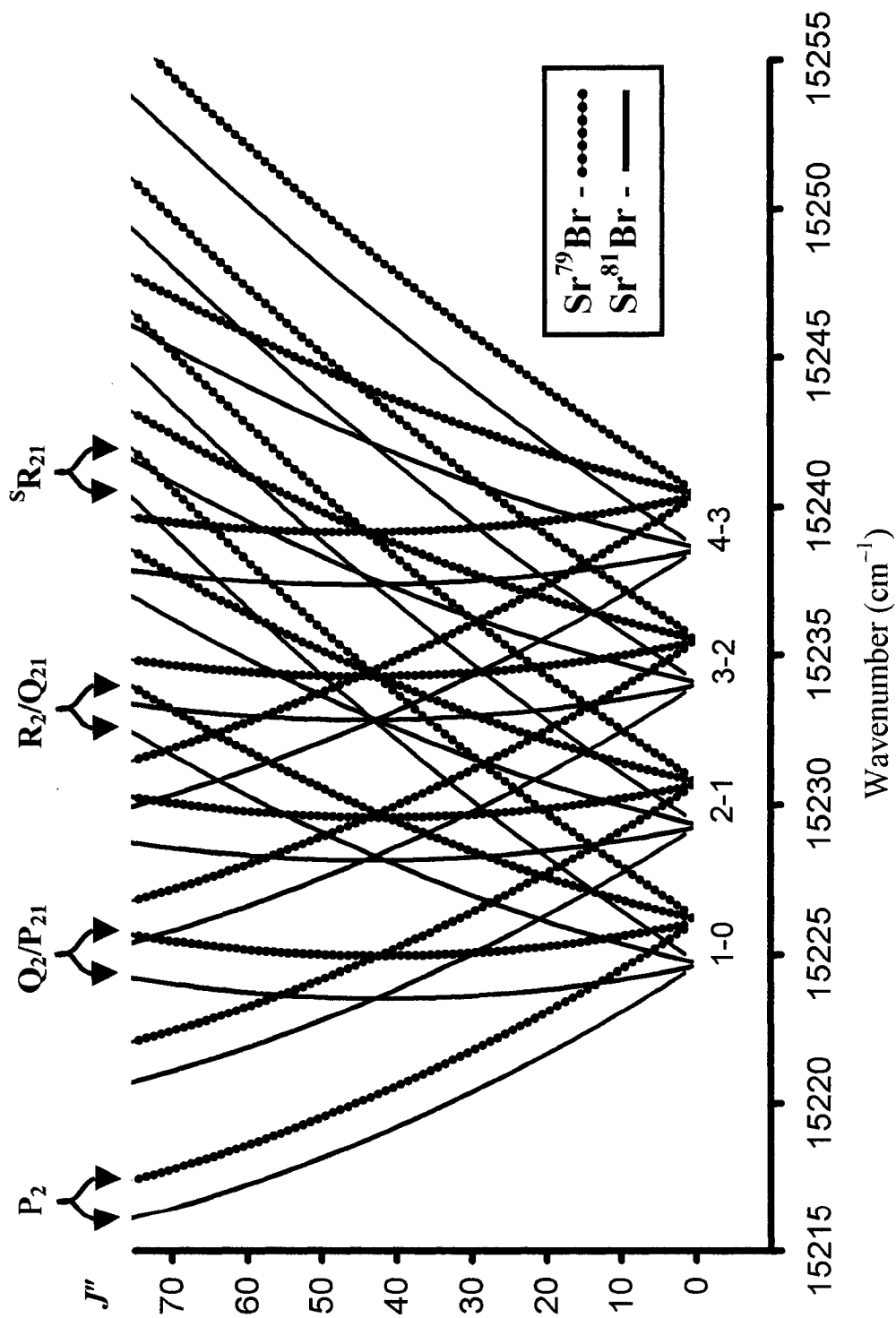


Figure 4.1 Fortrat Diagram of observed $\Delta v = +1$ bands in the $A^2\Pi_{3/2} - X^2\Sigma^+$ system of SrBr.

A non-linear least squares eigenvalue fitting routine was employed for the determination of molecular parameters. In order to properly describe the interaction between crossed levels of the $A^2\Pi(\nu + 3)$ and $B^2\Sigma^+(\nu)$ levels, the 3×3 Hamiltonian matrix described above was employed. A labeling convention for two bands involved in an $A \sim B$ level crossing is given as $[\nu_A - \nu_X^A] \sim [\nu_B - \nu_X^B]$, as fits of the $[3 - 2] \sim [0 - 0]$ and $[4 - 3] \sim [1 - 1]$ band pairs required a model that accounts for the two different levels in the ground state separately. The standard expressions of Table 2.1(b), for a $^2\Sigma^+$ state were employed for both levels (ν_X^A and ν_X^B) of the ground state. The difference between these ground state levels was labeled as ν_o^X , the value of which was determined in the least squares fits of the data. As there is no level crossing in the $\nu_A = 2$ level, the $2 - 1$ band was much simpler to characterize. The Hamiltonian matrix describing the upper state was the standard 2×2 matrix for a $^2\Pi$ state, given in Table 2.1(a), and did not include any level crossing interactions with the neighboring B state.

Fits that employed either the homogeneous parameter (α), or the heterogeneous parameter (β), were equally successful and produced parameters that represented the line positions within their estimated uncertainties in three of the four deperturbation fits ($[3 - 2] \sim [0 - 0]$ for $^{88}\text{Sr}^{79}\text{Br}$ and $^{88}\text{Sr}^{81}\text{Br}$, and $[4 - 3] \sim [1 - 1]$ for $^{88}\text{Sr}^{79}\text{Br}$). A fit of the $^{88}\text{Sr}^{81}\text{Br}$ $[4 - 3] \sim [1 - 1]$ crossing that converged was possible only when the homogeneous parameter (α) was employed to describe the interaction. This may be due to either the inadequacy of a purely heterogeneous model, or the situation in which the levels “cross” *prior* to the band origin (i.e. at $J < 0$), such that the data required to fit the β -parameter alone is unobtainable. Fits that allowed both parameters to be varied

independently failed to converge in all cases, most likely because of the high degree of correlation between α , β , A_v , and the band origins, as mentioned in Ref. [32]. Finally, fixing the parameter β to the value $\beta = \alpha(B_v / A_v)$, which was adopted in previous work [32] on CaI, was not employed here as the A and B states of SrBr cannot be described using a pure precession model, as outlined in Ref. [17].

All fitted parameters and their associated standard errors are listed in Table 4.1. Since the data for the $A - X$ and $B - X$ transitions have approximately the same accuracy ($\sim 0.004 \text{ cm}^{-1}$), weighted fits were not necessary. The observation of lines with high J values (≤ 100) made possible more accurate estimates of the distortion parameters than those found in previous work [4]. The average standard deviation for the fits was 0.0044 cm^{-1} , which lends testimony to both the reliability of the assignments for all of the bands, as well as the use of an adequate model to describe the perturbations.

4.5 Discussion

4.5.1 Extra Lines

As described above, simultaneous fits of the $A - X$ and $B - X$ data sets were employed to deperturb the level crossings between the B ($\nu = 0, 1$) and A ($\nu = 3, 4$) states. In preliminary fits, it became quite evident that some line positions in the $B - X$ data set [2], particularly those that involved the most perturbed rotational levels, had anomalously large errors and it was thus necessary to exclude such lines in subsequent fits. The present section provides an explanation and revised assignments for these erroneous line positions.

Table 4.1

Fitted parameters^a (cm⁻¹) for the $A^2\Pi \leftarrow X^2\Sigma^+$ and $B^2\Sigma^+ \leftarrow X^2\Sigma^+$ systems of $^{88}\text{Sr}^{79}\text{Br}$ and $^{88}\text{Sr}^{81}\text{Br}$.

		$^{88}\text{Sr}^{79}\text{Br}$			
$B - X_B$		0 - 0	1 - 1		
$B^2\Sigma^+$	ν_o^{Bb}	14925.580(5)	14932.997(3)		
	B_v	0.0552018(4)	0.0550072(6)		
	$10^8 D_v$	1.365(5)	1.357(9)		
	γ_v	-0.10172(2)	-0.10175(3)		
	$10^8 \gamma_{Dv}$	9.6(4)	11.2(7)		
$X_B^2\Sigma^+$	ν_o^{Xb}	-430.213(5)	-428.160(3)		
	B_v	[0.0540934]	[0.0539110]		
	$10^8 D_v$	[1.35617]	[1.35569]		
	γ_v	[0.002159647]	[0.002146278]		
	$10^9 \gamma_{Dv}$	[1.18]	[1.18]		
$A - X_A$		2 - 1	3 - 2	4 - 3	
$A^2\Pi$	ν_o^{Ab}	15079.643(2)	15084.187(1)	15088.683(1)	
	B_v	0.0545419(8)	0.0543540(7)	0.0541692(6)	
	$10^8 D_v$	1.359(9)	1.349(10)	1.349(7)	
	A_v	302.399(3)	302.379(1)	302.355(2)	
	$10^5 A_{Dv}$	-4.91(8)	-4.87(6)	-4.96(5)	
	p_v	-0.10084(6)	-0.10084(6)	-0.10079(5)	
	$10^8 p_{Dv}$	4.1(21)	5.6(17)	9.4(13)	
	$10^5 q_v$	8.6(7)	9.1(7)	7.9(6)	
	$X_A^2\Sigma^+$	B_v	[0.0539110]	[0.0537288]	[0.0535470]
		$10^8 D_v$	[1.35569]	[1.35521]	[1.35474]
γ_v		[0.002146278]	[0.002132909]	[0.002119540]	
$10^9 \gamma_{Dv}$		[1.18]	[1.18]	[1.18]	
$A \sim B$	α	-	0.1950(12)	0.3777(9)	
	N	156	507	409	
	$\hat{\sigma}$	0.0047	0.0044	0.0041	

Table 4.1. (con't)

$B - X_B$		$^{88}\text{Sr}^{81}\text{Br}$		
		0 - 0	1 - 1	
	v_o^{Bb}	14928.393(6)	14935.685(23)	
$B^2\Sigma^+$	B_v	0.0544846(4)	0.0542946(7)	
	$10^8 D_v$	1.340(5)	1.356(11)	
	γ_v	-0.10042(2)	-0.10031(5)	
	$10^8 \gamma_{Dv}$	9.9(4)	7.7(9)	
	v_o^{Ab}	-427.379(6)	-425.415(22)	
$X_B^2\Sigma^+$	B_v	[0.0533902]	[0.0532113]	
	$10^8 D_v$	[1.32113]	[1.32063]	
	γ_v	[0.002126428]	[0.002113444]	
	$10^9 \gamma_{Dv}$	[2.32]	[2.32]	
	$A - X_A$	2 - 1	3 - 2	4 - 3
$A^2\Pi$	v_o^{Ab}	15078.153(2)	15082.681(1)	15087.162(1)
	B_v	0.0538338(10)	0.0536516(6)	0.0534695(8)
	$10^8 D_v$	1.278(14)	1.287(9)	1.297(9)
	A_v	302.397(2)	302.383(1)	302.356(2)
	$10^5 A_{Dv}$	-4.95(6)	-5.11(5)	-4.94(6)
	p_v	-0.09928(6)	-0.09903(6)	-0.09947(6)
	$10^8 p_{Dv}$	1.0(16)	4.1(15)	8.3(13)
	$10^5 q_v$	7.9(10)	9.1(7)	7.2(7)
	B_v	[0.0532113]	[0.0530327]	[0.0528545]
	$10^8 D_v$	[1.32063]	[1.32013]	[1.31963]
$X_A^2\Sigma^+$	γ_v	[0.002113444]	[0.002100445]	[0.002087446]
	$10^9 \gamma_{Dv}$	[2.32]	[2.32]	[2.32]
$A \sim B$	α	-	0.1843(14)	0.3815(34)
	N	162	523	388
	$\hat{\sigma}$	0.0050	0.0042	0.0040

^aEstimates of one standard error are given in parentheses in units of the least significant digit of the corresponding parameter. Ground state parameters (in square brackets) were constrained to the values obtained in Ref. (40). N denotes the number of measured line positions included in each fit, and $\hat{\sigma}$ denotes the standard deviation of each fit (given in cm^{-1}).

^bAll band origins are referenced to the $X_A^2\Sigma^+$ state.

In the previous deperturbation analysis for the $B \leftarrow X$ transition by Ernst and Schröder [3], several of the perturbing A state parameters were held fixed, including the spin-orbit parameter A_v to the value reported in Ref. [39], the Λ -doubling parameter p_v ($v_A = 3,4$) to the corresponding B state spin-rotation parameter γ_v ($v_B = 0,1$), and q_v , which was determined using the relationship between p_v and q_v given in Ref. [17]. Using the $B - X$ ($0 - 0$) data sets, and fixing the B and X state parameters to the values in Ref. [2], Ernst and Schröder [3] were then able to fit the parameters v_{3-0}^{Π} , B_3^{Π} , and α_{3-0} for both isotopomers. Similarly, a fit of the $B - X$ ($1 - 1$) band for $^{88}\text{Sr}^{79}\text{Br}$ gave estimates of v_{4-1}^{Π} , B_4^{Π} , B_1^{Σ} , α_{4-1} and the heterogeneous parameter β_{4-1} . Although estimates of these parameters were close to the values determined in the present work, with differences determined to be 0.4 – 3.0 % (except for β_{4-1} , which was not considered in the present work), small changes in their values have a large effect on calculated rotational levels nearest the crossing point. By fixing the aforementioned parameters, the previous study [3] “restricted” the calculated positions of the perturbed rotational levels such that spectral lines at the crossing point could easily be misassigned. Ernst and Schröder’s [3] inclusion of these misassigned lines may explain the necessity to employ the parameters β_{4-1} and B_1^{Σ} in fits describing the $A(v_A = 4) \sim B(v_B = 1)$ interaction. Once these “erroneous” lines were excluded from the $B - X$ data sets, alternate assignments were sought.

As is well known [17], it is expected that the intensities of rotational lines are affected by mixing with neighboring states. In the case of a level crossing, this can result in the enhancement of rotational structure that may otherwise be unobservable; the

presence of “extra lines” in the spectrum is the consequence. Extra line positions in the enhanced $A - X_B$ system were calculated and compared to the erroneous lines with much success; the results are presented in Table 4.2. It is evident that the combination differences for both the previous and present assignments are equal, thus adding credence to these changes of assignment. The newly assigned lines, where indicated in Table 4.2, were subsequently included in the final fits, and agree with the calculated positions within the experimental uncertainty. The single line found for the $^{88}\text{Sr}^{81}\text{Br}$ isotopomer was not included in the final fit, as the assignment could not be determined unequivocally. Similarly, because extra lines in the present $A - X_A$ spectrum were only tentatively identified, they were not included in the final fits.

4.5.2 Interactions Between the $A^2\Pi$ and $B^2\Sigma^+$ states: Level Crossings, $^2\Pi$ state Λ -doubling and $^2\Sigma^+$ State “Spin-Rotation.”

As described previously [17], interactions between $^2\Pi$ and $^2\Sigma^+$ states can be observed either as *local* perturbations, such as a level crossing, or as *global* effects, as evident by Λ -doubling in the $^2\Pi$ state and “spin-rotation” splittings in the $^2\Sigma^+$ state. The *global* “effects” are usually described for each level separately using parameters defined through the Van Vleck transformation [20], namely p_v and q_v for $^2\Pi$ states, and γ_v for $^2\Sigma^+$ states (see Eqs. 4.1, 4.2 and 4.3). An alternate approach to the Van Vleck transformation, is to diagonalize the full $^2\Pi \sim ^2\Sigma^+$ Hamiltonian matrix, with off-diagonal matrix elements describing the interactions included explicitly. The form of these matrix elements are identical to those used to describe level crossings, as given in Table 2.2, but

Table 4.2
Calculated and observed extra lines (cm^{-1}) in the spectra of SrBr.

Isotopomer	Assignment ^a	Line Position (Calc.) ^b	Line Position (Exp.) ^c	$\Delta\nu$ (Exp. - Calc.)
⁸⁸ Sr ⁷⁹ Br	<i>B - X</i> (0-0)	15355.084 ^d		0.385
	<i>A - X</i> (3-0)	15255.471	15355.467	-0.004
	<i>B - X</i> (0-0)	15363.622 ^d		0.388
	<i>A - X</i> (3-0)	15364.009	15364.008	-0.001
	<i>B - X</i> (1-1)	15360.060 ^d		0.761
	<i>A - X</i> (4-1)	15360.816	15360.821	0.005
	<i>B - X</i> (1-1)	15365.555 ^d		0.759
	<i>A - X</i> (4-1)	15366.311	15366.314	0.003
⁸⁸ Sr ⁸¹ Br	<i>B - X</i> (0-0)	15358.859 ^d		0.048
	<i>A - X</i> (3-0)	15358.907 ^d	15358.907	0.000

^aAssignments for the *B - X* system made in Ref. [2]; Proposed assignments of extra lines for the perturbation enhanced *A - X* system.

^bCalculated line positions based on the parameters given in Table 4.1.

^cExperimental line positions from Ref. [2].

^dLine not included in fit.

a much larger matrix is thus required to account for the multitude of interactions with neighboring vibrational levels. A simultaneous characterization of both the *local* and the *global* effects can thus be accomplished by employing off-diagonal matrix elements between both degenerate and non-degenerate vibrational levels of the *A* and *B* states. It was hoped that the various α and β parameters from each off-diagonal interaction (either as crossings or from distant interactions), could be described using only the purely electronic parameters α_{AB} and b_{AB} .

Global deperturbation analyses have been carried out previously for several diatomic alkaline earth metal halides, CaI [32], CaF [5], CaCl [35], and SrI [36]. (It should be noted that there is an apparent typographical error with the matrix elements of Table 4.2 in Ref. [5]). As with these examples, the *A* and *B* states of SrBr interact almost solely with one another, and form a unique perturber pair. Evidence for this is provided by the nearly identical values of p_v and γ_v in the *A* and *B* states, respectively [17]. Because both bromine isotopomers were examined, the present study is unique in that both mechanical and electronic isotopic consistencies can be verified. In the latter case, the form of the α_{AB} and b_{AB} parameters is of particular interest.

As shown by Kaledin *et al.* [5], the off-diagonal matrix elements involving the α and β parameters describe the interaction between specific levels of $^2\Pi$ and $^2\Sigma^+$ states, and are dependent on either the vibrational overlap integral or the R^{-2} overlap integral,

$\langle R^{-2} \rangle_{\nu_A \nu_B}$, respectively³,

³ Calculated as $\langle \nu_A | \nu_B \rangle = \langle \Psi_{\text{vib}}(\nu_A) | \Psi_{\text{vib}}(\nu_B) \rangle$ and $\langle R^{-2} \rangle_{\nu_A \nu_B} = \langle \Psi_{\text{vib}}(\nu_A) | B(R) | \Psi_{\text{vib}}(\nu_B) \rangle$

$$\alpha_{\nu_A \sim \nu_B} = \frac{1}{2} \langle A^2 \Pi | \sum_i \hat{a}_i l_i^+ s_i^- | B^2 \Sigma^+ \rangle \langle \nu_A | \nu_B \rangle, \quad 4.4$$

$$\text{and } \beta_{\nu_A \sim \nu_B} = \langle A^2 \Pi | \sum_i l_i^+ | B^2 \Sigma^+ \rangle \langle \nu_A | B(R) | \nu_B \rangle, \quad 4.5$$

$$\text{where } B(R) = \frac{\hbar^2}{2\mu R^2}. \quad 4.6$$

Expressions 4.4 and 4.5 are both given as a sum of one-electron operators describing the spin-orbit and \hat{L} -uncoupling effects (respectively) on the metal-centered unpaired electron. The electronic portions of Eqs. 4.4 and 4.5 can thus be written as:

$$\alpha_{AB} / \text{cm}^{-1} = \langle A^2 \Pi | \sum_i \hat{a}_i l_i^+ s_i^- | B^2 \Sigma^+ \rangle = \frac{2\alpha}{\langle \nu_A | \nu_B \rangle}, \quad 4.7$$

$$\text{and } b_{AB} = \langle A^2 \Pi | \sum_i l_i^+ | B^2 \Sigma^+ \rangle = \frac{\beta}{\langle \nu_A | B(R) | \nu_B \rangle}, \quad 4.8$$

where it is assumed that the radial dependences of α_{AB} and b_{AB} are negligible.

In SrBr, estimates of the purely electronic interaction parameters (α_{AB} and b_{AB}) between the A and B states could thus be achieved by calculating both overlap integrals, $\langle \nu_A | \nu_B \rangle$ and $\langle R^{-2} \rangle_{\nu_A \nu_B}$, between all sampled vibrational levels in each state (as shown in Eqs 4.7 and 4.8), and identifying α and β with $(\frac{1}{2})\alpha_{AB} \langle \nu_A | \nu_B \rangle$ and $b_{AB} \langle \nu_A | B(R) | \nu_B \rangle$, respectively. The parameters α_{AB} and b_{AB} could thus be determined in least squares fits of the entire data set for each isotopomer. Since these parameters are not mass dependent, they should be identical for both SrBr isotopomers examined.

In the previous *global* studies of analogous MX species [5,32,35,36], it was determined that owing to the nearly identical potential curves of the A and B states, the magnitudes of the parameters α and β were greatest for $\Delta\nu_{B,A} = 0$, and thus estimates of

the a_{AB} and b_{AB} parameters were based mostly on such interactions. Since R -centroid⁴ values,

$$\bar{R}_{\nu_A\nu_B} = \frac{\langle \nu_A | R | \nu_B \rangle}{\langle \nu_A | \nu_B \rangle}, \quad 4.9$$

for diagonal interactions are almost constant, the approximation $a_{AB}(R) \approx a_{AB}$ and $b_{AB}(R) \approx b_{AB}$ is quite reasonable. For the present situation in SrBr, however, the level crossings at $A(\nu_A = 3,4,5) \sim B(\nu_B = 0,1,2)$ will occur at different values of $\bar{R}_{\nu_A\nu_B}$, and thus the possibility of employing the radially dependent forms $a_{AB}(R)$ and $b_{AB}(R)$ must be considered.

Potential energy curves for the A and B states of SrBr have been calculated using the RKR method described by Coxon [42]. A small correction was included to account for the radial dependence of the spin-orbit parameter [43]. For this purpose $A(R)$ was assumed to be linear in R . The radially dependent form for the two isotopomers is given as:

$$A(R)/\text{cm}^{-1} = 299.687 - 5.014R \quad 4.10$$

with R in units of Å. This approach leads to an effective potential energy curve for each of the $A^2\Pi$ sub-states. Figure 4.2 illustrates the proximity of levels in the $A^2\Pi_{1/2}$ and $B^2\Sigma^+$ states. Overlap integrals, $\langle \nu_A | \nu_B \rangle$ and $\langle R^{-2} \rangle_{\nu_A\nu_B}$, were calculated from the corrected RKR curves, using a standard numerical approach [44]. Results for the

⁴ The R -centroid approximation is used to estimate an "effective" value of R that exists between two electronic states. Although this value has no physical meaning, it is necessary to facilitate a description of the vibrational dependence (alternately given as radial dependence) of certain parameters.

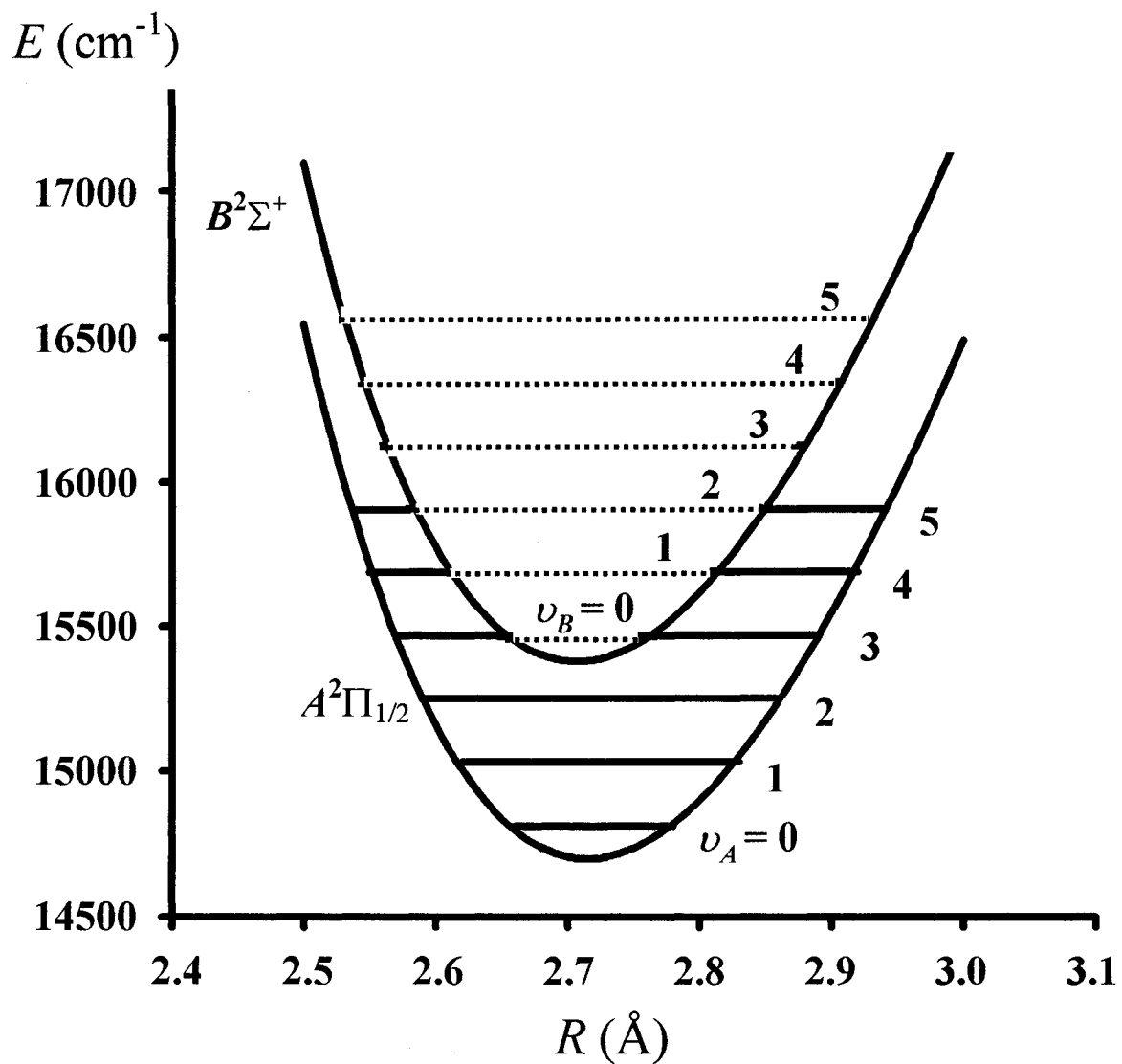


Figure 4.2 RKR Curves for the $A^2\Pi_{1/2}$ and $B^2\Sigma^+$ states of SrBr.

complete set of calculated $A^2\Pi_{1/2} \sim B^2\Sigma^+$ and $A^2\Pi_{3/2} \sim B^2\Sigma^+$ overlap integrals is available in Appendix I, while some selected overlaps are given in Table 4.3.

It was found empirically that the reliability of calculated values of the overlap integrals, $\langle \nu_A | \nu_B \rangle$ and $\langle R^{-2} \rangle_{\nu_A \nu_B}$, decreased rapidly with increasing magnitudes of $\Delta \nu_{BA} = \nu_B - \nu_A$. This result is a consequence of the almost parallel nature of the A and B state potential energy curves, as is apparent from the large (> 0.99) overlap integrals, $\langle \nu_A | \nu_B \rangle$, given in Table 4.3 (and Appendix I) for $\Delta \nu_{BA} = 0$. The magnitudes of $\langle \nu_A | \nu_B \rangle$ for the $\nu_B - \nu_A = -3$ series are exceedingly small, and are extremely sensitive to very small changes in the generated RKR potentials; even a change in sign can occur. Likewise, the magnitudes of $\langle R^{-2} \rangle_{\nu_A \nu_B}$ are small for the off-diagonal interactions, and largest for $\nu_B = \nu_A$. Since very small errors in the calculated RKR potentials thus cause large percentage errors in the calculated overlap integrals, these quantities could not be determined with enough accuracy to produce *global* expressions for the $\alpha_{AB}(R)$ and $b_{AB}(R)$ parameters such that the *local* level crossings and the *global* splitting effects could be properly represented simultaneously.

In accord with the previous paragraph, while *global* α_{AB} and b_{AB} parameters could be employed for interactions between all non-crossing levels, so as to account for the *global* splitting effects in the A and B states, it was necessary to treat each level crossing explicitly with its own α and/or β value. With this approach it was established that the parameters α_{AB} and b_{AB} could account very satisfactorily for most of the *global*

Table 4.3Overlap integrals^a for selected $A^2\Pi \sim B^2\Sigma^+$ interactions in $^{88}\text{Sr}^{79}\text{Br}$.

		$A^2\Pi_{1/2} \sim B^2\Sigma^+$		$A^2\Pi_{3/2} \sim B^2\Sigma^+$	
ν_A	ν_B	$\langle \nu_A \nu_B \rangle$	$\langle \nu_A B(R) \nu_B \rangle$	$\langle \nu_A \nu_B \rangle$	$\langle \nu_A B(R) \nu_B \rangle$
0	0	9.994E-01	5.500E-02	9.994E-01	5.500E-02
1	0	-3.314E-02	-3.551E-03	-3.410E-02	-3.604E-03
2	0	3.868E-03	4.119E-04	3.932E-03	4.178E-04
3	0	7.955E-05	-2.486E-05	7.088E-05	-2.572E-05
4	1	-3.294E-04	-7.406E-05	-3.457E-04	-7.570E-05
5	2	-8.503E-04	-1.337E-04	-8.753E-04	-1.363E-04

^aThe overlap integrals, $\langle \nu_A | \nu_B \rangle$, are dimensionless, while values of $\langle \nu_A | B(R) | \nu_B \rangle$ are in units of cm^{-1} .

splitting effects; however, small residual terms (p_ν^{res} , q_ν^{res} and γ_ν^{res}) were required to fit the line positions to within their estimated uncertainties. (The residual parameters are understood to account for all remaining n' , ν' interactions of Eqs. 4.1, 4.2 and 4.3.) A similar approach was also adopted by Kaledin *et al.* [5] for CaF, so as to account for weaker interactions with *all* neighboring $^2\Sigma^+$ and $^2\Pi$ states, for the A and B states, respectively.

As previously mentioned, the a_{AB} and b_{AB} parameters are determined largely by interactions that occur between $\Delta\nu_{AB} = 0$ levels, while interactions between the remaining $\Delta\nu_{AB} \neq 0$ levels contributed only slightly ($< 5\%$). To fully characterize the electronic interactions, contributions from levels not directly investigated were considered in the fits. Estimated parameters for levels up to $\nu_{A/B} = \nu_{B/A}^{max} + 3$ were extrapolated in an iterative fashion: a second order polynomial in ν was employed for the term values, T_ν ; a linear model in ν was used for B_ν and A_ν ; and the remaining parameters D_ν , p_ν , q_ν , $A_{D\nu}$, and γ_ν were estimated based on values obtained for sampled levels. A 17×17 Hamiltonian matrix (for each value of J and parity) was obtained in this way, with 70 individual off-diagonal elements employing the calculated $\langle \nu_A | \nu_B \rangle$ and $\langle R^{-2} \rangle_{\nu_A \nu_B}$ values.

Several different fits were employed using either α and/or β parameters to describe the individual level crossings. As was the case for the fits of individual crossings (Table 4.1), only fits with the α parameter were successful in representing all level crossings. Again it would seem that fits employing both α and β failed to converge

owing to the high degree of correlation of the parameters, and fits of level crossings that occur outside the data range could not be described by β alone. The results of the fits involving solely α are given in Table 4.4.

It should be mentioned that it was necessary to fix $\omega_e x_e$ for the X state of $^{88}\text{Sr}^{81}\text{Br}$ at the value calculated from the fitted value for $^{88}\text{Sr}^{79}\text{Br}$. The failure of the fit for $^{88}\text{Sr}^{81}\text{Br}$ to yield a fitted value of $\omega_e x_e$ is associated with the different situation for the $A(\nu_A = 4) \sim B(\nu_B = 1)$ interaction for the two isotopomers. For $^{88}\text{Sr}^{79}\text{Br}$, the level crossing occurs at $J > 0$, and is sampled directly; for $^{88}\text{Sr}^{81}\text{Br}$, however, the “crossing” occurs at $J < 0$. As a consequence, the data cannot provide an estimate of $G_3 - G_1$ in the X state, and only one vibrational separation ($G_2 - G_0$) is afforded by the data.

As can be seen from a comparison of Tables 4.1 and 4.4, estimates of the term values, spin-orbit coupling parameters, and rotational B_v values are quite different between the two models. This is readily understood in terms of the largely effective nature the parameters found in Table 4.1; while such parameters reproduce the line positions to within their estimated uncertainty, they arise as a mixture of electronic and mechanical effects. Conversely, the results given in Table 4.4 are closer to the “true” electronic (for T_e and A_v) and mechanical (for B_v and D_v) definitions, as the effects of interactions between the A and B states have been described explicitly. The values of R_e for the A and B states derived from Table 4.4 are 2.71314(9) Å and 2.71054(2) Å, respectively; these values are significantly different from the values obtained previously 2.7147(1) Å [4] and 2.707530(2) Å [2].

Table 4.4 Fitted parameters^a for $^{88}\text{Sr}^{79}\text{Br}$ and $^{88}\text{Sr}^{81}\text{Br}$ obtained from combined $[A - X] \sim [B - X]$ fits.

$^{88}\text{Sr}^{79}\text{Br } B^2\Sigma^+$								
ν	0	1	2	3	4	5	6	7
T_{00}	15447.660(1)	15668.630(2)	15888.478(2)	[16107.190]	[16324.770]	[16541.230]	[16756.550]	[16970.750]
B_v	0.0550768(4)	0.0548817(6)	0.0546888(7)	[0.0544964]	[0.0543030]	[0.0541097]	[0.0539164]	[0.0537231]
$10^8 D_v$	1.357(5)	1.34(1)	1.37(1)	[1.35]	[1.35]	[1.35]	[1.35]	[1.35]
$10^3 \gamma_v^{\text{re}}$	2.71(2)	2.45(3)	2.47(4)	[2.5]	[2.5]	[2.5]	[2.5]	[2.5]
$^{88}\text{Sr}^{79}\text{Br } A^2\Pi$								
ν	0	1	2	3	4	5	$A \sim B$	
T_{00}	14970.078(1)	15191.396(2)	15411.6550(2)	15630.799(2)	15848.871(4)	[16065.861]	a_{ab}	[-203.902]
B_v	0.054979(2)	0.054793(2)	0.0546045(7)	0.0544162(6)	0.0542314(6)	[0.0540432]	b_{ab}	[-3.112]
$10^8 D_v$	1.39(5)	1.45(5)	1.371(8)	1.353(9)	1.354(7)	[1.35]	$\alpha'_{v=0}$	0.197(1)
A_v	286.063(2)	286.036(2)	286.002(2)	285.969(2)	285.930(2)	[285.898]	$\alpha'_{v=1}$	0.3875(9)
$10^5 A_{\text{bv}}$	2.1(1)	2.19(9)	2.19(7)	2.28(6)	1.98(6)	[2.0]	$\alpha'_{v=2}$	0.600(2)
$10^3 p_v^{\text{re}}$	3.85(6)	3.72(6)	3.30(8)	2.9(1)	3.30(6)	[3.5]		
$10^4 q_v^{\text{re}}$	-1.2(3)	-2.0(4)	-0.5(5)	1.1(8)	-1.9(5)	[-1.0]		
$^{88}\text{Sr}^{79}\text{Br } \Lambda^2\Sigma^+$								
ν	0	1	2	3				
B_v^b	[0.0540934]	[0.0539110]	[0.0537288]	[0.0535470]				
$10^8 D_v^b$	[1.35665]	[1.35569]	[1.35521]	[1.35474]				
$10^3 \gamma_v^b$	[2.159615]	[2.146278]	[2.132909]	[2.119540]				
$10^9 \gamma_{\text{rv}}^b$	[1.18]	[1.18]	[1.18]	[1.18]				
ω_e			216.646(2)				N	1517
$\omega_e x_e$			0.5132(5)				$\hat{\sigma}$	1.049

Table 4.4 (con't)

$^{88}\text{Sr}^{81}\text{Br } B^2\Sigma^+$								
ν	0	1	2	3	4	5	6	7
$T_{\nu 0}$	15446.9260(7)	15666.454(2)	15884.876(3)	[16102.204]	[16318.420]	[16533.531]	[16747.537]	[16960.438]
B_{ν}	0.0543629(4)	0.0541722(7)	0.0539380(7)	[0.0537900]	[0.0535990]	[0.0534080]	[0.0532170]	[0.0530260]
$10^8 D_{\nu}$	1.335(5)	1.34(1)	1.31(1)	[1.32]	[1.32]	[1.32]	[1.32]	[1.32]
$10^3 \gamma_{\nu}^{\text{re}}$	2.71(2)	2.63(4)	2.54(5)	[2.5]	[2.5]	[2.5]	[2.5]	[2.5]
$^{88}\text{Sr}^{81}\text{Br } A^2\Pi$								
ν	0	1	2	3	4	5	$A \sim B$	
$T_{\nu 0}$	14969.356(1)	15189.233(2)	15408.0490(4)	15625.783(3)	15842.455(4)	[16058.075]	a_{AB}	[-203.902]
B_{ν}	0.054256(2)	0.054079(2)	0.0538968(8)	0.0537120(6)	0.0535301(8)	[0.0533485]	b_{AB}	[-3.112]
$10^8 D_{\nu}$	1.17(5)	1.33(5)	1.31(1)	1.289(8)	1.30(1)	[1.30]	α_{3-0}^c	0.194(1)
A_{ν}	286.059(2)	286.034(2)	286.006(2)	285.970(1)	285.929(2)	[285.898]	α_{4-1}^c	0.396(2)
$10^5 A_{\text{Dop}}$	1.8(1)	2.18(9)	1.86(4)	1.81(5)	1.88(5)	[2.0]	α_{5-2}^c	0.586(2)
$10^3 p_{\nu}^{\text{re}}$	3.82(5)	3.41(8)	3.02(7)	3.2(1)	3.1(1)	[3.5]		
$10^4 q_{\nu}^{\text{re}}$	-1.3(2)	0.3(5)	0.8(5)	2.6(8)	-0.8(7)	[-1.0]		
$^{88}\text{Sr}^{81}\text{Br } \Lambda^2\Sigma^+$								
ν	0	1	2	3				
B_{ν}^c	[0.0533902]	[0.0532113]	[0.0530327]	[0.0528545]				
$10^8 D_{\nu}^c$	[1.32113]	[1.32063]	[1.32013]	[1.31963]				
$10^3 \gamma_{\nu}^b$	[2.126428]	[2.113444]	[2.100445]	[2.087446]				
$10^9 \gamma_{\nu}^{\text{re}}$	[2.32]	[2.32]	[2.32]	[2.32]				
ω_c			215.2247(9)					
$\omega_c X_c$			[0.5067]		N		1499	
					σ		1.031	

Table 4.4 (con't)

^aAll parameters except for b_{iB} (dimensionless) are in cm^{-1} units. Estimated standard errors (1σ) are given in parentheses with uncertainties in the last significant digit; parameters constrained to fixed values are given in square brackets. See body of text for further explanation of fixed parameters. N denotes the number of measured line positions included in each fit, and $\hat{\sigma}$ denotes the reduced standard deviation of each fit (a value of 1.000 denotes all lines reproduced on average to within their estimated error).

^bValues fixed to those of Ref. [40].

^cDenoted as $\alpha_{i,4-10p}$.

It is apparent in Table 4.4 that values for the parameters α_{AB} and b_{AB} were fixed at constant values. Since this might appear to contradict the objectives of the present analysis, further explanation is needed. Discrepancies were found between the results of the fits for the separate isotopomers. In such fits, values of α_{AB} and b_{AB} were determined to be $-206.38(8) \text{ cm}^{-1}$ and $-3.067(4)$, respectively, for the $^{88}\text{Sr}^{79}\text{Br}$ isotopomer, and $-202.54(6) \text{ cm}^{-1}$ and $-3.137(8)$, respectively, for the $^{88}\text{Sr}^{81}\text{Br}$ isotopomer. As these parameters, and similarly the A_v parameters, are determined entirely by electronic effects, they should be essentially identical between the $^{88}\text{Sr}^{79}\text{Br}$ and $^{88}\text{Sr}^{81}\text{Br}$ isotopomers. (In principle an extremely small difference might occur due to sampling the identical potential energy curves at slightly different vibrational energies, and thus different R values). This was clearly an unsatisfactory result, and it was decided that final fits for each isotopomer should employ α_{AB} and b_{AB} that were fixed to their weighted averages. These final fits, shown in Table 4.4, demonstrate that by fixing the α_{AB} and b_{AB} parameters, the individual A_v values agree extremely well between the isotopomers, as expected. Interestingly, the reduced standard deviations changed by less than 0.1% between the fits where α_{AB} and b_{AB} were determined and the fits using fixed values.

The equally satisfactory nature of the two types of fits thus appears paradoxical, as the individual parameters changed by up to 30 standard deviations. While this is difficult to rationalize, it is possible that the large magnitudes of the correlation coefficients between parameters, as shown in Table 4.5, are involved. It was found that α_{AB} was highly correlated with the A_v , ω_e , $(\omega_e x_e)$, and T_B parameters, and similarly, the

Table 4.5

Correlation coefficients between the a_{AB} and b_{AB} parameters of $^{88}\text{Sr}^{81}\text{Br}$ and selected A , B and X state parameters from intermediate fit^a.

	a_{AB}		b_{AB}
A_0	0.98636	p_0^{res}	-0.97474
A_1	0.97929	p_1^{res}	-0.95898
A_2	0.98224	p_2^{res}	-0.96923
A_3	0.98679	p_3^{res}	-0.94105
A_4	0.97293	p_4^{res}	-0.95428
T_{00}^B	0.99802	γ_0^{res}	-0.99210
T_{10}^B	0.99322	γ_1^{res}	-0.98259
T_{20}^B	0.98846	γ_2^{res}	-0.98548
ω_e^X	0.94976		

^aSee text.

b_{AB} parameter showed a high degree of correlation with p_v^{res} and γ_v^{res} parameters. These high correlations for nearly one third of the parameter set might suggest that the model is so flexible that large changes in parameters can be tolerated.

A combined fit of the data for both isotopomers simultaneously would lead to single estimates of a_{AB} and b_{AB} . It is expected, however, that only marginal improvements in the estimated parameters would be achieved in such a fit, and the final model employed here, that uses fixed values of a_{AB} and b_{AB} , is regarded as satisfactory.

4.5.3 *Ab initio* Estimates of a_{AB} and b_{AB}

It is of interest to compare the present estimates of a_{AB} and b_{AB} with those that can be estimated from *ab initio* calculations, as also performed in the work of Kaledin *et al.* [5]. Similar to calcium fluoride, strontium bromide is highly ionic in character, with the unpaired electron predominantly on the Sr^+ metal center, and perturbed by the Br^- ion. It is thus possible to describe the electronic states of SrBr in terms of atomic Sr^+ $5s$, $5p$, and $4d$ orbitals. The results of an unpublished theoretical ligand field study undertaken by Allouche *et al.* [6], can be summarized as:

$$|A^2\Pi\rangle = 0.671|5p(\text{Sr}^+)\rangle - 0.721|4d(\text{Sr}^+)\rangle \quad 4.11$$

$$\text{and } |B^2\Sigma\rangle = 0.173|5s(\text{Sr}^+)\rangle - 0.510|5p(\text{Sr}^+)\rangle + 0.812|4d(\text{Sr}^+)\rangle. \quad 4.12$$

Thus using the spin-orbit parameters of Sr^+ , $\zeta_{5p} = 534.3\text{cm}^{-1}$, and $\zeta_{4d} = 112.1\text{cm}^{-1}$ [45], and with $l = 1$ and 2 for p and d orbitals, respectively, calculated values of:

$$a_{AB} = \left\langle A^2\Pi \left| \sum_i \hat{a}_i l_i^+ s_i^- \right| B^2\Sigma^+ \right\rangle$$

$$\begin{aligned}
&= (-0.510)(0.671)[I(I+1)]^{1/2}\zeta_{5p} + (-0.721)(0.812)[I(I+1)]^{1/2}\zeta_{4d} \\
&= -419.4 \text{ cm}^{-1}
\end{aligned} \tag{4.13}$$

$$\begin{aligned}
\text{and } b_{AB} &= \left\langle A^2\Pi \left| \sum_i I_i^+ \right| B^2\Sigma^+ \right\rangle \\
&= (-0.510)(0.671)[I(I+1)]^{1/2} + (-0.721)(0.812)[I(I+1)]^{1/2} \\
&= -1.918
\end{aligned} \tag{4.14}$$

are obtained.

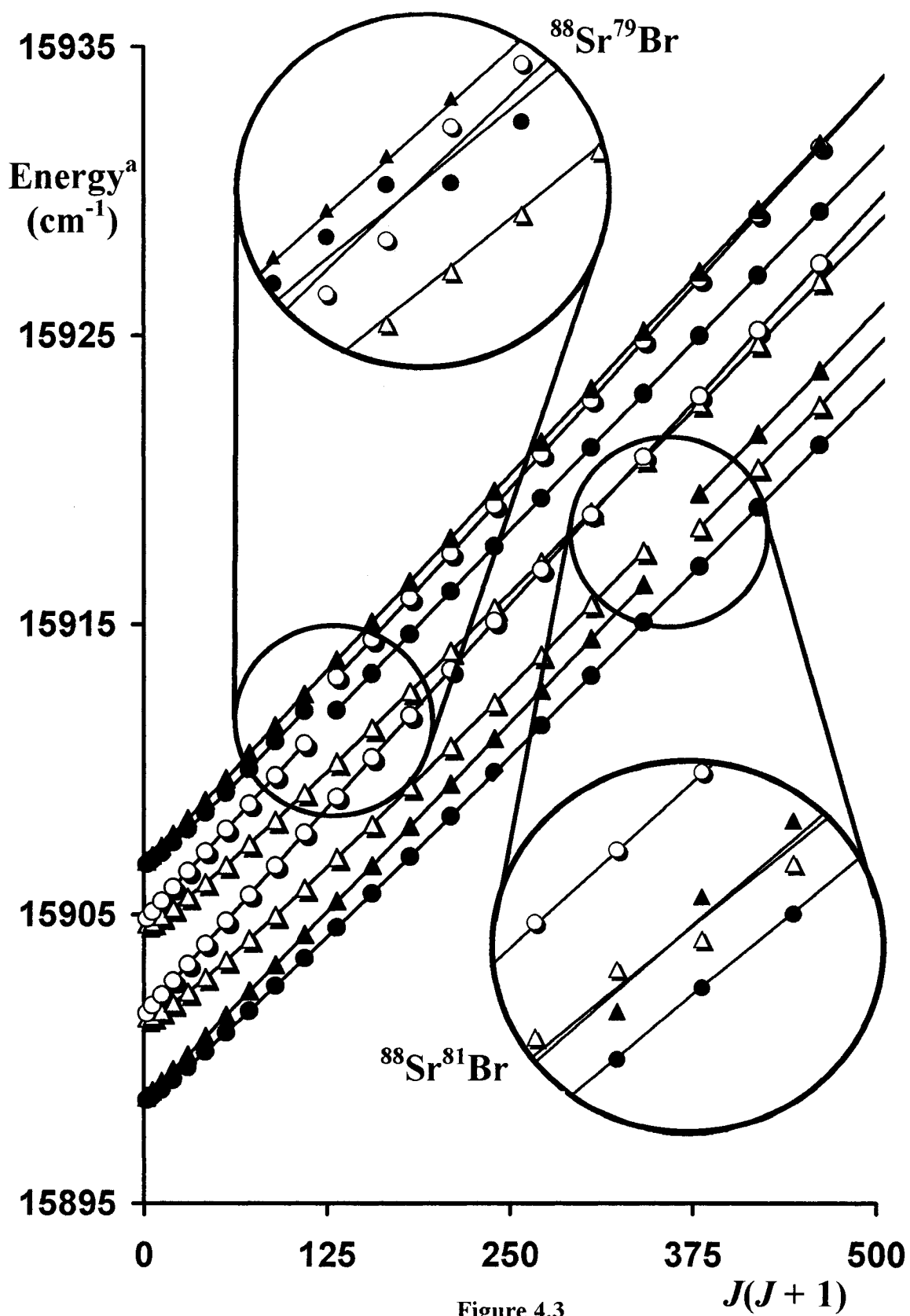
Comparisons of the *ab initio* estimates with the experimentally determined values suggests that a much larger degree of $5p$ character is present in the $A^2\Pi_{1/2}$ and $B^2\Sigma^+$ states than given in Eqs. 4.11 and 4.12. In fact, an order of magnitude change in the orbital mixing percentages would be required to achieve consistency with the experimental results.

4.5.4 Interaction of the B ($\nu = 2$) and A ($\nu = 5$) Levels

The simultaneous fits of all $A - X$ and $B - X$ data described above have enabled the interactions between the B ($\nu_B = 2$) and A ($\nu_A = 5$) levels to be deperturbed for the first time. A new level crossing of the e parities in $^{88}\text{Sr}^{81}\text{Br}$ is now predicted, as can be seen in Figure 4.3.

Schröder and Ernst's initial analysis [2] of the $2 - 2$ band of the $B - X$ transition for $^{88}\text{Sr}^{81}\text{Br}$ noted perturbed line positions for low N ($N'' = 28 - 50$ in the P_1 branch and $N'' = 13 - 50$ for the R_1 branch), which were not included in their final fit. In the present analysis, line positions in the $2 - 2$ band for both the P_1 and R_1 branches for $N'' = 28 - 50$

Figure 4.3 Rotational energy levels in the $A^2\Pi(\nu_A = 5)$ and $B^2\Sigma^+(\nu_B = 2)$ states, relative to the $\nu_X = 0$ level in the ground state, for both $^{88}\text{Sr}^{79}\text{Br}$ and $^{88}\text{Sr}^{81}\text{Br}$. Filled symbols indicate perturbed rotational levels in the $\nu_A = 5$ level of the $A^2\Pi$ state, while open symbols indicate perturbed rotational levels in the $\nu_B = 2$ level of the $B^2\Sigma^+$ state; circles denote levels of f parity, and triangles denote levels of e parity. Solid lines in the magnification windows indicate calculated unperturbed energies.



and $N'' = 30 - 50$, respectively, are satisfactorily deperturbed and are included in the fit. Measured lines given in Ref. [2] for the R_1 branch for $N'' = 13 - 29$, however, show large residuals, and it seems possible, then, that these low- N lines in the congested region near the origin were assigned incorrectly in Ref. [2]. Further data are required to resolve this issue unequivocally.

4.6 Conclusions

The electronic $A^2\Pi \sim B^2\Sigma^+$ interaction parameters a_{AB} and b_{AB} , determined from combined fits of $A^2\Pi \leftarrow X^2\Sigma^+$ and $B^2\Sigma^+ \leftarrow X^2\Sigma^+$ data, successfully describe the *global* splittings in the two states, namely Λ -doubling in the $^2\Pi$ state and “spin-rotation” in the $^2\Sigma^+$ state. Similarly, *local* level crossings between the two states are described satisfactorily, in each case, by a single parameter, $\alpha_{\nu_A \sim \nu_B}$. Comparison of experimental a_{AB} and b_{AB} values with *ab initio* results show large discrepancies. A level crossing between the B ($\nu_B = 2$) and A ($\nu_A = 5$) levels is also predicted, but has not yet been observed.

Chapter 5

A FTMW Study of the $X^2\Sigma^+$ States of YbF, YbCl and YbBr

5.1 Background

There has been increasing attention to the spectroscopy of lanthanide containing diatomic molecules in recent years. However, most studies have been limited to hydrides, oxides and fluorides. Several reports describe the spectroscopy of the ytterbium halides; YbF has been studied *via* optical [46,47], rf-optical double resonance [48], and electron spin resonance [49] spectroscopies. The visible $A^2\Pi \leftarrow X^2\Sigma^+$ and $B^2\Sigma^+ \leftarrow X^2\Sigma^+$ systems of YbCl has been recorded at high resolution and analyzed by Melville *et al.* [50] and Linton and Adam [51], respectively; and a vibrational analysis of the $A - X$ system of YbBr has been reported [52] from low-resolution spectra. Prior to the present work no information was available on the rotational energy level structure of YbBr.

Like the alkaline earth metals, the ytterbium atom has a filled s sub-shell in its ground state configuration ($[\text{Xe}]4f^{14}6s^2$). Consequently, $^2\Sigma^+$ ground states are adopted by its diatomic Yb^+X^- halide species. The metal-centered unpaired $6s$ electron couples to halide nuclei, which have $I > 0$, causing hyperfine effects to be observed in the rotational spectra of these molecules. Parameters describing these hyperfine interactions serve as a sensitive probe into several aspects of the electronic structure. For example, Fermi contact interactions in these molecules, with their associated parameters (b_F), provide useful information on the unpaired electron spin densities at the halogen nuclei, and on the amount of atomic s -orbital occupation on the halogen atoms. Similarly, the dipole-

dipole hyperfine parameter (c) can yield an estimate of the amount of p -orbital occupation on the halide ion. For quadrupolar nuclei with $I \geq 1$, the hyperfine effects also depend on the nuclear quadrupole moment; experimental quadrupolar coupling parameters can yield insight into the electric field gradient at the quadrupolar nuclei, and often the ionic characters of the molecules.

The present study employed Fourier transform microwave (FTMW) spectroscopic techniques to record pure rotational spectra of YbX ($X = \text{F}, \text{Cl}, \text{Br}$), from which rotational, fine and hyperfine parameters were determined. The four $N = 1 \leftarrow 0$ transitions of ^{174}YbF were recorded for both the $\nu = 0$ and $\nu = 1$ levels. The spectra of three isotopomers of the chloride, $^{174}\text{Yb}^{35}\text{Cl}$, $^{172}\text{Yb}^{35}\text{Cl}$ and $^{174}\text{Yb}^{37}\text{Cl}$, were recorded for the $\nu = 0$ level in the range $1 \leq N \leq 4$. For $\nu = 1$, however, spectra were obtained only for the principal $^{174}\text{Yb}^{35}\text{Cl}$ isotopomer. The investigation of YbBr , was limited to the $\nu = 0$ level for the two principal isotopomers ($^{174}\text{Yb}^{79}\text{Br}$ and $^{174}\text{Yb}^{81}\text{Br}$) in the range $2 \leq N \leq 8$. Least squares fits of the experimental line positions have provided reliable estimates of the rotational parameters (B_v , D_v), fine structure parameters (γ_v), and hyperfine parameters (b_{F} , c , eQq , C_{I}) for each isotopomer. Equilibrium bond lengths have been obtained for YbF and YbCl , and information extracted from the hyperfine parameters is discussed in terms of bonding trends in this series of halides.

5.2 Experimental Arrangement

The YbX molecules ($X \equiv \text{F}, \text{Cl}$ and Br) were produced in an ablation/super sonic expansion, the details of which are described in Chapter 3. A rod of ytterbium metal (5 mm diameter, *Goodfellow*, 99.9%) was the target of the ablating Nd:YAG pulse, and

SF₆, Cl₂ or Br₂ were the oxidants selected for the production of the respective halide diatomic molecule. The oxidant was 0.005 % - 0.015 % of the total 5-6 atmospheres of argon backing pressure.

The YbX radicals were directed between two aluminum mirrors that comprised the microwave cavity, again outlined in chapter 3. The free induction decay signal (FID) obtained from probing the molecules was transformed using the Fourier algorithm to produce a spectrum spanning 1 MHz.

Spectra typical to this study are shown in Figure 3.7, with the effects of Doppler splitting in both spectra, and Zeeman splitting owing to the earth's magnetic field shown in Figure 3.7b.

5.3 Results

5.3.1 YbF

Previous spectroscopic work on the ground state of YbF consists of a detailed analysis of the hyperfine structure in the $\nu = 0$ and 1 levels by Sauer *et al.* [46,48], and a high resolution study [47] by Dunfield *et al.* of the visible $A^2\Pi - X^2\Sigma^+$ system. The initial study reported by Sauer *et al.* [46] was concerned with the hyperfine structure of spin-doublets in $\nu = 0$ with $J = N \pm \frac{1}{2}$ for $N \leq 73$ obtained from Doppler-free laser radio-frequency fluorescence from specific levels of the $A^2\Pi$ state. This work revealed a very unusual behavior of the spin-rotation splittings in ^{174}YbF . The $\nu = 0$ spin-rotation parameter is small in magnitude but is subject to anomalously large centrifugal distortion effects such that γ actually changes sign at $N = 60$. In the later work [48], transitions between the hyperfine components of individual N levels were observed directly for

$\nu = 0$ and 1 by laser induced double resonance spectroscopy. This led to precise values for the spin-rotation and hyperfine parameters. In addition three hyperfine components of the $N = 1 \leftarrow 0$ pure rotational transition with $F'' = 1$ were observed by microwave optical double resonance in a molecular beam.

The value of B for $\nu = 0$ of ^{174}YbF given by Sauer *et al.* [48], differed substantially from that reported by Dunfield *et al.* [47]. In the present work, the three transitions previously reported [48] were observed along with a previously unobserved transition with $F'' = 0$. The measured frequencies are listed in Appendix II, and are in agreement with those of Sauer *et al.* [48] within our estimated uncertainties, though they are systematically 4 kHz less.

The present data on YbF from Appendix II, along with the radio-frequency data of Sauer *et al.* [48] for $0 < N < 10$, were employed in a weighted least squares fit that provided values for the rotational, fine structure and hyperfine parameters. These values are listed in Table 5.1. Higher order parameters (γ_D , γ_H and b_{fb}) were required in the fits described herein, and are defined by the general form (P) given in Eq. 5.1:

$$P(N) = P + P_D N(N+1) + P_H [N(N+1)]^2 + \dots \quad 5.1$$

The reduced standard deviation of the fit was $\hat{\sigma} = 1.3$, indicating that the residuals were, on average, only slightly larger than the corresponding measurement accuracies. Two parameters were constrained: the centrifugal distortion parameter, D_0 , was fixed at the value obtained by Dunfield *et al.* [47], and the parameter γ_H was set at the value obtained by Sauer *et al.* [48] from the data of Ref. 46. Although most of the results in Table 5.1 for $\nu = 0$ are in excellent agreement with the values obtained by Sauer *et al.*

Table 5.1

Molecular parameters^a (MHz) for the $\nu = 0$ and 1 levels of ^{174}YbF ($X^2\Sigma^+$).

	^{174}YbF ($\nu = 0$)		^{174}YbF ($\nu = 1$)	
	Sauer et al. ^b	This work	Sauer et al. ^b	This work
B_ν	7233.8007(2)	7233.8271(17)		7188.8919(7)
$10^3 D_\nu$	[7.159] ^c	[7.159] ^c		[6.904] ^c
γ	-13.42400(16)	-13.41679(13)	-33.8118(7)	-33.81036(57)
$10^3 \gamma_D$	-3.801(15)	3.9840(15)	4.323(6)	4.3205(24)
$10^8 \gamma_H$	-2.5(1)	[-2.5] ^d	-2.8(9)	[-2.8] ^d
b_F	170.2631(7)	170.26374(20)	168.81(4)	168.770(11)
$10^3 b_{F_D}$	-0.510(11) ^e	-0.522(15)	-0.7(4) ^e	-0.36(11)
c	85.4026(14)	85.4028(19)	86.75(5)	86.7120(80)
$10^3 C_1$	20.38(13)	13.099(52)	18.3(1)	17.20(80)

^aStandard errors of the fitted parameters are given in parentheses in units of least significant digit of the corresponding constant.

^bRef. 48.

^cConstrained values from Ref. 47.

^dConstrained values from Ref. 48.

^eValue corresponds to $10^3 b_D$.

[48], such that discrepancies are less than the combined standard error estimates, there are also some significant differences. The two estimates of B_0 , γ_0 and C_1 differ by between 14 and 40 combined standard errors. It is likely that such large discrepancies are due to the different approaches in the numerical fitting methods. In the present work all the data were fitted simultaneously with eigenvalues based on the full Hamiltonian matrix for each F -value (Table 2.3), including matrix elements off-diagonal in N . In the work of Sauer *et al.* [48], however, the microwave data were treated separately, with “corrections” being applied for hyperfine effects, and contributions to the eigenvalues from neglected off-diagonal matrix elements were applied by perturbation theory for the $c\hat{\mathbf{I}}_z \cdot \hat{\mathbf{S}}_z$ interaction, but not at all for the $C_1\hat{\mathbf{I}} \cdot \hat{\mathbf{N}}$ spin-rotation interaction.

For the $\nu = 1$ level, our measurements in Table 5.1 are the first precise pure rotational data from microwave spectroscopy. These new data were combined, in a similar fashion to the least-squares fit described above for $\nu = 0$, with the data of Sauer *et al.* [48] for transitions between the hyperfine components of individual N -levels. Two points of detail can be noted; first, the two transitions labeled as f_δ by Sauer *et al.* [48] for $\nu = 1$ are incorrectly labeled; in fact the two transitions occur between the $F = N$ and $F = N - 1$ components of the $J = N - \frac{1}{2}$ spin-rotation level; second, the data of Sauer *et al.* [48] are for the relatively small range $8 \leq N \leq 13$, whereas for $\nu = 0$, comparable data were obtained for most of the levels $0 \leq N \leq 10$. The parameter estimates obtained in Table 5.1 for $\nu = 1$, which are based on the combined data sets, might be expected therefore to be more reliable than those of Ref. 48. In fact agreement for all parameters is excellent; in all cases discrepancies are close to the combined standard errors.

As for $\nu = 0$, the present results and those of Ref. 48 are not in good agreement with those of Dunfield *et al.* [47] for B_1 and especially γ_1 . The very different estimates of γ_1 almost certainly arise from the unusually large centrifugal distortion effect (γ_D) and the failure to model this N -dependence of γ in Ref. 47.

The values of B_0 and B_1 in Table 5.1 give estimates of B_e and α_e^ν according to Eq 2.12 as:

$$B_\nu(^{174}\text{YbF})/\text{MHz} = 7256.2980(18) - 44.9373(17)(\nu + \frac{1}{2}). \quad 5.2$$

5.3.2 YbCl

Results from the rotational analysis of the $A^2\Pi - X^2\Sigma^+$ system of YbCl by Melville *et al.* [50] provided excellent initial estimates for the rotational and spin-rotation parameters. Relatively crude predictions of the quadrupole coupling were obtained based on the estimated ionic character, while the Fermi-contact, and dipole-dipole interaction terms were estimated from the hyperfine parameters determined for YbF. Transitions were sought first for the most abundant isotopomer, $^{174}\text{Yb}^{35}\text{Cl}$. From preliminary fits of the $^{174}\text{Yb}^{35}\text{Cl}$ data, initial parameter estimates for the other isotopomers were sufficiently reliable that transitions for these isotopomers were identified with very little difficulty. In all, data for three isotopomers ($^{174}\text{Yb}^{35}\text{Cl}$, $^{172}\text{Yb}^{35}\text{Cl}$ and $^{174}\text{Yb}^{37}\text{Cl}$) were collected for the $\nu = 0$ level, and data on the $^{174}\text{Yb}^{35}\text{Cl}$ isotopomer were collected also for the $\nu = 1$ level. Line positions and assignments are given in Appendix II.

Data for each of the isotopomers were fit separately, employing the same program as was used for YbF, and the fitted parameters are listed in Table 5.2. In accord with the

Table 5.2

Fitted parameters^a (MHz) for the $\nu = 0$ levels of $^{172}\text{Yb}^{35}\text{Cl}$ and $^{174}\text{Yb}^{37}\text{Cl}$, and the $\nu = 0$ and 1 levels of $^{174}\text{Yb}^{35}\text{Cl}$.

	$\nu = 0$			$\nu = 1$
	$^{172}\text{Yb}^{35}\text{Cl}$	$^{174}\text{Yb}^{35}\text{Cl}$	$^{174}\text{Yb}^{37}\text{Cl}$	$^{174}\text{Yb}^{35}\text{Cl}$
B_ν	2803.0060(13)	2797.5642(5)	2671.8451(24)	2785.8148(14)
$10^3 D_\nu$	0.988(48)	1.219(20)	0.716(75)	1.314(50)
γ_ν	135.6482(86)	135.3657(33)	129.324(10)	132.8276(81)
eQq	-1.65(15)	-1.627(85)	-2.16(31)	-1.92(13)
b_F	30.76(15)	31.339(49)	25.33 (24)	32.17(22)
c	21.95(13)	22.110(73)	18.32(17)	22.72(14)

^aAll uncertainties (1σ) are given in parentheses in units of the least significant digit of the corresponding parameter.

smaller magnetic moment of the Cl nucleus relative to that of F and Br, it was established that the nuclear spin-rotation interaction could be omitted from the model Hamiltonian for YbCl.

The results permit comparisons with quantities that are readily calculated from known physical data. Such comparisons provide appropriate measures of the precision of the fit with respect to the fine and hyperfine parameters. The spin-rotation parameter (γ), is inversely dependent on the reduced mass of the molecule, while the hyperfine parameters, b_F , and c , are proportional to the nuclear moments (see Tables 2.4 and 2.5). The magnitudes of various ratios derived from the experimental data are given in Table 5.3, alongside values that may be simply calculated from physical quantities [53] that are known to a high level of accuracy. Although the calculated ratios serve as a reliable estimate of the quality of the determined parameters, it should be mentioned that exact agreement is not expected. Since the experimental values are for the $\nu = 0$ level and not for the equilibrium position, these values represent sampling [9,54] at slightly different vibrational energies. In addition, the nuclear quadrupole coupling parameters for each of the isotopomers studied make only a small contribution to the total Hamiltonian of the molecule. It should be expected therefore that this parameter will not be determined with a high degree of precision. Typically, experimental and theoretical values do not differ more than four standard errors for $^{172}\text{Yb}^{35}\text{Cl}$ and three standard errors for $^{174}\text{Yb}^{37}\text{Cl}$.

For $^{174}\text{Yb}^{35}\text{Cl}$, the values of B_e and α_e^ν are defined by Eq. 2.12, and from the results for $\nu = 0$ and $\nu = 1$,

$$B_0(^{174}\text{Yb}^{35}\text{Cl})/\text{MHz} = 2803.4389(9) - 11.7494(5)(\nu + \frac{1}{2}). \quad 5.3$$

Table 5.3

Table of experimental and theoretical isotopomeric ratios for the fine and hyperfine parameters of YbCl.

	$^{172}\text{Yb}^{35}\text{Cl}$		$^{174}\text{Yb}^{37}\text{Cl}$	
	Experimental	Theoretical ^a	Experimental	Theoretical ^a
R_γ^a	1.00209(7)	1.00195	0.95536(8)	0.95502
R_{b_F}	0.982(5)	1.000	0.808(8)	0.832
R_c	0.993(7)	1.000	0.829(10)	0.832
R_{eQq}	1.0(1)	1.0	1.3(2)	0.8

^aThe quantities, R_X , are the ratios of $X(\text{YbCl})/X(^{174}\text{Yb}^{35}\text{Cl})$. The theoretical values are the following:

γ : the ratios of the reduced masses of the isotopomers; b_F , c : the ratios of the ^{35}Cl and ^{37}Cl nuclear magnetic moments; eQq : the ratios of the ^{35}Cl and ^{37}Cl nuclear quadrupole moments. These were calculated from the data in Ref. 53.

5.3.3 YbBr

Preliminary estimates of the rotational parameters were made through comparison with the analogous alkaline earth metal species [55-57], while the hyperfine parameters were estimated from those of the chloride and fluoride. Spectra calculated from these parameters were very helpful in guiding the searches for the corresponding transitions experimentally. Data were obtained for the $\nu = 0$ level of the two major isotopomers, $^{174}\text{Yb}^{79}\text{Br}$ and $^{174}\text{Yb}^{81}\text{Br}$, results are presented in Appendix II. Attempts were made to record spectra for the $\nu = 1$ level, but no lines were observed using either argon or neon as the backing gas.

The data were fit to the same model as used for YbCl, and the results are presented in Table 5.4. In fits that included the nuclear spin-rotation term $C_1 \hat{\mathbf{N}} \cdot \hat{\mathbf{I}}$, it was found that the C_1 parameter was indeterminate, and this parameter was excluded in the final fits. As with YbCl, the quality of the fitted parameters can be assessed by comparison of ratios for different isotopomers with corresponding theoretical ratios; such comparisons are given in Table 5.5. The experimental values are in excellent agreement with the calculated theoretical ratios; except for eQq discrepancies are about one standard error.

5.4 Discussion

5.4.1 Hyperfine Parameters

The spins of the various nuclei are $I = 0$ for $^{172,174}\text{Yb}$, $I = 1/2$ for ^{19}F , and $I = 3/2$ for $^{35,37}\text{Cl}$ and $^{79,81}\text{Br}$. Thus, for all the species investigated the hyperfine effects pertain

Table 5.4

Fitted parameters^a (MHz) for the $\nu = 0$ levels of $^{174}\text{Yb}^{79}\text{Br}$ and $^{174}\text{Yb}^{81}\text{Br}$.

	$^{174}\text{Yb}^{79}\text{Br}$	$^{174}\text{Yb}^{81}\text{Br}$
B_0	1328.2826(2)	1305.7381(2)
$10^3 D_0$	0.2736(23)	0.2603(20)
γ_0	115.9116(32)	113.9469(28)
eQq	25.41(10)	20.64(10)
b_F	157.455(32)	169.771(26)
c	133.649(58)	143.962(77)

All uncertainties (1σ) given in parentheses in units of the least significant digit of the corresponding parameters.

Table 5.5

Experimental and theoretical ratios for the fine and hyperfine parameters of $^{174}\text{Yb}^{79}\text{Br}$ and $^{174}\text{Yb}^{81}\text{Br}$.

	Experimental	Theoretical ^a
R_γ ^a	0.98303(4)	0.98301
R_{b_F}	1.0782(3)	1.0779
R_c	1.0772(9)	1.0779
R_{eQq}	0.812(6)	0.834

^aThe quantities R_X are the ratios of $X(^{174}\text{Yb}^{81}\text{Br})/X(^{174}\text{Yb}^{79}\text{Br})$. The theoretical ratios are those of the following:

γ : the ratios of the reduced masses of the isotopomers; b_F , c : the ratios of the ^{79}Br and ^{81}Br nuclear magnetic moments; eQq : the ratios of the ^{79}Br and ^{81}Br nuclear quadrupole moments. These were calculated from the data in Ref. 53.

solely to the halide nucleus. The Fermi-contact parameter, b_F , can be expressed [21] as a product of nuclear and electronic properties, and the unpaired spin electron density at the halide nucleus, $|\Psi(0)|^2$. Similarly, the dipole-dipole parameter, c , is proportional [21] to the expectation value $\langle(3\cos^2\Theta-1)/r^3\rangle$, where r is the vector separation between the unpaired electron and the halide nucleus, making an angle Θ with the molecular axis. In SI units:

$$b_F = \frac{2\mu_0}{3} g_e g_N \mu_B \mu_N |\Psi(0)|^2 \quad 5.4$$

and

$$c = \frac{3\mu_0}{8\pi} g_e g_N \mu_B \mu_N \langle(3\cos^2\Theta-1)/r^3\rangle. \quad 5.5$$

Here g_e and g_N are the electronic and nuclear g -factors respectively; μ_B is the Bohr magneton, and μ_N is the nuclear magneton.

Using parameters from Ref. 53, values for $|\Psi(0)|^2$ and $\langle(3\cos^2\Theta-1)/r^3\rangle$ were calculated, and are presented in Table 5.6. It can be seen that there is a trend whereby the unpaired spin density approximately doubles for each successive halide. This trend is also true of the expectation value $\langle(3\cos^2\Theta-1)/r^3\rangle$.

Comparison of the experimental values for $|\Psi(0)|^2$ and $\langle(3\cos^2\Theta-1)/r^3\rangle$ with values calculated for the corresponding halogen atoms yields insight into the fraction of halide s and p_z occupation of the unpaired electron. The halogen atom calculations were performed by Morton and Preston [58], and as mentioned in their paper, corrections were applied to the values of $|\Psi(0)|^2$ to account for relativistic effects. As well, the expectation values for angular dependence $\langle(3\cos^2\Theta-1)\rangle$ of the p_z orbital and $\langle r^{-3}\rangle$ for the halogen

Table 5.6

Trends in unpaired halide spin density in the $X^2\Sigma^+$ ground states of YbF, YbCl and YbBr.

	^{174}YbF	$^{174}\text{Yb}^{35}\text{Cl}$	$^{174}\text{Yb}^{79}\text{Br}$
b_F /MHz	170.2637	31.34	157.45
$ \Psi(0) ^2$ /a.u. ⁻³	0.04047	0.07147	0.14011
$\rho(s)$ /%	0.3221	0.5475	0.4906
c /MHz	85.403	22.11	133.65
$(3\cos^2\Theta-1)/r^3$ /a.u. ⁻³	0.13366	0.2816	0.6644
$\rho(p)$ /%	1.6166	4.196	5.446

atom were combined. The percentage occupations for all three halides are presented in Table 5.6. It can be seen that there is a trend towards increasing amounts of both s and p character with each consecutive halide. The actual percentages are very small, consistent with the unpaired electron being located almost entirely on the Yb atom. It is interesting to note that a similar trend has been observed by Bernath *et al.* [8] for the corresponding series of calcium mono-halides.

A measure of the ionic character of the ytterbium halides can be obtained from the formula given by Gordy and Cook [19]:

$$i_c = 1 + \frac{eQq_{\text{exp}}}{eQq_{n10}}, \quad 5.6$$

where eQq_{exp} is the experimentally determined quadrupolar coupling parameter, and eQq_{n10} is the coupling parameter for an np_z electron in the n^{th} subshell of the halide ($eQq_{310}(^{35}\text{Cl}) = 109.74$ MHz, $eQq_{410}(^{79}\text{Br}) = -769.76$ MHz [19]). Values of $100 \cdot i_c$ are given for the chlorides and bromides of ytterbium, magnesium and calcium in Table 5.7. The ionic character of YbBr was found to be slightly less than that of YbCl; this result is consistent with the lower electronegativity of Br, and the corresponding decrease, also shown in Table 5.7, for the Mg and Ca analogs [8-11].

The overall results obtained from all three hyperfine parameters are in accord with a highly ionic character for the YbX species, with the unpaired electron essentially localized on the metal center. This is in excellent agreement with the M^+X^- character inferred from previous studies for alkaline earth metal – halides [8].

Table 5.7

Comparison of percentage ionic character for the $X^2\Sigma^+$ ground states of alkaline earth (MX) and YbX molecules ($X = F, Cl, Br$).

M	M ³⁵ Cl	M ⁷⁹ Br
Yb	98.52	96.74
Mg	89.41 ^b	85.67 ^c
Ca	99.09 ^d	97.40 ^e

^aCalculations were performed using the method of Ref. 19, see text.

^bRef. 10; ^cRef. 11; ^dRef. 9; ^eRef. 8.

5.4.2 Bond Lengths

The rotational parameters determined in the present work have been used to determine estimates of the internuclear bond lengths. Considerable care must be taken in assessing the physical significance of these bond lengths, owing to their very high accuracy of seven or eight figures. Accordingly, careful consideration was given to the factors that contribute to the “raw” bond lengths.

In the first place, the small standard errors obtained in Eqs. 5.2 and 5.3 for the B_e values of ^{174}YbF and $^{174}\text{Yb}^{35}\text{Cl}$, and in Table 5.4 for the B_0 values of $^{174}\text{Yb}^{79}\text{Br}$ and $^{174}\text{Yb}^{81}\text{Br}$, are related directly to the high precision and accuracy of the FTMW technique and to the success of the model Hamiltonian in representing the data. The standard errors are in the range 0.15-0.36 ppm, similar to that found [11] for MgBr ($X^2\Sigma^+$), but larger than those (~ 0.04 ppm) found by Gerry *et al.* [59-61] from the spectra of molecules with $^1\Sigma^+$ ground states.

It is well known [18,62] that the fitted B_e values cannot be used directly to calculate meaningful bond lengths with correspondingly small errors. The experimentally determined B_e -values are in fact Dunham Y_{01} coefficients, and small corrections must be made

$$B_e = Y_{01} - \Delta Y_{01}^{\text{Dunham}} + \Delta Y_{01}^{\text{non-adiabatic}} \quad 5.7$$

Reliable estimates of the nonmechanical contributions from second-order nonadiabatic effects, $\Delta Y_{01}^{\text{non-adiabatic}}$, would require data for isotopomers with substitution at both nuclear centres. As no such data are available, estimates of the magnitude of this correction cannot be made.

The Dunham correction has been considered previously by Watson [62], and is

given as

$$\Delta Y_{01}^{\text{Dunham}} = \frac{B_e^3}{4\omega_e^2} \left[\frac{Y_{10}^2 Y_{21}}{4Y_{01}^3} + 16a_1 \left(\frac{Y_{20}}{3Y_{01}} \right) - 8a_1 - 6a_1^2 + 4a_1^3 \right], \quad 5.8$$

where a_i , the expansion parameters of the Dunham potential [63], can be expressed in terms of the Dunham coefficients, Y_{kl} , as presented in the following summation of rotational (or order l) and vibrational (of order k) energy contributions¹.

$$E_{\omega J} = \sum_{kl} Y_{kl} \left(\nu + \frac{1}{2} \right)^k (J(J+1))^l. \quad 5.9$$

Using Eq. 5.8, with a_1 defined by $a_1 = Y_{11}Y_{10}/(6Y_{01}^2 - 1)$ [63], the corrections to the bond lengths from $\Delta Y_{01}^{\text{Dun}}$ are found as $2.6(3) \times 10^{-6}$ (1.3 ppm) and $9.6(3) \times 10^{-6}$ Å (3.9 ppm) for ^{174}YbF and $^{174}\text{Yb}^{35}\text{Cl}$, respectively². The largest source of error is from the uncertainty of the Y_{21} (γ_e^ν) values (estimated at $-1.0(5) \times 10^{-3} \cdot \alpha_e^\nu$), derived above in the first term of Eq. 5.8.

In addition to the Dunham correction, it is necessary to consider the magnitude of systematic error introduced by the assumption in Eqs. 5.2 and 5.3 of a linear variation of B_ν with ν . Since the present data for YbF and YbCl are obtained only for the $\nu = 0$ and 1 levels, the contribution of the γ_e^ν -term in Eq. 2.12, is absorbed in the derived B_e and α_e^ν values. If the vibration-rotational parameter γ_e^ν is held fixed at an estimated value of $-1.0(5) \times 10^{-3} \cdot \alpha_e^\nu$ (a value that is typical of those found for alkaline earth halides), the

¹ Each Dunham parameter has an *approximate* relationship with a vibrational and/or rotational parameter. For example, $Y_{01} \approx B_e$, and it can be shown that $Y_{11} \approx -\alpha_e^\nu$, $Y_{21} \approx \gamma_e^\nu$, $Y_{10} \approx \omega_e$ and $Y_{20} \approx -\omega_e x_e$.

² These values are based on the vibrational parameters $Y_{10} = 506.6674(77)$ and $Y_{20} = -2.2451(34)$ cm^{-1} obtained by Dunfield *et al.* [47] for ^{174}YbF , and $Y_{10} = 294.24(42)$ and $Y_{20} = -0.944(2)$ cm^{-1} obtained by Lee and Zare [64] for YbCl.

calculated bond lengths of YbF and YbCl are decreased by $\approx 5.1 \times 10^{-6}$ and $\approx 4.0 \times 10^{-6}$ Å, respectively. Uncertainty in the assumed γ_e^v values introduces an uncertainty, then, of about 2.0×10^{-6} Å, or about 1.0 ppm, in the calculated bond lengths. This is about ten times the uncertainty introduced by the standard errors associated with the fitted B_e parameters.

Errors associated with the fundamental constants, recommended by CODATA in the 1998 paper of Mohr and Taylor [65], must also be considered. Expressions for bond length calculation are given as

$$R_e(\text{Å}) = C_1 [B_e(\text{cm}^{-1})\mu]^{-1/2}, \quad 5.10$$

or

$$R_e(\text{Å}) = C_2 [B_e(\text{MHz})\mu]^{-1/2}, \quad 5.11$$

where

$$C_1 = \sqrt{\frac{10^{21} h N_A}{8\pi^2 c}}, \quad 5.12$$

and

$$C_2 = \sqrt{\frac{10^{17} h N_A}{8\pi^2}}. \quad 5.13$$

with h , N_A and c being Planck's constant, Avogadro's number and the speed of light (m/s), respectively.

Using the 1998 set of constants [65], the uncertainties in N_A and h can be reduced by using the approach of Le Roy [66] and substituting

$$hN_A = cM_e\lambda_c, \quad 5.14$$

where λ_c is the Compton wavelength and M_e is the molar electron mass. This gives

$C_1 = 4.105\,804\,317(14) \text{ \AA cm}^{-1/2} u^{1/2}$ and $C_2 = 710.900\,137\,9(25) \text{ \AA MHz}^{1/2} u^{1/2}$, with a relative uncertainty of ≈ 0.0035 ppm. This is outside of the precision of the present study, but may be an important consideration in the study of $^1\Sigma^+$ states.

Finally, uncertainties associated with the atomic masses from the 1993 compilation of Audi and Wapstra [67] have been considered, and are typically ≈ 0.03 ppm, approaching the estimated uncertainty of fitted B_e values.

From Eqs. 5.2 and 5.3, the equilibrium bond lengths have been calculated for ^{174}YbF and $^{174}\text{Yb}^{35}\text{Cl}$, respectively, using Eq. 5.11. These are presented in Table 5.8 both with, and without the application of the estimated corrections as R_e^{corr} and R_e^{raw} , respectively. For YbBr, for which only B_0 values have been determined (Table 5.4), ground state effective (R_0) values have been obtained for $^{174}\text{Yb}^{79}\text{Br}$ and $^{174}\text{Yb}^{81}\text{Br}$, also given in Table 5.8.

One other consideration in the calculation of bond lengths is due to the isotopic *field effect*. Discussed in more detail in the following chapter, this effect arises from a change in the nuclear charge distribution between isotopes of heavy atoms, such as ytterbium, the net result of which is $R_e^{174\text{YbX}} \neq R_e^{172\text{YbX}}$. This difference in bond lengths is only observable when more than one isotopomer of the heavy element, in this case ytterbium, is studied. Although there is insufficient data in the present study to observe such an effect, a brief description is given here for completeness.

Schlembach and Tieman [12] discuss both the mechanism of the *field effect*, and the associated magnitude for a single isotopomer, which is obtained as;

$$\delta R_e = -\left(\frac{C^{\text{FS}}}{k_e}\right)\left(\frac{d\rho_{\text{Elec}}(R)}{dR}\right)_{R_e} \langle r_{\text{NC}}^2 \rangle_a \quad 5.15$$

Table 5.8

Bond lengths (Å) calculated for ^{174}YbF , $^{174}\text{Yb}^{35}\text{Cl}$, $^{174}\text{Yb}^{79}\text{Br}$ and $^{174}\text{Yb}^{81}\text{Br}$. Corrected values (denoted as R_e^{corr}) are adjusted to account for the effects of truncation and the Dunham correction.

	^{174}YbF	$^{174}\text{Yb}^{35}\text{Cl}$	$^{174}\text{Yb}^{79}\text{Br}^{\text{a}}$	$^{174}\text{Yb}^{81}\text{Br}^{\text{a}}$
R_e^{raw}	2.0165167(2)	2.4882877(4)	2.6473645(2)	2.6473477(2)
R_e^{corr}	2.016514(2)	2.488293(2)		

^aValues given are for R_0 .

where,

$$C^{\text{rFS}} = \frac{Z_x e^2}{6\epsilon_0}. \quad 5.16$$

In Eqs. 5.15 and 5.16, Z is the atomic number of isotope x , e is the proton charge, ϵ_0 is the permittivity of vacuum, and k_e is the vibrational force constant. Also present is the expectation value of the nuclear charge radius, r_{NC} , and the change in the electron density at the nucleus as a function of the change in R , is described by $d\rho_{\text{Elec}}(R)/dR$. (The definition of $\rho_{\text{Elec}}(R)$ is similar to $|\Psi(0)|^2$, but is for all electron density, and not only unpaired spin electron density.)

5.5 Conclusions

Rotational, fine and hyperfine effects have been characterized for the $X^2\Sigma^+$ ground states of several isotopomers of ytterbium monofluoride, monochloride and monobromide. Trends in the bonding characteristics of the ytterbium halides show that there is a small but increasing amount of unpaired spin density at the halide nucleus with increasing halide size.

Chapter 6

The $B^2\Sigma^+ \leftarrow X^2\Sigma^+$ System of YbBr

6.1 Background

Spectroscopic characterization of the low-lying electronic states of lanthanide-containing diatomic molecules, in particular several monohalide species [68-75], have been the focus of a number of electronic studies in recent years. The $4f^{14}6s^2$ ground state valence configuration of ytterbium makes it unique among the lanthanides, as it is similar to the ns^2 ground state configuration found in the alkaline earth metals. The alkaline earth metal monohalides have been the focus of numerous studies [2-5,32,35,36], making the analogous ytterbium monohalides an interesting class of molecules for investigation and comparison.

As discussed in chapter 5, the low-lying electronic states of the metal halides, MX, (where M = Ca, Sr, Ba or Yb and X = F, Cl, Br or I) have a high degree of ionic character, with the unpaired electron predominantly localized on the metal center [76], i.e. M^+X^- . This unpaired metal electron largely governs the electronic symmetry of the arising molecular states [70], and as such, several electronic states of the ytterbium halides, most notably the ground states, adopt symmetries analogous to those of the well-studied alkaline earth metal halides.

In contrast with the alkaline earth metal halides, however, ytterbium-containing diatomic molecules have additional low-lying electronic states that arise from the promotion of a $4f$ electron into higher valence orbitals, leading to an open $4f$ sub-shell. Such states have been observed directly [47,77] and indirectly [46-48] through perturbations with neighboring state(s). An example of this is YbF, where the $A^2\Pi$ and

$X^2\Sigma^+$ states are perturbed by electronic states arising from the promotion of $4f$ electrons [47].

Recently, a theoretical study on the low-lying electronic states of various lanthanide monohalides has been carried out using a ligand field model [70], and experimentally, several of the electronic states of YbF and YbCl have been vibrationally characterized [52,78-82] by employing both emission and absorption spectroscopic techniques. The 1978 study of Kramer [52] and the 1995 study by Uttam and Joshi [83] represent the only vibrational studies of the heavier YbBr and YbI molecules. In Kramer's original study of YbBr, several emission bands were assigned to the $A^2\Pi \rightarrow X^2\Sigma^+$ system, and three bands were tentatively assigned to the $B^2\Sigma^+ \rightarrow X^2\Sigma^+$ system. High-resolution studies of ytterbium halides have been performed on the $A^2\Pi$ [46-49] and $X^2\Sigma^+$ [46-48,76] states of YbF, the $B^2\Sigma^+$ [51], $A^2\Pi$ [50] and $X^2\Sigma^+$ [50,51,76] states of YbCl, and the $X^2\Sigma^+$ [76] state of YbBr.

A rotational analysis of the $B^2\Sigma^+ \leftarrow X^2\Sigma^+$ $0 - 0$, $1 - 0$, $0 - 1$ and $1 - 1$ bands for the four major isotopomers of YbBr, namely $^{174}\text{Yb}^{79}\text{Br}$, $^{174}\text{Yb}^{81}\text{Br}$, $^{172}\text{Yb}^{79}\text{Br}$ and $^{172}\text{Yb}^{81}\text{Br}$, is the subject of the present work. A linear least squares fitting program was developed to simultaneously model data for all four bands and four isotopomers, producing a single set of isotopically consistent parameters.

6.2 Experimental Arrangement

All experiments on the $B - X$ system were carried out at the University of New Brunswick (UNB). Gas phase YbBr was produced in a Broida oven, described in chapter 3. A mixture of approximately equal amounts of AlBr_3 and ytterbium metal was

resistively heated to produce YbBr vapor, which was carried by argon gas (4-5 torr) into the observation area of the oven. The output of a *Coherent 699-29* ring dye laser operating in single frequency mode with coumarin 480 dye and pumped by a *Coherent Innova Sabre* argon ion laser was used to probe the YbBr radicals. Laser induced fluorescence was observed perpendicular to the probe laser beam, and focused onto the entrance slit of a 0.5-m *Jarell-Ash* spectrometer equipped with a small photomultiplier tube. The absorption spectrum of either molecular iodine or atomic uranium was recorded simultaneously, and lines were compared with the appropriate atlas [30,33] to calibrate the spectral features of YbBr to within 0.004 cm^{-1} .

6.3 Results

6.3.1 General Description of Spectra

In each band, four of the six allowed branches increase in J to the blue of the band origin and are completely overlapped, making observation of individual unblended low- J lines impossible. Spectral lines in these branches could only be resolved at higher values of J , which is where initial efforts were focused. The P_1 and Q_1 branches (see Figure 2.4) form heads to the red of the band origin, and, although much less congested than the main head, lines from these branches were typically overlapped both with one another as well as with other isotopomers, making unequivocal assignment of the rotational structure difficult.

From initial survey work on the $B^2\Sigma^+ \leftarrow X^2\Sigma^+$ system, it was apparent that the previous assignments tentatively proposed by Kramer [52] were incorrect. The observed isotope shifts of both the P_1 and Q_1 heads, and the much more intense main heads, are not

consistent with Kramer's assignments for the 0 – 0 (19495.5 cm^{-1}), 0 – 1 (19303.5 cm^{-1}) and 1 – 1 (19516.4 cm^{-1}) bands. From estimated vibrational parameters [52] and measured isotope shifts, these have been reassigned in the present work as the 0 – 1, 0 – 2 and 1 – 2 bands, respectively.

6.3.2 Blended Spectral Lines

Owing to the 14 possible isotopomers of YbBr, and the small rotational parameter, $B \approx 0.045 \text{ cm}^{-1}$, which is similar for both states, the $B - X$ spectrum of YbBr is extremely congested. Analysis of YbBr spectra was further complicated by the similar line intensities of the isotopomers. The relative abundances of the four most prevalent isotopomers are 1.00, 0.97, 0.69 and 0.67 for the $^{174}\text{Yb}^{79}\text{Br}$, $^{174}\text{Yb}^{81}\text{Br}$, $^{172}\text{Yb}^{79}\text{Br}$ and $^{172}\text{Yb}^{81}\text{Br}$ isotopomers, respectively [53]. Because of the similarity of rotational B values between $^{174}\text{YbBr}$ and $^{172}\text{YbBr}$ isotopomers ($\sim 0.4\%$ different), and Yb^{79}Br and Yb^{81}Br isotopomers ($\sim 1.7\%$ different), the rotational spacing of lines varied only slightly between isotopomers of the same branch and at similar values of J .

As illustrated in Figure 6.1, blending of rotational lines into a single spectral feature, or "line", was observed frequently, owing to high spectral congestion, similarity of line intensities and spectral spacings between different isotopomers, and Doppler limited line widths. Although the presence of line blending is not unique to this molecule, these blended features remained unresolved over wide ranges of J -values, resulting in *blended branches*. Such blended lines were observed to be broadened up to three times the 0.02 cm^{-1} Doppler line width, and were found to contain as many as four

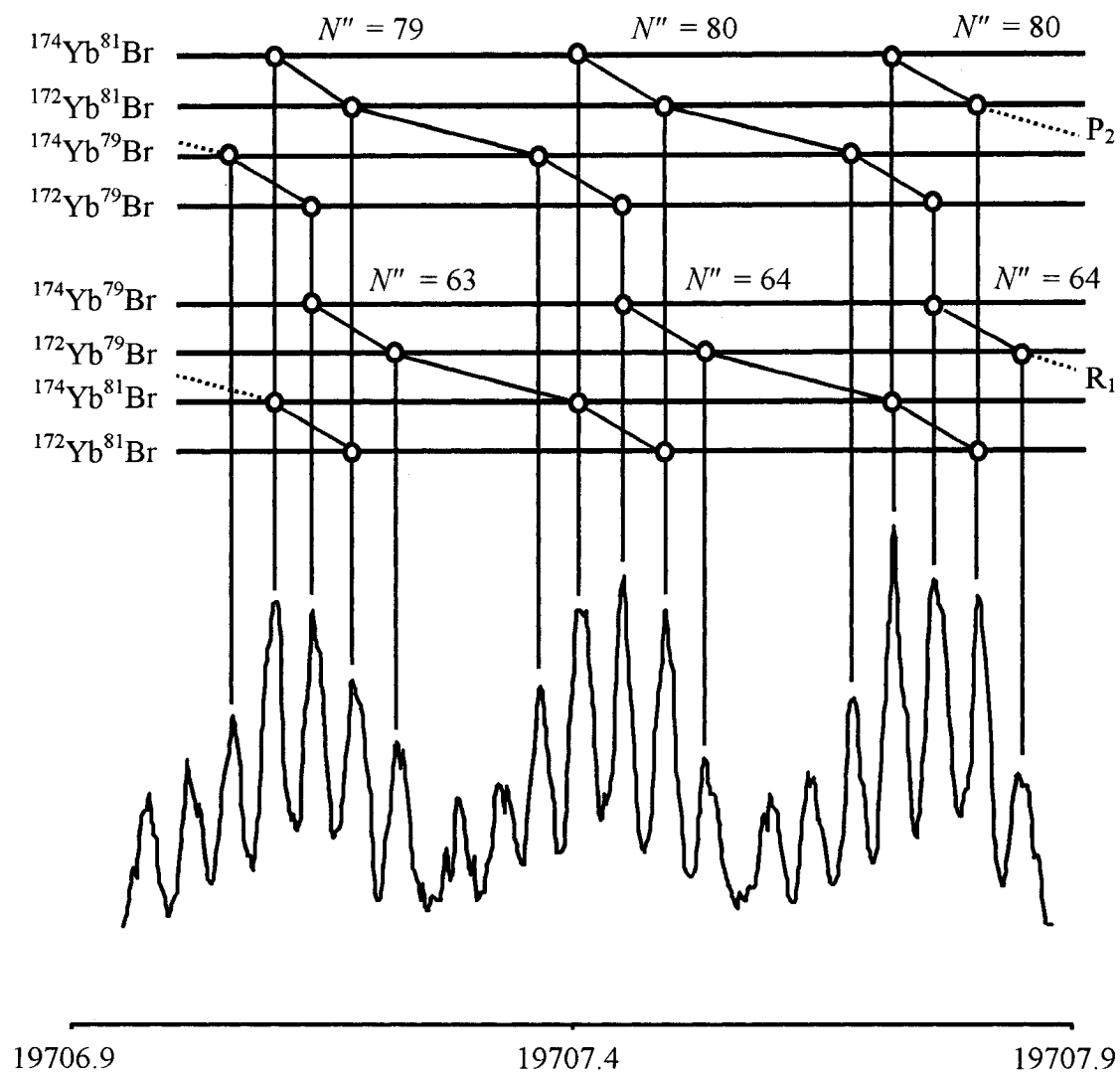


Figure 6.1 Part of the $0-0$ band of the $B \leftarrow X$ absorption spectrum of YbBr showing overlap of branches from different parity levels and different isotopomers.

individual lines simultaneously. The spectral shape of lines in these blended branches are an amalgamation of the individual line profiles, and can change dramatically with J , owing to the constituent lines changing both in intensity and in spectral separation relative to one another. It was not always obvious whether an individual line within a compounded profile would be detectable if it were unblended, thus casting doubt on the identification and subsequent assignment of individual lines within each profile.

Some of the spectral convolution was removed through selective detection of the same band, or by selectively detecting an alternate band that shared the same upper level. Because of the small spectral range of each band, (approximately 45 cm^{-1} , of which $\approx 90\%$ of the measured lines were within a 30 cm^{-1} range) the effectiveness of selective detection techniques was greatly reduced, and for many branches the observation of blended lines was unavoidable. In these instances, the intensity of individual lines within blended branches was estimated by the intensity of unblended lines from other isotopomers at similar values of J .

Owing to the increased uncertainty of line positions, the nearly identical B_v values for different isotopomers, and the nearly identical B_v values of both the X and B states, the assignment of spectral lines to values of J , and occasionally to the correct branch and isotopomer, could not be determined unequivocally from combination differences. It thus became apparent that the assignment of spectral lines required a more sophisticated method.

6.3.3 Rotational Assignment and Fitting Procedures

Lines in both the P_1 and Q_1 branches exhibit a high degree of blending, and, as mentioned above, combination differences calculated from lines in the well resolved R_1 branch did not provide unequivocal assignments. The assignment of lines in the P_2 and R_2/Q_2 ¹ branches using combination differences was even more equivocal, as both branches were blended.

Initial efforts to assign spectral lines focused only on the relatively large number of well-resolved R_1 lines that had been measured. By employing a model that ensured isotopic consistency between rotational and vibrational parameters² (as given in Table 2.4), it was hoped that unequivocal assignments of this single branch could be found, ultimately facilitating analysis of the remaining features of the spectra. Lines from the less abundant ¹⁷²YbBr isotopomers were also measured to ensure that the major features throughout the spectra would be assigned correctly.

As mentioned above, a least squares program was created to model the four bands for each of the four isotopomers simultaneously. Isotopically dependent expressions for the vibrational energy [16]

$$G(\nu) = \omega_e(\nu + \frac{1}{2}) - \omega_e x_e(\nu + \frac{1}{2})^2, \quad 6.1$$

and the rotational energy, given in Table 2.1(b), were employed to model the $B^2\Sigma^+$ and $X^2\Sigma^+$ states separately, in addition to a single, isotopically invariant term value, T_e . All parameters were identified with their respective equilibrium values given in Eq. 2.12.

¹ Lines in the R_2 branch are nearly identical in spacing with the Q_2 branch, differing by the relatively small spin-rotation splitting in the ground $X^2\Sigma^+$ state, and thus they are often grouped together as R_2/Q_2 .

² Implicit in this is that the vibrational combination differences are ensured, for example:
 $R_1(J) [0 - 0] - R_1(J) [0 - 1] = R_1(J) [1 - 0] - R_1(J) [1 - 1]$.

Initial efforts to assign R_1 lines required that the ground state parameters were fixed³ at the values of chapter 5. This procedure proved partially successful, as initial upper state parameters and rotational assignments could be determined from either the $^{174}\text{YbBr}$ isotopomer data set, or the $^{172}\text{YbBr}$ data set, but not from fits of all four isotopomers together.

Through examination of previous work [50,51] on the $A \leftarrow X$ and $B \leftarrow X$ systems of YbCl , a better understanding of the failings of this model were understood. Two observations were made: first, a small but statistically significant offset exists between observed and calculated isotope shifts of the $^{174}\text{YbCl}$ and $^{172}\text{YbCl}$ isotopomers, as shown in Table 6.1; and second, the fitted rotational parameters, B_v , and the vibrational parameters, α_v , were consistent with the relevant isotopomer relationships of Table 2.4. This evidence led to the development of a second model, and fitting program, in which each of the 16 band origins were fitted separately, while maintaining the appropriate isotopic relationship between all rotational and spin-rotational parameters. This model proved extremely successful, and simultaneous fits using data from all four isotopomers facilitated the final assignments of the R_1 lines unambiguously. From calculated line positions, assignments of blended lines in the P_1 branch were then made. Assignment of blended lines in the remaining P_2 , R_2 and Q_2 branches were made based on calculated line

³ The highly precise values of B_0'' , determined in Ref. [76], were used to estimate values of B_v'' and α_v'' as follows: assuming that the $^{174}\text{Yb}^{79}\text{Br}$ and $^{174}\text{Yb}^{81}\text{Br}$ isotopomers have identical potential energy curves, the two B_0'' values represent sampling at different vibrational energy, and thus can be used to calculate the vibrational dependence of the rotational B'' parameters. Unfortunately, the spin-rotation and centrifugal distortion parameters, γ_0'' and D_0'' , respectively, were not determined precisely enough to make analogous estimates, and the vibrational dependence of these parameters was initially assumed to be zero.

Table 6.1

Calculated ($\Delta\nu_{\nu'\nu''}^{\text{BO}}$) and observed ($\Delta\nu_{\nu'\nu''}^{\text{Obs}}$) isotope shifts for bands in the $A - X$ and $B - X$ systems of YbCl.

Isotopomer	System (Band)	$\Delta\nu_{\nu'\nu''}^{\text{Obs}}$	$\Delta\nu_{\nu'\nu''}^{\text{BO}}$	$\delta\Delta\nu^{\text{a}}$	$\#\sigma^{\text{b}}$
[174/35]–[172/35] ^c	$A - X (1 - 0)^{\text{c}}$	–0.339(1)	–0.312	–0.027(1)	19
	$A - X (0 - 0)^{\text{c}}$	–0.036(1)	–0.011	–0.025(1)	18
	$B - X (1 - 0)^{\text{d}}$	–0.345(3)	–0.315	–0.030(3)	10
	$B - X (0 - 0)^{\text{d}}$	–0.0422(8)	–0.0114	–0.0308(8)	39

^a $\delta\Delta\nu = \Delta\nu_{\nu'\nu''}^{\text{Obs}} - \Delta\nu_{\nu'\nu''}^{\text{BO}}$

^b Calculated as $\delta\Delta\nu/\sigma_{\text{Obs}}$

^c Defined as $^{174}\text{Yb}^{35}\text{Cl} - ^{172}\text{Yb}^{35}\text{Cl}$

^d Ref [50]

^e Ref [51]

positions, and for the $^{174}\text{Yb}^{81}\text{Br}$ and $^{172}\text{Yb}^{81}\text{Br}$ isotopomers of the 1 – 0 band, from both calculated line positions and combination differences. Although the assignment of experimental lines using calculated line positions was not ideal, from empirical study it was found that the estimated upper-state parameters, determined from fits employing only R_1 lines, restricted the possible assignments of lines in the remaining branches. In fact, fits employing an assignment of $\Delta J = \pm 1, 2$ in one of the remaining branches produced reduced standard deviations that were (~8-15%) larger, suggesting that the assignment of all lines had been made unequivocally⁴. Due to the complexity of many of the spectra recorded, only lines that could be identified with a definite branch pattern were used to fit molecular parameters. All line positions, their estimated uncertainties, and the associated differences from calculated values are given in Appendix III.

The final fitting program employed a weighted linear-least squares routine, where the weights were defined as the inverse squares of the estimated uncertainties. The uncertainty for each “line” was determined from estimates of the number of coincident lines: $\pm 0.004 \text{ cm}^{-1}$ for unblended lines, and $\pm 0.006 \text{ cm}^{-1}$ for 2 or more coincident lines. The use of weights allowed for the inclusion of blended lines, although it should be mentioned that a small degree of systematic error was introduced by including such lines in the fits. The effect of this systematic offset on the final parameter set, however, was almost completely cancelled by the inclusion of data for all four isotopomers in fits employing an isotopically consistent model.

The final weighted fit also allowed the ground state parameters of chapter 5 to be included in the fit as “data”, with the respective weights based on the estimated

⁴ Single isotopomer, single band fits gave negligible (<4%) differences between the reduced standard deviations of fits that altered the various branch assignments by $\Delta J = 0, \pm 1, \pm 2$.

uncertainty of each parameter. This approach was particularly beneficial, as estimates of the parameters D_0'' and γ_0'' from chapter 5 were not determined with sufficient precision such that these parameters could be held fixed, while the precision associated with the parameter B_0'' was much better than that which could be obtained from the present work.

Estimated parameters for both the B and X states are given in Table 6.2, with all parameters referenced to the $^{174}\text{Yb}^{79}\text{Br}$ isotopomer, and all 16 band origins determined individually. Table 6.3 compares the previous $v'' = 0$ parameter set of chapter 5 with values calculated from the parameters of Table 6.2.

From the B_e values given in Table 6.2, estimates of the equilibrium bond lengths for the B and X states of YbBr were calculated using Eqs 5.10 and 5.12 as 2.58275(1) and 2.645386(4) Å, respectively; atomic masses were obtained from Ref. [67].

6.4 Discussion

6.4.1 Isotopic Electronic Energy Shifts in YbBr: Evidence of Born Oppenheimer Breakdown in a “Heavy” Molecule?

As for YbCl, systematic differences have been found in the present work between calculated and observed isotope shifts for the $^{174}\text{YbBr}$ and $^{172}\text{YbBr}$ isotopomers. These offsets, or shifts, labeled as $\delta\Delta\nu$, were calculated for the four bands of the $B - X$ system of YbBr and are given in Table 6.4. The weighted average value for the B state of YbBr is calculated as $-0.0281(3) \text{ cm}^{-1}$, which can be compared with values of $-0.026(1) \text{ cm}^{-1}$ and $-0.0308(2) \text{ cm}^{-1}$, calculated from values in Table 6.1, for the A and B states of YbCl, respectively.

Table 6.2

Fitted parameters^a (cm^{-1}) from combined fits of the $0-0$, $0-1$, $1-0$ and $1-1$ bands of $^{174}\text{Yb}^{79}\text{Br}$, $^{174}\text{Yb}^{81}\text{Br}$, $^{172}\text{Yb}^{79}\text{Br}$ and $^{172}\text{Yb}^{81}\text{Br}$.

	B_e'	0.04655156(38)
	$\alpha_e' \times 10^4$	1.3415(16)
$^{174}\text{Yb}^{79}\text{Br}$	$D_e' \times 10^8$	9.038(52)
	γ_e'	-0.111636(17)
	$\gamma_D' \times 10^8$	6.03(27)
	B_e'	0.04437305(12)
	$\alpha_e' \times 10^4$	1.3262(24)
$^{174}\text{Yb}^{79}\text{Br}$	$D_e' \times 10^8$	9.126(47)
	γ_e'	0.0038377(52)
	$\alpha_\gamma'' \times 10^5$	5.8(11)
	ν_{00}	19696.378(1)
$^{174}\text{Yb}^{79}\text{Br}$	ν_{01}	19500.747(1)
	ν_{10}	19910.641(1)
	ν_{11}	19715.030(1)
	ν_{00}	19696.293(1)
$^{174}\text{Yb}^{81}\text{Br}$	ν_{01}	19502.326(1)
	ν_{10}	19908.738(1)
	ν_{11}	19714.789(1)
	ν_{00}	19696.422(1)
$^{172}\text{Yb}^{79}\text{Br}$	ν_{01}	19500.439(1)
	ν_{10}	19911.074(1)
	ν_{11}	19715.114(1)
	ν_{00}	19696.337(1)
$^{172}\text{Yb}^{81}\text{Br}$	ν_{01}	19502.015(1)
	ν_{10}	19909.171(1)
	ν_{11}	19714.870(1)
	$\hat{\sigma}$	1.0744
	# Lines	1506

^aAll parameters are referenced to the $^{174}\text{Yb}^{79}\text{Br}$ isotopomer, except for the band origins.

Table 6.3

Comparison of $\nu = 0$ parameters from chapter 5 (P_{C5}), and calculated from values of Table 6.2 (P_{C6}).

		P_{C5}	$P_{C6} - P_{C5}$	$\#\sigma^a$
$^{174}\text{Yb}^{79}\text{Br}$	B_0	0.0443067380(67)	1.58E-10	0.0
	$10^9 D_0$	9.126(77)	4.58E-13	0.0
	γ_0	0.00386639(11)	-2.15E-07	2.0
$^{174}\text{Yb}^{81}\text{Br}$	B_0	0.0435547350(67)	-1.02E-10	0.0
	$10^9 D_0$	8.683(67)	-1.36E-10	2.0
	γ_0	0.003800859(93)	1.67E-07	1.8

^aCalculated as $|(P_{C6} - P_{C5})/(\sigma_{C5})|$

Table 6.4

Calculated ($\Delta\nu_{v'v''}^{\text{BO}}$) and observed ($\Delta\nu_{v'v''}^{\text{Obs}}$) isotope shifts for bands in the $B-X$ system of YbBr.

Isotopomer	System (Band)	$\Delta\nu_{v'v''}^{\text{Obs}}$	$\Delta\nu_{v'v''}^{\text{BO}}$	$\delta\Delta\nu^{\text{a}}$	$\#\sigma^{\text{b}}$
[174/79]-[172/79] ^c	$B-X(1-0)$	-0.433(2)	-0.404	-0.029(2)	18
	$B-X(0-0)$	-0.044(1)	-0.017	-0.027(1)	14
	$B-X(0-1)$	0.308(2)	0.337	-0.029(2)	22
	$B-X(1-1)$	-0.084(2)	-0.051	-0.033(2)	21
[174/81]-[172/81] ^c	$B-X(1-0)$	-0.433(1)	-0.408	-0.025(1)	17
	$B-X(0-0)$	-0.044(2)	-0.017	-0.027(2)	15
	$B-X(0-1)$	0.311(1)	0.340	-0.029(1)	21
	$B-X(1-1)$	-0.081(1)	-0.051	-0.030(1)	22
[174/79]-[174/81] ^c	$B-X(1-0)$	1.903(2)	1.899	-0.004(2)	2
	$B-X(0-0)$	0.085(2)	0.080	0.005(2)	3
	$B-X(0-1)$	-1.579(1)	-1.581	0.002(1)	2
	$B-X(1-1)$	0.241(2)	0.238	-0.003(2)	2
[172/79]-[172/81] ^c	$B-X(1-0)$	1.903(1)	1.895	0.008(1)	7
	$B-X(0-0)$	0.085(1)	0.080	0.005(1)	4
	$B-X(0-1)$	-1.576(1)	-1.578	0.002(1)	2
	$B-X(1-1)$	0.244(1)	0.238	0.006(1)	6

$$^{\text{a}} \delta\Delta\nu = \Delta\nu_{v'v''}^{\text{Obs}} - \Delta\nu_{v'v''}^{\text{BO}}$$

^bCalculated as $\delta\Delta\nu/\sigma_{\text{Obs}}$

^cDefined as $[x/y] - [x'/y'] \equiv {}^x\text{Yb}^y\text{Br} - {}^{x'}\text{Yb}^{y'}\text{Br}$

Vibrational perturbations are often observed in metal-containing diatomic molecules, the result of which would be deviations from the expected isotope shifts. This was the case for YbO [77], and it was initially thought that perturbations were the main cause of the observed differences in YbBr and YbCl. Certain characteristics, however, prompted further investigation:

1. There appears to be negligible deviation from calculated isotope shifts for the $\text{Yb}^{79}\text{Br} - \text{Yb}^{81}\text{Br}$ isotopomers. Homogeneous interactions with a perturbing state would cause the isotope shift to be similar, or possibly greater, for bromine isotopomers than for ytterbium isotopomers [17]. This is not the case as the calculated shifts between bromine isotopomers agree well with experimental values.
2. The vibrational parameters are isotopically consistent within each state. Table 6.5 shows calculated values for ω_e and $\omega_e x_e$, for both the X and B states of YbBr. As was the case for YbCl [50,51], all parameters were found to be isotopically consistent with one another. Again, a homogeneously perturbing state would likely cause the vibrational spacings to be inconsistent. This would imply that the observed difference is in the electronic energy of the ytterbium isotopomers, and not due to a difference of vibrational energy.
3. The magnitude and sign of the difference between calculated and observed isotope shifts of ytterbium isotopomers is similar for both the $A - X$ and $B - X$ systems of YbCl and the $B - X$ system of YbBr. This also would be consistent with an electronic effect, as both the $A^2\Pi$ and $B^2\Sigma^+$ states in the ytterbium halides are predicted to arise from the $6p\pi$ and $6p\sigma$ orbitals, respectively, of the $\text{Yb}^+(4f^{14}6p)X^-$ configuration ($X \equiv \text{halogen}$), while

Table 6.5Calculated vibrational constants for the B and X states of YbBr.

		$^{174}\text{Yb}^{79}\text{Br}$	$^{174}\text{Yb}^{81}\text{Br}$	$^{172}\text{Yb}^{79}\text{Br}$	$^{172}\text{Yb}^{81}\text{Br}$
$B^2\Sigma^+$	ω_e^a	215.229(2)	213.394(2)	215.621(2)	213.790(2)
	$\omega_e x_e^b$	0.483(1)	0.475(1)	0.485(1)	0.478(1)
	$\omega_e/\omega_e^{174/79}$	1.00000	0.99147(1)	1.00182(1)	0.99331(1)
$X^2\Sigma^+$	ω_e^a	196.521(2)	194.846(2)	196.876(2)	195.201(2)
	$\omega_e x_e^b$	0.455(1)	0.448(1)	0.458(1)	0.451(1)
	$\omega_e/\omega_e^{174/79}$	1.00000	0.99147(1)	1.00181(1)	0.99328(1)
Theoretical	$\omega_e/\omega_e^{174/79}$	1.00000	0.99147	1.00182	0.99330

^aCalculated from values of ω_0 and $\omega_e x_e$ ^bCalculated in an iterative fashion using the Pekeris relationship and experimental values of B_e , α_e , and ω_0 [16]

the $X^2\Sigma^+$ ground state for both molecules arises from a $\text{Yb}^+(4f^{14}6s)X^-$ configuration [51]. It would seem unlikely that this effect could be the result of perturbations affecting two different states, and two different analogous molecules by essentially the same amount.

A shift in the isotopic electronic energy of YbBr would be inconsistent with the well-known Born-Oppenheimer (BO) approximation, and an alternate explanation of this phenomenon was sought. Initial efforts focused on results for atomic ytterbium, specifically the Yb^+ ion. Mårtensson-Pendrill *et al.* [84] have performed a study of the hyperfine structure in the 369.4 nm $\text{Yb}^+ 6s - 6p_{1/2}$ transition; measurable differences in transition energy were found between the various isotopes. The measured shift between atomic lines of $^{174}\text{Yb}^+$ and $^{172}\text{Yb}^+$ isotopes was reported in Ref. [84] as $-0.04254(2) \text{ cm}^{-1}$, and both the relative magnitude and sign are consistent with values obtained for YbCl and YbBr molecules. The shift reported in Ref. [84] was attributed to two phenomena, namely atomic *mass shifts* and *field shifts* (alternately called *volume shifts*); these effects will now be considered for molecular spectra.

6.4.2 Mass Shifts – Born-Oppenheimer Breakdown

In the spectroscopy of “light” atoms, defined as atoms with $Z < 10$, there is a small but measurable effect due to the breakdown in the assumption that the nucleus is infinitely more massive than that of the electron(s). In reality the nucleus and electron(s) orbit about the center of mass, rather than the electron(s) orbiting about a “fixed” nucleus, causing a slight mass dependent shift in the electronic energy, known as the mass shift [85].

A similar effect is known for molecules, and is usually called Born-Oppenheimer breakdown [86]. In the Born-Oppenheimer approximation [16-18], the energetic contribution from mechanical, mass dependent, motion is separated from purely electronic, mass independent, interactions. Rotational and vibrational energies for a $^2\Sigma^+ - ^2\Sigma^+$ transition are described using Eq. 6.1 and Table 2.1(b), while electronic effects are described by a single parameter, T_e [16]. Shifts of the electronic energy between isotopomers are known for “lighter” molecules, and are an example of Born-Oppenheimer Breakdown (BOB). For such molecules, the contribution to the electronic term value is given as [86]

$$T_e = T_e^{\text{BO}} \left[1 + \left(\left(\Delta_x / M_x \right) + \left(\Delta_y / M_y \right) \right) \right], \quad 6.2$$

where $\Delta_{x,y}$ are mass independent isotope shift parameters for each atomic centre, $M_{x,y}$ are the masses of each atom (x or y), and T_e^{BO} is the term value calculated from the Born-Oppenheimer approximation.

The effects of mass shifts between $^{174}\text{YbBr}$ and $^{172}\text{YbBr}$ isotopomers can be determined from

$$\delta\Delta\nu^{\text{MS}} = \Delta T_e^{\text{BOB}} = T_e^{\text{BO}} \cdot \Delta_{\text{Yb}} \left(\left(1/M_{^{174}\text{Yb}} \right) - \left(1/M_{^{172}\text{Yb}} \right) \right). \quad 6.3$$

As described by McCaffrey *et al.* [15], it was shown that this could be approximated by

$$\delta\Delta\nu^{\text{MS}} = \Delta T_e^{\text{BOB}} \approx \left(B_e^{174} - B_e^{172} \right)_B \langle \hat{L}^2 \rangle_B - \left(B_e^{174} - B_e^{172} \right)_X \langle \hat{L}^2 \rangle_X. \quad 6.4$$

In this expression, B_e is the equilibrium rotational parameter of either $^{172}\text{YbBr}$ or $^{174}\text{YbBr}$, B and X denote the upper and lower electronic molecular states, respectively,

and $\langle \hat{L}^2 \rangle$ is the square of the orbital angular momentum. As outlined in Ref. [15], values of $\langle \hat{L}^2 \rangle$ can be estimated from

$$\langle \hat{L}^2 \rangle = [l_x(l_x + 1) + l_y(l_y + 1)], \quad 6.5$$

where l_i is the orbital angular momentum for atoms x and y at the asymptotic dissociation limit. Assuming YbBr molecules dissociate into ions for all relevant electronic states, the excited states arising from the $\text{Yb}^+(4f^{14}6p)\text{X}^-$ configuration will dissociate to give $\text{Yb}^+(^2\text{P})$ ($l_x = 1$) and $\text{X}^-(^1\text{S})$ ($l_y = 0$) products, while the ground state $\text{Yb}^+(4f^{14}6s)\text{X}^-$ configuration will dissociate to give $\text{Yb}^+(^2\text{S})$ ($l_x = 0$) and $\text{X}^-(^1\text{S})$ ($l_y = 0$) products. An estimate of the electronic offset due to a mass shifts is given as

$$\Delta T_e^{\text{BOB}} = \delta \Delta \nu^{\text{MS}} = -1.8 \times 10^{-4} \text{ cm}^{-1}, \quad 6.6$$

which is smaller in magnitude than the precision of the present experiments and is therefore unlikely to be the cause of the observed isotope shifts.

6.4.3 Field Shifts (*Volume Shifts*)

As outlined in the work of Kuhn [85], the nucleus of an atom is often treated as a point charge of zero volume. In reality, a nucleus has a finite, albeit small, nuclear charge volume, and the charges from the individual protons within that volume constitute a distribution. A difference in the volume of this nucleus, from isotopic substitution, causes a distinctive Coulombic potential that the electrons of each isotope experience: there is thus a possibility of a slight change in the difference of electronic energy between states. In “light” atoms, this difference in the distributed charge between isotopes is small, but as the volume of a nucleus increases in size, so too will differences in the

charge distributions. For “heavy” ($Z \geq 55$) atoms, the Coulombic difference will be observed as a difference of atomic transition energy when studied using high-resolution spectroscopic techniques.

In addition to the size of nuclear charge radii, the magnitude of this effect is also governed by the change in electron density at the nucleus between the electronic states observed in the transition [85]. As discussed in chapter 5, the electron density at the nucleus is representative of the amount of s orbital occupation for a given state, and a change in electron density at the nucleus will be greatest for transitions where the occupation of s orbitals change between electronic states, such as an $ns - np$ transition [85].

Molecular field shifts [12] are relatively unknown, though this effect has been observed in $PbCh$ ($Ch \equiv O, S, Se, Te$) [12-14], TlX ($X \equiv F, Cl, Br, I$) [12], and Cu_2 [15] molecules. The lack of literature on field shifts for diatomic molecules containing “heavy” atoms is not surprising, as highly precise molecular parameters for several bands and several isotopomers are required for such effects to be observed. Based on the large atomic mass of ytterbium, and the $Yb^+(4f^{14}6s)X^-$ and $Yb^+(4f^{14}6p)X^-$ configurations that give rise to the X and A/B states, respectively, the $A - X$ and $B - X$ transitions observed in ytterbium halides make ideal candidates to observe the field shift effect, and appear to be the cause of the offsets observed in Table 6.1 and 6.4.

6.4.4 Effects of Field Shifts on Bond Length

As outlined in Schlembach and Tiemann [12], the change in nuclear charge radii associated with field shifts will slightly alter the force constant, k_e , and the internuclear

distance, R_e , between isotopomers. As seen from Table 6.5, the magnitude of such an effect on k_e , and by extension ω_e , is below the accuracy of the present study. Of greater interest is the magnitude of δR_e , which was assumed to be zero in the combined isotopomer fit of Table 6.2. In the molecular Hamiltonian, the expression for the Coulomb electron-nuclear attraction energy operator is given, in atomic units, as [17]

$$V^{eN}(R) = -\sum_{i=1}^n \left(\frac{Z_x e^2}{r_{xi}} + \frac{Z_y e^2}{r_{yi}} \right) \quad 6.7$$

where each particle, either nucleus or electron, is treated as a point charge with zero volume. In this expression, Z is the atomic number for atoms x and y , e is the elementary unit of charge, and r is the electron-nucleus distance between nucleus “ x ” or “ y ” and each of the n electrons.

By replacing the nucleus-electron distance with a distribution for nucleus x , Schlembach and Tiemann [12] have evaluated the molecular Hamiltonian for a diatomic molecule with a single heavy atom. Their results show that the electronic field shift between molecules containing isotopes x and x' , is described by

$$\Delta T_e^{\text{FS}} / \text{cm}^{-1} = \delta \Delta v^{\text{FS}} / \text{cm}^{-1} = \frac{C^{\text{FS}}}{hc^*} \Delta \rho_{\text{Elec}} \cdot \delta \langle r_{\text{NC}}^2 \rangle_{\text{xx}'} \quad 6.8$$

$$\text{where, } \Delta \rho_{\text{Elec}} = \rho'_{\text{Elec}}(R'_e) - \rho''_{\text{Elec}}(R''_e), \quad 6.9$$

$$\delta \langle r_{\text{NC}}^2 \rangle_{\text{xx}'} = \langle r_{\text{NC}}^2 \rangle_{x'} - \langle r_{\text{NC}}^2 \rangle_x, \quad 6.10$$

$$\text{and } C^{\text{FS}} = \frac{Z_x e^2}{6\epsilon_0}, \quad 6.11$$

where ϵ_0 is the permittivity of vacuum, h is Planck's constant, c^* is the speed of light (in cm/s), and $\delta \langle r_{\text{NC}}^2 \rangle_{\text{xx}'}$ is the change in the mean square nuclear charge radius between

isotopomers x and x' , or in this case ^{174}Yb and ^{172}Yb , respectively. The electron density at the nucleus is given as

$$\rho_{\text{Elec}}(R) = \sum_{i=1}^N |\phi_i(0, R)|^2, \quad 6.12$$

with the parameter $\Delta\rho_{\text{Elec}}$ representing the *total* change in electron density between two states (e.g. X and B)⁵, given the individual electron orbital functions $\phi_i(0, R)$.

Ref. [12] defines the difference in equilibrium bond lengths between isotopomers as:

$$\delta R_e^{xx'} = \left(\frac{C^{\text{FS}}}{k_e} \right) \left(\frac{d\rho_{\text{Elec}}(R)}{dR} \right)_{R_e} \delta \langle r_{\text{NC}}^2 \rangle_{xx'}. \quad 6.13$$

For YbBr , an order of magnitude estimate of $\delta R_e^{174/172}$ can be easily made as follows [12]: $d\rho_{\text{Elec}}(R)$ can be approximated by $\Delta\rho_{\text{Elec}}(R)$, the difference in bond lengths between the B and X states, dR , can be roughly estimated as ΔR_e^{BX} , and the force constant k_e , was calculated to be 148.169(3) N/m from the values in Table 6.5. Eq. 6.13 can be approximated by

$$\delta R_e^{xx'} / \text{m} \approx \frac{C^{\text{FS}} \Delta\rho_{\text{Elec}} \delta \langle r_{\text{NC}}^2 \rangle_{xx'}}{k_e \Delta R_e^{BX}} = \frac{hc^* \delta \Delta\nu^{\text{FS}}}{k_e \Delta R_e^{BX}}. \quad 6.14$$

Assuming that the observed electronic isotope shift in YbBr is due entirely to the effects of the field shift, (i.e. $\delta \Delta\nu^{\text{FS}} = \delta \Delta\nu$ from Table 6.4), the upper limit of the difference in R_e values between $^{174}\text{YbBr}$ and $^{172}\text{YbBr}$ isotopomers is estimated at $\delta R_e^{174/172} \leq 6.0(4) \times 10^{-6} \text{ \AA}$. This is of the same order of magnitude as the estimated

⁵ This is similar to the value $\Delta|\Psi(0)|^2$ discussed in the microwave study of chapter 5, although the summation given in Eq. 6.12 is for *all* electron density at the nucleus and not just unpaired spin density.

uncertainty in the equilibrium bond lengths, and may account for a slightly higher $\hat{\sigma}$ in the combined isotopomer fit given in Table 6.2.

It is unfortunate that there have been no *ab initio* estimates of $\Delta\rho_{\text{Elec}}$ for either YbCl or YbBr, as this could provide further insight into the origin of the observed electronic isotope shifts. It is also regrettable that the *A* and *X* state of YbF [46-48] are perturbed, negating the possibility of observing this effect in a third ytterbium halide. However, work is currently underway in our laboratory to characterize YbI, though the extremely dense rotational structure may preclude the study of both ytterbium isotopomers.

6.5 Conclusions

The *B* ← *X* absorption spectrum of YbBr is extremely complicated, owing to the large number of isotopomers with similar (small) rotational parameters. A combined isotopomer fitting procedure was required to assign lines in the spectrum, and to estimate rotational parameters of the *B* state. The field shift effect was identified through observation of small shifts in the electronic energy between the $^{172}\text{YbBr}$ and $^{174}\text{YbBr}$ isotopomers. Calculations show that this effect might also be observable as a difference in the internuclear bond length, R_e , between the ytterbium isotopomers.

Chapter 7

The $A^2\Pi \leftarrow X^2\Sigma^+$ System of YbBr

7.1 Background

Previous work performed on ytterbium halides, and on analogous alkaline earth metal halides, has been outlined in chapters 5 and 6, and only a brief introduction will be given here.

The first spectroscopic study of YbBr was performed by Kramer [52], in which emission spectra were photo-electrically recorded, using a high-pressure, electrodeless microwave arc discharge source. Several violet degraded bands in the visible 500-575 nm region were observed, and assigned to either a $^2\Pi \rightarrow ^2\Sigma^+$ or a $^2\Sigma^+ \rightarrow ^2\Sigma^+$ transition, which were subsequently labeled as the $A - X$ and $B - X$ systems, respectively. From bands spanning $0 \leq \nu_{A,X} \leq 8$, estimates of the vibrational constants for the A and X states were determined. A more recent study of pure rotational spectra for the $\nu = 0$ level of the $X^2\Sigma^+$ state is discussed in chapter 5 (and Ref. [76]), and highly accurate estimates of the rotational B_0 values for the $^{174}\text{Yb}^{79}\text{Br}$ and $^{174}\text{Yb}^{81}\text{Br}$ isotopomers are provided.

The present work represents the first characterization of rotational fine structure within the $A^2\Pi$ state of YbBr, through study of rotational transitions of the $A^2\Pi \leftarrow X^2\Sigma^+$ system. More specifically, spectra of the 0 - 0 and 1 - 0 bands have been analyzed for both $^{174}\text{Yb}^{79}\text{Br}$ and $^{174}\text{Yb}^{81}\text{Br}$ isotopomers.

7.2 Experimental Arrangement

Experiments on the $A^2\Pi_{1/2} \leftarrow X^2\Sigma^+$ system were conducted at Dalhousie University, while studies of the $A^2\Pi_{3/2} \leftarrow X^2\Sigma^+$ system were carried out at the University of New Brunswick (UNB). All measured spectra were referenced to the standard iodine atlas [30] (with the offset of Ref. [31] applied), and the uncertainty of spectral lines was estimated at 0.004 cm^{-1} for both facilities.

7.2.1 Dalhousie Arrangement

Production of YbBr radicals was facilitated using a Broida oven, whereby vaporized ytterbium (*Strem*, 99.99%) was entrained in a flow of argon gas (4-5 torr) and reacted with CH_3Br , as outlined in chapter 3. The product YbBr molecules were probed using the output of a *Coherent 699-29* ring dye laser operating in single frequency mode, and pumped by either a *Coherent Innova 100* or *Coherent Innova Sabre* argon ion laser. Both Rhodamine 110 and Pyrromethene 556 dyes were used to produce the desired green laser light. Fluorescence was detected perpendicular to the incident laser beam, and focused onto the entrance slit of a 1.26 m *SPEX* spectrometer equipped with both a phase sensitive photoelectric arrangement, and a liquid nitrogen cooled CCD array detector (see chapter 3 for details).

7.2.2 UNB arrangement

Similar to the Dalhousie arrangement, a Broida oven was employed in the production of YbBr molecules. In this arrangement, however, ytterbium metal and aluminum tribromide were mixed in approximately equal amounts by mass, and then

resistively heated to produce gaseous YbBr molecules. The resulting molecules were carried into the observation area using a flow of argon gas, and total oven pressures were typically 4-5 torr.

The technique of laser ablation/supersonic expansion, outlined in chapter 3, was also used as a production source in this study. The output of a Nd:YAG laser, operating at the 2nd harmonic, was focused onto an ytterbium rod (*Goodfellow*, 99.9%), vapourizing the metal. This vapour was reacted with bromomethane (1-3% CH₃Br in 5-6 atmospheres Ar) to produce the desired YbBr molecules, which were then pulsed into the ultra low-pressure cavity (maintained using a diffusion pump) at supersonic velocities. The output of a *Coherent 699-29* ring dye laser, using Coumarin 480 dye and pumped by a *Coherent Innova Sabre* operating in the UV, was used to probe the YbBr radicals.

7.3 Results

7.3.1 General Description of Spectra

The P₁₂ and P₂₂ branches (see Figure 2.3), for the $A^2\Pi_{1/2} \leftarrow X^2\Sigma^+$ and $A^2\Pi_{3/2} \leftarrow X^2\Sigma^+$ systems, respectively, were both observed to increase in J to the red of the band origin and formed heads at $J \approx 54.5$ and 38.5 , respectively. Similar to the branch structure in the $B - X$ system, the remaining branches in each system are overlapped, increasing in J to the blue of the band origin and thus making assignment of rotational lines in these branches impossible at low values of J .

As was observed in spectra of the $B - X$ system, rotational lines in many of the branches were blended systematically into single features, which remained unresolved over a wide range of J values (see section 6.3.2). An example of this is shown in Figure

7.1, where lines from two branches of two different ytterbium isotopomers are coalesced. This blending of lines caused problems in assigning spectral lines, particularly in bands of the $A^2\Pi_{3/2} \leftarrow X^2\Sigma^+$ system, and thus fits employing blended lines were weighted based on the estimated uncertainty of each line: $\pm 0.004 \text{ cm}^{-1}$ for unblended lines, $\pm 0.006 \text{ cm}^{-1}$ for two blended lines and $\pm 0.008 \text{ cm}^{-1}$ for three (or more) blended lines. A model containing isotopically consistent parameters was also employed to offset the effects of line blending, and to aid in the assignment of rotational lines.

7.3.2 The $A^2\Pi_{1/2} \leftarrow X^2\Sigma^+$ System

From preliminary estimates of the A state parameters¹, and the known ground state parameters reported in chapter 5, it was predicted that two of the six branches in this system, P_{12} and R_{11} , could be observed in isolation using the technique of selective detection [32]. The remaining four branches in this system, however, were predicted to occur as pairs (Q_{11}/R_{12} and P_{11}/Q_{12}), which could not be isolated owing to both branches within the pair having similar² line spacings. Spectral analysis of these branches would thus be considerably more challenging, and so initial efforts focused on recording spectral lines in the P_{12} and R_{11} branches alone, through selective detection of the Q_{11}/R_{12} and P_{11}/Q_{12} branch pairs, respectively.

Selectively detected spectra of the R_{11} branch showed lines in this branch that were typically well resolved and exhibiting the expected isotopomer intensity patterns. Resolved fluorescence spectra of lines in this branch, however, were often complicated

¹ Based on the previous study of YbCl [50].

² For a given value of J , they differ by only the relatively small ground state spin-rotation splitting [16].

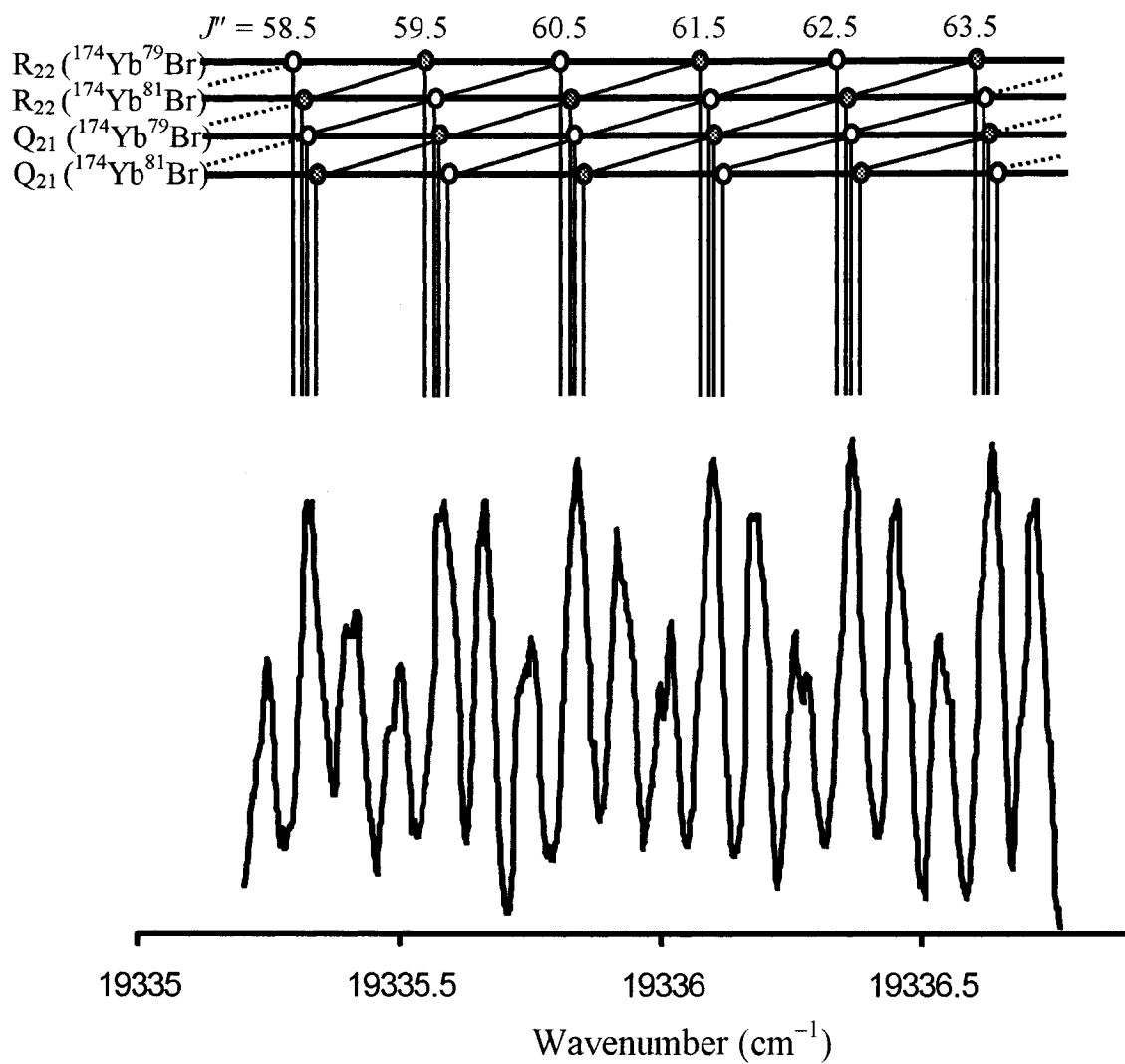


Figure 7.1 Recorded spectra of Q_{21} and R_{22} lines in the $0 - 0$ band of YbBr. Designations for the ^{172}Yb and ^{176}Yb isotopomers (to the right and left of the ^{174}Yb , respectively) have been removed for clarity. Consecutive values of J are differentiated using either filled or unfilled markers. Line widths (FWHM) in this scan are $\sim 0.06 \text{ cm}^{-1}$, 2 - 3 times the width for an unblended line.

by the simultaneous observation of several fluorescence patterns, due almost certainly to coincidental overlap of R_{11} lines and lines in the Q_{11}/R_{12} and/or P_{11}/Q_{12} branches. This made rotational assignments from combination differences extremely difficult, as lines acquired from resolved fluorescence spectra were often so broadened that assignments from combination differences were not unambiguous.

Similarly, lines in the P_{12} branch in both the $0 - 0$ and $1 - 0$ bands, were observed to be overlapped for high and low values of J , and were also found to be coincident for the $^{172}\text{YbBr}$ and $^{174}\text{YbBr}$ isotopomers in the $0 - 0$ band, consistent with previous studies (50,87). Thus, efforts to assign lines in this branch using resolved fluorescence were also hampered by the simultaneous observation of several fluorescence patterns.

Lines in the P_{12} and R_{11} branches were ultimately assigned by recording resolved fluorescence spectra for nearly all of the measured lines, and determining combination differences for the few resolved fluorescence spectra that were free from coincidental overlap(s). This is in contrast to previous studies [4,50] where unequivocal rotational line assignments were made by recording fewer resolved fluorescence spectra.

Owing to the fact that these two branches sample levels of different parity in the excited state, it was possible to characterize the $\nu = 0$ and 1 levels of the $A^2\Pi_{1/2}$ state from fits employing the fixed ground state parameters of chapter 5. Fits including $A^2\Pi_{1/2} \leftarrow X^2\Sigma^+$ data, constrained ground state parameters, and constrained values³ of q_ν , A_e and α_A , provided excellent initial estimates of the rotational and Λ -doubling parameters for the entire $A^2\Pi$ state, which was extremely helpful in analysis of the $A^2\Pi_{3/2}$ spin-orbit component.

³ Estimated from the previous study of YbCl [50].

7.3.3 The $A^2\Pi_{3/2} \leftarrow X^2\Sigma^+$ System

The assignment of lines in sub-bands of the $A^2\Pi_{3/2} \leftarrow X^2\Sigma^+$ system was very similar to the method used for lines in the $B^2\Sigma^+ \leftarrow X^2\Sigma^+$ system. Many of the lines in this system were found to occur as “blended branches” (see section 6.3.2) making their assignment using combination differences not possible. The assignment of lines in this system was thus based on the comparison of calculated line positions with experimental spectra, and final assignments were then made based on fits with the lowest value of $\hat{\sigma}$. Lines in all six branches were sought to ensure that the correct assignments had been made. The inclusion of data for the other spin-orbit component (i.e. from the $A^2\Pi_{1/2} \leftarrow X^2\Sigma^+$ system) introduced constraints on the parameter set, and thus made assignment of lines in the $A^2\Pi_{3/2} \leftarrow X^2\Sigma^+$ system less ambiguous.

Further aiding in the assignment of lines in this system, was the collection of P_{22} lines at low- J values, recorded using the “cold” ablation source. These lines were closest to the band origin, and were thus more “sensitive” to their respective assignments than higher J -lines. Once the P_{22} lines were assigned, blended lines in the remaining five branches were carefully identified, and their respective assignments were then determined unambiguously.

7.3.4 Fits of the $A^2\Pi \leftarrow X^2\Sigma^+$ data

A simultaneous fit including all data for both $^{174}\text{Yb}^{79}\text{Br}$ and $^{174}\text{Yb}^{81}\text{Br}$ isotopomers for the 0 – 0 and 1 – 0 bands was employed to characterize the $A^2\Pi \leftarrow X^2\Sigma^+$ system, with the complete list of line positions given in Appendix IV. Similar to the $B - X$ study of chapter 6, the parameters were referenced to the $^{174}\text{Yb}^{79}\text{Br}$ isotopomer

through the isotopic relationships of Table 2.4, with the exception of the band origins that were determined independently. In the final fit, the ground state parameters were held fixed to values found in Table 6.2. Fixing of ground state parameters was justified in this instance, as the previous $B - X$ study included both the highly accurate B_0 values from the FTMW study of chapter 5, and extensive electronic data of the $B - X$ system at high J -values. Fits of the $A^2\Pi$ equilibrium rotational, spin-orbit and Λ -doubling parameters are given in Table 7.1, with the estimated uncertainties in the last digit denoted in parentheses. The reduced standard deviation of the fit is close to unity, which lends evidence to the selection of an adequate model for this system, and the correct analysis and assignment of weights to the features in the spectra.

From Eqs. 5.10 and 5.12 and the value of B'_e , given in Table 7.1, an estimate of the equilibrium bond length for the $A^2\Pi$ state was calculated as 2.595406(5) Å.

7.4 Discussion

Several comparisons can be made between the results of the present analysis of the $A - X$ system of YbBr, and previous studies of the visible electronic spectra of YbF [46-48] and YbCl [50,51].

In their study of YbF, Dunfield *et al.* [47] reported a previously unobserved $^2\Pi_{1/2}$ state, believed to be the cause of perturbations in the nearby $A^2\Pi$ state. As a consequence of these perturbations, the fitted B_ν and p_ν parameters ($\nu = 0,1$) of the A state of YbF were found to be inconsistent with the vibrational expression of Eq. 2.12,

Table 7.1

Fitted parameters^a from simultaneous fits of the 0 – 0 and 1 – 0 bands of the $A^2\Pi \leftarrow X^2\Sigma^+$ system for $^{174}\text{Yb}^{79}\text{Br}$ and $^{174}\text{Yb}^{81}\text{Br}$.

	B_e'	0.04609858(18)
	$\alpha_e' \times 10^4$	1.2935(15)
	$D_e' \times 10^8$	8.819(20)
	A_e'	1520.38104(83)
$A^2\Pi$	α_A'	1.26799(91)
	$A_D' \times 10^7$	-6.2(22)
	p_e'	-0.111284(80)
	$\alpha_p' \times 10^4$	5.15(15)
	$q_e' \times 10^4$	2.53(40)
	$p_D' \times 10^8$	5.04(36)
	B_e''	[0.04437305]
	$\alpha_e'' \times 10^4$	[1.3262]
$X^2\Sigma^+$	$D_e'' \times 10^8$	[9.126]
	γ_e''	[0.0038377]
	$\alpha_\gamma'' \times 10^5$	[5.8]
$^{174}\text{Yb}^{79}\text{Br}$	ν_{00}	18565.8903(4)
	ν_{10}	18777.7544(8)
$^{174}\text{Yb}^{81}\text{Br}$	ν_{00}	18565.8209(4)
	ν_{10}	18775.8851(8)
	$\hat{\sigma}$	1.0518
	# Lines	856

^aAll parameters are referenced to the $^{174}\text{Yb}^{79}\text{Br}$ isotopomer, except for the band origins, and are given in units of cm^{-1} . Values in parentheses indicate the uncertainty of 1σ , while brackets indicate constrained parameters.

and similarly, the vibrational spacings were found to be inconsistent with Eq. 6.1⁴.

A similar state was not observed for either YbCl or in the present study of YbBr, nor was anomalous behavior in any of the fitted parameters of the $X^2\Sigma^+$, $A^2\Pi$ or $B^2\Sigma^+$ states observed, as seen from Tables 5.2, 5.4, 6.3, 7.1 and Refs. 50 and 51. Similarly, in the previous $A^2\Pi \leftarrow X^2\Sigma^+$ bandhead study of YbCl and YbBr by Kramer [52], neither irregular vibrational structure nor the observation of an unidentified system was reported. In an effort to predict the term value of the analogous $^2\Pi_{1/2}$ state in YbCl and YbBr, comparisons of both theoretical and experimental results are made.

Dunfield *et al.* [47] hypothesized that the perturbing $^2\Pi_{1/2}$ state in YbF arose from one of the $4f^{13}6s^2$, $4f^{13}6p6s$ or $4f^{13}5d6s$ Yb⁺ configurations, based on the theoretical predictions of Kaledin *et al.* [70] and Dolg *et al.* [88]. Although Kaledin's energy level calculations were reasonable for the $A^2\Pi_{1/2}$ states of YbF, YbCl and YbBr, estimates of the perturbing $^2\Pi_{1/2}$ state arising from either the $4f^{13}6p6s$ or $4f^{13}5d6s$ Yb⁺ configurations⁵ in YbF, are 1200 to 4900 cm⁻¹ above the state observed by Dunfield *et al.* Assuming that the predictions made by Kaledin *et al.* describe reasonably well the *relative* term values of electronic states of the different analogous molecules, the same perturbing state arising from either the $4f^{13}6p6s$ or $4f^{13}5d6s$ Yb⁺ configurations would lie between 20000 and 27000 cm⁻¹ in YbCl and/or YbBr. This would mean that such a perturbing state would likely lie above the $B^2\Sigma^+$ states of both molecules, and would not be observable in the present study of the $A^2\Pi \leftarrow X^2\Sigma^+$ system of YbBr.

⁴ For the $A^2\Pi$ state of ¹⁷⁴YbF: $B_0 = 0.248064(24)$, $B_1 = 0.255305(27)$, $\gamma_0 = -0.39635(13)$, $\gamma_1 = -0.89614(25)$, $\Delta G(v + \frac{1}{2}) = 474.333$ and $\Delta G(v + \frac{3}{2}) = 544.707$ cm⁻¹ [47].

⁵ Kaledin *et al.* [70] predicted the lowest energy state from a given configuration, which may not necessarily be $^2\Pi_{1/2}$ in symmetry. Thus, it is assumed that the differences between the various electronic states arising from the same configuration will be small.

As was determined in the previous studies of YbCl [50,51], the $A^2\Pi$ and $B^2\Sigma^+$ states form a unique perturber pair, as seen from the nearly identical fitted values for p_e and γ_e . The unique perturber pair model is also found for YbBr, as $p_e = -0.111284(80) \text{ cm}^{-1}$ for the $A^2\Pi$ state and $\gamma_e = -0.111636(17) \text{ cm}^{-1}$ for the $B^2\Sigma^+$ state.

7.5 Conclusions

From analyses of spectra for the 0 – 0 and 1 – 0 bands of the $A^2\Pi \leftarrow X^2\Sigma^+$ system of $^{174}\text{Yb}^{79}\text{Br}$ and $^{174}\text{Yb}^{81}\text{Br}$ isotopomers, the first characterization of the $A^2\Pi$ state of YbBr has been achieved. Although perturbations were observed in the $A^2\Pi$ state of YbF [46-48], no perturbations were observed in the present analysis of YbBr, as was the case for the analogous YbCl molecule [50,51].

Appendix I

SrBr Laser Excitation Line Positions

Measured and calculated line positions (given in units of cm^{-1}) in the $A^2\Pi \leftarrow X^2\Sigma^+$ and $B^2\Sigma^+ \leftarrow X^2\Sigma^+$ systems of $^{88}\text{Sr}^{79}\text{Br}$ and $^{88}\text{Sr}^{81}\text{Br}$ from the fits of Table 4.4. Each branch is labeled in accordance with Ref. [16], and by system and band (given as $\nu' - \nu''$). The symbol “**” indicates a line position that was not included in the final fits; line positions in bold indicate crossing points in the data. All lines from the 0 – 0 and 1 – 0 bands of the $A^2\Pi \leftarrow X^2\Sigma^+$ system are from Ref. [4]. All lines measured in the $B - X$ system are from Ref. [2]; some lines in this data set were assigned to two different values of J on opposites sides of a band head, and were excluded from the final fit of this analysis.

Page 136: $^{88}\text{Sr}^{79}\text{Br}$

Page 157: $^{88}\text{Sr}^{81}\text{Br}$

Overlap integrals, $\langle \nu_A | \nu_B \rangle$ and $\langle R^{-2} \rangle_{\nu_A \nu_B}$, used in the final fits of Table 4.3. See text for an explanation of the method of calculation.

Page 177

$^{88}\text{Sr}^{79}\text{Br}$

$A^2\Pi_{1/2} \leftarrow X^2\Sigma^+ (0-0) R_{11}(ee)$				$A^2\Pi_{1/2} \leftarrow X^2\Sigma^+ (0-0) P_{12}(ff)$			
J	OBS	CALC	DIFF	OBS	CALC	DIFF	
15.5	-	14706.218		14699.396	14699.395	0.001	
16.5	-	14706.459		14699.211	14699.209	0.002	
17.5	-	14706.701		14699.026	14699.026	0.000	
18.5	-	14706.946		14698.846	14698.844	0.002	
19.5	-	14707.191		14698.667	14698.663	0.004	
20.5	-	14707.439		14698.488	14698.484	0.004	
21.5	-	14707.688		14698.310	14698.307	0.003	
22.5	-	14707.939		14698.135	14698.132	0.003	
23.5	-	14708.191		14697.960	14697.958	0.002	
24.5	-	14708.445		14697.787	14697.786	0.001	
25.5	-	14708.701		14697.618	14697.616	0.002	
26.5	14708.951	14708.958	-0.007	14697.450	14697.447	0.003	
27.5	14709.212	14709.217	-0.005	14697.282	14697.280	0.002	
28.5	14709.476	14709.478	-0.002	14697.119	14697.115	0.004	
29.5	14709.738	14709.740	-0.002	14696.952	14696.952	0.000	
30.5	14710.002	14710.004	-0.002	14696.789	14696.790	-0.001	
31.5	14710.263	14710.270	-0.007	14696.631	14696.630	0.001	
32.5	14710.541	14710.537	0.004	14696.476	14696.471	0.005	
33.5	14710.801	14710.806	-0.005	14696.313	14696.314	-0.001	
34.5	14711.078	14711.077	0.001	14696.160	14696.159	0.001	
35.5	14711.344	14711.349	-0.005	14696.005	14696.006	-0.001	
36.5	14711.616	14711.623	-0.007	14695.856	14695.854	0.002	
37.5	14711.900	14711.899	0.001	14695.703	14695.704	-0.001	
38.5	14712.178	14712.176	0.002	14695.557	14695.556	0.001	
39.5	14712.451	14712.455	-0.004	14695.407	14695.409	-0.002	
40.5	14712.730	14712.735	-0.005	14695.264	14695.264	0.000	
41.5	14713.021	14713.017	0.004	14695.119	14695.121	-0.002	
42.5	14713.298	14713.301	-0.003	14694.979	14694.980	-0.001	
43.5	14713.588	14713.586	0.002	14694.840	14694.840	0.000	
44.5	14713.869	14713.873	-0.004	14694.698	14694.702	-0.004	
45.5	14714.164	14714.162	0.002	14694.561	14694.565	-0.004	
46.5	14714.457	14714.452	0.005	14694.425	14694.431	-0.006	
47.5	14714.749	14714.744	0.005	14694.294	14694.298	-0.004	
48.5	14715.037	14715.038	-0.001	-	14694.166		
49.5	14715.336	14715.333	0.003	-	14694.037		
50.5	14715.632	14715.630	0.002	-	14693.909		
51.5	14715.933	14715.928	0.005	-	14693.783		
52.5	14716.235	14716.228	0.007	-	14693.658		

$A^2\Pi_{3/2} \leftarrow X^2\Sigma^+ (0-0) P_{22}(ff)$				$A^2\Pi_{3/2} \leftarrow X^2\Sigma^+ (0-0) R_{21}(ee)$			
J	OBS	CALC	DIFF	OBS	CALC	DIFF	
12.5	-	15002.881		15007.104	15007.114	-0.010	
13.5	-	15002.740		15007.306	15007.299	0.007	
14.5	-	15002.601		15007.479	15007.485	-0.006	
15.5	-	15002.463		15007.677	15007.673	0.004	

16.5	-	15002.327		15007.855	15007.862	-0.007
17.5	15002.190	15002.193	-0.003	15008.055	15008.053	0.002
18.5	15002.058	15002.060	-0.002	15008.249	15008.246	0.003
19.5	15001.927	15001.929	-0.002	15008.442	15008.440	0.002
20.5	15001.797	15001.799	-0.002	15008.635	15008.636	-0.001
21.5	15001.667	15001.671	-0.004	15008.834	15008.833	0.001
22.5	15001.544	15001.545	-0.001	15009.036	15009.032	0.004
23.5	15001.416	15001.420	-0.004	15009.236	15009.233	0.003
24.5	15001.296	15001.297	-0.001	15009.436	15009.435	0.001
25.5	15001.174	15001.176	-0.002	15009.635	15009.639	-0.004
26.5	15001.054	15001.056	-0.002	15009.845	15009.844	0.001
27.5	15000.937	15000.938	-0.001	15010.054	15010.051	0.003
28.5	15000.820	15000.821	-0.001	15010.259	15010.260	-0.001
29.5	15000.705	15000.706	-0.001	15010.473	15010.470	0.003
30.5	15000.599	15000.593	0.006	15010.688	15010.682	0.006
31.5	15000.488	15000.481	0.007	15010.899	15010.896	0.003
32.5	15000.373	15000.371	0.002	15011.114	15011.111	0.003
33.5	15000.260	15000.263	-0.003	15011.327	15011.327	0.000
34.5	15000.155	15000.156	-0.001	15011.542	15011.545	-0.003
35.5	15000.051	15000.051	0.000	-	15011.765	
36.5	14999.948	14999.948	0.000	-	15011.987	
37.5	14999.848	14999.846	0.002	15012.211	15012.210	0.001
38.5	14999.746	14999.746	0.000	15012.432	15012.434	-0.002
39.5	14999.647	14999.647	0.000	15012.663	15012.660	0.003
40.5	14999.551	14999.550	0.001	15012.891	15012.888	0.003
41.5	14999.456	14999.455	0.001	15013.116	15013.117	-0.001
42.5	14999.362	14999.361	0.001	15013.350	15013.348	0.002
43.5	14999.270	14999.269	0.001	15013.582	15013.581	0.001
44.5	14999.181	14999.179	0.002	15013.816	15013.815	0.001
45.5	14999.092	14999.090	0.002	15014.048	15014.051	-0.003
46.5	14999.004	14999.003	0.001	15014.288	15014.288	0.000
47.5	14998.917	14998.917	0.000	15014.525	15014.527	-0.002
48.5	14998.834	14998.833	0.001	15014.767	15014.767	0.000
49.5	14998.749	14998.751	-0.002	15015.007	15015.009	-0.002
50.5	-	14998.670		15015.246	15015.253	-0.007
51.5	14998.597	14998.591	0.006	15015.494	15015.498	-0.004
52.5	14998.519	14998.514	0.005	15015.744	15015.745	-0.001
53.5	14998.441	14998.438	0.003	15015.997	15015.993	0.004
54.5	14998.366	14998.364	0.002	15016.239	15016.243	-0.004
55.5	14998.293	14998.292	0.001	15016.489	15016.495	-0.006
56.5	14998.221	14998.221	0.000	15016.747	15016.748	-0.001
57.5	14998.149	14998.152	-0.003	-	15017.002	

$$A^2\Pi_{1/2} \leftarrow X^2\Sigma^+ (1-0) R_{11}(ee)$$

$$A^2\Pi_{1/2} \leftarrow X^2\Sigma^+ (1-0) P_{12}(ff)$$

J	OBS	CALC	DIFF	OBS	CALC	DIFF
18.5	14928.189	14928.187	0.002	-	14920.097	
19.5	14928.423	14928.425	-0.002	-	14919.910	
20.5	14928.662	14928.665	-0.003	-	14919.724	
21.5	14928.903	14928.906	-0.003	-	14919.539	
22.5	14929.139	14929.148	-0.009	-	14919.356	
23.5	14929.386	14929.391	-0.005	-	14919.174	
24.5	14929.628	14929.636	-0.008	-	14918.993	
25.5	14929.882	14929.882	0.000	-	14918.813	

26.5	-	14930.129		-	14918.635	
27.5	-	14930.377		-	14918.458	
28.5	14930.626	14930.627	-0.001	14918.289	14918.283	0.006
29.5	14930.876	14930.878	-0.002	14918.112	14918.109	0.003
30.5	14931.131	14931.130	0.001	14917.941	14917.936	0.005
31.5	14931.384	14931.384	0.000	14917.758	14917.764	-0.006
32.5	14931.642	14931.639	0.003	14917.598	14917.594	0.004
33.5	14931.897	14931.895	0.002	14917.429	14917.425	0.004
34.5	14932.149	14932.152	-0.003	14917.260	14917.257	0.003
35.5	14932.416	14932.411	0.005	14917.093	14917.091	0.002
36.5	14932.674	14932.670	0.004	14916.929	14916.926	0.003
37.5	14932.934	14932.932	0.002	14916.763	14916.762	0.001
38.5	14933.193	14933.194	-0.001	14916.598	14916.600	-0.002
39.5	14933.454	14933.458	-0.004	14916.441	14916.439	0.002
40.5	14933.720	14933.722	-0.002	14916.279	14916.279	0.000
41.5	14933.985	14933.989	-0.004	14916.120	14916.121	-0.001
42.5	14934.258	14934.256	0.002	14915.966	14915.963	0.003
43.5	14934.521	14934.525	-0.004	14915.809	14915.808	0.001
44.5	14934.794	14934.795	-0.001	14915.656	14915.653	0.003
45.5	14935.061	14935.066	-0.005	14915.501	14915.500	0.001
46.5	14935.337	14935.338	-0.001	14915.349	14915.348	0.001
47.5	14935.613	14935.612	0.001	14915.199	14915.198	0.001
48.5	14935.885	14935.887	-0.002	14915.045	14915.048	-0.003
49.5	14936.168	14936.163	0.005	-	14914.901	
50.5	14936.441	14936.440	0.001	-	14914.754	
51.5	14936.721	14936.719	0.002	14914.610	14914.609	0.001
52.5	14937.002	14936.998	0.004	14914.465	14914.465	0.000
53.5	14937.284	14937.279	0.005	14914.325	14914.322	0.003
54.5	14937.565	14937.562	0.003	14914.178	14914.181	-0.003
55.5	-	14937.845		14914.037	14914.041	-0.004
56.5	-	14938.130		14913.898	14913.902	-0.004
57.5	-	14938.416		14913.758	14913.764	-0.006
58.5	-	14938.703		14913.623	14913.628	-0.005

$$A^2\Pi_{3/2} \leftarrow X^2\Sigma^+ (1-0) P_{22}(ff)$$

$$A^2\Pi_{3/2} \leftarrow X^2\Sigma^+ (1-0) R_{21}(ee)$$

J	OBS	CALC	DIFF	OBS	CALC	DIFF
18.5	15223.307	15223.305	0.002	-	15229.476	
19.5	15223.168	15223.167	0.001	-	15229.663	
20.5	15223.030	15223.030	0.000	-	15229.851	
21.5	15222.899	15222.894	0.005	-	15230.040	
22.5	15222.760	15222.760	0.000	-	15230.230	
23.5	15222.630	15222.627	0.003	-	15230.422	
24.5	15222.499	15222.495	0.004	-	15230.615	
25.5	15222.370	15222.365	0.005	-	15230.809	
26.5	15222.240	15222.235	0.005	-	15231.004	
27.5	15222.109	15222.107	0.002	-	15231.200	
28.5	15221.976	15221.981	-0.005	-	15231.398	
29.5	15221.854	15221.855	-0.001	-	15231.597	
30.5	15221.727	15221.731	-0.004	-	15231.797	
31.5	15221.602	15221.608	-0.006	-	15231.998	
32.5	15221.481	15221.486	-0.005	-	15232.201	
33.5	15221.372	15221.366	0.006	15232.410	15232.404	0.006

34.5	15221.239	15221.246	-0.007	15232.604	15232.609	-0.005
35.5	15221.131	15221.128	0.003	15232.816	15232.815	0.001
36.5	-	15221.012		15233.025	15233.023	0.002
37.5	15220.891	15220.896	-0.005	15233.225	15233.231	-0.006
38.5	15220.786	15220.782	0.004	15233.443	15233.441	0.002
39.5	15220.670	15220.669	0.001	15233.645	15233.652	-0.007
40.5	15220.551	15220.557	-0.006	15233.866	15233.865	0.001
41.5	15220.442	15220.447	-0.005	-	15234.078	
42.5	15220.329	15220.337	-0.008	-	15234.293	
43.5	15220.230	15220.230	0.000	15234.513	15234.508	0.005
44.5	15220.122	15220.123	-0.001	15234.729	15234.725	0.004
45.5	15220.017	15220.017	0.000	15234.947	15234.944	0.003
46.5	15219.910	15219.913	-0.003	15235.169	15235.163	0.006
47.5	15219.808	15219.810	-0.002	15235.390	15235.384	0.006
48.5	15219.706	15219.708	-0.002	15235.613	15235.606	0.007
49.5	15219.606	15219.608	-0.002	15235.830	15235.829	0.001
50.5	15219.505	15219.509	-0.004	15236.059	15236.053	0.006
51.5	15219.409	15219.411	-0.002	15236.283	15236.278	0.005
52.5	15219.312	15219.314	-0.002	15236.510	15236.505	0.005
53.5	15219.214	15219.219	-0.005	15236.738	15236.733	0.005
54.5	15219.121	15219.125	-0.004	15236.959	15236.962	-0.003
55.5	15219.028	15219.032	-0.004	15237.193	15237.192	0.001
56.5	15218.933	15218.940	-0.007	15237.429	15237.423	0.006
57.5	15218.842	15218.849	-0.007	15237.664	15237.656	0.008
58.5	15218.758	15218.760	-0.002	-	15237.889	

 $A^2\Pi_{1/2} \leftarrow X^2\Sigma^+ (2-1) R_{11}(ee)$ $A^2\Pi_{1/2} \leftarrow X^2\Sigma^+ (2-1) P_{12}(ff)$

J	OBS	CALC	DIFF	OBS	CALC	DIFF
15.5	14932.115	14932.111	0.004	-	14925.317	
16.5	14932.348	14932.345	0.003	-	14925.126	
17.5	14932.582	14932.580	0.002	-	14924.937	
18.5	14932.812	14932.816	-0.004	-	14924.748	
19.5	-	14933.053		-	14924.561	
20.5	-	14933.292		-	14924.376	
21.5	-	14933.532		-	14924.191	
22.5	-	14933.773		-	14924.008	
23.5	-	14934.016		-	14923.826	
24.5	14934.257	14934.259	-0.002	-	14923.646	
25.5	14934.494	14934.504	-0.010	-	14923.467	
26.5	14934.748	14934.751	-0.003	-	14923.289	
27.5	-	14934.998		14923.115	14923.112	0.003
28.5	-	14935.247		14922.938	14922.937	0.001
29.5	14935.497	14935.497	0.000	14922.764	14922.763	0.001
30.5	14935.747	14935.749	-0.002	14922.591	14922.590	0.001
31.5	14935.997	14936.002	-0.005	-	14922.419	
32.5	14936.251	14936.256	-0.005	-	14922.249	
33.5	14936.501	14936.511	-0.010	14922.081	14922.080	0.001
34.5	14936.778	14936.767	0.011	14921.907	14921.913	-0.006
35.5	14937.025	14937.025	0.000	14921.750	14921.747	0.003
36.5	14937.279	14937.284	-0.005	14921.577	14921.582	-0.005
37.5	14937.542	14937.544	-0.002	14921.423	14921.419	0.004
38.5	14937.802	14937.806	-0.004	14921.257	14921.256	0.001
39.5	14938.063	14938.069	-0.006	14921.101	14921.096	0.005

40.5	14938.333	14938.333	0.000	14920.941	14920.936	0.005
41.5	-	14938.598		14920.778	14920.778	0.000
42.5	-	14938.865		14920.621	14920.621	0.000
43.5	14939.125	14939.133	-0.008	14920.464	14920.465	-0.001
44.5	14939.409	14939.402	0.007	14920.314	14920.311	0.003
45.5	-	14939.672		14920.161	14920.158	0.003
46.5	14939.949	14939.944	0.005	14920.014	14920.007	0.007
47.5	14940.216	14940.217	-0.001	14919.864	14919.856	0.008
48.5	14940.500	14940.491	0.009	14919.710	14919.707	0.003
49.5	14940.773	14940.766	0.007	14919.547	14919.560	-0.013**
50.5	14941.050	14941.043	0.007	14919.410	14919.413	-0.003
51.5	14941.330	14941.321	0.009	14919.267	14919.268	-0.001
52.5	14941.597	14941.600	-0.003	14919.123	14919.125	-0.002
53.5	14941.881	14941.881	0.000	14918.983	14918.982	0.001
54.5	14942.164	14942.162	0.002	14918.840	14918.841	-0.001
55.5	14942.448	14942.445	0.003	14918.700	14918.701	-0.001
56.5	14942.728	14942.729	-0.001	14918.553	14918.563	-0.010
57.5	14943.015	14943.015	0.000	14918.426	14918.426	0.000
58.5	14943.298	14943.301	-0.003	14918.289	14918.290	-0.001
59.5	14943.589	14943.589	0.000	-	14918.156	
60.5	14943.875	14943.879	-0.004	-	14918.023	
61.5	14944.172	14944.169	0.003	-	14917.891	
62.5	14944.462	14944.461	0.001	-	14917.760	
63.5	14944.749	14944.754	-0.005	-	14917.631	
64.5	-	14945.048		14917.502	14917.503	-0.001
65.5	-	14945.343		14917.372	14917.377	-0.005
66.5	-	14945.640		14917.252	14917.252	0.000
67.5	-	14945.938		14917.129	14917.128	0.001
68.5	-	14946.237		14917.008	14917.005	0.003
69.5	-	14946.537		14916.878	14916.884	-0.006

$$A^2\Pi_{3/2} \leftarrow X^2\Sigma^+ (2-1) P_{22}(ff)$$

$$A^2\Pi_{3/2} \leftarrow X^2\Sigma^+ (2-1) R_{21}(ee)$$

J	OBS	CALC	DIFF	OBS	CALC	DIFF
34.5	-	15225.881		15237.205	15237.205	0.000
35.5	-	15225.763		-	15237.411	
36.5	-	15225.647		15237.619	15237.617	0.002
37.5	-	15225.531		15237.782	15237.825	-0.043**
38.5	-	15225.417		15238.026	15238.034	-0.008
39.5	-	15225.305		15238.243	15238.244	-0.001
40.5	-	15225.193		15238.459	15238.455	0.004
41.5	-	15225.083		15238.666	15238.668	-0.002
42.5	-	15224.974		-	15238.881	
43.5	-	15224.866		-	15239.096	
44.5	-	15224.760		-	15239.313	
45.5	-	15224.654		-	15239.530	
46.5	-	15224.550		-	15239.749	
47.5	-	15224.448		-	15239.968	
48.5	15224.350	15224.346	0.004	-	15240.189	
49.5	15224.243	15224.246	-0.003	-	15240.411	
50.5	15224.138	15224.147	-0.009	-	15240.635	
51.5	15224.046	15224.049	-0.003	-	15240.859	
52.5	15223.949	15223.953	-0.004	-	15241.085	
53.5	-	15223.858		15241.309	15241.312	-0.003

54.5	-	15223.764		15241.543	15241.540	0.003
55.5	-	15223.671		15241.776	15241.770	0.006
56.5	-	15223.580		15242.006	15242.000	0.006
57.5	15223.492	15223.490	0.002	15242.240	15242.232	0.008
58.5	-	15223.401		15242.473	15242.465	0.008
59.5	15223.316	15223.313	0.003	15242.717	15242.699	0.018**
60.5	15223.227	15223.227	0.000	15242.944	15242.935	0.009
61.5	-	15223.142		15243.174	15243.171	0.003
62.5	15223.065	15223.058	0.007	15243.404	15243.409	-0.005
63.5	15222.963	15222.976	-0.013	15243.643	15243.648	-0.005
64.5	15222.895	15222.894	0.001	15243.884	15243.888	-0.004
65.5	15222.815	15222.814	0.001	15244.132	15244.129	0.003
66.5	15222.744	15222.736	0.008	15244.369	15244.372	-0.003
67.5	15222.654	15222.658	-0.004	15244.611	15244.616	-0.005
68.5	15222.583	15222.582	0.001	15244.866	15244.861	0.005
69.5	15222.508	15222.507	0.001	15245.102	15245.107	-0.005
70.5	15222.437	15222.433	0.004	15245.355	15245.354	0.001
71.5	15222.371	15222.361	0.010	15245.598	15245.603	-0.005
72.5	15222.288	15222.290	-0.002	15245.859	15245.852	0.007
73.5	15222.216	15222.220	-0.004	15246.098	15246.103	-0.005
74.5	15222.148	15222.151	-0.003	15246.356	15246.355	0.001
75.5	15222.085	15222.084	0.001	15246.599	15246.608	-0.009
76.5	15222.017	15222.018	-0.001	15246.853	15246.863	-0.010
77.5	15221.950	15221.953	-0.003	15247.118	15247.118	0.000
78.5	15221.886	15221.890	-0.004	15247.389	15247.375	0.014
79.5	15221.832	15221.828	0.004	15247.631	15247.633	-0.002
80.5	15221.769	15221.767	0.002	15247.889	15247.892	-0.003
81.5	15221.705	15221.707	-0.002	15248.151	15248.153	-0.002
82.5	15221.638	15221.648	-0.010	15248.417	15248.414	0.003
83.5	15221.598	15221.591	0.007	15248.671	15248.677	-0.006
84.5	15221.532	15221.535	-0.003	15248.937	15248.941	-0.004
85.5	15221.482	15221.481	0.001	15249.202	15249.206	-0.004
86.5	15221.436	15221.428	0.008	15249.472	15249.472	0.000
87.5	15221.378	15221.376	0.002	15249.738	15249.739	-0.001
88.5	-	15221.325		15250.008	15250.008	0.000
89.5	-	15221.275		15250.274	15250.278	-0.004
90.5	-	15221.227		15250.551	15250.549	0.002
91.5	-	15221.180		15250.824	15250.821	0.003
92.5	-	15221.134		15251.095	15251.094	0.001
93.5	-	15221.090		15251.370	15251.368	0.002
94.5	-	15221.047		15251.638	15251.644	-0.006
95.5	-	15221.005		15251.931	15251.921	0.010
96.5	-	15220.965		15252.179	15252.199	-0.020**
97.5	-	15220.925		15252.480	15252.478	0.002
98.5	-	15220.887		15252.752	15252.758	-0.006
99.5	-	15220.851		15253.041	15253.040	0.001
100.5	-	15220.815		15253.285	15253.322	-0.037**
101.5	-	15220.781		15253.564	15253.606	-0.042**

$A^2\Pi_{1/2} \leftarrow X^2\Sigma^+ (3-2) R_{11}(ee)$				$A^2\Pi_{1/2} \leftarrow X^2\Sigma^+ (3-2) P_{12}(ff)$			
J	OBS	CALC	DIFF	OBS	CALC	DIFF	
18.5	14937.355	14937.359	-0.004	-	14929.320		
19.5	-	14937.596		-	14929.134		
20.5	14937.826	14937.834	-0.008	-	14928.949		
21.5	14938.073	14938.073	0.000	-	14928.766		
22.5	14938.316	14938.313	0.003	-	14928.583		
23.5	14938.540	14938.555	-0.015**	-	14928.402		
24.5	14938.796	14938.798	-0.002	-	14928.223		
25.5	14939.043	14939.042	0.001	14928.037	14928.045	-0.008	
26.5	14939.293	14939.287	0.006	14927.867	14927.868	-0.001	
27.5	14939.526	14939.534	-0.008	14927.701	14927.693	0.008	
28.5	14939.780	14939.782	-0.002	14927.526	14927.519	0.007	
29.5	14940.027	14940.031	-0.004	14927.358	14927.347	0.011	
30.5	14940.284	14940.281	0.003	14927.184	14927.176	0.008	
31.5	14940.530	14940.533	-0.003	14927.021	14927.007	0.014**	
32.5	14940.782	14940.786	-0.004	14926.850	14926.840	0.010	
33.5	14941.032	14941.040	-0.008	14926.691	14926.676	0.015**	
34.5	14941.295	14941.296	-0.001	14926.527	14926.513	0.014**	
35.5	14941.555	14941.552	0.003	14926.361	14926.355	0.006	
36.5	14941.812	14941.811	0.001	14926.204	14926.202	0.002	
37.5	14942.072	14942.070	0.002	14926.057	14926.059	-0.002	
38.5	14942.326	14942.330	-0.004	14925.927	14925.935	-0.008	
39.5	14942.589	14942.592	-0.003	-	14925.855		
40.5	14942.856	14942.855	0.001	14925.384	14925.391	-0.007	
41.5	14943.131	14943.119	0.012	14925.270	14925.273	-0.003	
42.5	14943.401	14943.385	0.016**	14925.133	14925.137	-0.004	
43.5	14943.661	14943.652	0.009	14924.990	14924.993	-0.003	
44.5	14943.927	14943.920	0.007	14924.850	14924.847	0.003	
45.5	14944.190	14944.189	0.001	14924.706	14924.699	0.007	
46.5	14944.447	14944.460	-0.013**	14924.553	14924.551	0.002	
47.5	14944.728	14944.732	-0.004	14924.403	14924.404	-0.001	
48.5	14945.004	14945.005	-0.001	14924.253	14924.257	-0.004	
49.5	14945.281	14945.279	0.002	-	14924.111		
50.5	14945.551	14945.555	-0.004	-	14923.966		
51.5	14945.847	14945.832	0.015**	-	14923.823		
52.5	14946.112	14946.110	0.002	14923.671	14923.680	-0.009	
53.5	14946.389	14946.389	0.000	14923.534	14923.538	-0.004	
54.5	14946.669	14946.670	-0.001	14923.391	14923.398	-0.007	
55.5	14946.966	14946.952	0.014**	14923.251	14923.259	-0.008	
56.5	14947.236	14947.235	0.001	14923.117	14923.121	-0.004	
57.5	14947.523	14947.519	0.004	14922.984	14922.984	0.000	
58.5	14947.810	14947.805	0.005	14922.850	14922.849	0.001	
59.5	14948.087	14948.091	-0.004	14922.714	14922.715	-0.001	
60.5	-	14948.380		14922.580	14922.582	-0.002	
61.5	14948.661	14948.669	-0.008	14922.450	14922.450	0.000	
62.5	-	14948.960		14922.317	14922.320	-0.003	
63.5	14949.251	14949.251	0.000	14922.183	14922.191	-0.008	
64.5	-	14949.544		14922.067	14922.063	0.004	
65.5	-	14949.839		14921.940	14921.937	0.003	
66.5	-	14950.134		14921.813	14921.812	0.001	
67.5	-	14950.431		14921.690	14921.688	0.002	
68.5	-	14950.729		14921.570	14921.565	0.005	
69.5	-	14951.029		14921.449	14921.444	0.005	

70.5	-	14951.329		14921.326	14921.324	0.002
71.5	-	14951.631		14921.213	14921.205	0.008
72.5	-	14951.934		14921.079	14921.088	-0.009
73.5	-	14952.238		14920.969	14920.972	-0.003
74.5	-	14952.544		14920.862	14920.857	0.005

 $A^2\Pi_{1/2} \leftarrow X^2\Sigma^+ (3-2) Q_{11}(ef)$
 $A^2\Pi_{1/2} \leftarrow X^2\Sigma^+ (3-2) R_{12}(ff)$

J	OBS	CALC	DIFF	OBS	CALC	DIFF
55.5	-	14935.124		14935.323	14935.319	0.004
56.5	14935.196	14935.199	-0.003	14935.390	14935.398	-0.008
57.5	14935.273	14935.275	-0.002	14935.480	14935.477	0.003
58.5	14935.350	14935.353	-0.003	14935.557	14935.558	-0.001
59.5	14935.433	14935.431	0.002	14935.640	14935.640	0.000
60.5	14935.507	14935.511	-0.004	14935.727	14935.724	0.003
61.5	14935.590	14935.593	-0.003	14935.810	14935.808	0.002
62.5	14935.667	14935.675	-0.008	14935.900	14935.894	0.006
63.5	14935.757	14935.759	-0.002	14935.987	14935.981	0.006
64.5	14935.840	14935.844	-0.004	14936.077	14936.069	0.008
65.5	14935.934	14935.930	0.004	-	14936.159	
66.5	14936.017	14936.017	0.000	-	14936.250	

 $A^2\Pi_{3/2} \leftarrow X^2\Sigma^+ (3-2) P_{22}(ff)$
 $A^2\Pi_{3/2} \leftarrow X^2\Sigma^+ (3-2) R_{21}(ee)$

J	OBS	CALC	DIFF	OBS	CALC	DIFF
20.5	15232.190	15232.205	-0.015**	-	15238.980	
21.5	15232.056	15232.070	-0.014**	-	15239.167	
22.5	15231.940	15231.936	0.004	-	15239.356	
23.5	15231.806	15231.804	0.002	-	15239.546	
24.5	-	15231.673		-	15239.737	
25.5	15231.559	15231.543	0.016**	-	15239.929	
26.5	15231.406	15231.414	-0.008	-	15240.123	
27.5	15231.279	15231.286	-0.007	-	15240.317	
28.5	15231.156	15231.160	-0.004	-	15240.513	
29.5	15231.039	15231.035	0.004	-	15240.710	
30.5	15230.919	15230.911	0.008	-	15240.909	
31.5	15230.809	15230.789	0.020**	-	15241.108	
32.5	15230.692	15230.667	0.025**	-	15241.309	
33.5	15230.549	15230.547	0.002	-	15241.511	
34.5	15230.442	15230.428	0.014**	-	15241.714	
35.5	15230.305	15230.311	-0.006	-	15241.918	
36.5	15230.228	15230.195	0.033**	-	15242.124	
37.5	15230.088	15230.079	0.009	-	15242.331	
38.5	15229.958	15229.966	-0.008	-	15242.539	
39.5	15229.868	15229.853	0.015**	-	15242.748	
40.5	-	15229.742		-	15242.958	
41.5	-	15229.631		-	15243.170	
42.5	-	15229.523		-	15243.383	
43.5	15229.398	15229.415	-0.017**	-	15243.597	
44.5	15229.311	15229.309	0.002	-	15243.812	
45.5	15229.201	15229.203	-0.002	-	15244.028	
46.5	15229.088	15229.100	-0.012	-	15244.246	

47.5	15228.998	15228.997	0.001	-	15244.464		
48.5	15228.897	15228.895	0.002	-	15244.684		
49.5	15228.801	15228.795	0.006	-	15244.905		
50.5	15228.701	15228.696	0.005	-	15245.128		
51.5	15228.604	15228.599	0.005	-	15245.351		
52.5	15228.504	15228.502	0.002	-	15245.576		
53.5	15228.404	15228.407	-0.003	-	15245.802		
54.5	15228.314	15228.313	0.001	-	15246.029		
55.5	-	15228.221		15246.264	15246.257	0.007	
56.5	-	15228.130		15246.491	15246.487	0.004	
57.5	-	15228.039		15246.715	15246.717	-0.002	
58.5	15227.946	15227.951	-0.005	15246.945	15246.949	-0.004	
59.5	-	15227.863		15247.182	15247.182	0.000	
60.5	-	15227.777		15247.418	15247.417	0.001	
61.5	15227.686	15227.692	-0.006	15247.656	15247.652	0.004	
62.5	15227.604	15227.608	-0.004	15247.896	15247.889	0.007	
63.5	15227.523	15227.525	-0.002	15248.149	15248.126	0.023**	
64.5	15227.443	15227.444	-0.001	15248.402	15248.365	0.037**	
65.5	15227.374	15227.364	0.010	15248.603	15248.606	-0.003	
66.5	15227.286	15227.285	0.001	15248.843	15248.847	-0.004	
67.5	15227.208	15227.208	0.000	15249.093	15249.090	0.003	
68.5	15227.129	15227.132	-0.003	15249.327	15249.333	-0.006	
69.5	15227.071	15227.057	0.014**	15249.581	15249.578	0.003	
70.5	15226.997	15226.983	0.014**	15249.831	15249.824	0.007	
71.5	15226.911	15226.910	0.001	15250.070	15250.072	-0.002	
72.5	15226.837	15226.839	-0.002	15250.314	15250.320	-0.006	
73.5	15226.761	15226.769	-0.008	15250.574	15250.570	0.004	
74.5	15226.712	15226.701	0.011	15250.814	15250.821	-0.007	
75.5	15226.638	15226.633	0.005	15251.081	15251.073	0.008	
76.5	15226.573	15226.567	0.006	15251.324	15251.326	-0.002	
77.5	15226.501	15226.503	-0.002	15251.578	15251.580	-0.002	
78.5	-	15226.439		15251.831	15251.836	-0.005	
79.5	15226.370	15226.377	-0.007	15252.089	15252.093	-0.004	
80.5	15226.318	15226.316	0.002	15252.349	15252.351	-0.002	
81.5	-	15226.256		15252.602	15252.610	-0.008	
82.5	-	15226.198		15252.875	15252.870	0.005	
83.5	15226.141	15226.140	0.001	15253.132	15253.132	0.000	
84.5	-	15226.085		15253.396	15253.394	0.002	
85.5	15226.037	15226.030	0.007	-	15253.658		
86.5	15225.980	15225.977	0.003	15253.930	15253.923	0.007	
87.5	15225.917	15225.924	-0.007	-	15254.189		
88.5	15225.877	15225.874	0.003	-	15254.457		
89.5	15225.823	15225.824	-0.001	-	15254.725		
90.5	15225.772	15225.776	-0.004	-	15254.995		
91.5	-	15225.729		-	15255.266		
92.5	15225.681	15225.683	-0.002	-	15255.538		

$$A^2\Pi_{1/2} \leftarrow X^2\Sigma^+ (4-3) R_{11}(ee)$$

J	OBS	CALC	DIFF
18.5	-	14941.872	
19.5	-	14942.108	
20.5	-	14942.344	
21.5	-	14942.583	

$$A^2\Pi_{1/2} \leftarrow X^2\Sigma^+ (4-3) P_{12}(ff)$$

J	OBS	CALC	DIFF
18.5	14933.931	14933.926	0.005
19.5	14933.758	14933.753	0.005
20.5	14933.588	14933.585	0.003
21.5	14933.433	14933.423	0.010

22.5	-	14942.822		14933.287	14933.271	0.016**
23.5	-	14943.063		14933.121	14933.132	-0.011
24.5	-	14943.305		14932.990	14933.010	-0.020**
25.5	-	14943.548		14932.914	14932.913	0.001
26.5	-	14943.792		14932.070	14932.068	0.002
27.5	-	14944.038		14931.960	14931.960	0.000
28.5	14944.283	14944.285	-0.002	14931.842	14931.834	0.008
29.5	14944.533	14944.533	0.000	14931.698	14931.696	0.002
30.5	14944.780	14944.783	-0.003	14931.555	14931.550	0.005
31.5	14945.030	14945.034	-0.004	14931.396	14931.398	-0.002
32.5	14945.283	14945.286	-0.003	14931.242	14931.243	-0.001
33.5	14945.537	14945.539	-0.002	14931.086	14931.087	-0.001
34.5	-	14945.794		14930.926	14930.929	-0.003
35.5	14946.048	14946.050	-0.002	14930.773	14930.771	0.002
36.5	14946.308	14946.307	0.001	14930.612	14930.613	-0.001
37.5	14946.558	14946.565	-0.007	14930.452	14930.456	-0.004
38.5	-	14946.825		14930.296	14930.299	-0.003
39.5	-	14947.085		14930.142	14930.142	0.000
40.5	14947.343	14947.348	-0.005	14929.988	14929.987	0.001
41.5	14947.613	14947.611	0.002	14929.831	14929.832	-0.001
42.5	14947.870	14947.875	-0.005	14929.681	14929.678	0.003
43.5	14948.140	14948.141	-0.001	14929.528	14929.526	0.002
44.5	14948.412	14948.408	0.004	14929.374	14929.374	0.000
45.5	14948.673	14948.677	-0.004	14929.221	14929.224	-0.003
46.5	14948.950	14948.946	0.004	14929.074	14929.074	0.000
47.5	14949.217	14949.217	0.000	14928.927	14928.926	0.001
48.5	14949.490	14949.489	0.001	14928.774	14928.779	-0.005
49.5	14949.755	14949.763	-0.008	14928.627	14928.633	-0.006
50.5	14950.032	14950.037	-0.005	14928.490	14928.488	0.002
51.5	14950.305	14950.313	-0.008	14928.347	14928.345	0.002
52.5	14950.591	14950.590	0.001	14928.200	14928.203	-0.003
53.5	14950.864	14950.868	-0.004	14928.063	14928.062	0.001
54.5	-	14951.148		14927.927	14927.922	0.005
55.5	-	14951.429		14927.783	14927.783	0.000
56.5	-	14951.711		14927.647	14927.646	0.001
57.5	-	14951.994		14927.513	14927.510	0.003
58.5	14952.288	14952.278	0.010	14927.380	14927.376	0.004
59.5	14952.572	14952.564	0.008	14927.240	14927.242	-0.002
60.5	14952.855	14952.851	0.004	14927.106	14927.110	-0.004
61.5	14953.148	14953.139	0.009	14926.979	14926.979	0.000
62.5	14953.432	14953.429	0.003	14926.846	14926.850	-0.004
63.5	14953.729	14953.719	0.010	14926.719	14926.721	-0.002
64.5	14954.016	14954.011	0.005	14926.592	14926.594	-0.002
65.5	14954.310	14954.304	0.006	14926.469	14926.469	0.000
66.5	14954.613	14954.599	0.014**	14926.346	14926.344	0.002
67.5	-	14954.894		14926.222	14926.221	0.001
68.5	-	14955.191		-	14926.099	
69.5	-	14955.489		-	14925.979	
70.5	-	14955.788		-	14925.860	
71.5	-	14956.089		-	14925.742	
72.5	-	14956.390		-	14925.625	
73.5	14956.693	14956.693	0.000	-	14925.510	
74.5	14957.000	14956.997	0.003	-	14925.396	
75.5	14957.303	14957.303	0.000	-	14925.284	
76.5	14957.600	14957.609	-0.009	-	14925.172	
77.5	14957.917	14957.917	0.000	-	14925.062	
78.5	14958.241	14958.226	0.015**	-	14924.954	

79.5	14958.531	14958.536	-0.005	-	14924.846
80.5	14958.845	14958.848	-0.003	-	14924.740

 $A^2\Pi_{3/2} \leftarrow X^2\Sigma^+ (4-3) P_{22}(ff)$

<i>J</i>	OBS	CALC	DIFF
27.5	15235.779	15235.784	-0.005
28.5	-	15235.658	
29.5	-	15235.534	
30.5	-	15235.410	
31.5	15235.285	15235.288	-0.003
32.5	15235.165	15235.167	-0.002
33.5	15235.045	15235.047	-0.002
34.5	-	15234.928	
35.5	-	15234.811	
36.5	-	15234.695	
37.5	-	15234.580	
38.5	-	15234.466	
39.5	15234.358	15234.354	0.004
40.5	15234.241	15234.243	-0.002
41.5	-	15234.133	
42.5	-	15234.024	
43.5	15233.910	15233.916	-0.006
44.5	15233.814	15233.810	0.004
45.5	15233.710	15233.705	0.005
46.5	15233.600	15233.601	-0.001
47.5	15233.493	15233.499	-0.006
48.5	15233.403	15233.398	0.005
49.5	15233.293	15233.298	-0.005
50.5	15233.203	15233.199	0.004
51.5	15233.103	15233.101	0.002
52.5	15233.010	15233.005	0.005
53.5	15232.916	15232.910	0.006
54.5	15232.813	15232.816	-0.003
55.5	-	15232.724	
56.5	-	15232.633	
57.5	-	15232.543	
58.5	15232.459	15232.454	0.005
59.5	15232.369	15232.366	0.003
60.5	15232.283	15232.280	0.003
61.5	15232.199	15232.195	0.004
62.5	15232.113	15232.111	0.002
63.5	15232.029	15232.029	0.000
64.5	15231.949	15231.947	0.002
65.5	15231.869	15231.867	0.002
66.5	15231.792	15231.789	0.003
67.5	15231.715	15231.711	0.004
68.5	15231.636	15231.635	0.001
69.5	15231.562	15231.560	0.002
70.5	15231.485	15231.486	-0.001
71.5	15231.412	15231.414	-0.002
72.5	15231.345	15231.343	0.002

 $A^2\Pi_{3/2} \leftarrow X^2\Sigma^+ (4-3) R_{21}(ee)$

OBS	CALC	DIFF
-	15244.785	
-	15244.980	
-	15245.176	
-	15245.374	
-	15245.572	
-	15245.772	
-	15245.973	
-	15246.176	
-	15246.379	
-	15246.584	
-	15246.790	
-	15246.997	
-	15247.205	
-	15247.415	
-	15247.625	
-	15247.837	
-	15248.050	
-	15248.264	
15248.481	15248.480	0.001
15248.694	15248.696	-0.002
15248.914	15248.914	0.000
15249.128	15249.133	-0.005
-	15249.353	
-	15249.575	
15249.795	15249.797	-0.002
15250.018	15250.021	-0.003
15250.249	15250.246	0.003
15250.472	15250.472	0.000
-	15250.699	
15250.930	15250.928	0.002
15251.156	15251.158	-0.002
15251.400	15251.388	0.012
15251.620	15251.621	-0.001
15251.853	15251.854	-0.001
15252.084	15252.088	-0.004
15252.314	15252.324	-0.010
15252.554	15252.561	-0.007
15252.824	15252.799	0.025**
15253.038	15253.038	0.000
15253.281	15253.278	0.003
15253.525	15253.520	0.005
15253.765	15253.762	0.003
15254.005	15254.006	-0.001
15254.248	15254.251	-0.003
15254.495	15254.498	-0.003
15254.749	15254.745	0.004

73.5	15231.278	15231.273	0.005	15254.989	15254.994	-0.005
74.5	15231.205	15231.204	0.001	15255.243	15255.243	0.000
75.5	15231.138	15231.137	0.001	15255.491	15255.494	-0.003
76.5	15231.074	15231.071	0.003	15255.745	15255.747	-0.002
77.5	15231.005	15231.006	-0.001	15255.992	15256.000	-0.008
78.5	15230.951	15230.942	0.009	15256.248	15256.254	-0.006
79.5	15230.881	15230.880	0.001	15256.518	15256.510	0.008
80.5	15230.814	15230.819	-0.005	15256.768	15256.767	0.001
81.5	15230.754	15230.759	-0.005	15257.028	15257.025	0.003
82.5	15230.691	15230.701	-0.010	15257.282	15257.284	-0.002
83.5	15230.641	15230.643	-0.002	15257.539	15257.545	-0.006
84.5	15230.588	15230.587	0.001	15257.809	15257.806	0.003
85.5	15230.531	15230.533	-0.002	15258.069	15258.069	0.000
86.5	15230.474	15230.479	-0.005	-	15258.333	
87.5	15230.421	15230.427	-0.006	-	15258.598	
88.5	15230.371	15230.376	-0.005	-	15258.864	
89.5	15230.324	15230.327	-0.003	-	15259.132	
90.5	15230.277	15230.278	-0.001	-	15259.401	
91.5	15230.231	15230.231	0.000	-	15259.670	
92.5	-	15230.186		15259.940	15259.941	-0.001
93.5	-	15230.141		15260.214	15260.214	0.000
94.5	-	15230.098		15260.487	15260.487	0.000
95.5	-	15230.056		15260.761	15260.761	0.000
96.5	-	15230.015		15261.048	15261.037	0.011
97.5	-	15229.976		15261.318	15261.314	0.004
98.5	-	15229.938		15261.595	15261.592	0.003

 $B^2\Sigma^+ \leftarrow X^2\Sigma^+ (0-0) P_1$
 $B^2\Sigma^+ \leftarrow X^2\Sigma^+ (0-0) P_2$

<i>N</i>	OBS	CALC	DIFF	OBS	CALC	DIFF
1	15355.687	15355.680	0.007	-	-	
2	15355.527	15355.522	0.005	15355.685	15355.679	0.006
3	-	15355.366		-	15355.627	
4	-	15355.213		-	15355.578	
5	-	15355.062		-	15355.530	
6	15354.917	15354.913	0.004	15355.490	15355.485	0.005
7	-	15354.766		-	15355.442	
8	-	15354.621		15355.397	15355.401	-0.004
9	-	15354.479		15355.355	15355.362	-0.007
10	15354.331	15354.339	-0.008	15355.326	15355.326	0.000
11	15354.197	15354.201	-0.004	15355.291	15355.292	-0.001
12	15354.058	15354.065	-0.007	15355.258	15355.260	-0.002
13	15353.928	15353.932	-0.004	15355.224	15355.230	-0.006
14	15353.798	15353.801	-0.003	15355.198	15355.202	-0.004
15	15353.674	15353.672	0.002	15355.170	15355.177	-0.007
16	15353.542	15353.545	-0.003	15355.153	15355.153	0.000
17	15353.417	15353.421	-0.004	15355.134	15355.132	0.002
18	15353.295	15353.298	-0.003	15355.117	15355.113	0.004**
19	15353.173	15353.178	-0.005	15355.091	15355.097	-0.006**
20	15353.056	15353.060	-0.004	15355.076	15355.082	-0.006
21	15352.938	15352.945	-0.007	15355.046	15355.070	-0.024**
22	15352.824	15352.831	-0.007	15355.046	15355.060	-0.014**
23	15352.717	15352.720	-0.003	15355.044	15355.052	-0.008**
24	15352.609	15352.611	-0.002	15355.044	15355.046	-0.002**

25	15352.502	15352.504	-0.002	15355.035	15355.042	-0.007**
26	15352.398	15352.400	-0.002	15355.035	15355.040	-0.005**
27	15352.296	15352.298	-0.002	15355.035	15355.041	-0.006**
28	15352.198	15352.198	0.000	15355.035	15355.044	-0.009**
29	15352.101	15352.100	0.001	15355.035	15355.048	-0.013**
30	15352.006	15352.004	0.002	15355.044	15355.055	-0.011
31	15351.912	15351.911	0.001	15355.064	15355.063	0.001**
32	15351.822	15351.820	0.002	15355.064	15355.073	-0.009**
33	15351.728	15351.731	-0.003	15355.076	15355.085	-0.009
34	15351.643	15351.644	-0.001	15355.091	15355.098	-0.007**
35	15351.560	15351.560	0.000	15355.107	15355.112	-0.005
36	15351.483	15351.478	0.005	15355.117	15355.126	-0.009**
37	15351.403	15351.398	0.005	15355.135	15355.138	-0.003**
38	15351.322	15351.320	0.002	15355.135	15355.144	-0.009**
39	15351.246	15351.245	0.001	15355.135	15355.133	0.002**
40	15351.169	15351.172	-0.003	15355.467	15355.083	0.384**
41	15351.101	15351.101	0.000	15355.414	15355.420	-0.006
42	15351.032	15351.032	0.000	15355.397	15355.414	-0.017**
43	15350.963	15350.965	-0.002	15355.428	15355.430	-0.002
44	15350.897	15350.901	-0.004	15355.457	15355.458	-0.001
45	15350.839	15350.839	0.000	15355.490	15355.491	-0.001
46	15350.775	15350.779	-0.004	15355.529	15355.529	0.000
47	15350.720	15350.722	-0.002	15355.572	15355.571	0.001
48	15350.667	15350.667	0.000	15355.613	15355.616	-0.003
49	15350.608	15350.614	-0.006	15355.659	15355.664	-0.005
50	15350.556	15350.563	-0.007	15355.712	15355.715	-0.003
51	15350.511	15350.514	-0.003	15355.766	15355.768	-0.002
52	15350.466	15350.468	-0.002	15355.823	15355.824	-0.001
53	15350.424	15350.424	0.000	15355.881	15355.881	0.000
54	15350.383	15350.382	0.001	15355.937	15355.942	-0.005
55	15350.341	15350.342	-0.001	15356.000	15356.004	-0.004
56	15350.304	15350.305	-0.001	15356.066	15356.069	-0.003
57	15350.274	15350.270	0.004	15356.134	15356.137	-0.003
58	15350.243	15350.237	0.006	15356.204	15356.206	-0.002
59	15350.216	15350.207	0.009	15356.272	15356.278	-0.006
60	15350.184	15350.178	0.006	15356.350	15356.352	-0.002
61	15350.151	15350.152	-0.001	15356.426	15356.429	-0.003
62	15350.128	15350.128	0.000	15356.505	15356.507	-0.002
63	15350.102	15350.107	-0.005	15356.588	15356.588	0.000
64	15350.081	15350.087	-0.006	15356.673	15356.671	0.002
65	15350.064	15350.070	-0.006	15356.758	15356.757	0.001
66	15350.051	15350.055	-0.004	15356.842	15356.844	-0.002
67	15350.039	15350.043	-0.004	15356.931	15356.934	-0.003
68	-	15350.033		15357.024	15357.026	-0.002
69	-	15350.024		15357.121	15357.120	0.001
70	15350.013	15350.019	-0.006	15357.216	15357.217	-0.001
71	15350.013	15350.015	-0.002	15357.316	15357.315	0.001
72	15350.013	15350.014	-0.001	15357.416	15357.416	0.000
73	15350.013	15350.015	-0.002	15357.518	15357.520	-0.002
74	15350.013	15350.018	-0.005	15357.624	15357.625	-0.001
75	-	15350.023		15357.732	15357.733	-0.001
76	15350.028	15350.031	-0.003	15357.843	15357.842	0.001
77	15350.039	15350.041	-0.002	15357.955	15357.955	0.000
78	15350.051	15350.053	-0.002	15358.072	15358.069	0.003
79	15350.064	15350.068	-0.004	15358.188	15358.185	0.003
80	15350.081	15350.084	-0.003	15358.307	15358.304	0.003
81	15350.102	15350.103	-0.001	15358.422	15358.425	-0.003

82	15350.122	15350.125	-0.003	15358.549	15358.548	0.001
83	15350.151	15350.148	0.003	15358.674	15358.674	0.000
84	15350.168	15350.174	-0.006	15358.794	15358.801	-0.007
85	15350.201	15350.202	-0.001	15358.924	15358.931	-0.007
86	15350.234	15350.232	0.002	15359.064	15359.063	0.001
87	15350.274	15350.265	0.009	15359.197	15359.197	0.000
88	15350.304	15350.300	0.004	15359.334	15359.334	0.000
89	-	15350.337		15359.471	15359.472	-0.001
90	-	15350.376		15359.614	15359.613	0.001
91	-	15350.418		15359.754	15359.756	-0.002
92	-	15350.461		15359.899	15359.902	-0.003
93	-	15350.508		15360.045	15360.049	-0.004

$$B^2\Sigma^+ \leftarrow X^2\Sigma^+ (0-0) R_1$$

$$B^2\Sigma^+ \leftarrow X^2\Sigma^+ (0-0) R_2$$

<i>N</i>	OBS	CALC	DIFF	OBS	CALC	DIFF
2	15355.976	15355.972	0.004	-	15356.333	
3	-	15356.037		15356.512	15356.502	0.010
4	-	15356.105		15356.679	15356.673	0.006
5	-	15356.174		15356.847	15356.846	0.001
6	15356.252	15356.246	0.006	15357.028	15357.022	0.006
7	15356.324	15356.320	0.004	15357.206	15357.199	0.007
8	15356.400	15356.397	0.003	15357.381	15357.379	0.002
9	15356.477	15356.475	0.002	15357.560	15357.561	-0.001
10	15356.556	15356.556	0.000	15357.749	15357.746	0.003
11	15356.642	15356.639	0.003	15357.935	15357.932	0.003
12	15356.726	15356.724	0.002	15358.126	15358.121	0.005
13	15356.811	15356.811	0.000	15358.311	15358.312	-0.001
14	15356.899	15356.901	-0.002	15358.509	15358.505	0.004
15	15356.994	15356.992	0.002	15358.703	15358.700	0.003
16	15357.090	15357.086	0.004	15358.907	15358.897	0.010
17	15357.184	15357.183	0.001	15359.105	15359.097	0.008
18	15357.276	15357.281	-0.005	15359.303	15359.298	0.005
19	15357.376	15357.382	-0.006	15359.501	15359.502	-0.001
20	15357.486	15357.484	0.002	15359.712	15359.708	0.004
21	15357.588	15357.589	-0.001	15359.914	15359.917	-0.003
22	15357.697	15357.697	0.000	15360.124	15360.127	-0.003
23	15357.805	15357.806	-0.001	15360.341	15360.339	0.002
24	15357.915	15357.918	-0.003	15360.554	15360.554	0.000
25	15358.030	15358.032	-0.002	15360.774	15360.771	0.003
26	15358.148	15358.148	0.000	15360.994	15360.989	0.005
27	15358.265	15358.266	-0.001	15361.207	15361.210	-0.003
28	15358.384	15358.387	-0.003	15361.431	15361.433	-0.002
29	15358.505	15358.509	-0.004	15361.658	15361.657	0.001
30	15358.632	15358.634	-0.002	15361.884	15361.884	0.000
31	15358.755	15358.762	-0.007	15362.112	15362.111	0.001
32	15358.886	15358.891	-0.005	15362.344	15362.341	0.003
33	15359.022	15359.023	-0.001	15362.578	15362.571	0.007
34	15359.155	15359.156	-0.001	15362.803	15362.800	0.003
35	15359.289	15359.292	-0.003	15363.033	15363.028	0.005
36	15359.428	15359.431	-0.003	15363.248	15363.250	-0.002
37	15359.568	15359.571	-0.003	15363.456	15363.455	0.001
38	15359.715	15359.714	0.001	15364.008	15363.621	0.387**
39	15359.860	15359.859	0.001	15364.180	15364.174	0.006

40	15360.002	15360.006	-0.004	15364.377	15364.384	-0.007
41	15360.153	15360.155	-0.002	15364.623	15364.616	0.007
42	15360.304	15360.307	-0.003	15364.862	15364.859	0.003
43	15360.464	15360.460	0.004	15365.110	15365.108	0.002
44	15360.621	15360.616	0.005	15365.358	15365.362	-0.004
45	15360.778	15360.774	0.004	15365.623	15365.620	0.003
46	15360.943	15360.935	0.008	15365.886	15365.880	0.006
47	15361.097	15361.097	0.000	15366.143	15366.144	-0.001
48	15361.268	15361.262	0.006	15366.411	15366.410	0.001
49	15361.431	15361.429	0.002	15366.679	15366.679	0.000
50	15361.601	15361.598	0.003	15366.950	15366.950	0.000
51	15361.776	15361.770	0.006	15367.228	15367.223	0.005
52	15361.948	15361.943	0.005	15367.501	15367.499	0.002
53	15362.123	15362.119	0.004	15367.778	15367.777	0.001
54	15362.302	15362.297	0.005	15368.059	15368.057	0.002
55	15362.482	15362.478	0.004	15368.341	15368.340	0.001
56	15362.662	15362.660	0.002	15368.627	15368.625	0.002
57	15362.848	15362.845	0.003	15368.915	15368.912	0.003
58	15363.036	15363.032	0.004	15369.201	15369.201	0.000
59	15363.223	15363.221	0.002	15369.491	15369.493	-0.002
60	15363.418	15363.412	0.006	15369.786	15369.787	-0.001
61	15363.612	15363.606	0.006	15370.083	15370.083	0.000
62	15363.803	15363.801	0.002	15370.383	15370.381	0.002
63	15363.998	15363.999	-0.001	15370.689	15370.681	0.008
64	15364.199	15364.200	-0.001	15370.989	15370.984	0.005
65	15364.401	15364.402	-0.001	15371.289	15371.289	0.000
66	15364.608	15364.607	0.001	15371.595	15371.596	-0.001
67	15364.810	15364.813	-0.003	15371.905	15371.905	0.000
68	15365.023	15365.022	0.001	15372.217	15372.216	0.001
69	15365.237	15365.234	0.003	15372.531	15372.530	0.001
70	15365.447	15365.447	0.000	15372.844	15372.845	-0.001
71	15365.664	15365.663	0.001	15373.167	15373.163	0.004
72	15365.882	15365.880	0.002	15373.481	15373.483	-0.002
73	15366.100	15366.100	0.000	15373.805	15373.805	0.000
74	15366.323	15366.323	0.000	15374.135	15374.130	0.005
75	15366.550	15366.547	0.003	15374.455	15374.456	-0.001
76	15366.778	15366.774	0.004	15374.786	15374.785	0.001
77	15367.001	15367.003	-0.002	15375.116	15375.116	0.000
78	15367.236	15367.234	0.002	15375.459	15375.449	0.010
79	15367.463	15367.467	-0.004	15375.786	15375.784	0.002
80	15367.699	15367.702	-0.003	15376.128	15376.122	0.006
81	15367.938	15367.940	-0.002	15376.466	15376.461	0.005
82	15368.181	15368.180	0.001	15376.804	15376.803	0.001
83	15368.422	15368.422	0.000	15377.138	15377.147	-0.009
84	15368.666	15368.666	0.000	-	15377.493	
85	15368.919	15368.913	0.006	15377.842	15377.841	0.001
86	15369.165	15369.162	0.003	-	15378.192	

J	$B^2\Sigma^+ \leftarrow X^2\Sigma^+ (1-1) P_1$			$B^2\Sigma^+ \leftarrow X^2\Sigma^+ (1-1) P_2$		
	OBS	CALC	DIFF	OBS	CALC	DIFF
13	15359.280	15359.280	0.000	-	15360.546	
14	15359.152	15359.149	0.003	-	15360.515	
15	15359.019	15359.021	-0.002	-	15360.485	
16	15358.895	15358.894	0.001	15360.450	15360.456	-0.006
17	15358.768	15358.770	-0.002	15360.422	15360.428	-0.006
18	15358.646	15358.648	-0.002	15360.400	15360.401	-0.001
19	15358.531	15358.528	0.003	15360.375	15360.375	0.000
20	15358.412	15358.411	0.001	15360.347	15360.347	0.000
21	15358.301	15358.295	0.006	15360.312	15360.319	-0.007
22	15358.186	15358.182	0.004	15360.283	15360.287	-0.004
23	15358.072	15358.071	0.001	15360.245	15360.249	-0.004
24	15357.964	15357.962	0.002	15360.197	15360.202	-0.005
25	15357.853	15357.855	-0.002	15360.045	15360.140	-0.095**
26	15357.748	15357.751	-0.003	15360.821	15360.059	0.762**
27	15357.647	15357.648	-0.001	15360.726	15360.727	-0.001
28	15357.545	15357.548	-0.003	15360.658	15360.663	-0.005
29	15357.448	15357.450	-0.002	15360.608	15360.619	-0.011**
30	15357.352	15357.355	-0.003	15360.593	15360.592	0.001
31	15357.255	15357.261	-0.006	15360.565	15360.577	-0.012**
32	15357.162	15357.170	-0.008	15360.565	15360.570	-0.005**
33	15357.071	15357.081	-0.010	-	15360.569	
34	15356.988	15356.994	-0.006	15360.565	15360.574	-0.009**
35	15356.904	15356.909	-0.005	15360.570	15360.584	-0.014**
36	15356.823	15356.827	-0.004	15360.589	15360.597	-0.008
37	15356.741	15356.746	-0.005	15360.608	15360.614	-0.006**
38	15356.667	15356.668	-0.001	15360.629	15360.634	-0.005
39	15356.592	15356.592	0.000	15360.659	15360.657	0.002
40	15356.511	15356.519	-0.008	15360.700	15360.682	0.018**
41	15356.445	15356.447	-0.002	15360.700	15360.711	-0.011**
42	15356.376	15356.378	-0.002	15360.738	15360.742	-0.004
43	15356.308	15356.311	-0.003	15360.773	15360.775	-0.002
44	15356.244	15356.246	-0.002	15360.804	15360.811	-0.007
45	15356.183	15356.184	-0.001	15360.850	15360.850	0.000
46	-	15356.123		15360.890	15360.891	-0.001
47	-	15356.065		15360.934	15360.934	0.000
48	-	15356.009		15360.981	15360.980	0.001
49	-	15355.956		15361.011	15361.027	-0.016**
50	-	15355.904		15361.067	15361.078	-0.011
51	-	15355.855		15361.121	15361.130	-0.009
52	-	15355.808		15361.181	15361.185	-0.004
53	-	15355.763		15361.248	15361.242	0.006
54	-	15355.721		15361.296	15361.301	-0.005
55	-	15355.680		15361.361	15361.363	-0.002
56	-	15355.642		15361.424	15361.427	-0.003
57	-	15355.606		15361.493	15361.493	0.000
58	-	15355.573		15361.561	15361.561	0.000
59	-	15355.541		15361.634	15361.632	0.002
60	-	15355.512		15361.707	15361.705	0.002
61	-	15355.485		15361.787	15361.780	0.007
62	-	15355.460		15361.863	15361.857	0.006
63	-	15355.438		15361.937	15361.937	0.000
64	-	15355.417		15362.028	15362.018	0.010

65	-	15355.399		15362.104	15362.102	0.002
66	-	15355.383		15362.188	15362.188	0.000
67	-	15355.370		15362.278	15362.277	0.001
68	-	15355.358		15362.368	15362.367	0.001
69	-	15355.349		-	15362.460	
70	-	15355.342		15362.552	15362.555	-0.003
71	15355.339	15355.338	0.001**	15362.651	15362.653	-0.002
72	15355.339	15355.335	0.004**	15362.750	15362.752	-0.002
73	15355.339	15355.335	0.004**	15362.852	15362.854	-0.002
74	15355.339	15355.337	0.002**	15362.958	15362.957	0.001
75	15355.339	15355.342	-0.003**	15363.063	15363.063	0.000
76	-	15355.348		15363.169	15363.172	-0.003
77	-	15355.357		15363.271	15363.282	-0.011

$$B^2\Sigma^+ \leftarrow X^2\Sigma^+ (1-1) R_1$$

$$B^2\Sigma^+ \leftarrow X^2\Sigma^+ (1-1) R_2$$

<i>N</i>	OBS	CALC	DIFF	OBS	CALC	DIFF
5	-	15361.514		15362.170	15362.172	-0.002
6	-	15361.586		15362.349	15362.345	0.004
7	-	15361.660		15362.524	15362.521	0.003
8	-	15361.736		15362.699	15362.698	0.001
9	-	15361.814		15362.879	15362.876	0.003
10	-	15361.895		15363.059	15363.057	0.002
11	-	15361.978		15363.241	15363.239	0.002
12	-	15362.062		15363.427	15363.423	0.004
13	-	15362.149		15363.618	15363.609	0.009
14	-	15362.239		15363.799	15363.796	0.003
15	-	15362.330		15363.987	15363.984	0.003
16	15362.421	15362.423	-0.002	15364.173	15364.172	0.001
17	15362.514	15362.519	-0.005	15364.364	15364.361	0.003
18	15362.615	15362.617	-0.002	15364.553	15364.549	0.004
19	15362.717	15362.717	0.000	15364.740	15364.736	0.004
20	15362.821	15362.819	0.002	15364.922	15364.920	0.002
21	15362.929	15362.924	0.005	15365.102	15365.098	0.004
22	15363.033	15363.030	0.003	15365.269	15365.266	0.003
23	-	15363.139		15365.330	15365.420	-0.090**
24	15363.256	15363.250	0.006	15366.314	15365.553	0.761**
25	15363.367	15363.363	0.004	15366.440	15366.438	0.002
26	-	15363.478		15366.591	15366.588	0.003
27	-	15363.596		15366.764	15366.761	0.003
28	15363.709	15363.715	-0.006	15366.954	15366.949	0.005
29	15363.840	15363.837	0.003	15367.142	15367.148	-0.006
30	15363.963	15363.961	0.002	15367.366	15367.357	0.009
31	15364.081	15364.088	-0.007	15367.587	15367.572	0.015**
32	15364.216	15364.216	0.000	15367.790	15367.792	-0.002
33	15364.349	15364.346	0.003	15368.016	15368.017	-0.001
34	15364.482	15364.479	0.003	15368.246	15368.245	0.001
35	15364.616	15364.614	0.002	15368.476	15368.477	-0.001
36	15364.755	15364.751	0.004	15368.714	15368.712	0.002
37	15364.894	15364.891	0.003	15368.951	15368.951	0.000
38	15365.038	15365.032	0.006	15369.185	15369.191	-0.006
39	15365.177	15365.176	0.001	15369.433	15369.435	-0.002
40	15365.325	15365.322	0.003	15369.679	15369.681	-0.002

41	15365.473	15365.470	0.003	15369.929	15369.930	-0.001
42	15365.615	15365.620	-0.005	15370.184	15370.181	0.003
43	15365.776	15365.773	0.003	15370.437	15370.434	0.003
44	15365.933	15365.927	0.006	15370.693	15370.690	0.003
45	15366.082	15366.084	-0.002	15370.952	15370.948	0.004
46	15366.241	15366.243	-0.002	15371.214	15371.209	0.005
47	15366.405	15366.404	0.001	15371.471	15371.472	-0.001
48	15366.568	15366.568	0.000	15371.736	15371.737	-0.001
49	15366.735	15366.733	0.002	15372.006	15372.004	0.002
50	15366.908	15366.901	0.007	15372.274	15372.274	0.000
51	15367.068	15367.071	-0.003	15372.546	15372.546	0.000
52	15367.239	15367.243	-0.004	15372.820	15372.820	0.000
53	15367.422	15367.417	0.005	15373.094	15373.096	-0.002
54	15367.596	15367.594	0.002	15373.374	15373.375	-0.001
55	15367.778	15367.773	0.005	15373.655	15373.655	0.000
56	15367.957	15367.954	0.003	15373.945	15373.938	0.007
57	15368.141	15368.137	0.004	15374.225	15374.223	0.002
58	15368.318	15368.322	-0.004	15374.511	15374.511	0.000
59	15368.505	15368.510	-0.005	15374.799	15374.800	-0.001
60	15368.701	15368.699	0.002	15375.093	15375.092	0.001
61	15368.890	15368.891	-0.001	15375.390	15375.386	0.004
62	15369.089	15369.085	0.004	15375.685	15375.682	0.003
63	15369.283	15369.281	0.002	15375.979	15375.980	-0.001
64	15369.481	15369.480	0.001	15376.284	15376.281	0.003
65	15369.679	15369.680	-0.001	15376.583	15376.583	0.000
66	15369.880	15369.883	-0.003	15376.889	15376.888	0.001
67	15370.086	15370.088	-0.002	15377.195	15377.195	0.000
68	15370.295	15370.295	0.000	15377.505	15377.504	0.001
69	15370.506	15370.505	0.001	15377.811	15377.815	-0.004
70	15370.718	15370.716	0.002	15378.131	15378.129	0.002
71	15370.932	15370.930	0.002	15378.447	15378.444	0.003
72	15371.140	15371.146	-0.006	15378.762	15378.762	0.000
73	15371.360	15371.364	-0.004	15379.085	15379.082	0.003
74	15371.585	15371.585	0.000	15379.405	15379.404	0.001
75	15371.808	15371.807	0.001	15379.723	15379.728	-0.005
76	15372.036	15372.032	0.004	-	15380.055	
77	15372.262	15372.259	0.003	-	15380.383	
78	15372.488	15372.488	0.000	-	15380.714	
79	15372.725	15372.719	0.006	-	15381.047	
80	15372.952	15372.953	-0.001	-	15381.382	
81	15373.186	15373.188	-0.002	-	15381.719	
82	15373.425	15373.426	-0.001	-	15382.058	
83	15373.667	15373.666	0.001	-	15382.400	

$$B^2\Sigma^+ \leftarrow X^2\Sigma^+ (2-2) P_1$$

$$B^2\Sigma^+ \leftarrow X^2\Sigma^+ (2-2) P_2$$

<i>N</i>	OBS	CALC	DIFF	OBS	CALC	DIFF
10	-	15364.874		-	15365.440	
11	-	15364.741		-	15366.495	
12	-	15364.610		-	15366.387	
13	-	15364.480		-	15366.292	
14	-	15364.353		15366.206	15366.211	-0.005**
15	-	15364.227		15366.135	15366.140	-0.005**
16	-	15364.103		15366.077	15366.080	-0.003**

17	-	15363.981		15366.015	15366.028	-0.013**
18	-	15363.861		15365.931	15365.984	-0.053**
19	-	15363.744		15365.943	15365.945	-0.002**
20	-	15363.628		15365.901	15365.913	-0.012**
21	-	15363.514		15365.878	15365.885	-0.007**
22	-	15363.402		15365.844	15365.861	-0.017**
23	-	15363.293		15365.830	15365.842	-0.012**
24	-	15363.185		15365.817	15365.826	-0.009**
25	15363.084	15363.080	0.004	-	15365.813	
26	15362.977	15362.976	0.001	-	15365.804	
27	15362.878	15362.875	0.003	-	15365.797	
28	15362.781	15362.776	0.005	15365.791	15365.794	-0.003**
29	15362.684	15362.679	0.005	-	15365.794	
30	15362.589	15362.584	0.005	-	15365.796	
31	15362.491	15362.491	0.000	-	15365.800	
32	15362.400	15362.400	0.000	-	15365.808	
33	15362.308	15362.312	-0.004	15365.817	15365.818	-0.001
34	15362.223	15362.226	-0.003	15365.830	15365.830	0.000
35	15362.141	15362.141	0.000	15365.844	15365.845	-0.001
36	15362.063	15362.059	0.004	15365.859	15365.862	-0.003
37	15361.983	15361.979	0.004	15365.878	15365.882	-0.004
38	15361.903	15361.901	0.002	15365.901	15365.904	-0.003
39	15361.827	15361.826	0.001	15365.926	15365.928	-0.002
40	15361.754	15361.752	0.002	15365.952	15365.955	-0.003
41	15361.677	15361.681	-0.004	15365.981	15365.984	-0.003
42	15361.607	15361.612	-0.005	15366.015	15366.015	0.000
43	15361.541	15361.545	-0.004	15366.039	15366.049	-0.010
44	15361.479	15361.480	-0.001	15366.077	15366.085	-0.008
45	15361.414	15361.417	-0.003	15366.103	15366.123	-0.020**
46	15361.355	15361.356	-0.001	15366.158	15366.164	-0.006
47	15361.293	15361.298	-0.005	15366.193	15366.206	-0.013**
48	15361.240	15361.242	-0.002	15366.241	15366.251	-0.010
49	15361.183	15361.188	-0.005	15366.295	15366.299	-0.004
50	15361.125	15361.136	-0.011	15366.346	15366.348	-0.002
51	-	15361.086		15366.399	15366.400	-0.001
52	-	15361.039		15366.454	15366.454	0.000
53	-	15360.993		15366.505	15366.510	-0.005
54	-	15360.950		15366.567	15366.568	-0.001
55	-	15360.909		15366.629	15366.629	0.000
56	-	15360.870		15366.689	15366.691	-0.002
57	-	15360.834		15366.756	15366.756	0.000
58	-	15360.799		15366.825	15366.823	0.002
59	-	15360.767		15366.895	15366.893	0.002
60	-	15360.737		15366.961	15366.964	-0.003
61	-	15360.709		15367.052	15367.038	0.014**
62	-	15360.683		15367.124	15367.114	0.010
63	-	15360.660		15367.192	15367.192	0.000
64	-	15360.638		15367.285	15367.273	0.012
65	-	15360.619		15367.355	15367.355	0.000
66	-	15360.602		15367.436	15367.440	-0.004
67	-	15360.587		15367.523	15367.527	-0.004
68	-	15360.575		15367.613	15367.616	-0.003
69	-	15360.564		15367.705	15367.707	-0.002
70	-	15360.556		15367.800	15367.801	-0.001
71	15360.544	15360.550	-0.006**	15367.892	15367.896	-0.004
72	15360.544	15360.546	-0.002**	15367.987	15367.994	-0.007
73	15360.544	15360.544	0.000**	15368.093	15368.094	-0.001

74	15360.544	15360.545	-0.001**	15368.187	15368.196	-0.009
75	15360.544	15360.548	-0.004**	15368.290	15368.301	-0.011
76	-	15360.553		15368.398	15368.407	-0.009
77	-	15360.560		15368.499	15368.516	-0.017**

$$B^2\Sigma^+ \leftarrow X^2\Sigma^+ (2-2) R_1$$

$$B^2\Sigma^+ \leftarrow X^2\Sigma^+ (2-2) R_2$$

<i>N</i>	OBS	CALC	DIFF	OBS	CALC	DIFF
8	-	15366.918		-	15367.480	
9	-	15367.000		-	15368.749	
10	-	15367.083		-	15368.856	
11	15367.169	15367.169	0.000	-	15368.976	
12	15367.259	15367.256	0.003	15369.115	15369.110	0.005
13	15367.347	15367.345	0.002	15369.261	15369.254	0.007
14	15367.439	15367.436	0.003	15369.413	15369.409	0.004
15	15367.529	15367.529	0.000	15369.571	15369.572	-0.001**
16	15367.623	15367.624	-0.001	15369.743	15369.742	0.001
17	15367.722	15367.721	0.001	15369.917	15369.919	-0.002
18	15367.821	15367.820	0.001	15370.098	15370.101	-0.003
19	15367.927	15367.921	0.006	15370.287	15370.287	0.000
20	15368.021	15368.024	-0.003	15370.474	15370.479	-0.005
21	15368.132	15368.129	0.003	15370.677	15370.674	0.003
22	15368.236	15368.236	0.000	15370.872	15370.873	-0.001
23	15368.344	15368.346	-0.002	15371.071	15371.075	-0.004
24	15368.455	15368.457	-0.002	15371.272	15371.280	-0.008
25	15368.570	15368.570	0.000	15371.482	15371.489	-0.007
26	15368.690	15368.686	0.004	15371.695	15371.700	-0.005
27	15368.804	15368.804	0.000	15371.906	15371.914	-0.008
28	15368.924	15368.923	0.001	15372.137	15372.131	0.006
29	15369.047	15369.045	0.002	15372.357	15372.350	0.007
30	15369.170	15369.169	0.001	15372.581	15372.572	0.009
31	15369.294	15369.295	-0.001	15372.802	15372.797	0.005
32	15369.421	15369.423	-0.002	15373.026	15373.024	0.002
33	15369.549	15369.553	-0.004	15373.251	15373.253	-0.002
34	15369.686	15369.686	0.000	15373.483	15373.485	-0.002
35	15369.817	15369.820	-0.003	15373.721	15373.719	0.002
36	15369.955	15369.957	-0.002	15373.960	15373.955	0.005
37	15370.092	15370.096	-0.004	15374.198	15374.194	0.004
38	15370.240	15370.237	0.003	15374.433	15374.435	-0.002
39	15370.380	15370.380	0.000	15374.678	15374.679	-0.001
40	15370.529	15370.525	0.004	15374.924	15374.925	-0.001
41	15370.678	15370.672	0.006	15375.172	15375.173	-0.001
42	15370.824	15370.822	0.002	15375.421	15375.423	-0.002
43	15370.973	15370.973	0.000	15375.676	15375.675	0.001
44	15371.119	15371.127	-0.008	15375.929	15375.930	-0.001
45	15371.275	15371.283	-0.008	15376.181	15376.187	-0.006
46	15371.433	15371.441	-0.008	15376.447	15376.446	0.001
47	15371.602	15371.601	0.001	15376.704	15376.707	-0.003
48	15371.761	15371.763	-0.002	15376.970	15376.971	-0.001
49	15371.925	15371.928	-0.003	15377.245	15377.237	0.008
50	15372.095	15372.094	0.001	15377.507	15377.505	0.002
51	15372.266	15372.263	0.003	15377.775	15377.775	0.000
52	15372.437	15372.434	0.003	15378.051	15378.047	0.004
53	15372.611	15372.607	0.004	15378.330	15378.322	0.008

54	15372.777	15372.782	-0.005	15378.605	15378.598	0.007
55	15372.959	15372.959	0.000	15378.887	15378.877	0.010
56	15373.139	15373.138	0.001	15379.163	15379.158	0.005
57	15373.319	15373.320	-0.001	15379.452	15379.442	0.010
58	15373.511	15373.504	0.007	15379.736	15379.727	0.009
59	15373.695	15373.689	0.006	15380.024	15380.014	0.010
60	15373.878	15373.877	0.001	15380.307	15380.304	0.003
61	15374.071	15374.068	0.003	15380.599	15380.596	0.003
62	15374.261	15374.260	0.001	15380.900	15380.890	0.010
63	15374.452	15374.454	-0.002	15381.192	15381.186	0.006
64	15374.651	15374.651	0.000	15381.486	15381.484	0.002
65	15374.848	15374.849	-0.001	15381.787	15381.785	0.002
66	15375.052	15375.050	0.002	15382.094	15382.087	0.007
67	15375.252	15375.253	-0.001	15382.395	15382.392	0.003
68	15375.458	15375.458	0.000	15382.695	15382.699	-0.004
69	15375.664	15375.666	-0.002	15383.006	15383.008	-0.002
70	15375.876	15375.875	0.001	-	15383.319	
71	15376.088	15376.087	0.001	-	15383.632	
72	15376.294	15376.300	-0.006	-	15383.948	
73	15376.515	15376.516	-0.001	-	15384.265	
74	15376.739	15376.734	0.005	-	15384.585	
75	15376.957	15376.954	0.003	-	15384.906	
76	15377.179	15377.177	0.002	-	15385.230	
77	15377.397	15377.401	-0.004	-	15385.556	
78	15377.627	15377.627	0.000	-	15385.885	
79	15377.855	15377.856	-0.001	-	15386.215	
80	15378.089	15378.087	0.002	-	15386.547	
81	15378.325	15378.320	0.005	-	15386.882	
82	15378.553	15378.555	-0.002	-	15387.218	
83	15378.793	15378.792	0.001	-	15387.557	
84	15379.037	15379.032	0.005	-	15387.898	
85	15379.272	15379.273	-0.001	-	15388.241	

Extra Lines

$A^2\Pi_{1/2} \leftarrow X^2\Sigma^+ (3-0) R_{12}(ff)$				$A^2\Pi_{1/2} \leftarrow X^2\Sigma^+ (3-0) P_{12}(ff)$		
<i>J</i>	OBS	CALC	DIFF	OBS	CALC	DIFF
37.5	15364.008	15364.008	0.000	-	15355.732	
38.5	-	15363.730		-	15355.580	
39.5	-	15363.798		15355.467	15355.470	-0.003

$A^2\Pi_{1/2} \leftarrow X^2\Sigma^+ (0-0) R_{12}(ff)$				$A^2\Pi_{1/2} \leftarrow X^2\Sigma^+ (4-1) P_{12}(ff)$		
<i>J</i>	OBS	CALC	DIFF	OBS	CALC	DIFF
23.5	15366.314	15366.312	0.002	-	15361.073	
24.5	-	15365.663		-	15360.934	
25.5	-	15365.750		15360.821	15360.817	0.004

$^{88}\text{Sr}^{81}\text{Br}$

$A^2\Pi_{1/2} \leftarrow X^2\Sigma^+ (0-0) R_{11}(ee)$				$A^2\Pi_{1/2} \leftarrow X^2\Sigma^+ (0-0) P_{12}(ff)$		
J	OBS	CALC	DIFF	OBS	CALC	DIFF
15.5	-	14706.155		14699.421	14699.421	0.000
16.5	-	14706.392		14699.241	14699.237	0.004
17.5	-	14706.631		14699.056	14699.056	0.000
18.5	-	14706.872		14698.882	14698.876	0.006
19.5	-	14707.115		14698.693	14698.698	-0.005
20.5	-	14707.359		14698.522	14698.521	0.001
21.5	-	14707.605		14698.347	14698.346	0.001
22.5	-	14707.852		14698.174	14698.173	0.001
23.5	-	14708.101		14698.001	14698.001	0.000
24.5	-	14708.352		14697.834	14697.831	0.003
25.5	-	14708.604		14697.664	14697.663	0.001
26.5	-	14708.858		14697.499	14697.496	0.003
27.5	14709.109	14709.113	-0.004	14697.331	14697.331	0.000
28.5	14709.366	14709.370	-0.004	14697.171	14697.168	0.003
29.5	14709.628	14709.629	-0.001	14697.006	14697.007	-0.001
30.5	14709.884	14709.890	-0.006	14696.848	14696.847	0.001
31.5	14710.149	14710.152	-0.003	14696.690	14696.689	0.001
32.5	14710.418	14710.416	0.002	14696.537	14696.532	0.005
33.5	14710.680	14710.681	-0.001	14696.378	14696.377	0.001
34.5	14710.947	14710.948	-0.001	14696.225	14696.224	0.001
35.5	14711.217	14711.217	0.000	14696.071	14696.073	-0.002
36.5	14711.481	14711.487	-0.006	14695.923	14695.923	0.000
37.5	14711.757	14711.759	-0.002	14695.774	14695.775	-0.001
38.5	14712.030	14712.033	-0.003	14695.629	14695.628	0.001
39.5	14712.304	14712.308	-0.004	14695.487	14695.484	0.003
40.5	14712.585	14712.585	0.000	14695.339	14695.341	-0.002
41.5	14712.862	14712.863	-0.001	14695.200	14695.199	0.001
42.5	14713.147	14713.144	0.003	14695.059	14695.060	-0.001
43.5	14713.423	14713.425	-0.002	14694.919	14694.922	-0.003
44.5	14713.708	14713.709	-0.001	14694.788	14694.786	0.002
45.5	14713.995	14713.994	0.001	14694.648	14694.651	-0.003
46.5	14714.284	14714.281	0.003	14694.516	14694.518	-0.002
47.5	14714.574	14714.569	0.005	14694.384	14694.387	-0.003
48.5	14714.865	14714.859	0.006	14694.253	14694.258	-0.005
49.5	14715.153	14715.151	0.002	-	14694.130	
50.5	14715.445	14715.445	0.000	-	14694.005	
51.5	14715.742	14715.740	0.002	-	14693.880	
52.5	14716.040	14716.036	0.004	-	14693.758	

$A^2\Pi_{3/2} \leftarrow X^2\Sigma^+ (0-0) P_{22}(ff)$				$A^2\Pi_{3/2} \leftarrow X^2\Sigma^+ (0-0) R_{21}(ee)$		
J	OBS	CALC	DIFF	OBS	CALC	DIFF
12.5	-	15002.891		15007.058	15007.068	-0.010
13.5	-	15002.752		15007.256	15007.250	0.006
14.5	-	15002.614		15007.438	15007.434	0.004
15.5	-	15002.478		15007.619	15007.619	0.000

16.5	-	15002.343		15007.798	15007.806	-0.008
17.5	15002.209	15002.210	-0.001	15007.993	15007.994	-0.001
18.5	15002.075	15002.079	-0.004	15008.184	15008.184	0.000
19.5	15001.948	15001.949	-0.001	15008.377	15008.376	0.001
20.5	15001.819	15001.821	-0.002	15008.566	15008.569	-0.003
21.5	15001.690	15001.695	-0.005	15008.765	15008.763	0.002
22.5	15001.569	15001.570	-0.001	15008.956	15008.959	-0.003
23.5	15001.445	15001.446	-0.001	15009.158	15009.157	0.001
24.5	15001.326	15001.325	0.001	15009.359	15009.357	0.002
25.5	15001.204	15001.205	-0.001	15009.558	15009.557	0.001
26.5	15001.086	15001.086	0.000	15009.764	15009.760	0.004
27.5	15000.969	15000.969	0.000	15009.963	15009.964	-0.001
28.5	15000.854	15000.854	0.000	15010.170	15010.170	0.000
29.5	15000.741	15000.740	0.001	15010.381	15010.377	0.004
30.5	15000.637	15000.628	0.009	15010.585	15010.586	-0.001
31.5	15000.527	15000.518	0.009	15010.802	15010.796	0.006
32.5	-	15000.409		15011.007	15011.008	-0.001
33.5	-	15000.302		15011.218	15011.222	-0.004
34.5	-	15000.196		15011.434	15011.437	-0.003
35.5	-	15000.092		-	15011.654	
36.5	-	14999.990		15011.872	15011.872	0.000
37.5	14999.892	14999.889	0.003	15012.091	15012.092	-0.001
38.5	14999.792	14999.790	0.002	15012.310	15012.314	-0.004
39.5	14999.696	14999.692	0.004	15012.537	15012.537	0.000
40.5	14999.598	14999.596	0.002	15012.760	15012.761	-0.001
41.5	14999.505	14999.502	0.003	15012.990	15012.988	0.002
42.5	14999.414	14999.410	0.004	15013.215	15013.216	-0.001
43.5	14999.323	14999.319	0.004	15013.442	15013.445	-0.003
44.5	-	14999.229		15013.676	15013.676	0.000
45.5	14999.147	14999.142	0.005	15013.910	15013.909	0.001
46.5	14999.060	14999.056	0.004	15014.138	15014.143	-0.005
47.5	14998.975	14998.971	0.004	15014.372	15014.379	-0.007
48.5	14998.893	14998.889	0.004	15014.613	15014.617	-0.004
49.5	14998.809	14998.808	0.001	15014.851	15014.856	-0.005
50.5	14998.731	14998.728	0.003	15015.087	15015.096	-0.009
51.5	-	14998.650		15015.333	15015.339	-0.006
52.5	14998.571	14998.574	-0.003	15015.581	15015.583	-0.002
53.5	14998.499	14998.500	-0.001	15015.825	15015.828	-0.003
54.5	14998.427	14998.427	0.000	15016.067	15016.075	-0.008
55.5	14998.358	14998.356	0.002	-	15016.324	
56.5	14998.291	14998.287	0.004	-	15016.574	
57.5	14998.225	14998.219	0.006	-	15016.826	
58.5	14998.159	14998.153	0.006	-	15017.080	

$$A^2\Pi_{1/2} \leftarrow X^2\Sigma^+ (1-0) R_{11}(ee)$$

$$A^2\Pi_{1/2} \leftarrow X^2\Sigma^+ (1-0) P_{12}(ff)$$

J	OBS	CALC	DIFF	OBS	CALC	DIFF
16.5	-	14926.209		14919.066	14919.067	-0.001
17.5	-	14926.441		14918.879	14918.880	-0.001
18.5	-	14926.675		14918.695	14918.694	0.001
19.5	-	14926.910		14918.510	14918.509	0.001
20.5	-	14927.146		14918.325	14918.325	0.000
21.5	-	14927.384		14918.144	14918.143	0.001
22.5	-	14927.623		14917.959	14917.962	-0.003

23.5	-	14927.863		14917.781	14917.782	-0.001
24.5	-	14928.104		14917.602	14917.604	-0.002
25.5	14928.349	14928.347	0.002	14917.428	14917.426	0.002
26.5	14928.590	14928.591	-0.001	14917.249	14917.251	-0.002
27.5	14928.834	14928.836	-0.002	14917.077	14917.076	0.001
28.5	14929.078	14929.082	-0.004	14916.900	14916.903	-0.003
29.5	14929.333	14929.330	0.003	14916.730	14916.731	-0.001
30.5	14929.577	14929.579	-0.002	14916.562	14916.560	0.002
31.5	14929.821	14929.829	-0.008	14916.393	14916.391	0.002
32.5	14930.078	14930.081	-0.003	14916.225	14916.223	0.002
33.5	14930.334	14930.333	0.001	14916.059	14916.056	0.003
34.5	14930.589	14930.587	0.002	14915.890	14915.891	-0.001
35.5	14930.838	14930.843	-0.005	14915.730	14915.727	0.003
36.5	14931.097	14931.099	-0.002	14915.568	14915.564	0.004
37.5	14931.363	14931.357	0.006	14915.407	14915.402	0.005
38.5	14931.618	14931.616	0.002	14915.245	14915.242	0.003
39.5	14931.874	14931.876	-0.002	14915.089	14915.083	0.006
40.5	14932.139	14932.138	0.001	14914.924	14914.926	-0.002
41.5	14932.402	14932.401	0.001	14914.772	14914.770	0.002
42.5	14932.666	14932.665	0.001	14914.613	14914.615	-0.002
43.5	14932.931	14932.930	0.001	14914.463	14914.461	0.002
44.5	14933.196	14933.197	-0.001	14914.304	14914.309	-0.005
45.5	14933.467	14933.465	0.002	14914.158	14914.158	0.000
46.5	14933.735	14933.734	0.001	14914.005	14914.008	-0.003
47.5	14934.005	14934.004	0.001	14913.857	14913.860	-0.003
48.5	14934.273	14934.276	-0.003	14913.711	14913.712	-0.001
49.5	14934.551	14934.549	0.002	14913.566	14913.567	-0.001
50.5	14934.825	14934.823	0.002	14913.423	14913.422	0.001
51.5	14935.095	14935.098	-0.003	14913.276	14913.279	-0.003
52.5	14935.374	14935.375	-0.001	14913.135	14913.137	-0.002
53.5	14935.649	14935.653	-0.004	14912.998	14912.997	0.001
54.5	14935.929	14935.932	-0.003	14912.858	14912.858	0.000
55.5	14936.213	14936.212	0.001	14912.721	14912.720	0.001
56.5	14936.500	14936.494	0.006	14912.581	14912.583	-0.002
57.5	14936.779	14936.777	0.002	14912.446	14912.448	-0.002

$$A^2\Pi_{3/2} \leftarrow X^2\Sigma^+ (1-0) P_{22}(ff)$$

$$A^2\Pi_{3/2} \leftarrow X^2\Sigma^+ (1-0) R_{21}(ee)$$

J	OBS	CALC	DIFF	OBS	CALC	DIFF
25.5	-	15220.959		15229.291	15229.293	-0.002
26.5	-	15220.831		15229.470	15229.486	-0.016**
27.5	-	15220.705		15229.674	15229.680	-0.006
28.5	-	15220.580		15229.873	15229.875	-0.002
29.5	15220.455	15220.456	-0.001	15230.067	15230.071	-0.004
30.5	-	15220.333		15230.269	15230.268	0.001
31.5	15220.209	15220.212	-0.003	15230.462	15230.467	-0.005
32.5	15220.090	15220.092	-0.002	15230.672	15230.667	0.005
33.5	15219.988	15219.973	0.015**	15230.871	15230.868	0.003
34.5	15219.863	15219.855	0.008	15231.077	15231.071	0.006
35.5	15219.742	15219.739	0.003	15231.275	15231.274	0.001
36.5	15219.637	15219.623	0.014	15231.480	15231.479	0.001
37.5	15219.512	15219.509	0.003	15231.684	15231.685	-0.001
38.5	15219.396	15219.397	-0.001	15231.896	15231.892	0.004
39.5	15219.286	15219.285	0.001	15232.103	15232.101	0.002

40.5	15219.176	15219.175	0.001	15232.304	15232.310	-0.006
41.5	15219.068	15219.066	0.002	15232.523	15232.521	0.002
42.5	15218.973	15218.959	0.014**	15232.729	15232.733	-0.004
43.5	15218.844	15218.852	-0.008	15232.946	15232.946	0.000
44.5	15218.741	15218.747	-0.006	15233.161	15233.161	0.000
45.5	15218.632	15218.643	-0.011	15233.375	15233.376	-0.001
46.5	15218.537	15218.540	-0.003	15233.601	15233.593	0.008
47.5	15218.438	15218.439	-0.001	15233.808	15233.811	-0.003
48.5	15218.332	15218.339	-0.007	15234.034	15234.030	0.004
49.5	15218.231	15218.240	-0.009	15234.260	15234.251	0.009
50.5	15218.139	15218.142	-0.003	15234.484	15234.472	0.012
51.5	-	15218.046		15234.704	15234.695	0.009
52.5	15217.952	15217.951	0.001	15234.924	15234.919	0.005
53.5	15217.852	15217.857	-0.005	15235.137	15235.145	-0.008
54.5	15217.761	15217.764	-0.003	15235.392	15235.371	0.021**
55.5	15217.673	15217.673	0.000	15235.608	15235.599	0.009
56.5	15217.582	15217.583	-0.001	15235.822	15235.828	-0.006
57.5	15217.491	15217.494	-0.003	15236.063	15236.058	0.005
58.5	15217.403	15217.407	-0.004	-	15236.289	
59.5	15217.321	15217.320	0.001	-	15236.521	

 $A^2\Pi_{1/2} \leftarrow X^2\Sigma^+ (2-1) R_{11}(ee)$
 $A^2\Pi_{1/2} \leftarrow X^2\Sigma^+ (2-1) P_{12}(ff)$

J	OBS	CALC	DIFF	OBS	CALC	DIFF
14.5	14930.349	14930.343	0.006	-	14924.056	
15.5	14930.576	14930.572	0.004	-	14923.866	
16.5	14930.806	14930.803	0.003	-	14923.678	
17.5	14931.036	14931.035	0.001	-	14923.491	
18.5	14931.263	14931.268	-0.005	-	14923.305	
19.5	14931.507	14931.502	0.005	-	14923.120	
20.5	14931.737	14931.738	-0.001	-	14922.937	
21.5	14931.964	14931.975	-0.011**	-	14922.755	
22.5	14932.207	14932.213	-0.006**	-	14922.575	
23.5	-	14932.453		-	14922.395	
24.5	14932.691	14932.694	-0.003	-	14922.217	
25.5	-	14932.936		-	14922.041	
26.5	-	14933.179		-	14921.865	
27.5	-	14933.424		-	14921.691	
28.5	-	14933.669		-	14921.518	
29.5	-	14933.917		-	14921.347	
30.5	-	14934.165		-	14921.176	
31.5	-	14934.415		-	14921.007	
32.5	-	14934.666		14920.837	14920.840	-0.003
33.5	-	14934.918		14920.671	14920.674	-0.003
34.5	-	14935.171		14920.497	14920.508	-0.011
35.5	14935.422	14935.426	-0.004	14920.347	14920.345	0.002**
36.5	14935.689	14935.682	0.007	14920.177	14920.182	-0.005
37.5	14935.946	14935.939	0.007	14920.017	14920.021	-0.004
38.5	14936.196	14936.198	-0.002	14919.857	14919.861	-0.004
39.5	14936.463	14936.458	0.005	14919.703	14919.703	0.000**
40.5	14936.727	14936.719	0.008	-	14919.546	
41.5	14936.980	14936.981	-0.001	14919.384	14919.390	-0.006
42.5	-	14937.245		14919.245	14919.235	0.010**
43.5	-	14937.510		14919.084	14919.082	0.002**

44.5	-	14937.776		14918.931	14918.930	0.001**
45.5	-	14938.043		14918.774	14918.779	-0.005
46.5	-	14938.312		14918.627	14918.630	-0.003
47.5	-	14938.582		14918.480	14918.482	-0.002
48.5	-	14938.853		14918.340	14918.335	0.005
49.5	14939.129	14939.125	0.004	14918.197	14918.190	0.007
50.5	14939.410	14939.399	0.011**	14918.050	14918.046	0.004
51.5	14939.686	14939.674	0.012**	14917.900	14917.903	-0.003
52.5	14939.953	14939.950	0.003	14917.760	14917.761	-0.001
53.5	14940.223	14940.227	-0.004	14917.616	14917.621	-0.005**
54.5	14940.507	14940.506	0.001	14917.486	14917.483	0.003
55.5	14940.784	14940.786	-0.002	14917.346	14917.345	0.001
56.5	14941.067	14941.067	0.000	14917.213	14917.209	0.004
57.5	14941.351	14941.349	0.002	14917.075	14917.074	0.001
58.5	14941.631	14941.633	-0.002	14916.964	14916.940	0.024**
59.5	14941.921	14941.918	0.003	-	14916.808	
60.5	-	14942.204		-	14916.677	
61.5	14942.501	14942.492	0.009**	-	14916.548	
62.5	14942.788	14942.781	0.007	-	14916.419	
63.5	14943.072	14943.071	0.001	-	14916.292	
64.5	14943.358	14943.362	-0.004	-	14916.167	
65.5	14943.651	14943.654	-0.003	14916.045	14916.042	0.003
66.5	14943.941	14943.948	-0.007	14915.922	14915.919	0.003
67.5	-	14944.243		14915.795	14915.798	-0.003
68.5	14944.532	14944.539	-0.007	14915.678	14915.678	0.000
69.5	14944.832	14944.837	-0.005	14915.555	14915.559	-0.004
70.5	-	14945.135		14915.441	14915.441	0.000
71.5	-	14945.435		14915.325	14915.325	0.000
72.5	-	14945.737		14915.214	14915.210	0.004
73.5	-	14946.039		14915.098	14915.096	0.002
74.5	-	14946.343		14914.981	14914.983	-0.002
75.5	-	14946.648		14914.874	14914.872	0.002
76.5	-	14946.954		14914.768	14914.763	0.005
77.5	-	14947.262		14914.657	14914.654	0.003
78.5	-	14947.570		14914.547	14914.547	0.000
79.5	-	14947.880		14914.441	14914.442	-0.001
80.5	-	14948.192		14914.341	14914.337	0.004
81.5	-	14948.504		14914.207	14914.234	-0.027**
82.5	-	14948.818		14914.127	14914.133	-0.006
83.5	-	14949.133		14914.037	14914.033	0.004
84.5	-	14949.449		14913.930	14913.934	-0.004
85.5	-	14949.766		14913.837	14913.836	0.001
86.5	-	14950.085		14913.734	14913.740	-0.006
87.5	-	14950.405		14913.650	14913.645	0.005

 $A^2\Pi_{3/2} \leftarrow X^2\Sigma^+ (2-1) P_{22}(ff)$
 $A^2\Pi_{3/2} \leftarrow X^2\Sigma^+ (2-1) R_{21}(ee)$

J	OBS	CALC	DIFF	OBS	CALC	DIFF
31.5	-	15224.815		15235.035	15235.036	-0.001
32.5	-	15224.695		15235.235	15235.235	0.000
33.5	-	15224.577		15235.438	15235.436	0.002
34.5	-	15224.459		-	15235.637	
35.5	-	15224.343		15235.846	15235.840	0.006
36.5	-	15224.228		15236.051	15236.044	0.007

37.5	-	15224.114		15236.246	15236.249	-0.003
38.5	-	15224.002		15236.453	15236.455	-0.002
39.5	-	15223.891		15236.656	15236.663	-0.007
40.5	-	15223.781		15236.873	15236.871	0.002
41.5	-	15223.672		15237.083	15237.081	0.002
42.5	-	15223.565		15237.293	15237.292	0.001
43.5	-	15223.458		15237.507	15237.505	0.002
44.5	-	15223.353		15237.713	15237.718	-0.005
45.5	15223.250	15223.250	0.000	-	15237.933	
46.5	15223.150	15223.147	0.003	15238.147	15238.149	-0.002
47.5	15223.050	15223.046	0.004	15238.364	15238.366	-0.002
48.5	15222.952	15222.946	0.006	-	15238.584	
49.5	15222.851	15222.847	0.004	15238.804	15238.804	0.000
50.5	15222.738	15222.750	-0.012**	15239.031	15239.025	0.006
51.5	15222.654	15222.654	0.000	15239.244	15239.246	-0.002
52.5	15222.567	15222.559	0.008	15239.462	15239.470	-0.008
53.5	-	15222.465		15239.688	15239.694	-0.006
54.5	15222.370	15222.372	-0.002	15239.921	15239.919	0.002
55.5	15222.280	15222.281	-0.001	15240.138	15240.146	-0.008
56.5	15222.194	15222.191	0.003	15240.368	15240.374	-0.006
57.5	15222.100	15222.103	-0.003	15240.598	15240.603	-0.005
58.5	-	15222.015		15240.831	15240.833	-0.002
59.5	-	15221.929		15241.065	15241.065	0.000
60.5	-	15221.844		15241.289	15241.297	-0.008
61.5	15221.761	15221.760	0.001	15241.532	15241.531	0.001
62.5	15221.698	15221.678	0.020**	15241.768	15241.766	0.002
63.5	15221.595	15221.597	-0.002	15242.006	15242.002	0.004
64.5	15221.522	15221.517	0.005	15242.233	15242.240	-0.007
65.5	15221.435	15221.438	-0.003	15242.476	15242.478	-0.002
66.5	15221.364	15221.361	0.003	15242.720	15242.718	0.002
67.5	15221.284	15221.285	-0.001	15242.960	15242.959	0.001
68.5	15221.214	15221.210	0.004	15243.200	15243.201	-0.001
69.5	15221.138	15221.137	0.001	15243.447	15243.445	0.002
70.5	15221.064	15221.064	0.000	15243.690	15243.689	0.001
71.5	15221.001	15220.993	0.008	-	15243.935	
72.5	15220.928	15220.923	0.005	15244.181	15244.182	-0.001
73.5	15220.857	15220.855	0.002	15244.428	15244.430	-0.002
74.5	15220.791	15220.788	0.003	-	15244.680	
75.5	15220.724	15220.722	0.002	-	15244.930	
76.5	15220.654	15220.657	-0.003	15245.178	15245.182	-0.004
77.5	15220.594	15220.594	0.000	15245.434	15245.435	-0.001
78.5	15220.531	15220.532	-0.001	15245.691	15245.689	0.002
79.5	15220.471	15220.471	0.000	15245.945	15245.944	0.001
80.5	15220.411	15220.411	0.000	-	15246.201	
81.5	15220.354	15220.353	0.001	15246.469	15246.458	0.011**
82.5	15220.297	15220.296	0.001	15246.722	15246.717	0.005
83.5	15220.240	15220.240	0.000	-	15246.977	
84.5	15220.184	15220.186	-0.002	-	15247.238	
85.5	15220.134	15220.133	0.001	-	15247.501	
86.5	15220.080	15220.081	-0.001	-	15247.764	
87.5	15220.027	15220.030	-0.003	-	15248.029	

$A^2\Pi_{1/2} \leftarrow X^2\Sigma^+ (3-2) R_{11}(ee)$				$A^2\Pi_{1/2} \leftarrow X^2\Sigma^+ (3-2) P_{12}(ff)$			
J	OBS	CALC	DIFF	OBS	CALC	DIFF	
12.5	-	14934.422		14929.019	14929.020	-0.001	
13.5	-	14934.647		14928.822	14928.834	-0.012	
14.5	-	14934.874		14928.679	14928.652	0.027**	
15.5	-	14935.102		14928.480	14928.474	0.006	
16.5	-	14935.332		14928.286	14928.306	-0.020**	
17.5	-	14935.562		14928.140	14928.153	-0.013**	
18.5	-	14935.794		14928.039	14928.030	0.009	
19.5	-	14936.028		14927.563	14927.543	0.020**	
20.5	-	14936.262		14927.413	14927.405	0.008	
21.5	-	14936.498		14927.242	14927.248	-0.006	
22.5	-	14936.735		14927.085	14927.083	0.002	
23.5	-	14936.973		14926.918	14926.913	0.005	
24.5	-	14937.213		14926.745	14926.742	0.003	
25.5	-	14937.454		14926.571	14926.571	0.000	
26.5	-	14937.696		14926.398	14926.399	-0.001	
27.5	-	14937.939		14926.234	14926.228	0.006	
28.5	-	14938.184		14926.064	14926.058	0.006	
29.5	14938.414	14938.430	-0.016**	14925.891	14925.889	0.002	
30.5	14938.671	14938.677	-0.006	14925.711	14925.721	-0.010	
31.5	14938.928	14938.925	0.003	14925.557	14925.554	0.003	
32.5	14939.171	14939.175	-0.004	14925.394	14925.388	0.006	
33.5	14939.421	14939.426	-0.005	14925.224	14925.223	0.001	
34.5	14939.675	14939.678	-0.003	-	14925.059		
35.5	14939.930	14939.932	-0.002	-	14924.896		
36.5	14940.190	14940.187	0.003	14924.731	14924.735	-0.004	
37.5	14940.442	14940.443	-0.001	14924.577	14924.575	0.002	
38.5	14940.692	14940.700	-0.008	14924.414	14924.416	-0.002	
39.5	14940.952	14940.958	-0.006	14924.254	14924.258	-0.004	
40.5	14941.213	14941.218	-0.005	14924.100	14924.102	-0.002	
41.5	14941.473	14941.479	-0.006	14923.947	14923.947	0.000	
42.5	14941.743	14941.741	0.002	14923.797	14923.793	0.004	
43.5	14942.000	14942.005	-0.005	14923.647	14923.640	0.007	
44.5	-	14942.270		14923.490	14923.489	0.001	
45.5	-	14942.536		14923.343	14923.339	0.004	
46.5	-	14942.803		14923.190	14923.190	0.000	
47.5	-	14943.072		14923.040	14923.043	-0.003	
48.5	-	14943.342		14922.897	14922.896	0.001	
49.5	14943.621	14943.613	0.008	14922.750	14922.751	-0.001	
50.5	14943.894	14943.885	0.009	14922.600	14922.608	-0.008	
51.5	14944.161	14944.159	0.002	14922.463	14922.465	-0.002	
52.5	14944.440	14944.434	0.006	14922.330	14922.324	0.006	
53.5	14944.718	14944.710	0.008	14922.186	14922.184	0.002	
54.5	14944.993	14944.987	0.006	14922.040	14922.046	-0.006	
55.5	14945.270	14945.266	0.004	14921.906	14921.909	-0.003	
56.5	14945.549	14945.546	0.003	14921.766	14921.773	-0.007	
57.5	14945.830	14945.827	0.003	14921.636	14921.638	-0.002	
58.5	14946.111	14946.109	0.002	14921.503	14921.505	-0.002	
59.5	14946.391	14946.393	-0.002	14921.366	14921.373	-0.007	
60.5	14946.678	14946.678	0.000	14921.236	14921.242	-0.006	
61.5	14946.965	14946.964	0.001	14921.106	14921.113	-0.007	
62.5	14947.251	14947.251	0.000	14920.989	14920.985	0.004	
63.5	14947.538	14947.540	-0.002	14920.859	14920.858	0.001	

64.5	14947.832	14947.830	0.002	14920.731	14920.732	-0.001
65.5	14948.125	14948.121	0.004	14920.611	14920.608	0.003
66.5	14948.416	14948.413	0.003	-	14920.485	
67.5	14948.702	14948.707	-0.005	14920.368	14920.364	0.004
68.5	14949.003	14949.002	0.001	14920.251	14920.244	0.007
69.5	14949.296	14949.298	-0.002	-	14920.125	
70.5	14949.588	14949.596	-0.008	-	14920.007	
71.5	14949.893	14949.894	-0.001	14919.897	14919.891	0.006
72.5	14950.187	14950.194	-0.007	-	14919.776	

$$A^2\Pi_{3/2} \leftarrow X^2\Sigma^+ (3-2) P_{22}(ff)$$

$$A^2\Pi_{3/2} \leftarrow X^2\Sigma^+ (3-2) R_{21}(ee)$$

<i>J</i>	OBS	CALC	DIFF	OBS	CALC	DIFF
26.5	15229.963	15229.961	0.002	15238.562	15238.557	0.005
27.5	15229.839	15229.836	0.003	15238.745	15238.750	-0.005
28.5	15229.713	15229.711	0.002	15238.935	15238.943	-0.008
29.5	-	15229.587		15239.135	15239.138	-0.003
30.5	15229.469	15229.465	0.004	15239.339	15239.333	0.006
31.5	15229.346	15229.344	0.002	15239.526	15239.530	-0.004
32.5	15229.226	15229.225	0.001	15239.729	15239.729	0.000
33.5	15229.112	15229.106	0.006	15239.926	15239.928	-0.002
34.5	15228.992	15228.989	0.003	15240.126	15240.128	-0.002
35.5	15228.911	15228.873	0.038**	15240.329	15240.330	-0.001
36.5	15228.765	15228.758	0.007	15240.533	15240.533	0.000
37.5	15228.645	15228.644	0.001	15240.740	15240.737	0.003
38.5	15228.532	15228.532	0.000	15240.943	15240.943	0.000
39.5	15228.425	15228.421	0.004	15241.147	15241.149	-0.002
40.5	15228.312	15228.311	0.001	15241.353	15241.357	-0.004
41.5	15228.202	15228.202	0.000	15241.560	15241.566	-0.006
42.5	-	15228.095		15241.774	15241.776	-0.002
43.5	-	15227.989		15241.981	15241.987	-0.006
44.5	15227.879	15227.884	-0.005	15242.201	15242.199	0.002
45.5	15227.762	15227.780	-0.018**	15242.414	15242.413	0.001
46.5	15227.680	15227.677	0.003	15242.628	15242.628	0.000
47.5	15227.583	15227.576	0.007	15242.845	15242.844	0.001
48.5	15227.470	15227.476	-0.006	15243.061	15243.061	0.000
49.5	15227.375	15227.378	-0.003	15243.275	15243.280	-0.005
50.5	15227.279	15227.280	-0.001	15243.498	15243.499	-0.001
51.5	15227.186	15227.184	0.002	15243.719	15243.720	-0.001
52.5	15227.073	15227.089	-0.016**	15243.939	15243.942	-0.003
53.5	15226.987	15226.995	-0.008	15244.162	15244.165	-0.003
54.5	15226.899	15226.902	-0.003	15244.389	15244.389	0.000
55.5	15226.818	15226.811	0.007	15244.609	15244.615	-0.006
56.5	15226.716	15226.721	-0.005	15244.839	15244.842	-0.003
57.5	15226.628	15226.632	-0.004	15245.083	15245.069	0.014**
58.5	15226.550	15226.545	0.005	15245.304	15245.298	0.006
59.5	15226.462	15226.459	0.003	15245.527	15245.529	-0.002
60.5	15226.370	15226.374	-0.004	15245.764	15245.760	0.004
61.5	15226.287	15226.290	-0.003	15245.987	15245.993	-0.006
62.5	15226.213	15226.207	0.006	-	15246.227	
63.5	15226.123	15226.126	-0.003	-	15246.462	
64.5	-	15226.046		-	15246.698	
65.5	15225.971	15225.967	0.004	-	15246.935	

66.5	15225.890	15225.890	0.000	15247.175	15247.174	0.001
67.5	15225.817	15225.814	0.003	15247.412	15247.414	-0.002
68.5	15225.737	15225.739	-0.002	-	15247.655	
69.5	15225.673	15225.665	0.008	15247.892	15247.897	-0.005
70.5	15225.597	15225.593	0.004	15248.136	15248.140	-0.004
71.5	15225.523	15225.522	0.001	15248.393	15248.384	0.009
72.5	15225.450	15225.452	-0.002	15248.633	15248.630	0.003
73.5	15225.386	15225.383	0.003	15248.886	15248.877	0.009
74.5	15225.310	15225.316	-0.006	15249.123	15249.125	-0.002
75.5	15225.253	15225.250	0.003	15249.373	15249.374	-0.001
76.5	15225.183	15225.185	-0.002	15249.623	15249.625	-0.002
77.5	15225.120	15225.121	-0.001	15249.877	15249.876	0.001
78.5	15225.060	15225.059	0.001	15250.134	15250.129	0.005
79.5	15225.000	15224.998	0.002	-	15250.383	
80.5	15224.936	15224.938	-0.002	15250.644	15250.639	0.005
81.5	15224.886	15224.880	0.006	15250.897	15250.895	0.002
82.5	15224.823	15224.823	0.000	15251.154	15251.152	0.002
83.5	15224.769	15224.767	0.002	15251.411	15251.411	0.000
84.5	15224.716	15224.712	0.004	15251.661	15251.671	-0.010
85.5	15224.656	15224.659	-0.003	15251.932	15251.932	0.000
86.5	15224.603	15224.607	-0.004	15252.192	15252.195	-0.003
87.5	15224.553	15224.556	-0.003	15252.462	15252.458	0.004
88.5	-	15224.507		15252.722	15252.723	-0.001
89.5	-	15224.459		15252.989	15252.989	0.000
90.5	-	15224.412		15253.259	15253.256	0.003
91.5	-	15224.366		15253.519	15253.524	-0.005

$$A^2\Pi_{1/2} \leftarrow X^2\Sigma^+ (4-3) R_{11}(ee)$$

$$A^2\Pi_{1/2} \leftarrow X^2\Sigma^+ (4-3) P_{12}(ff)$$

J	OBS	CALC	DIFF	OBS	CALC	DIFF
22.5	14941.264	14941.256	0.008	-	14931.587	
23.5	14941.497	14941.492	0.005	14931.412	14931.410	0.002
24.5	14941.728	14941.730	-0.002	14931.239	14931.235	0.004
25.5	14941.971	14941.970	0.001	14931.068	14931.061	0.007
26.5	-	14942.210		-	14930.887	
27.5	14942.481	14942.452	0.029**	14930.718	14930.715	0.003
28.5	14942.705	14942.695	0.010	14930.534	14930.545	-0.011
29.5	14942.942	14942.940	0.002	14930.385	14930.375	0.010
30.5	-	14943.185		14930.201	14930.206	-0.005
31.5	14943.435	14943.432	0.003	14930.044	14930.039	0.005
32.5	14943.679	14943.681	-0.002	14929.874	14929.873	0.001
33.5	14943.932	14943.931	0.001	-	14929.708	
34.5	14944.183	14944.181	0.002	-	14929.545	
35.5	14944.434	14944.434	0.000	-	14929.382	
36.5	14944.684	14944.687	-0.003	14929.221	14929.221	0.000
37.5	14944.941	14944.942	-0.001	14929.061	14929.061	0.000
38.5	14945.198	14945.198	0.000	14928.901	14928.903	-0.002
39.5	14945.451	14945.455	-0.004	14928.741	14928.745	-0.004
40.5	14945.712	14945.714	-0.002	14928.594	14928.589	0.005
41.5	14945.972	14945.974	-0.002	14928.430	14928.434	-0.004
42.5	14946.232	14946.235	-0.003	14928.284	14928.280	0.004
43.5	14946.485	14946.497	-0.012	14928.124	14928.128	-0.004
44.5	14946.762	14946.761	0.001	14927.974	14927.977	-0.003
45.5	14947.026	14947.025	0.001	14927.827	14927.827	0.000

46.5	14947.283	14947.292	-0.009	14927.680	14927.679	0.001
47.5	14947.556	14947.559	-0.003	-	14927.531	
48.5	14947.826	14947.828	-0.002	14927.380	14927.385	-0.005
49.5	14948.090	14948.097	-0.007	14927.236	14927.241	-0.005
50.5	14948.367	14948.368	-0.001	14927.096	14927.097	-0.001
51.5	14948.643	14948.641	0.002	14926.956	14926.955	0.001
52.5	14948.910	14948.914	-0.004	14926.813	14926.814	-0.001
53.5	14949.187	14949.189	-0.002	14926.673	14926.674	-0.001
54.5	14949.463	14949.465	-0.002	14926.533	14926.536	-0.003
55.5	14949.744	14949.743	0.001	14926.396	14926.399	-0.003
56.5	14950.030	14950.021	0.009	14926.259	14926.263	-0.004
57.5	14950.307	14950.301	0.006	-	14926.129	
58.5	14950.591	14950.582	0.009	-	14925.996	
59.5	14950.864	14950.864	0.000	-	14925.864	
60.5	14951.148	14951.148	0.000	14925.739	14925.733	0.006
61.5	14951.432	14951.433	-0.001	14925.605	14925.604	0.001
62.5	-	14951.719		14925.475	14925.476	-0.001
63.5	-	14952.006		14925.348	14925.350	-0.002
64.5	-	14952.295		14925.225	14925.224	0.001
65.5	-	14952.584		14925.095	14925.100	-0.005
66.5	14952.874	14952.875	-0.001	14924.978	14924.977	0.001
67.5	-	14953.167		14924.855	14924.856	-0.001
68.5	14953.468	14953.461	0.007	14924.738	14924.736	0.002
69.5	-	14953.756		14924.614	14924.617	-0.003
70.5	14954.051	14954.051	0.000	14924.501	14924.499	0.002
71.5	14954.345	14954.349	-0.004	14924.384	14924.383	0.001
72.5	-	14954.647		14924.268	14924.268	0.000
73.5	-	14954.947		14924.159	14924.155	0.004
74.5	-	14955.247		14924.042	14924.042	0.000
75.5	-	14955.550		14923.935	14923.932	0.003
76.5	-	14955.853		14923.822	14923.822	0.000
77.5	-	14956.157		-	14923.714	
78.5	-	14956.463		-	14923.607	
79.5	-	14956.770		-	14923.501	
80.5	-	14957.078		14923.401	14923.396	0.005

$$A^2\Pi_{3/2} \leftarrow X^2\Sigma^+ (4-3) P_{22}(ff)$$

$$A^2\Pi_{3/2} \leftarrow X^2\Sigma^+ (4-3) R_{21}(ee)$$

J	OBS	CALC	DIFF	OBS	CALC	DIFF
35.5	-	15233.356		15244.782	15244.775	0.007
36.5	-	15233.241		15244.979	15244.977	0.002
37.5	-	15233.128		-	15245.180	
38.5	-	15233.016		15245.379	15245.385	-0.006
39.5	-	15232.905		15245.589	15245.591	-0.002
40.5	-	15232.795		15245.793	15245.797	-0.004
41.5	-	15232.687		15246.003	15246.005	-0.002
42.5	-	15232.580		15246.216	15246.215	0.001
43.5	-	15232.474		15246.423	15246.425	-0.002
44.5	-	15232.369		15246.636	15246.637	-0.001
45.5	-	15232.265		15246.843	15246.850	-0.007
46.5	-	15232.163		15247.057	15247.063	-0.006
47.5	-	15232.062		15247.280	15247.279	0.001
48.5	-	15231.962		15247.494	15247.495	-0.001

49.5	-	15231.864		15247.707	15247.712	-0.005
50.5	-	15231.766		15247.931	15247.931	0.000
51.5	-	15231.670		15248.147	15248.151	-0.004
52.5	15231.583	15231.575	0.008	15248.378	15248.372	0.006
53.5	-	15231.482		15248.597	15248.594	0.003
54.5	-	15231.389		15248.818	15248.818	0.000
55.5	15231.303	15231.298	0.005	15249.041	15249.042	-0.001
56.5	15231.212	15231.208	0.004	15249.264	15249.268	-0.004
57.5	-	15231.119		-	15249.495	
58.5	15231.045	15231.032	0.013**	15249.725	15249.723	0.002
59.5	15230.939	15230.946	-0.007	15249.952	15249.952	0.000
60.5	-	15230.861		15250.180	15250.183	-0.003
61.5	-	15230.777		15250.414	15250.414	0.000
62.5	-	15230.695		15250.647	15250.647	0.000
63.5	15230.609	15230.613	-0.004	15250.888	15250.881	0.007
64.5	15230.532	15230.533	-0.001	15251.118	15251.116	0.002
65.5	15230.449	15230.455	-0.006	15251.361	15251.353	0.008
66.5	-	15230.377		15251.591	15251.590	0.001
67.5	15230.312	15230.301	0.011	-	15251.829	
68.5	15230.225	15230.226	-0.001	15252.085	15252.069	0.016**
69.5	15230.145	15230.152	-0.007	15252.322	15252.310	0.012
70.5	15230.079	15230.080	-0.001	15252.559	15252.552	0.007
71.5	15230.007	15230.009	-0.002	15252.799	15252.796	0.003
72.5	-	15229.939		15253.039	15253.040	-0.001
73.5	15229.864	15229.870	-0.006	15253.286	15253.286	0.000
74.5	15229.800	15229.802	-0.002	15253.449	15253.533	-0.084**
75.5	15229.737	15229.736	0.001	15253.776	15253.781	-0.005
76.5	15229.674	15229.671	0.003	-	15254.030	
77.5	15229.617	15229.608	0.009	15254.203	15254.281	-0.078**
78.5	15229.547	15229.545	0.002	15254.533	15254.532	0.001
79.5	-	15229.484		15254.787	15254.785	0.002
80.5	15229.424	15229.424	0.000	15255.037	15255.039	-0.002
81.5	15229.367	15229.366	0.001	15255.297	15255.294	0.003
82.5	15229.313	15229.308	0.005	15255.551	15255.551	0.000
83.5	15229.247	15229.252	-0.005	15255.811	15255.808	0.003
84.5	15229.197	15229.197	0.000	15256.070	15256.067	0.003
85.5	15229.140	15229.144	-0.004	15256.325	15256.327	-0.002
86.5	15229.090	15229.092	-0.002	15256.591	15256.588	0.003
87.5	15229.037	15229.041	-0.004	15256.848	15256.850	-0.002
88.5	15228.987	15228.991	-0.004	15257.112	15257.114	-0.002
89.5	-	15228.942		15257.375	15257.378	-0.003
90.5	-	15228.895		15257.646	15257.644	0.002
91.5	-	15228.849		15257.909	15257.911	-0.002
92.5	-	15228.805		15258.179	15258.179	0.000
93.5	-	15228.761		15258.449	15258.448	0.001
94.5	-	15228.719		15258.716	15258.719	-0.003
95.5	-	15228.678		15258.990	15258.991	-0.001

$$B^2\Sigma^+ \leftarrow X^2\Sigma^+ (0-0) P_1$$

$$B^2\Sigma^+ \leftarrow X^2\Sigma^+ (0-0) P_2$$

N	OBS	CALC	DIFF	OBS	CALC	DIFF
1	15355.653	15355.654	-0.001	-	-	
2	15355.501	15355.498	0.003	15355.662	15355.653	0.009
3	-	15355.345		-	15355.601	
4	-	15355.194		-	15355.551	
5	-	15355.045		-	15355.503	
6	-	15354.898		-	15355.458	
7	-	15354.754		-	15355.414	
8	-	15354.611		-	15355.373	
9	-	15354.471		-	15355.333	
10	15354.328	15354.333	-0.005	15355.291	15355.295	-0.004
11	15354.197	15354.197	0.000	15355.258	15355.259	-0.001
12	15354.059	15354.063	-0.004	15355.223	15355.224	-0.001
13	15353.928	15353.932	-0.004	15355.186	15355.191	-0.005**
14	15353.798	15353.803	-0.005	15355.170	15355.158	0.012**
15	15353.674	15353.675	-0.001	15355.135	15355.126	0.009**
16	15353.547	15353.550	-0.003	15355.091	15355.091	0.000**
17	15353.424	15353.428	-0.004	15355.044	15355.052	-0.008
18	15353.305	15353.307	-0.002	15354.996	15355.000	-0.004
19	15353.185	15353.189	-0.004	15354.968	15354.922	0.046**
20	15353.070	15353.072	-0.002	15355.211	15355.211	0.000
21	15352.952	15352.958	-0.006	15355.153	15355.155	-0.002
22	15352.838	15352.846	-0.008	15355.117	15355.121	-0.004
23	15352.736	15352.737	-0.001	15355.107	15355.099	0.008
24	15352.631	15352.629	0.002	15355.076	15355.084	-0.008
25	15352.526	15352.524	0.002	15355.064	15355.075	-0.011**
26	15352.416	15352.421	-0.005	15355.064	15355.069	-0.005**
27	15352.317	15352.320	-0.003	15355.064	15355.067	-0.003
28	15352.223	15352.222	0.001	15355.064	15355.068	-0.004**
29	15352.128	15352.125	0.003	15355.064	15355.071	-0.007**
30	15352.030	15352.031	-0.001	15355.064	15355.078	-0.014**
31	15351.939	15351.939	0.000	15355.076	15355.086	-0.010
32	15351.849	15351.849	0.000	15355.091	15355.097	-0.006
33	15351.761	15351.761	0.000	15355.107	15355.111	-0.004
34	15351.672	15351.676	-0.004	15355.117	15355.126	-0.009
35	15351.593	15351.593	0.000	15355.135	15355.144	-0.009
36	15351.515	15351.512	0.003	15355.153	15355.165	-0.012
37	15351.437	15351.433	0.004	15355.186	15355.187	-0.001
38	15351.361	15351.356	0.005	15355.211	15355.212	-0.001
39	15351.284	15351.282	0.002	15355.237	15355.239	-0.002
40	15351.212	15351.209	0.003	15355.268	15355.269	-0.001
41	15351.138	15351.139	-0.001	15355.296	15355.300	-0.004
42	15351.071	15351.072	-0.001	15355.332	15355.334	-0.002
43	15351.004	15351.006	-0.002	15355.368	15355.370	-0.002
44	15350.937	15350.943	-0.006	15355.410	15355.408	0.002
45	15350.880	15350.881	-0.001	15355.446	15355.449	-0.003
46	15350.824	15350.822	0.002	15355.490	15355.491	-0.001
47	15350.764	15350.766	-0.002	15355.529	15355.536	-0.007
48	15350.711	15350.711	0.000	15355.583	15355.583	0.000
49	15350.662	15350.659	0.003	15355.629	15355.633	-0.004
50	15350.608	15350.609	-0.001	15355.677	15355.684	-0.007
51	15350.562	15350.561	0.001	15355.735	15355.738	-0.003
52	15350.511	15350.515	-0.004	15355.791	15355.794	-0.003

53	15350.466	15350.472	-0.006	15355.851	15355.852	-0.001
54	15350.424	15350.430	-0.006	15355.907	15355.912	-0.005
55	15350.392	15350.391	0.001	15355.959	15355.974	-0.015**
56	15350.354	15350.354	0.000	15356.035	15356.039	-0.004
57	15350.323	15350.320	0.003	15356.102	15356.106	-0.004
58	15350.283	15350.287	-0.004	15356.171	15356.175	-0.004
59	15350.255	15350.257	-0.002	15356.246	15356.246	0.000
60	15350.234	15350.229	0.005	15356.315	15356.320	-0.005
61	15350.210	15350.203	0.007	15356.392	15356.395	-0.003
62	-	15350.180		15356.470	15356.473	-0.003
63	15350.154	15350.158	-0.004	15356.551	15356.553	-0.002
64	15350.144	15350.139	0.005	15356.634	15356.635	-0.001
65	15350.122	15350.122	0.000	15356.720	15356.719	0.001
66	15350.102	15350.108	-0.006	15356.803	15356.806	-0.003
67	-	15350.095		15356.892	15356.895	-0.003
68	15350.081	15350.085	-0.004**	15356.982	15356.986	-0.004
69	15350.081	15350.077	0.004	15357.078	15357.079	-0.001
70	-	15350.071		15357.175	15357.174	0.001
71	-	15350.068		15357.272	15357.271	0.001
72	15350.064	15350.066	-0.002**	15357.370	15357.371	-0.001
73	15350.064	15350.067	-0.003	15357.470	15357.473	-0.003
74	15350.064	15350.070	-0.006**	15357.575	15357.577	-0.002
75	-	15350.075		15357.683	15357.683	0.000
76	-	15350.083		15357.790	15357.791	-0.001
77	15350.084	15350.093	-0.009	15357.902	15357.902	0.000
78	15350.102	15350.104	-0.002	15358.016	15358.015	0.001
79	15350.122	15350.119	0.003	15358.134	15358.130	0.004
80	15350.128	15350.135	-0.007	15358.250	15358.247	0.003
81	15350.151	15350.154	-0.003	15358.362	15358.366	-0.004
82	15350.168	15350.174	-0.006	15358.486	15358.488	-0.002
83	15350.194	15350.197	-0.003	15358.611	15358.611	0.000
84	15350.216	15350.223	-0.007	15358.738	15358.737	0.001
85	15350.255	15350.250	0.005	15358.858	15358.865	-0.007
86	15350.283	15350.280	0.003	15358.996	15358.995	0.001
87	15350.304	15350.312	-0.008	15359.130	15359.128	0.002
88	15350.341	15350.346	-0.005	15359.261	15359.262	-0.001
89	15350.382	15350.382	0.000	15359.397	15359.399	-0.002
90	15350.424	15350.421	0.003	15359.537	15359.538	-0.001
91	15350.466	15350.462	0.004	15359.676	15359.679	-0.003
92	15350.511	15350.505	0.006	15359.820	15359.822	-0.002
93	-	15350.550		15359.966	15359.968	-0.002
94	-	15350.598		15360.108	15360.115	-0.007

$$B^2\Sigma^+ \leftarrow X^2\Sigma^+ (0-0) R_1$$

$$B^2\Sigma^+ \leftarrow X^2\Sigma^+ (0-0) R_2$$

N	OBS	CALC	DIFF	OBS	CALC	DIFF
3	-	15356.008		15356.467	15356.462	0.005
4	-	15356.075		15356.638	15356.630	0.008
5	-	15356.144		15356.808	15356.800	0.008
6	-	15356.215		15356.977	15356.972	0.005
7	-	15356.288		15357.155	15357.146	0.009
8	15356.368	15356.364	0.004	15357.326	15357.322	0.004
9	15356.444	15356.442	0.002	15357.501	15357.499	0.002
10	15356.524	15356.521	0.003	15357.684	15357.678	0.006

11	15356.606	15356.603	0.003	15357.862	15357.858	0.004
12	15356.693	15356.687	0.006	15358.045	15358.039	0.006
13	15356.776	15356.774	0.002	15358.220	15358.220	0.000
14	15356.854	15356.862	-0.008	15358.399	15358.399	0.000
15	15356.946	15356.953	-0.007	15358.574	15358.573	0.001
16	15357.040	15357.046	-0.006	15358.744	15358.735	0.009
17	15357.138	15357.141	-0.003	15358.907	15358.870	0.037**
18	15357.235	15357.238	-0.003	15359.383	15359.372	0.011
19	15357.331	15357.338	-0.007	15359.538	15359.530	0.008
20	15357.434	15357.439	-0.005	15359.712	15359.709	0.003
21	15357.544	15357.543	0.001	15359.914	15359.900	0.014
22	15357.649	15357.649	0.000	15360.098	15360.099	-0.001
23	15357.761	15357.757	0.004	15360.305	15360.303	0.002
24	15357.866	15357.867	-0.001	15360.510	15360.511	-0.001
25	15357.979	15357.980	-0.001	15360.724	15360.722	0.002
26	15358.097	15358.094	0.003	15360.942	15360.937	0.005
27	15358.212	15358.211	0.001	15361.152	15361.153	-0.001
28	15358.329	15358.330	-0.001	15361.371	15361.373	-0.002
29	15358.449	15358.452	-0.003	15361.595	15361.595	0.000
30	15358.573	15358.575	-0.002	15361.823	15361.819	0.004
31	15358.700	15358.701	-0.001	15362.050	15362.046	0.004
32	15358.822	15358.828	-0.006	15362.280	15362.275	0.005
33	15358.957	15358.958	-0.001	15362.510	15362.506	0.004
34	15359.090	15359.090	0.000	15362.742	15362.739	0.003
35	15359.222	15359.225	-0.003	15362.983	15362.975	0.008
36	15359.358	15359.361	-0.003	15363.213	15363.213	0.000
37	15359.495	15359.500	-0.005	15363.456	15363.453	0.003
38	15359.639	15359.641	-0.002	15363.700	15363.696	0.004
39	15359.781	15359.784	-0.003	15363.943	15363.940	0.003
40	15359.930	15359.929	0.001	15364.180	15364.187	-0.007
41	15360.074	15360.076	-0.002	15364.437	15364.436	0.001
42	15360.222	15360.226	-0.004	15364.692	15364.687	0.005
43	15360.376	15360.378	-0.002	15364.947	15364.941	0.006
44	15360.535	15360.532	0.003	15365.198	15365.196	0.002
45	15360.694	15360.688	0.006	15365.464	15365.454	0.010
46	15360.849	15360.846	0.003	15365.721	15365.714	0.007
47	15361.013	15361.007	0.006	15365.981	15365.976	0.005
48	15361.169	15361.169	0.000	15366.241	15366.240	0.001
49	15361.340	15361.334	0.006	15366.505	15366.507	-0.002
50	15361.503	15361.501	0.002	15366.769	15366.775	-0.006
51	15361.674	15361.670	0.004	15367.052	15367.046	0.006
52	15361.841	15361.842	-0.001	15367.327	15367.319	0.008
53	15362.020	15362.015	0.005	15367.597	15367.594	0.003
54	15362.192	15362.191	0.001	15367.873	15367.871	0.002
55	15362.369	15362.369	0.000	15368.156	15368.151	0.005
56	15362.553	15362.549	0.004	15368.429	15368.432	-0.003
57	15362.732	15362.731	0.001	15368.718	15368.716	0.002
58	15362.920	15362.916	0.004	15369.002	15369.002	0.000
59	15363.107	15363.103	0.004	15369.288	15369.290	-0.002
60	15363.296	15363.291	0.005	15369.581	15369.580	0.001
61	15363.488	15363.482	0.006	15369.873	15369.873	0.000
62	15363.684	15363.675	0.009	15370.169	15370.167	0.002
63	15363.855	15363.871	-0.016**	15370.466	15370.464	0.002
64	15364.065	15364.068	-0.003	15370.764	15370.762	0.002
65	15364.271	15364.268	0.003	15371.069	15371.063	0.006
66	15364.470	15364.470	0.000	15371.366	15371.366	0.000
67	15364.674	15364.674	0.000	15371.674	15371.671	0.003

68	15364.877	15364.880	-0.003	15371.980	15371.979	0.001
69	15365.088	15365.089	-0.001	15372.286	15372.288	-0.002
70	15365.300	15365.299	0.001	15372.603	15372.600	0.003
71	15365.513	15365.512	0.001	15372.914	15372.914	0.000
72	15365.727	15365.727	0.000	15373.231	15373.230	0.001
73	15365.944	15365.944	0.000	15373.548	15373.548	0.000
74	15366.163	15366.163	0.000	15373.868	15373.868	0.000
75	15366.386	15366.385	0.001	15374.194	15374.190	0.004
76	15366.613	15366.608	0.005	15374.514	15374.514	0.000
77	15366.838	15366.834	0.004	15374.840	15374.841	-0.001
78	15367.062	15367.062	0.000	15375.172	15375.170	0.002
79	15367.294	15367.292	0.002	15375.496	15375.500	-0.004
80	15367.518	15367.524	-0.006	15375.838	15375.833	0.005
81	15367.754	15367.759	-0.005	15376.176	15376.169	0.007
82	15367.994	15367.996	-0.002	15376.513	15376.506	0.007
83	15368.239	15368.234	0.005	15376.842	15376.845	-0.003
84	15368.476	15368.475	0.001	15377.186	15377.187	-0.001
85	15368.717	15368.719	-0.002	15377.533	15377.530	0.003
86	15368.972	15368.964	0.008	15377.882	15377.876	0.006
87	15369.214	15369.211	0.003	-	15378.224	

$$B^2\Sigma^+ \leftarrow X^2\Sigma^+ (1-1) P_1$$

$$B^2\Sigma^+ \leftarrow X^2\Sigma^+ (1-1) P_2$$

<i>N</i>	OBS	CALC	DIFF	OBS	CALC	DIFF
16	15358.838	15358.831	0.007	-	15360.543	
17	15358.714	15358.710	0.004	-	15360.518	
18	15358.595	15358.592	0.003	-	15360.495	
19	15358.483	15358.476	0.007	-	15360.476	
20	15358.363	15358.362	0.001	-	15360.459	
21	15358.254	15358.249	0.005	-	15360.444	
22	15358.138	15358.139	-0.001	15360.422	15360.432	-0.010**
23	15358.028	15358.031	-0.003	15360.422	15360.422	0.000**
24	15357.923	15357.924	-0.001	15360.413	15360.414	-0.001**
25	15357.816	15357.820	-0.004	15360.400	15360.409	-0.009**
26	15357.714	15357.718	-0.004	15360.400	15360.407	-0.007**
27	15357.616	15357.618	-0.002	15360.400	15360.406	-0.006**
28	15357.516	15357.520	-0.004	15360.400	15360.408	-0.008
29	15357.422	15357.424	-0.002	-	15360.412	
30	15357.331	15357.331	0.000	15360.413	15360.418	-0.005
31	15357.237	15357.239	-0.002	15360.422	15360.427	-0.005
32	-	15357.150		-	15360.438	
33	-	15357.062		15360.450	15360.451	-0.001
34	-	15356.977		-	15360.466	
35	-	15356.894		15360.477	15360.484	-0.007
36	15356.812	15356.813	-0.001	15360.499	15360.503	-0.004
37	15356.731	15356.735	-0.004	15360.508	15360.525	-0.017**
38	15356.658	15356.658	0.000	15360.540	15360.549	-0.009
39	15356.582	15356.584	-0.002	15360.565	15360.576	-0.011
40	15356.517	15356.511	0.006	15360.594	15360.604	-0.010
41	15356.445	15356.441	0.004	15360.629	15360.635	-0.006
42	15356.376	15356.373	0.003	15360.659	15360.668	-0.009
43	15356.308	15356.307	0.001	15360.700	15360.703	-0.003
44	15356.244	15356.244	0.000	15360.726	15360.741	-0.015**
45	15356.183	15356.182	0.001	15360.773	15360.780	-0.007

46	-	15356.123		15360.821	15360.822	-0.001
47	-	15356.066		15360.867	15360.866	0.001
48	-	15356.011		15360.912	15360.912	0.000
49	-	15355.958		15360.961	15360.960	0.001
50	-	15355.907		15361.011	15361.011	0.000
51	-	15355.859		15361.067	15361.063	0.004
52	-	15355.812		15361.118	15361.118	0.000
53	-	15355.768		15361.171	15361.175	-0.004
54	-	15355.726		15361.237	15361.234	0.003
55	-	15355.686		15361.296	15361.296	0.000
56	-	15355.649		15361.361	15361.359	0.002
57	-	15355.613		15361.424	15361.425	-0.001
58	-	15355.580		15361.493	15361.493	0.000
59	-	15355.549		15361.565	15361.563	0.002
60	-	15355.520		15361.634	15361.635	-0.001
61	-	15355.493		15361.707	15361.709	-0.002
62	-	15355.469		15361.787	15361.786	0.001
63	-	15355.446		15361.867	15361.865	0.002
64	-	15355.426		15361.946	15361.946	0.000
65	-	15355.408		15362.028	15362.029	-0.001
66	-	15355.392		15362.114	15362.114	0.000
67	-	15355.379		15362.203	15362.201	0.002
68	-	15355.367		15362.292	15362.291	0.001
69	-	15355.358		15362.384	15362.382	0.002
70	-	15355.351		15362.478	15362.476	0.002
71	15355.339	15355.346	-0.007**	15362.566	15362.572	-0.006
72	15355.339	15355.343	-0.004**	15362.668	15362.671	-0.003
73	15355.339	15355.343	-0.004**	15362.771	15362.771	0.000
74	15355.339	15355.344	-0.005**	15362.872	15362.873	-0.001
75	15355.339	15355.348	-0.009**	15362.977	15362.978	-0.001
76	-	15355.354		15363.085	15363.085	0.000
77	-	15355.362		15363.194	15363.194	0.000
78	-	15355.373		15363.304	15363.305	-0.001

$$B^2\Sigma^+ \leftarrow X^2\Sigma^+ (1 - 1) R_1$$

$$B^2\Sigma^+ \leftarrow X^2\Sigma^+ (1 - 1) R_2$$

<i>N</i>	OBS	CALC	DIFF	OBS	CALC	DIFF
4	-	15361.290		15362.170	15362.166	0.004
5	-	15361.370		15362.305	15362.308	-0.003
6	-	15361.450		15362.459	15362.458	0.001
7	-	15361.530		15362.613	15362.616	-0.003
8	-	15361.612		15362.779	15362.778	0.001
9	-	15361.695		15362.966	15362.946	0.020**
10	-	15361.779		15363.120	15363.118	0.002
11	-	15361.864		15363.295	15363.293	0.002
12	-	15361.952		15363.474	15363.472	0.002
13	-	15362.041		15363.659	15363.654	0.005
14	-	15362.131		15363.839	15363.839	0.000
15	-	15362.224		15364.029	15364.027	0.002
16	15362.326	15362.319	0.007	15364.216	15364.218	-0.002
17	15362.421	15362.415	0.006	15364.409	15364.411	-0.002
18	15362.514	15362.513	0.001	15364.608	15364.606	0.002
19	15362.615	15362.614	0.001	15364.807	15364.804	0.003
20	15362.715	15362.716	-0.001	15365.010	15365.005	0.005

21	15362.824	15362.821	0.003	15365.213	15365.208	0.005
22	15362.929	15362.927	0.002	15365.419	15365.413	0.006
23	15363.033	15363.035	-0.002	15365.619	15365.620	-0.001
24	15363.146	15363.146	0.000	15365.831	15365.830	0.001
25	15363.256	15363.259	-0.003	15366.047	15366.042	0.005
26	15363.367	15363.373	-0.006	15366.251	15366.257	-0.006
27	15363.484	15363.490	-0.006	15366.476	15366.474	0.002
28	15363.600	15363.609	-0.009	15366.699	15366.692	0.007
29	15363.727	15363.730	-0.003	15366.919	15366.914	0.005
30	15363.850	15363.853	-0.003	15367.142	15367.137	0.005
31	15363.979	15363.978	0.001	15367.366	15367.363	0.003
32	15364.103	15364.106	-0.003	15367.587	15367.590	-0.003
33	15364.233	15364.235	-0.002	15367.819	15367.820	-0.001
34	15364.364	15364.367	-0.003	15368.054	15368.053	0.001
35	15364.500	15364.500	0.000	15368.288	15368.287	0.001
36	15364.636	15364.636	0.000	15368.524	15368.523	0.001
37	15364.778	15364.774	0.004	15368.764	15368.762	0.002
38	15364.917	15364.914	0.003	15369.006	15369.003	0.003
39	15365.060	15365.056	0.004	15369.241	15369.246	-0.005
40	15365.204	15365.201	0.003	15369.491	15369.492	-0.001
41	15365.352	15365.347	0.005	15369.737	15369.739	-0.002
42	15365.502	15365.496	0.006	15369.985	15369.989	-0.004
43	15365.638	15365.647	-0.009	15370.244	15370.240	0.004
44	15365.795	15365.799	-0.004	15370.495	15370.494	0.001
45	15365.957	15365.954	0.003	15370.751	15370.750	0.001
46	15366.108	15366.112	-0.004	15371.011	15371.009	0.002
47	15366.264	15366.271	-0.007	15371.273	15371.269	0.004
48	15366.428	15366.432	-0.004	15371.534	15371.532	0.002
49	15366.594	15366.596	-0.002	15371.797	15371.796	0.001
50	15366.769	15366.762	0.007	15372.065	15372.063	0.002
51	15366.935	15366.929	0.006	15372.334	15372.332	0.002
52	15367.103	15367.099	0.004	15372.607	15372.603	0.004
53	15367.279	15367.271	0.008	15372.875	15372.877	-0.002
54	15367.452	15367.446	0.006	15373.149	15373.152	-0.003
55	15367.621	15367.622	-0.001	15373.428	15373.429	-0.001
56	15367.798	15367.801	-0.003	15373.711	15373.709	0.002
57	15367.983	15367.981	0.002	15373.998	15373.991	0.007
58	15368.158	15368.164	-0.006	15374.278	15374.275	0.003
59	15368.343	15368.349	-0.006	15374.562	15374.561	0.001
60	15368.533	15368.536	-0.003	15374.850	15374.849	0.001
61	15368.725	15368.726	-0.001	15375.140	15375.140	0.000
62	15368.916	15368.917	-0.001	15375.437	15375.432	0.005
63	15369.112	15369.110	0.002	15375.730	15375.727	0.003
64	15369.307	15369.306	0.001	15376.024	15376.023	0.001
65	15369.500	15369.504	-0.004	15376.325	15376.322	0.003
66	15369.705	15369.704	0.001	15376.624	15376.623	0.001
67	15369.913	15369.906	0.007	15376.928	15376.926	0.002
68	15370.114	15370.110	0.004	15377.234	15377.231	0.003
69	15370.317	15370.317	0.000	15377.537	15377.539	-0.002
70	15370.524	15370.525	-0.001	15377.846	15377.848	-0.002
71	15370.739	15370.736	0.003	15378.162	15378.160	0.002
72	15370.951	15370.949	0.002	15378.477	15378.474	0.003
73	15371.161	15371.164	-0.003	15378.789	15378.789	0.000
74	15371.376	15371.381	-0.005	15379.108	15379.107	0.001
75	15371.598	15371.600	-0.002	15379.428	15379.427	0.001
76	15371.821	15371.821	0.000	15379.742	15379.749	-0.007
77	15372.047	15372.045	0.002	-	15380.074	

78	15372.269	15372.270	-0.001	-	15380.400
79	15372.495	15372.498	-0.003	-	15380.728

$$B^2\Sigma^+ \leftarrow X^2\Sigma^+ (2-2) P_1$$

$$B^2\Sigma^+ \leftarrow X^2\Sigma^+ (2-2) P_2$$

<i>N</i>	OBS	CALC	DIFF	OBS	CALC	DIFF
13	-	15364.823		15365.859	15365.863	-0.004**
14	-	15364.726		15365.830	15365.834	-0.004**
15	-	15364.636		15365.807	15365.806	0.001**
16	-	15364.553		15365.791	15365.781	0.010**
17	-	15364.479		15365.756	15365.758	-0.002**
18	-	15364.412		15365.737	15365.738	-0.001**
19	-	15363.208		15365.711	15365.720	-0.009**
20	-	15363.149		15365.695	15365.703	-0.008**
21	-	15363.084		-	15365.690	
22	-	15363.015		-	15365.678	
23	-	15362.943		-	15365.669	
24	-	15362.867		-	15365.661	
25	-	15362.790		-	15365.656	
26	-	15362.710		-	15365.654	
27	-	15362.630		15365.653	15365.653	0.000**
28	15362.561	15362.550	0.011	-	15365.655	
29	15362.470	15362.469	0.001	-	15365.659	
30	15362.389	15362.388	0.001	-	15365.665	
31	15362.308	15362.308	0.000	-	15365.673	
32	15362.223	15362.228	-0.005	-	15365.683	
33	15362.141	15362.150	-0.009	15365.670	15365.696	-0.026**
34	15362.063	15362.073	-0.010	-	15365.711	
35	15361.994	15361.997	-0.003	15365.711	15365.728	-0.017
36	15361.919	15361.922	-0.003	15365.736	15365.747	-0.011
37	15361.849	15361.849	0.000	15365.756	15365.768	-0.012
38	15361.776	15361.777	-0.001	15365.791	15365.792	-0.001
39	15361.708	15361.707	0.001	15365.817	15365.817	0.000
40	15361.641	15361.639	0.002	15365.844	15365.845	-0.001
41	15361.574	15361.572	0.002	15365.878	15365.875	0.003
42	15361.508	15361.508	0.000	15365.901	15365.907	-0.006
43	15361.447	15361.445	0.002	15365.943	15365.942	0.001
44	15361.381	15361.384	-0.003	-	15365.978	
45	-	15361.324		15366.015	15366.017	-0.002
46	15361.263	15361.267	-0.004	15366.055	15366.058	-0.003
47	15361.207	15361.212	-0.005	15366.103	15366.101	0.002
48	15361.159	15361.158	0.001	15366.148	15366.146	0.002
49	15361.113	15361.107	0.006	15366.193	15366.193	0.000
50	15361.065	15361.058	0.007	15366.242	15366.243	-0.001
51	15361.007	15361.010	-0.003	15366.295	15366.294	0.001
52	15360.972	15360.965	0.007	-	15366.348	
53	-	15360.922		15366.404	15366.404	0.000
54	15360.883	15360.881	0.002	15366.460	15366.462	-0.002
55	15360.844	15360.842	0.002	15366.525	15366.523	0.002
56	15360.806	15360.804	0.002	15366.586	15366.585	0.001
57	15360.770	15360.769	0.001	15366.652	15366.650	0.002
58	-	15360.736		15366.722	15366.717	0.005
59	-	15360.706		15366.790	15366.786	0.004
60	-	15360.677		15366.863	15366.857	0.006

61	-	15360.650		15366.936	15366.930	0.006
62	-	15360.626		15367.007	15367.005	0.002
63	-	15360.603		15367.088	15367.083	0.005
64	-	15360.583		15367.169	15367.163	0.006
65	-	15360.565		15367.254	15367.245	0.009
66	-	15360.549		15367.339	15367.329	0.010
67	-	15360.535		15367.412	15367.415	-0.003
68	-	15360.523		15367.501	15367.503	-0.002
69	-	15360.513		15367.598	15367.594	0.004
70	-	15360.506		15367.684	15367.687	-0.003
71	-	15360.500		15367.781	15367.782	-0.001
72	15360.495	15360.497	-0.002**	-	15367.879	
73	15360.495	15360.496	-0.001**	-	15367.978	
74	15360.495	15360.497	-0.002**	-	15368.079	
75	15360.495	15360.500	-0.005**	-	15368.183	
76	15360.495	15360.505	-0.010**	-	15368.288	

$$B^2\Sigma^+ \leftarrow X^2\Sigma^+ (2-2) R_1$$

$$B^2\Sigma^+ \leftarrow X^2\Sigma^+ (2-2) R_2$$

N	OBS	CALC	DIFF	OBS	CALC	DIFF
3	-	15366.744		15367.135	15367.138	-0.003
4	-	15366.821		15367.299	15367.301	-0.002
5	-	15366.901		15367.471	15367.467	0.004
6	-	15366.986		15367.634	15367.635	-0.001
7	-	15367.074		15367.801	15367.806	-0.005
8	-	15367.167		15367.984	15367.979	0.005
9	-	15367.265		15368.159	15368.155	0.004
10	-	15367.368		15368.330	15368.333	-0.003
11	-	15367.477		15368.517	15368.513	0.004
12	-	15367.592		15368.699	15368.695	0.004
13	15367.169	15367.714	-0.545**	15368.885	15368.880	0.005
14	15367.259	15367.843	-0.584**	15369.074	15369.067	0.007
15	15367.347	15367.980	-0.633**	15369.261	15369.256	0.005
16	15367.439	15368.125	-0.686**	15369.452	15369.447	0.005
17	15367.529	15367.134	0.395**	15369.643	15369.641	0.002
18	15367.623	15367.286	0.337**	15369.838	15369.837	0.001
19	15367.722	15367.434	0.288**	15370.036	15370.035	0.001
20	15367.821	15367.577	0.244**	15370.240	15370.236	0.004
21	15367.927	15367.716	0.211**	15370.443	15370.438	0.005
22	15368.021	15367.853	0.168**	15370.651	15370.643	0.008
23	15368.132	15367.987	0.145**	15370.861	15370.850	0.011
24	15368.236	15368.120	0.116**	15371.071	15371.059	0.012
25	15368.344	15368.252	0.092**	15371.272	15371.271	0.001
26	15368.455	15368.383	0.072**	15371.482	15371.484	-0.002
27	15368.570	15368.514	0.056**	15371.695	15371.700	-0.005
28	15368.690	15368.645	0.045**	15371.906	15371.918	-0.012
29	15368.804	15368.777	0.027**	15372.137	15372.138	-0.001
30	15368.924	15368.909	0.015	15372.357	15372.360	-0.003
31	15369.047	15369.043	0.004	15372.581	15372.584	-0.003
32	15369.170	15369.177	-0.007	15372.802	15372.811	-0.009
33	15369.302	15369.313	-0.011	15373.036	15373.040	-0.004
34	15369.445	15369.450	-0.005	15373.264	15373.271	-0.007
35	15369.587	15369.589	-0.002	15373.499	15373.504	-0.005
36	15369.732	15369.729	0.003	15373.734	15373.739	-0.005

37	15369.868	15369.870	-0.002	15373.975	15373.976	-0.001
38	15370.014	15370.014	0.000	15374.217	15374.216	0.001
39	15370.157	15370.159	-0.002	15374.454	15374.457	-0.003
40	15370.309	15370.305	0.004	15374.702	15374.701	0.001
41	15370.453	15370.454	-0.001	15374.945	15374.947	-0.002
42	15370.606	15370.605	0.001	15375.192	15375.195	-0.003
43	15370.754	15370.757	-0.003	15375.446	15375.445	0.001
44	15370.916	15370.911	0.005	15375.703	15375.698	0.005
45	15371.066	15371.067	-0.001	15375.948	15375.952	-0.004
46	15371.211	15371.225	-0.014**	15376.208	15376.209	-0.001
47	15371.380	15371.386	-0.006	15376.470	15376.467	0.003
48	15371.538	15371.548	-0.010	15376.727	15376.728	-0.001
49	15371.708	15371.712	-0.004	15376.992	15376.991	0.001
50	15371.877	15371.878	-0.001	15377.256	15377.256	0.000
51	15372.047	15372.046	0.001	15377.518	15377.524	-0.006
52	15372.222	15372.216	0.006	15377.787	15377.793	-0.006
53	15372.391	15372.388	0.003	15378.066	15378.065	0.001
54	15372.562	15372.562	0.000	15378.343	15378.338	0.005
55	15372.738	15372.738	0.000	15378.615	15378.614	0.001
56	15372.914	15372.916	-0.002	15378.887	15378.892	-0.005
57	15373.101	15373.096	0.005	15379.167	15379.172	-0.005
58	15373.276	15373.279	-0.003	15379.452	15379.454	-0.002
59	15373.462	15373.463	-0.001	15379.736	15379.738	-0.002
60	15373.652	15373.649	0.003	15380.024	15380.025	-0.001
61	15373.841	15373.838	0.003	15380.307	15380.313	-0.006
62	15374.032	15374.028	0.004	15380.599	15380.604	-0.005
63	15374.226	15374.221	0.005	15380.900	15380.897	0.003
64	15374.415	15374.416	-0.001	15381.192	15381.192	0.000
65	15374.615	15374.612	0.003	15381.486	15381.489	-0.003
66	15374.808	15374.811	-0.003	15381.787	15381.788	-0.001
67	15375.011	15375.012	-0.001	15382.094	15382.089	0.005
68	15375.212	15375.215	-0.003	15382.395	15382.392	0.003
69	15375.421	15375.420	0.001	15382.695	15382.698	-0.003
70	15375.628	15375.628	0.000	15383.006	15383.005	0.001
71	15375.836	15375.837	-0.001	-	15383.315	
72	15376.050	15376.048	0.002	-	15383.627	
73	15376.257	15376.262	-0.005	-	15383.941	
74	15376.474	15376.478	-0.004	-	15384.257	
75	15376.698	15376.695	0.003	-	15384.575	
76	15376.917	15376.915	0.002	-	15384.895	
77	15377.138	15377.137	0.001	-	15385.218	
78	15377.357	15377.361	-0.004	-	15385.542	
79	15377.586	15377.587	-0.001	-	15385.869	
80	15377.812	15377.816	-0.004	-	15386.197	
81	15378.043	15378.046	-0.003	-	15386.528	
82	15378.279	15378.278	0.001	-	15386.861	
83	15378.511	15378.513	-0.002	-	15387.196	
84	-	15378.750		-	15387.533	
85	15378.988	15378.988	0.000	-	15387.872	

Calculated Overlap Integrals

		$A^2\Pi_{1/2} \sim B^2\Sigma^+$		$A^2\Pi_{3/2} \sim B^2\Sigma^+$	
ν_A	ν_B	$\langle \nu_A \nu_B \rangle$	$\langle \nu_A B(R) \nu_B \rangle$	$\langle \nu_A \nu_B \rangle$	$\langle \nu_A B(R) \nu_B \rangle$
0	0	9.99E-01	5.50E-02	9.99E-01	5.50E-02
1	0	3.43E-02	1.53E-04	3.33E-02	9.97E-05
0	1	-3.41E-02	-3.60E-03	-3.31E-02	-3.55E-03
1	1	9.98E-01	5.48E-02	9.99E-01	5.48E-02
0	2	3.93E-03	4.18E-04	3.87E-03	4.12E-04
1	2	-4.47E-02	-4.89E-03	-4.33E-02	-4.81E-03
0	3	7.09E-05	-2.57E-05	7.96E-06	-2.49E-05
1	3	6.47E-03	6.93E-04	6.36E-03	6.83E-04
0	4	-1.30E-04	-3.79E-06	-1.30E-04	-3.85E-06
1	4	-3.46E-04	-7.57E-05	-3.29E-05	-7.41E-05
0	5	-8.94E-05	-5.02E-06	-8.99E-05	-5.04E-06
1	5	-9.51E-05	3.52E-06	-9.61E-05	3.31E-06
2	0	-2.38E-03	-8.80E-05	-2.41E-03	-8.70E-05
3	0	-4.27E-04	-2.13E-05	-4.23E-04	-2.12E-05
2	1	4.51E-02	3.59E-05	4.37E-02	-3.94E-05
3	1	-4.07E-03	-1.44E-04	-4.11E-03	-1.42E-04
2	2	9.98E-01	5.45E-02	9.98E-01	5.45E-02
3	2	5.35E-02	-4.84E-05	5.18E-02	-1.41E-04
2	3	-5.28E-02	-5.86E-03	-5.11E-02	-5.77E-03
3	3	9.97E-01	5.43E-02	9.97E-01	5.43E-02
2	4	8.98E-03	9.62E-04	8.83E-03	9.49E-04
3	4	-5.94E-02	-6.66E-03	-5.75E-02	-6.55E-03
2	5	-8.75E-04	-1.36E-04	-8.50E-05	-1.34E-04
3	5	1.15E-02	1.23E-03	1.13E-02	1.21E-03

Calculated Overlap Integrals (con't)

		$A^2\Pi_{1/2} \sim B^2\Sigma^+$		$A^2\Pi_{3/2} \sim B^2\Sigma^+$	
ν_A	ν_B	$\langle \nu_A \nu_B \rangle$	$\langle \nu_A B(R) \nu_B \rangle$	$\langle \nu_A \nu_B \rangle$	$\langle \nu_A B(R) \nu_B \rangle$
4	0	1.30E-04	7.56E-06	1.30E-04	7.57E-06
5	0	1.10E-04	5.83E-06	1.10E-04	5.82E-06
4	1	-3.15E-04	-1.30E-05	-3.07E-04	-1.29E-05
5	1	1.48E-04	7.98E-06	1.48E-04	8.00E-06
4	2	-5.81E-03	-2.01E-04	-5.86E-03	-1.99E-04
5	2	-1.29E-04	-4.48E-07	-1.16E-04	-1.36E-07
4	3	6.05E-02	-1.22E-04	5.85E-02	-2.30E-04
5	3	-7.65E-03	-2.62E-04	-7.72E-03	-2.58E-04
4	4	9.96E-01	5.41E-02	9.96E-01	5.41E-02
5	4	6.60E-02	-2.18E-04	6.38E-02	-3.38E-04
4	5	-6.46E-02	-7.32E-03	-6.24E-02	-7.20E-03
5	5	9.95E-01	5.38E-02	9.96E-01	5.38E-02
6	0	-7.75E-05	-4.47E-06	-7.76E-05	-4.48E-06
7	0	-8.43E-06	-2.67E-07	-8.29E-06	-2.60E-07
6	1	1.33E-04	7.12E-06	1.33E-04	7.14E-06
7	1	-1.19E-04	-6.75E-06	-1.19E-04	-6.76E-06
6	2	1.20E-04	5.90E-06	1.20E-04	5.89E-06
7	2	9.93E-05	5.42E-06	9.90E-05	5.40E-06
6	3	-2.63E-05	7.82E-06	-6.58E-06	8.26E-06
7	3	1.00E-04	4.40E-06	1.00E-04	4.38E-06
6	4	-9.57E-03	-3.23E-04	-9.66E-03	-3.19E-04
7	4	-6.80E-06	1.19E-05	1.97E-05	1.24E-05
6	5	7.02E-02	-3.43E-04	6.78E-02	-4.76E-04
7	5	-1.15E-02	-3.82E-04	-1.16E-02	-3.76E-04

Appendix II

YbF, YbCl and YbBr FTMW Line Positions

All line positions are given in units of MHz, with the exception of the residuals, ($\Delta\nu = \nu_{\text{obs}} - \nu_{\text{calc}}$) which are in units of kHz. The symbol “*” denotes data points not included in the final least squares fit.

Measured line positions for the $\nu = 0$ and 1 levels of ^{174}YbF ($X^2\Sigma^+$).

Page 180

Line positions for $^{172}\text{Yb}^{35}\text{Cl}$, $^{174}\text{Yb}^{35}\text{Cl}$ and $^{174}\text{Yb}^{37}\text{Cl}$ in the $\nu = 0$ level ($X^2\Sigma^+$), and for $^{174}\text{Yb}^{35}\text{Cl}$ in the $\nu = 1$ level ($X^2\Sigma^+$).

Page 181

Line positions for $^{174}\text{Yb}^{79}\text{Br}$ and $^{174}\text{Yb}^{81}\text{Br}$ in the $\nu = 0$ level ($X^2\Sigma^+$).

Page 182

YbF

Transition						$\nu = 0$		$\nu = 1$		
N'	J'	F'	N''	J''	F''	Sauer et al. ^a	This work	$\Delta\nu$	This work	$\Delta\nu$
1	$\frac{3}{2}$	1	0	$\frac{1}{2}$	0		14467.1551	-0.4	14374.9325	-5.7
1	$\frac{1}{2}$	0	0	$\frac{1}{2}$	1	14452.5660(5)	14452.5624	-0.3	14382.6501	3.8
1	$\frac{1}{2}$	1	0	$\frac{1}{2}$	1	14489.0420(1)	14489.0378	0.7	14411.9345	6.0
1	$\frac{3}{2}$	2	0	$\frac{1}{2}$	1	14458.0878(3)	14458.0839	0.0	14357.9726	-4.2

^aRef [48].

YbCl

Transition													
$\nu = 0$													
N'	J'	F'	N''	J''	F''	$^{172}\text{Yb}^{35}\text{Cl}$	$\Delta\nu$	$^{174}\text{Yb}^{35}\text{Cl}$	$\Delta\nu$	$^{174}\text{Yb}^{37}\text{Cl}$	$\Delta\nu$	$^{174}\text{Yb}^{35}\text{Cl}$	$\Delta\nu$
2	$\frac{3}{2}$	3	1	$\frac{1}{2}$	2	11139.9160	-0.9	11118.2582	1.5	10618.9032	-32*		
2	$\frac{3}{2}$	4	1	$\frac{3}{2}$	3	11278.9119	-0.4	11256.9896	0.4	10751.2877	6.3	11208.7020	2.4
2	$\frac{3}{2}$	3	1	$\frac{3}{2}$	2	11282.8805	-4.4	11260.9858	-0.2				
2	$\frac{3}{2}$	2	1	$\frac{3}{2}$	1			11265.5025	0.9				
3	$\frac{3}{2}$	4	2	$\frac{3}{2}$	3	16748.2245	6.9	16715.6694	0.9	15964.6784	0.1	16646.4321	-0.2
3	$\frac{3}{2}$	3	2	$\frac{3}{2}$	2	16749.1002	2.4	16716.5422	2.2	15965.4288	-2.8	16647.3180	0.3
3	$\frac{3}{2}$	2	2	$\frac{3}{2}$	1	16750.0516	-1.7	16717.4942	-0.9			16648.2486	0.2
3	$\frac{3}{2}$	5	2	$\frac{3}{2}$	4	16885.2498	-1.2	16852.4297	-0.3	16095.2408	-4.5	16780.6390	-4.1
3	$\frac{3}{2}$	4	2	$\frac{3}{2}$	3			16854.1710	-4.8	16096.8319	53*	16782.3873	1.2
4	$\frac{7}{2}$	3	3	$\frac{3}{2}$	2					21309.6741	2.6		
4	$\frac{7}{2}$	4	3	$\frac{3}{2}$	3	22355.2040	-6.0	22311.7406	-4.3	21309.2537	8.3		
4	$\frac{7}{2}$	5	3	$\frac{3}{2}$	4	22354.8930	-1.4	22311.4339	0.8	21308.9706	-7.5		
4	$\frac{7}{2}$	3	3	$\frac{7}{2}$	3					21440.4353	-2.4		
4	$\frac{7}{2}$	4	3	$\frac{7}{2}$	3	22492.9694	5.4						
4	$\frac{7}{2}$	5	3	$\frac{7}{2}$	4	22492.2190	-58*			21439.8475	7.1		
4	$\frac{7}{2}$	6	3	$\frac{7}{2}$	5			22447.5665	4.4	21438.9728	-5.8	22352.2672	0.8

YbBr

Transition						$\nu = 0$			
N'	J'	F'	N''	J''	F''	$^{174}\text{Yb}^{79}\text{Br}$	$\Delta\nu$	$^{174}\text{Yb}^{81}\text{Br}$	$\Delta\nu$
3	$\frac{5}{2}$	4	2	$\frac{3}{2}$	3	7917.2158	-1.4		
3	$\frac{5}{2}$	3	2	$\frac{3}{2}$	2	7925.4526	-3.2		
3	$\frac{7}{2}$	4	2	$\frac{5}{2}$	3	8017.3071	-1.8		
3	$\frac{7}{2}$	5	2	$\frac{5}{2}$	4	8024.2051	7.4		
4	$\frac{7}{2}$	5	3	$\frac{5}{2}$	4	10571.7551	4.0	10393.2811	-0.1
4	$\frac{7}{2}$	4	3	$\frac{5}{2}$	3	10576.5506	-4.0	10398.7557	-3.6
4	$\frac{7}{2}$	3	3	$\frac{5}{2}$	2	10577.6881	-3.5	10400.1492	-0.8
4	$\frac{9}{2}$	4	3	$\frac{7}{2}$	3	10679.7801	1.3	10497.0918	19*
4	$\frac{9}{2}$	5	3	$\frac{7}{2}$	4	10677.5670	-8.7	10495.2128	3.7
4	$\frac{9}{2}$	6	3	$\frac{7}{2}$	5	10681.9695	3.6	10500.5286	12*
4	$\frac{9}{2}$	3	3	$\frac{7}{2}$	2	10683.3634	0.4		
5	$\frac{9}{2}$	6	4	$\frac{7}{2}$	5	13227.1371	-7.6	13003.3669	1.1
5	$\frac{9}{2}$	3	4	$\frac{7}{2}$	2	13228.2166	8.9	13003.9283	-9.2
5	$\frac{9}{2}$	5	4	$\frac{7}{2}$	4	13230.2983	2.8	13007.0275	-2.1
5	$\frac{9}{2}$	4	4	$\frac{7}{2}$	3	13230.9538	2.9	13007.8101	7.1
5	$\frac{11}{2}$	6	4	$\frac{9}{2}$	5	13336.1189	-1.5	13108.9258	-5.7
5	$\frac{11}{2}$	5	4	$\frac{9}{2}$	4	13336.9852	2.6	13109.4653	-3.7
5	$\frac{11}{2}$	4	4	$\frac{9}{2}$	3			13111.7191	8.0
5	$\frac{11}{2}$	7	4	$\frac{9}{2}$	6	13339.1334	-1.2	13112.6366	2.3
6	$\frac{11}{2}$	7	5	$\frac{9}{2}$	6	15882.9443	-0.2	15613.9294	3.5
6	$\frac{11}{2}$	4	5	$\frac{9}{2}$	3	15883.4079	2.2		
6	$\frac{11}{2}$	6	5	$\frac{9}{2}$	5	15885.1603	2.3	15616.5293	0.8
6	$\frac{11}{2}$	5	5	$\frac{9}{2}$	4	15885.5430	-4.5	15616.9541	-3.3
6	$\frac{13}{2}$	7	5	$\frac{11}{2}$	6	15993.8168	0.6	15721.7240	1.3
6	$\frac{13}{2}$	6	5	$\frac{11}{2}$	5	15994.2096	-6.2	15721.8505	-3.7
6	$\frac{13}{2}$	8	5	$\frac{11}{2}$	7	15996.0079	5.3	15724.4419	2.8
6	$\frac{13}{2}$	5	5	$\frac{11}{2}$	4	15995.8137	-4.7		

YbBr (con't)

Transition						$\nu = 0$			
N'	J'	F'	N''	J''	F''	$^{174}\text{Yb}^{79}\text{Br}$	$\Delta\nu$	$^{174}\text{Yb}^{81}\text{Br}$	$\Delta\nu$
7	$\frac{13}{2}$	5	6	$\frac{11}{2}$	4			18224.6087	-0.7
7	$\frac{13}{2}$	8	6	$\frac{11}{2}$	7	18538.9298	-13*	18224.7332	1.7
7	$\frac{13}{2}$	7	6	$\frac{11}{2}$	6	18540.5951	19*	18226.6610	-3.4
7	$\frac{13}{2}$	6	6	$\frac{11}{2}$	5	18540.8184	-1.6	18226.9142	5.6
7	$\frac{15}{2}$	8	6	$\frac{13}{2}$	7	18651.0349	-0.9	18333.9827	-2.8
7	$\frac{15}{2}$	6	6	$\frac{13}{2}$	5			18335.2510	2.7
7	$\frac{15}{2}$	7	6	$\frac{13}{2}$	6	18651.2475	3.6		
7	$\frac{15}{2}$	9	6	$\frac{13}{2}$	8	18652.6951	5.8	18336.0566	-0.6
8	$\frac{15}{2}$	6	7	$\frac{13}{2}$	5			20835.4807	0.6
8	$\frac{15}{2}$	9	7	$\frac{13}{2}$	8	21195.0349	2.4	20835.6639	2.2
8	$\frac{17}{2}$	7	7	$\frac{15}{2}$	6	21309.0181	-10.2	20945.9124	-3.7
8	$\frac{17}{2}$	10	7	$\frac{15}{2}$	9	21309.2526	4.6	20947.5442	0.9

Appendix III

YbBr Laser Excitation Line Positions - $B^2\Sigma^+ \leftarrow X^2\Sigma^+$ System

Line positions (cm^{-1}) in the 0 - 0, 0 - 1, 1 - 0 and 1 - 1 bands of the $B^2\Sigma^+ \leftarrow X^2\Sigma^+$ system of $^{174}\text{Yb}^{79}\text{Br}$, $^{174}\text{Yb}^{81}\text{Br}$, $^{172}\text{Yb}^{79}\text{Br}$ and $^{172}\text{Yb}^{81}\text{Br}$ calculated from the parameters of Table 6.2. Each band is labeled as $\nu' - \nu''$, while the symbol "*" indicates exclusion of the line from final fits. The uncertainty of each line (U) is estimated based on the number of coincident lines, and is given in units of 10^3 cm^{-1} .

Page 185: $^{174}\text{Yb}^{79}\text{Br}$

Page 193: $^{174}\text{Yb}^{81}\text{Br}$

Page 202: $^{172}\text{Yb}^{79}\text{Br}$

Page 210: $^{172}\text{Yb}^{81}\text{Br}$

$^{174}\text{Yb}^{79}\text{Br}$

0 - 0 Band

N	P ₁			Q ₁			R ₁		
	CALC	DIFF	U	CALC	DIFF	U	CALC	DIFF	U
45	19694.166			19694.342			19702.508		
46	19694.216			19694.396			19702.744		
47	19694.271			19694.454			19702.984		
48	19694.329			19694.517			19703.228		
49	19694.393			19694.584			19703.477		
50	19694.460			19694.655			19703.730	0.000	6
51	19694.532			19694.731			19703.987	0.006	6
52	19694.608			19694.811			19704.249	0.001	6
53	19694.689			19694.896			19704.515	0.000	6
54	19694.774			19694.985			19704.785	0.002	6
55	19694.864			19695.078			19705.060	0.001	6
56	19694.958			19695.176			19705.339	-0.005	6
57	19695.056			19695.278			19705.622	0.003	6
58	19695.158			19695.385			19705.910	0.001	6
59	19695.265			19695.495			19706.202	-0.004	6
60	19695.377			19695.611			19706.499	0.000	6
61	19695.493			19695.730			19706.800	-0.003	6
62	19695.613			19695.854			19707.105	-0.007	6
63	19695.737			19695.983			19707.415	-0.003	6
64	19695.866			19696.116			19707.729	-0.007	6
65	19695.999			19696.253			19708.047	-0.008	6
66	19696.137	0.010	6	19696.394			19708.370	-0.001	6
67	19696.279	0.014	6	19696.540			19708.697	-0.004	6
68	19696.426	0.024*	6	19696.691	-0.004	6	19709.028		
69	19696.577	0.020*	6	19696.845	-0.001	6	19709.364		
70	19696.732	0.018	6	19697.004	0.003	6	19709.704		
71	19696.891	0.016	6	19697.168	0.003	6	19710.049		
72	19697.055	0.012	6	19697.336	0.005	6	19710.398		
73	19697.224	0.007	6	19697.508	0.010	6	19710.751	-0.011	6
74	19697.397	0.000	6	19697.685	0.009	6	19711.108	0.002	6
75	19697.574	0.000	6	19697.866	0.018*	6	19711.470	0.007	6
76	19697.755	-0.004	6	19698.051	-0.003	6	19711.837	0.003	6
77	19697.941	-0.003	6	19698.241	-0.006	6	19712.207	0.000	6
78	19698.132			19698.435	-0.006	6	19712.582	0.002	6
79	19698.326			19698.634	-0.005	6	19712.962	0.000	6
80	19698.526			19698.837	-0.005	6	19713.345	0.001	6
81	19698.729			19699.044	-0.001	6	19713.734	0.000	6
82	19698.937			19699.256	-0.007	6	19714.126	-0.001	6
83	19699.149			19699.472			19714.523	0.000	6
84	19699.366			19699.693			19714.924	-0.001	6
85	19699.587			19699.918			19715.329	-0.002	6
86	19699.813			19700.147			19715.739	-0.003	4
87	19700.043	0.011	4	19700.381			19716.154	-0.004	4
88	19700.277	0.007	4	19700.619	-0.011	4	19716.572	-0.003	4
89	19700.516	-0.002	4	19700.862			19716.995	-0.006	4
90	19700.759	-0.001	4	19701.109	0.002	4	19717.422	-0.002	4
91	19701.006	-0.005	4	19701.360	-0.002	4	19717.854	-0.004	4
92	19701.258	-0.003	4	19701.616	-0.001	4	19718.290	0.000	4

93	19701.515	-0.007	4	19701.876	-0.004	4	19718.731	-0.001	4
94	19701.775	-0.006	4	19702.141	0.001	4	19719.175	-0.001	4
95	19702.040			19702.410	0.002	4	19719.625	0.003	4
96	19702.310	0.006	4	19702.683	0.006	4	19720.078		
97	19702.584	0.005	4	19702.961	0.005	6	19720.536		
98	19702.862	0.007	4	19703.243	-0.003	6	19720.998		
99	19703.145			19703.530	0.003	6	19721.465		
100	19703.432			19703.821			19721.936		
101	19703.724			19704.116			19722.411		
102	19704.020			19704.416			19722.891		
103	19704.320			19704.720			19723.375		
104	19704.625			19705.029			19723.863		

P_2				Q_2			R_2			
N	CALC	DIFF	U	CALC	DIFF	U	CALC	DIFF	U	
49	19699.991			19709.106			19709.298			
50	19700.174			19709.471			19709.666			
51	19700.361			19709.839			19710.038			
52	19700.552			19710.212			19710.415			
53	19700.748			19710.589			19710.796			
54	19700.948	-0.011	6	19710.971			19711.181			
55	19701.153	0.001	6	19711.356			19711.571			
56	19701.362	-0.001	6	19711.747			19711.965			
57	19701.575	-0.004	6	19712.141			19712.363			
58	19701.792	-0.001	6	19712.540			19712.766			
59	19702.014	0.001	6	19712.943			19713.173			
60	19702.240	-0.002	6	19713.351			19713.585			
61	19702.471	-0.003	6	19713.763			19714.000			
62	19702.706	-0.001	6	19714.179			19714.420			
63	19702.945	0.006	6	19714.599			19714.845			
64	19703.189	-0.001	6	19715.024			19715.273			
65	19703.437	-0.002	6	19715.453			19715.707			
66	19703.690	0.005	6	19715.887			19716.144			
67	19703.946	0.004	6	19716.325			19716.586			
68	19704.207	0.003	6	19716.767			19717.032			
69	19704.473	-0.003	6	19717.213			19717.482			
70	19704.743	-0.002	6	19717.664			19717.937			
71	19705.017	-0.003	6	19718.119			19718.396			
72	19705.296	0.002	6	19718.579			19718.859			
73	19705.579	-0.004	6	19719.043			19719.327			
74	19705.866	-0.001	6	19719.511			19719.799			
75	19706.158	0.000	6	19719.984			19720.275			
76	19706.454	0.001	6	19720.460			19720.756			
77	19706.754	0.001	6	19720.942			19721.241			
78	19707.059	0.003	6	19721.427			19721.731			
79	19707.368	-0.002	6	19721.917			19722.224			
80	19707.682	0.001	6	19722.411			19722.722			
81	19708.000	-0.001	6	19722.910			19723.225			
82	19708.322	0.000	6	19723.412			19723.731			
83	19708.648	0.001	6	19723.920			19724.243			
84	19708.979			19724.431			19724.758			
85	19709.315			19724.947			19725.278			
86	19709.654	0.002	6	19725.467			19725.802			

87	19709.999	-0.006	6	19725.992	19726.330
88	19710.347	-0.007	6	19726.520	19726.863
89	19710.700	-0.003	6	19727.054	19727.400
90	19711.057	0.003	6	19727.591	19727.941
91	19711.419	0.005	6	19728.133	19728.487
92	19711.784	0.003	6	19728.679	19729.037
93	19712.155	-0.001	6	19729.229	19729.591
94	19712.529	0.006	6	19729.784	19730.150
95	19712.908	0.000	6	19730.343	19730.712
96	19713.292	0.006	6	19730.907	19731.280
97	19713.680	-0.005	6	19731.474	19731.851
98	19714.072	0.004	6	19732.046	19732.427
99	19714.468	0.001	6	19732.623	19733.008
100	19714.869	0.003	6	19733.204	19733.592
101	19715.274			19733.789	19734.181
102	19715.684			19734.378	19734.774
103	19716.098			19734.972	19735.372
104	19716.516			19735.570	19735.974
105	19716.939			19736.172	19736.580

0 - 1 Band

N	P ₁			Q ₁			R ₁		
	CALC	DIFF	U	CALC	DIFF	U	CALC	DIFF	U
26	19498.506			19498.610			19503.321		
27	19498.481			19498.588			19503.481		
28	19498.459			19498.571			19503.645		
29	19498.443			19498.559			19503.815		
30	19498.431			19498.551			19503.988		
31	19498.424			19498.547			19504.167	0.003	6
32	19498.421			19498.548			19504.350	0.003	6
33	19498.423			19498.554			19504.538	0.002	6
34	19498.429			19498.565			19504.730	0.000	6
35	19498.441			19498.580			19504.927	0.003	6
36	19498.456			19498.600			19505.128	0.006	6
37	19498.477			19498.624			19505.334	0.000	6
38	19498.502			19498.653			19505.545	0.000	6
39	19498.532			19498.687			19505.761	-0.005	6
40	19498.566			19498.725			19505.981	-0.005	6
41	19498.605			19498.768			19506.205	0.004	6
42	19498.649			19498.816			19506.434	0.002	6
43	19498.697			19498.868			19506.668	-0.002	6
44	19498.750			19498.925			19506.907	0.006	6
45	19498.808			19498.986	-0.001	6	19507.150	0.003	4
46	19498.870			19499.053	0.002	6	19507.398	-0.001	4
47	19498.937			19499.123	-0.001	6	19507.650		
48	19499.009	0.003	6	19499.199			19507.907		
49	19499.085	0.003	4	19499.279	0.006	4	19508.169	-0.004	6
50	19499.166	0.002	4	19499.364	-0.039*	6	19508.435	-0.004	6
51	19499.251	0.007	6	19499.453	-0.014	6	19508.706	-0.001	6
52	19499.341	0.004	6	19499.547	-0.005	6	19508.981	0.001	6
53	19499.436	0.003	6	19499.646	0.003	6	19509.261	-0.002	6
54	19499.535	0.007	6	19499.749	-0.004	6	19509.546	0.003	6

55	19499.639	0.010	6	19499.857	-0.008	6	19509.835	-0.003	6
56	19499.748	-0.003	6	19499.970	0.006	6	19510.129		
57	19499.861	-0.012	6	19500.087	-0.008	4	19510.428		
58	19499.979	-0.003	6	19500.209	-0.004	6	19510.731	0.004	4
59	19500.102	-0.010	4	19500.335	0.000	6	19511.039	0.000	4
60	19500.229	-0.007	6	19500.467	0.005	6	19511.351	0.005	4
61	19500.361			19500.602			19511.668	-0.004	4
62	19500.498	-0.009	6	19500.743			19511.990	0.004	4
63	19500.639	0.003	6	19500.888	-0.006	6	19512.316	0.002	4
64	19500.785			19501.038	-0.006	6	19512.647	0.005	4
65	19500.935	0.004	6	19501.192	0.001	6	19512.983	-0.001	4
66	19501.090			19501.351	0.005	6	19513.323	0.002	4
67	19501.250			19501.515			19513.668	0.001	4
68	19501.415			19501.683			19514.017	0.008	4
69	19501.584			19501.857			19514.371	-0.005	4
70	19501.758			19502.034			19514.730	0.000	4
71	19501.936			19502.217			19515.093	0.004	4
72	19502.119			19502.404			19515.461	-0.001	4
73	19502.307			19502.595			19515.834	-0.004	4
74	19502.499			19502.792			19516.211	0.003	4
75	19502.696			19502.993			19516.593	-0.002	4
76	19502.898			19503.198			19516.979	0.002	4
77	19503.104			19503.408			19517.370		
78	19503.315			19503.623			19517.766		
79	19503.531			19503.843			19518.166		
80	19503.751			19504.067			19518.571		
81	19503.976			19504.296			19518.981		

	P_2			Q_2			R_2		
N	CALC	DIFF	U	CALC	DIFF	U	CALC	DIFF	U
32	19502.063			19508.087			19508.215		
33	19502.180			19508.387			19508.518		
34	19502.302			19508.690			19508.826		
35	19502.429			19508.999			19509.138		
36	19502.560			19509.311			19509.455		
37	19502.696	0.001	6	19509.629			19509.776		
38	19502.836	0.002	6	19509.951			19510.102		
39	19502.981	0.000	6	19510.278			19510.433		
40	19503.131	0.007	6	19510.609			19510.768		
41	19503.285	-0.001	6	19510.945			19511.108		
42	19503.444	0.004	6	19511.286			19511.452		
43	19503.608			19511.631			19511.802		
44	19503.776			19511.981			19512.155		
45	19503.949			19512.335			19512.514		
46	19504.126	0.000	6	19512.694			19512.876		
47	19504.308	0.002	6	19513.058			19513.244		
48	19504.495	-0.002	6	19513.426			19513.616		
49	19504.686	-0.003	6	19513.799			19513.993		
50	19504.882	-0.002	6	19514.176			19514.374		
51	19505.083	-0.003	6	19514.558			19514.760		
52	19505.288	0.011	6	19514.945			19515.151		
53	19505.498	0.004	6	19515.336			19515.546		
54	19505.712	0.000	6	19515.732			19515.945		
55	19505.931	0.001	6	19516.132			19516.350		

56	19506.155	-0.009	6	19516.537	19516.759
57	19506.383	0.000	6	19516.947	19517.172
58	19506.616	0.000	6	19517.361	19517.590
59	19506.854	-0.004	4	19517.780	19518.013
60	19507.096	0.004	4	19518.203	19518.440
61	19507.343	0.000	4	19518.631	19518.872
62	19507.594			19519.064	19519.309
63	19507.851			19519.501	19519.750
64	19508.111			19519.943	19520.196
65	19508.377	-0.009	6	19520.389	19520.646
66	19508.647	-0.009	6	19520.840	19521.101
67	19508.921	-0.003	6	19521.296	19521.561
68	19509.200	0.002	6	19521.756	19522.025
69	19509.484	0.005	6	19522.221	19522.493
70	19509.773	-0.011	6	19522.690	19522.967
71	19510.066	0.000	6	19523.164	19523.445
72	19510.364	-0.005	6	19523.643	19523.927
73	19510.666			19524.126	19524.414
74	19510.973			19524.614	19524.906
75	19511.284			19525.106	19525.402
76	19511.601			19525.603	19525.903
77	19511.922			19526.105	19526.409

1 - 0 Band

N	P ₁			Q ₁			R ₁		
	CALC	DIFF	U	CALC	DIFF	U	CALC	DIFF	U
55	19908.728			19908.943			19918.895		
56	19908.807			19909.026			19919.159		
57	19908.891			19909.113			19919.426		
58	19908.978			19909.204			19919.698		
59	19909.069			19909.299			19919.975		
60	19909.165			19909.399			19920.255	-0.003	4
61	19909.265			19909.502			19920.539	0.011	4
62	19909.368			19909.610			19920.827	0.003	4
63	19909.476			19909.722			19921.120	0.004	4
64	19909.588			19909.838			19921.416	0.004	4
65	19909.704			19909.958			19921.717	0.003	4
66	19909.825			19910.082			19922.022	0.002	4
67	19909.949			19910.210			19922.331	0.000	4
68	19910.078			19910.342			19922.644	-0.003	4
69	19910.210			19910.479			19922.961	0.000	4
70	19910.347			19910.619			19923.282	0.003	4
71	19910.488			19910.764			19923.607	0.002	4
72	19910.633			19910.913			19923.936	-0.001	4
73	19910.782			19911.066			19924.269	0.003	4
74	19910.935			19911.223			19924.607	-0.001	4
75	19911.092			19911.384			19924.948	0.001	4
76	19911.254			19911.550			19925.294	-0.020*	4
77	19911.419			19911.719			19925.644	-0.005	4
78	19911.589			19911.893			19925.998	0.012	4
79	19911.763			19912.070			19926.355	-0.001	4
80	19911.941			19912.252			19926.717	0.001	4

81	19912.123			19912.438			19927.084	0.001	4
82	19912.309			19912.628			19927.454	0.000	4
83	19912.499			19912.822			19927.828	0.000	4
84	19912.694			19913.021			19928.206	0.003	4
85	19912.892			19913.223			19928.589	0.003	4
86	19913.095			19913.430	0.001	6	19928.975	0.001	4
87	19913.302	-0.001	6	19913.640	0.005	6	19929.366	-0.003	4
88	19913.513	0.001	6	19913.855	0.017	6	19929.761	-0.001	4
89	19913.728	0.007	6	19914.074	0.004	6	19930.160	-0.003	4
90	19913.947	0.005	6	19914.297	0.002	6	19930.562	-0.005	4
91	19914.171	0.011	6	19914.525	0.007	6	19930.969	0.002	4
92	19914.398	0.001	6	19914.756	0.000	6	19931.381	0.004	4
93	19914.630	0.005	6	19914.991	-0.005	6	19931.796	0.009	4
94	19914.866			19915.231			19932.215	0.000	4
95	19915.106			19915.475	0.008	4	19932.638	-0.006	4
96	19915.350	0.003	4	19915.723	-0.001	4	19933.066	-0.005	4
97	19915.598	-0.005	4	19915.975			19933.497	-0.002	4
98	19915.850	0.004	4	19916.231			19933.933	-0.008	4
99	19916.106	0.004	4	19916.491			19934.373	-0.001	4
100	19916.367	0.006	4	19916.756			19934.817	0.006	4
101	19916.632	-0.006	4	19917.024			19935.265	0.005	4
102	19916.901	-0.011	4	19917.297			19935.717	-0.004	4
103	19917.174			19917.574			19936.173		
104	19917.451			19917.855			19936.633	-0.006	4
105	19917.732			19918.140			19937.097	0.003	4
106	19918.017			19918.429			19937.566	0.002	4
107	19918.307			19918.723			19938.038	-0.001	4
108	19918.601			19919.020			19938.515	0.001	4
109	19918.898			19919.322			19938.995	0.000	4
110	19919.200			19919.628			19939.480	0.008	4
111	19919.507			19919.938			19939.969		
112	19919.817			19920.252			19940.462		
113	19920.131			19920.570			19940.959		
114	19920.450			19920.893			19941.460		

N	P ₂			Q ₂			R ₂		
	CALC	DIFF	U	CALC	DIFF	U	CALC	DIFF	U
50	19914.108			19923.378			19923.573		
51	19914.282			19923.732			19923.931		
52	19914.460			19924.091			19924.294		
53	19914.642			19924.454			19924.661		
54	19914.827			19924.820			19925.031		
55	19915.017	-0.002	4	19925.191			19925.406		
56	19915.211	0.000	4	19925.566			19925.785		
57	19915.410	-0.002	4	19925.945			19926.167		
58	19915.612	-0.002	4	19926.328			19926.554		
59	19915.818	-0.005	4	19926.715			19926.945		
60	19916.029	0.005	4	19927.106			19927.340		
61	19916.243	-0.002	4	19927.502			19927.739		
62	19916.462			19927.901			19928.143		
63	19916.684	0.004	4	19928.304			19928.550		
64	19916.911	-0.002	4	19928.712			19928.961		
65	19917.142	-0.007	4	19929.123			19929.376		
66	19917.377	-0.008	4	19929.539			19929.796		

67	19917.616	-0.014*	4	19929.958		19930.219
68	19917.859	-0.002	4	19930.382		19930.647
69	19918.107	-0.006	4	19930.810		19931.078
70	19918.358	-0.004	4	19931.242		19931.514
71	19918.613	-0.005	4	19931.677		19931.954
72	19918.873	-0.008	4	19932.117		19932.398
73	19919.137	-0.008	4	19932.561		19932.846
74	19919.404	-0.007	4	19933.009		19933.297
75	19919.676	-0.008	4	19933.462		19933.753
76	19919.952			19933.918		19934.214
77	19920.232			19934.378		19934.678
78	19920.516			19934.842		19935.146
79	19920.805			19935.311		19935.618
80	19921.097			19935.783		19936.094

1 - 1 Band

N	P ₁			Q ₁			R ₁		
	CALC	DIFF	U	CALC	DIFF	U	CALC	DIFF	U
48	19712.988			19713.179			19721.861		
49	19713.052			19713.246			19722.109		
50	19713.119			19713.318			19722.362		
51	19713.191			19713.394			19722.619		
52	19713.268			19713.474			19722.880		
53	19713.349			19713.559			19723.145	0.002	8
54	19713.434			19713.648			19723.415	-0.004	8
55	19713.523			19713.741			19723.690	0.001	8
56	19713.617			19713.839			19723.968	-0.006	8
57	19713.716			19713.941			19724.251	-0.003	8
58	19713.818			19714.048	-0.013	6	19724.539	0.000	8
59	19713.925			19714.159	-0.010	6	19724.830	0.002	8
60	19714.037	-0.002	6	19714.274	-0.009	6	19725.127	-0.002	8
61	19714.153	-0.004	6	19714.394	-0.008	6	19725.427	-0.004	8
62	19714.273	-0.008	6	19714.518	-0.009	6	19725.732	0.001	8
63	19714.397	-0.011	6	19714.647	-0.008	6	19726.041	0.002	8
64	19714.526	-0.017	6	19714.779	0.001	6	19726.354	0.006	8
65	19714.660	-0.021*	6	19714.917	-0.014	6	19726.672	-0.002	8
66	19714.797	-0.017	6	19715.058	0.008	6	19726.994	-0.004	8
67	19714.939	-0.010	6	19715.204			19727.321	-0.004	8
68	19715.086	-0.020*	6	19715.355			19727.652	0.002	8
69	19715.237	-0.018*	6	19715.510			19727.987	0.001	8
70	19715.392	0.014	6	19715.669			19728.327	0.004	8
71	19715.552	0.008	6	19715.832			19728.671	0.004	8
72	19715.716	0.013	6	19716.000			19729.019	-0.004	8
73	19715.884	0.016	6	19716.173			19729.372	0.007	8
74	19716.057	0.003	6	19716.349			19729.729	-0.010	8
75	19716.234	0.003	6	19716.530			19730.090	0.002	8
76	19716.416	0.001	6	19716.716			19730.456	-0.003	8
77	19716.602	-0.002	6	19716.906			19730.826	0.004	8
78	19716.792	-0.008	6	19717.100			19731.201	0.002	8
79	19716.987	0.000	6	19717.299			19731.579	-0.002	8
80	19717.186	0.005	6	19717.502			19731.963	-0.001	8
81	19717.390	0.020*	6	19717.709			19732.350	-0.003	8

82	19717.597	0.014	6	19717.921	19732.742	-0.001	8
83	19717.810			19718.137	19733.138		
84	19718.026			19718.358	19733.539		
85	19718.248			19718.583	19733.944		
86	19718.473			19718.813	19734.353		
87	19718.703			19719.046	19734.767		

P_2				Q_2			R_2		
N	CALC	DIFF	U	CALC	DIFF	U	CALC	DIFF	U
45	19717.966			19726.327			19726.506		
46	19718.131			19726.674			19726.856		
47	19718.301			19727.025			19727.211		
48	19718.475			19727.380			19727.570		
49	19718.653			19727.739			19727.933		
50	19718.836	0.004	4	19728.103			19728.301		
51	19719.023	-0.019*	6	19728.471			19728.673		
52	19719.215	0.005	4	19728.843			19729.049		
53	19719.411	-0.004	6	19729.220			19729.430		
54	19719.611	0.006	6	19729.601			19729.815		
55	19719.816	0.001	6	19729.986			19730.204		
56	19720.024	0.007	4	19730.376			19730.598		
57	19720.238	-0.003	6	19730.770			19730.996		
58	19720.455	-0.007	6	19731.168			19731.398		
59	19720.677	-0.009	6	19731.571			19731.805		
60	19720.904	0.001	6	19731.978			19732.216		
61	19721.135	-0.003	6	19732.389			19732.631		
62	19721.370	0.005	6	19732.805			19733.050		
63	19721.609	0.003	6	19733.225			19733.474		
64	19721.853	0.002	6	19733.650			19733.903		
65	19722.101	0.011	6	19734.078			19734.335		
66	19722.354	0.002	6	19734.511			19734.772		
67	19722.610	0.003	6	19734.949			19735.214		
68	19722.872	0.004	6	19735.390			19735.659		
69	19723.137	0.006	6	19735.836			19736.109		
70	19723.407	0.002	6	19736.287			19736.563		
71	19723.682	0.008	6	19736.741			19737.022		
72	19723.960	0.004	6	19737.200			19737.485		
73	19724.243	0.004	6	19737.664			19737.952		
74	19724.531			19738.131			19738.424		
75	19724.822			19738.603			19738.900		
76	19725.119			19739.080			19739.380		
77	19725.419			19739.560			19739.865		
78	19725.724			19740.045			19740.353		

$^{174}\text{Yb}^{81}\text{Br}$

0 - 0 Band

N	P ₁			Q ₁			R ₁		
	CALC	DIFF	U	CALC	DIFF	U	CALC	DIFF	U
47	19694.221			19694.402			19702.787		
48	19694.279			19694.463			19703.027		
49	19694.341			19694.529			19703.271		
50	19694.408			19694.600			19703.520		
51	19694.478			19694.674			19703.773		
52	19694.553			19694.753			19704.030	-0.007	6
53	19694.633			19694.836			19704.292		
54	19694.716			19694.924			19704.557	-0.005	6
55	19694.804			19695.015			19704.828	0.001	6
56	19694.897			19695.111			19705.102	-0.007	6
57	19694.993			19695.212			19705.381	0.002	6
58	19695.094			19695.316			19705.664	-0.001	6
59	19695.199			19695.425			19705.951	-0.001	6
60	19695.309			19695.539			19706.242	0.002	6
61	19695.422			19695.656			19706.538	-0.003	6
62	19695.541			19695.778			19706.838	0.000	6
63	19695.663			19695.904			19707.143	-0.001	6
64	19695.790			19696.035			19707.451	0.001	6
65	19695.921			19696.170			19707.764	0.005	6
66	19696.056			19696.309			19708.081	0.001	6
67	19696.196			19696.452			19708.403	0.003	6
68	19696.340			19696.600	0.001	6	19708.729	0.007	6
69	19696.488			19696.752	-0.004	6	19709.059	0.000	6
70	19696.640	0.007	6	19696.908	0.003	6	19709.393	-0.001	6
71	19696.797	0.007	6	19697.069	0.002	6	19709.732	-0.003	6
72	19696.959	-0.005	6	19697.234	-0.009	6	19710.075	-0.006	6
73	19697.124	-0.003	6	19697.403	-0.005	6	19710.422	0.001	6
74	19697.294	-0.003	6	19697.577	-0.002	6	19710.774	0.002	6
75	19697.468	-0.007	6	19697.755	0.000	6	19711.129	0.001	6
76	19697.647	-0.006	6	19697.937	0.005	6	19711.489		
77	19697.829	-0.001	6	19698.124	0.005	6	19711.854		
78	19698.016			19698.315	0.004	6	19712.222		
79	19698.208			19698.510	0.009	6	19712.595	-0.011	6
80	19698.404			19698.710			19712.972	-0.010	6
81	19698.604			19698.913			19713.354	-0.008	6
82	19698.808			19699.122			19713.740	-0.006	6
83	19699.017	-0.010	6	19699.334	0.000	6	19714.130	-0.005	6
84	19699.230	0.000	6	19699.551	-0.004	6	19714.524	-0.001	6
85	19699.447	0.003	6	19699.772	0.002	6	19714.923	0.000	6
86	19699.669	-0.002	6	19699.998	0.003	6	19715.326	0.001	6
87	19699.895	-0.001	6	19700.227	0.001	6	19715.733	0.000	6
88	19700.125	-0.001	6	19700.461	0.003	6	19716.144	0.008	6
89	19700.360	-0.012	6	19700.700	-0.005	6	19716.560		
90	19700.599	-0.008	6	19700.943	0.005	6	19716.980		
91	19700.842	0.006	6	19701.190	-0.002	6	19717.405		
92	19701.090	-0.009	6	19701.441	0.001	6	19717.833		
93	19701.341			19701.697	0.012	6	19718.266		
94	19701.598			19701.957	-0.005	6	19718.703		

95	19701.858		19702.221	-0.005	6	19719.145
96	19702.123		19702.490			19719.591
97	19702.392		19702.763			19720.041
98	19702.666		19703.040			19720.495
99	19702.944		19703.322			19720.954
100	19703.226		19703.608			19721.417

P_2				Q_2			R_2		
N	CALC	DIFF	U	CALC	DIFF	U	CALC	DIFF	U
55	19700.987			19711.017			19711.228		
56	19701.192			19711.401			19711.616		
57	19701.401			19711.789			19712.007		
58	19701.615			19712.181			19712.403		
59	19701.833			19712.577			19712.803		
60	19702.056	0.004	6	19712.978			19713.208		
61	19702.283	0.002	6	19713.383			19713.616		
62	19702.514	0.002	6	19713.792			19714.029		
63	19702.749	0.000	6	19714.205			19714.447		
64	19702.988	0.003	6	19714.623			19714.868		
65	19703.232	0.002	6	19715.045			19715.294		
66	19703.480	0.010	6	19715.471			19715.724		
67	19703.733	-0.003	6	19715.901			19716.158		
68	19703.989	0.004	6	19716.336			19716.596		
69	19704.250	0.000	6	19716.775			19717.039		
70	19704.516	0.001	6	19717.218			19717.486		
71	19704.785	0.002	6	19717.666			19717.938		
72	19705.059	0.002	6	19718.118			19718.393		
73	19705.337	-0.003	6	19718.574			19718.853		
74	19705.620	0.005	6	19719.034			19719.317		
75	19705.907	0.004	6	19719.498			19719.785		
76	19706.198	0.000	6	19719.967			19720.258		
77	19706.493	0.006	6	19720.440			19720.735		
78	19706.793	0.004	6	19720.917			19721.216		
79	19707.096	0.002	6	19721.399			19721.701		
80	19707.405	0.007	6	19721.885			19722.191		
81	19707.717	0.005	6	19722.375			19722.685		
82	19708.034	0.005	6	19722.869			19723.183		
83	19708.355	0.014	6	19723.368			19723.685		
84	19708.680	0.013	6	19723.871			19724.192		
85	19709.010	-0.001	6	19724.378			19724.703		
86	19709.344	0.002	6	19724.889			19725.218		
87	19709.682	0.000	6	19725.405			19725.737		
88	19710.025	0.004	6	19725.924			19726.261		
89	19710.371	0.005	6	19726.449			19726.789		
90	19710.723	0.000	6	19726.977			19727.321		
91	19711.078	-0.008	6	19727.509			19727.857		
92	19711.438			19728.046			19728.398		
93	19711.802			19728.587			19728.943		
94	19712.170			19729.133			19729.492		
95	19712.542	-0.007	6	19729.682			19730.045		
96	19712.919	-0.011	6	19730.236			19730.603		
97	19713.301	-0.003	6	19730.795			19731.165		
98	19713.686	-0.011	6	19731.357			19731.731		
99	19714.076	0.000	6	19731.924			19732.302		

100	19714.470	-0.001	6	19732.494	19732.876
101	19714.868	0.004	6	19733.070	19733.455
102	19715.271	0.005	6	19733.649	19734.039
103	19715.678			19734.233	19734.626
104	19716.089			19734.821	19735.218
105	19716.504			19735.413	19735.814
106	19716.924			19736.009	19736.414
107	19717.348			19736.610	19737.018

0 - 1 Band

N	P ₁			Q ₁			R ₁		
	CALC	DIFF	U	CALC	DIFF	U	CALC	DIFF	U
17	19500.556			19500.624			19503.645		
18	19500.490			19500.561			19503.761		
19	19500.428			19500.503			19503.882		
20	19500.371			19500.450			19504.008		
21	19500.318			19500.401			19504.138		
22	19500.270			19500.357			19504.272	0.011	6
23	19500.226			19500.317			19504.411	-0.001	6
24	19500.187			19500.282			19504.555		
25	19500.153			19500.251			19504.703	0.004	6
26	19500.123			19500.225			19504.855		
27	19500.097			19500.203			19505.012	0.001	6
28	19500.076			19500.186			19505.174	-0.004	6
29	19500.060			19500.174			19505.340	-0.006	6
30	19500.048			19500.166			19505.511	-0.011	6
31	19500.041			19500.162			19505.687	0.004	6
32	19500.038			19500.163			19505.866	0.001	6
33	19500.040			19500.169			19506.051	0.003	6
34	19500.046			19500.179			19506.240	0.004	6
35	19500.057			19500.194			19506.433	0.001	6
36	19500.073			19500.213			19506.631	0.006	6
37	19500.093			19500.237			19506.834	0.001	6
38	19500.117			19500.266			19507.041	0.004	6
39	19500.147			19500.299			19507.253	0.002	6
40	19500.180			19500.336			19507.469	-0.004	6
41	19500.219			19500.379			19507.690	0.010	6
42	19500.261			19500.425			19507.915	0.002	6
43	19500.309			19500.477			19508.145	-0.001	6
44	19500.361			19500.532			19508.379	-0.002	6
45	19500.417			19500.593			19508.618	0.000	6
46	19500.478			19500.658			19508.861	-0.003	6
47	19500.544			19500.727			19509.109	-0.004	4
48	19500.614			19500.801			19509.362	-0.007	4
49	19500.689			19500.880			19509.619		
50	19500.768			19500.963			19509.880	-0.001	4
51	19500.852			19501.051			19510.147	-0.011	6
52	19500.941			19501.143			19510.417	0.006	6
53	19501.034	-0.001	6	19501.240			19510.692	0.004	6
54	19501.131	0.005	6	19501.341			19510.972		
55	19501.233	0.007	6	19501.447			19511.257	0.003	6
56	19501.340	0.007	6	19501.558			19511.545	-0.001	6

57	19501.451	-0.004	6	19501.673	19511.839	-0.005	6
58	19501.567	-0.007	6	19501.793	19512.137	-0.006	4
59	19501.687			19501.917	19512.439	0.002	4
60	19501.812			19502.046	19512.746	0.005	4
61	19501.942			19502.179	19513.058	-0.003	4
62	19502.076			19502.317	19513.374		
63	19502.215			19502.460	19513.694		
64	19502.358			19502.607	19514.020		
65	19502.506			19502.758	19514.349		
66	19502.658			19502.915	19514.684		

P_2				Q_2			R_2		
N	CALC	DIFF	U	CALC	DIFF	U	CALC	DIFF	U
34	19503.853			19510.133			19510.266		
35	19503.978			19510.436			19510.573		
36	19504.107			19510.743			19510.884		
37	19504.240			19511.056			19511.200		
38	19504.378			19511.372			19511.521		
39	19504.521	0.004	6	19511.693			19511.846		
40	19504.668	0.001	6	19512.019			19512.175		
41	19504.819	0.003	6	19512.349			19512.509		
42	19504.975	0.004	6	19512.684			19512.848		
43	19505.136	0.006	6	19513.023			19513.191		
44	19505.301	-0.005	6	19513.367			19513.538		
45	19505.471	0.003	6	19513.715			19513.890		
46	19505.645	-0.001	6	19514.068			19514.247		
47	19505.824	0.003	6	19514.425			19514.608		
48	19506.008	-0.001	6	19514.787			19514.974		
49	19506.196	0.002	6	19515.153			19515.344		
50	19506.388	0.000	6	19515.524			19515.719		
51	19506.585	0.003	6	19515.899			19516.098		
52	19506.787	-0.001	6	19516.279			19516.482		
53	19506.993	-0.003	6	19516.664			19516.870		
54	19507.204	0.003	6	19517.053			19517.263		
55	19507.419	-0.005	6	19517.446			19517.660		
56	19507.639	-0.005	6	19517.844			19518.062		
57	19507.863	-0.002	6	19518.247			19518.469		
58	19508.092	-0.005	6	19518.654			19518.880		
59	19508.325	-0.001	6	19519.066			19519.295		
60	19508.563	0.005	6	19519.482			19519.715		
61	19508.806	0.002	6	19519.902			19520.139		
62	19509.053	-0.002	6	19520.327			19520.568		
63	19509.304	-0.006	6	19520.757			19521.002		
64	19509.560	-0.002	6	19521.191			19521.440		
65	19509.821	0.011	6	19521.630			19521.883		
66	19510.086	-0.020*	6	19522.073			19522.330		
67	19510.356	0.003	6	19522.521			19522.781		
68	19510.630	0.006	6	19522.973			19523.237		
69	19510.909	-0.006	6	19523.430			19523.698		
70	19511.193	0.004	6	19523.891			19524.163		
71	19511.481	-0.007	6	19524.357			19524.633		
72	19511.773	-0.003	6	19524.827			19525.107		
73	19512.070	0.001	6	19525.302			19525.586		
74	19512.372	-0.005	6	19525.781			19526.069		

75	19512.678	0.000	6	19526.265	19526.557
76	19512.989	-0.001	6	19526.754	19527.049
77	19513.304			19527.247	19527.546
78	19513.624			19527.744	19528.047
79	19513.948			19528.246	19528.553
80	19514.277			19528.752	19529.063
81	19514.610			19529.263	19529.578

1 - 0 Band

N	P ₁			Q ₁			R ₁		
	CALC	DIFF	U	CALC	DIFF	U	CALC	DIFF	U
62	19907.490			19907.728			19918.755		
63	19907.596			19907.838			19919.043		
64	19907.707			19907.952			19919.335		
65	19907.821			19908.070			19919.630		
66	19907.939			19908.192			19919.930		
67	19908.062			19908.318			19920.234	-0.011	4
68	19908.188			19908.448			19920.541	0.009	4
69	19908.319			19908.583			19920.853	0.004	4
70	19908.453	-0.009	4	19908.721			19921.169		
71	19908.592	0.001	4	19908.863			19921.489	-0.002	4
72	19908.734	-0.003	4	19909.010			19921.813	-0.002	4
73	19908.881	0.010	4	19909.160			19922.141	0.003	4
74	19909.032	-0.027*	4	19909.315			19922.472	0.019*	4
75	19909.187	0.008	4	19909.474			19922.808	0.003	4
76	19909.346	-0.007	4	19909.636			19923.148	-0.003	4
77	19909.508	-0.003	4	19909.803			19923.492	0.003	4
78	19909.675	0.000	4	19909.974	-0.008	4	19923.840	-0.005	4
79	19909.846	0.003	4	19910.149	-0.007	4	19924.192	0.000	4
80	19910.021	-0.002	4	19910.327	0.006	4	19924.548	0.001	4
81	19910.201	0.004	4	19910.510	0.019*	4	19924.908	-0.002	4
82	19910.384	0.015	4	19910.697	0.012	4	19925.272	0.003	4
83	19910.571	-0.002	4	19910.888	0.012	4	19925.641	-0.002	4
84	19910.762	0.007	4	19911.084	-0.014*	4	19926.013	-0.003	4
85	19910.958	0.002	4	19911.283	0.000	4	19926.389	-0.002	4
86	19911.157	-0.001	4	19911.486	-0.003	4	19926.769	-0.005	4
87	19911.361	0.002	4	19911.693	0.000	4	19927.153	0.005	4
88	19911.568	-0.005	4	19911.905	-0.001	4	19927.541	0.001	4
89	19911.780	0.007	6	19912.120	0.010	6	19927.934	0.001	4
90	19911.996	0.008	6	19912.340	0.007	6	19928.330	-0.005	4
91	19912.215	0.009	6	19912.563	0.001	6	19928.730	-0.004	4
92	19912.439	-0.002	6	19912.791	-0.003	6	19929.135	-0.006	4
93	19912.667	0.020*	6	19913.022	-0.004	6	19929.543	-0.007	4
94	19912.899	-0.005	6	19913.258	-0.003	6	19929.955	-0.005	4
95	19913.135	-0.017	6	19913.498			19930.372	-0.001	4
96	19913.375	-0.021*	6	19913.742			19930.792	-0.001	4
97	19913.619	-0.038*	6	19913.990			19931.217	0.001	4
98	19913.867	0.005	4	19914.242			19931.645	0.000	4
99	19914.120			19914.498			19932.077	-0.002	4
100	19914.376	0.023*	4	19914.758			19932.514	-0.002	4
101	19914.636			19915.022			19932.955	-0.006	4
102	19914.901			19915.290			19933.399	0.004	4

103	19915.169		19915.563		19933.848	0.004	4
104	19915.442		19915.839		19934.300	0.002	4
105	19915.719		19916.120		19934.757	-0.008	4
106	19915.999		19916.404		19935.218	-0.006	4
107	19916.284		19916.693		19935.683	-0.007	4
108	19916.573		19916.985		19936.151		
109	19916.866		19917.282		19936.624		
110	19917.163		19917.583		19937.101		
111	19917.464		19917.888		19937.582		
112	19917.769		19918.197		19938.067		

N	P ₂			Q ₂			R ₂		
	CALC	DIFF	U	CALC	DIFF	U	CALC	DIFF	U
25	19909.187			19913.846			19913.943		
26	19909.257			19914.095			19914.196		
27	19909.332			19914.347			19914.452		
28	19909.410			19914.604			19914.712		
29	19909.492			19914.864			19914.977		
30	19909.578			19915.129			19915.245	-0.002	4
31	19909.669			19915.398	-0.001	4	19915.517	0.003	4
32	19909.763			19915.670	0.007	4	19915.794	0.003	4
33	19909.861			19915.947	-0.007	4	19916.074	0.006	4
34	19909.964			19916.227	-0.003	4	19916.358	-0.007	4
35	19910.070			19916.512	-0.003	4	19916.647	-0.005	4
36	19910.180			19916.800	0.009	4	19916.939	-0.002	4
37	19910.295			19917.093	0.000	4	19917.235	0.004	4
38	19910.413			19917.389	0.003	6	19917.536	0.000	6
39	19910.536			19917.690	-0.001	6	19917.840	0.006	6
40	19910.662			19917.995	0.002	6	19918.149	0.002	6
41	19910.793			19918.303	-0.001	6	19918.461	-0.001	6
42	19910.927	-0.002	4	19918.616	-0.002	6	19918.777	-0.002	6
43	19911.066	0.005	4	19918.933	-0.003	6	19919.098	0.003	6
44	19911.209	0.015*	4	19919.253	-0.004	6	19919.422	0.005	6
45	19911.355	0.005	4	19919.578	-0.001	6	19919.751	-0.005	6
46	19911.506	0.005	4	19919.906	-0.014	6	19920.083		
47	19911.660	0.002	4	19920.239			19920.420		
48	19911.819	0.007	4	19920.576			19920.760		
49	19911.982	0.006	4	19920.916			19921.104		
50	19912.149	0.005	4	19921.261			19921.453		
51	19912.319	0.009	4	19921.610			19921.805		
52	19912.494	0.005	4	19921.962			19922.162		
53	19912.673	-0.001	4	19922.319			19922.522		
54	19912.856	0.001	4	19922.680			19922.887		
55	19913.043	-0.002	4	19923.044			19923.255		
56	19913.233	-0.003	4	19923.413			19923.628		
57	19913.428	-0.003	4	19923.786			19924.004		
58	19913.627	-0.006	4	19924.162			19924.385		
59	19913.830	-0.002	4	19924.543			19924.769		
60	19914.037			19924.928			19925.158		
61	19914.248	0.003	4	19925.316			19925.550		
62	19914.463	0.002	4	19925.709			19925.946		
63	19914.682	0.014	6	19926.106			19926.347		
64	19914.905	0.007	6	19926.506			19926.751		
65	19915.133	0.003	6	19926.911			19927.160		

66	19915.364	-0.003	6	19927.320	19927.572
67	19915.599	-0.001	6	19927.732	19927.989
68	19915.838	-0.010	6	19928.149	19928.409
69	19916.081			19928.570	19928.834
70	19916.328			19928.994	19929.262
71	19916.580	-0.007	4	19929.423	19929.695
72	19916.835	-0.007	4	19929.855	19930.131
73	19917.094			19930.292	19930.571
74	19917.358			19930.733	19931.016
75	19917.625			19931.177	19931.464
76	19917.897	0.003	4	19931.626	19931.917
77	19918.172	-0.011	4	19932.079	19932.373
78	19918.451			19932.535	19932.834
79	19918.735			19932.996	19933.298
80	19919.023			19933.461	19933.767
81	19919.314			19933.929	19934.239
82	19919.610			19934.402	19934.715

1 - 1 Band

N	P ₁			Q ₁			R ₁		
	CALC	DIFF	U	CALC	DIFF	U	CALC	DIFF	U
43	19712.535			19712.703			19720.349		
44	19712.576			19712.748			19720.571		
45	19712.621			19712.797			19720.798		
46	19712.670			19712.850			19721.029		
47	19712.724			19712.907			19721.265		
48	19712.782			19712.969			19721.504	-0.024*	4
49	19712.844			19713.035			19721.748	-0.001	4
50	19712.911			19713.106			19721.997	-0.026*	4
51	19712.982			19713.180			19722.249	-0.012	4
52	19713.057			19713.259			19722.506	0.041*	4
53	19713.136			19713.342			19722.767	0.014*	4
54	19713.220			19713.430			19723.032	0.006	4
55	19713.308			19713.522			19723.302	0.012	4
56	19713.400			19713.618			19723.576	0.002	4
57	19713.497			19713.718			19723.854	0.001	4
58	19713.598			19713.823			19724.137	-0.005	4
59	19713.703			19713.932			19724.423	-0.004	4
60	19713.812			19714.046			19724.714	0.005	4
61	19713.926			19714.163			19725.010	-0.008	4
62	19714.044			19714.285			19725.309	0.000	4
63	19714.167			19714.412			19725.613	0.003	4
64	19714.294			19714.542			19725.922	-0.006	4
65	19714.425			19714.677			19726.234	0.002	4
66	19714.560			19714.817			19726.551	-0.004	4
67	19714.700			19714.960			19726.872	-0.005	4
68	19714.844			19715.108			19727.197	-0.003	4
69	19714.992			19715.260			19727.527	0.000	4
70	19715.145	0.001	4	19715.417			19727.860	0.001	4
71	19715.301	0.002	4	19715.577			19728.199	0.002	4
72	19715.463	-0.003	4	19715.742			19728.541	0.004	4
73	19715.628	0.002	4	19715.912			19728.888	-0.003	4

74	19715.798	-0.005	4	19716.085	19729.239	0.000	4
75	19715.972	0.001	6	19716.263	19729.594	0.001	4
76	19716.151	-0.011	6	19716.446	19729.954	-0.002	4
77	19716.334	-0.007	6	19716.632	19730.317	0.001	4
78	19716.521	-0.007	6	19716.823	19730.686	-0.002	4
79	19716.712			19717.019	19731.058	-0.001	4
80	19716.908			19717.218	19731.435	0.001	4
81	19717.108			19717.422	19731.816	-0.003	4
82	19717.312			19717.630	19732.201	0.001	4
83	19717.521			19717.843	19732.590	-0.001	4
84	19717.734			19718.060	19732.984		
85	19717.951			19718.281	19733.382		
86	19718.173			19718.507	19733.785		
87	19718.399			19718.736	19734.191		

	P ₂			Q ₂			R ₂		
N	CALC	DIFF	U	CALC	DIFF	U	CALC	DIFF	U
17	19714.862			19718.093			19718.161		
18	19714.904			19718.314			19718.385		
19	19714.951			19718.539			19718.615		
20	19715.003			19718.769			19718.848		
21	19715.058			19719.003			19719.086		
22	19715.118	-0.001	6	19719.241			19719.328		
23	19715.182	0.005	6	19719.483			19719.574		
24	19715.250	-0.002	6	19719.730			19719.824		
25	19715.323	-0.002	6	19719.981			19720.079		
26	19715.400	-0.006	6	19720.236			19720.338		
27	19715.481	-0.007	6	19720.495			19720.601		
28	19715.567	-0.002	6	19720.759			19720.869		
29	19715.656	-0.001	6	19721.027			19721.141		
30	19715.750	-0.009	6	19721.299			19721.417		
31	19715.849	-0.021*	6	19721.576			19721.697		
32	19715.951	-0.013	6	19721.857			19721.982		
33	19716.058	0.000	6	19722.142			19722.271		
34	19716.169	-0.024*	6	19722.431			19722.564		
35	19716.285	0.007	6	19722.725			19722.862		
36	19716.405	0.000	6	19723.022			19723.163		
37	19716.529	-0.011	6	19723.325			19723.469		
38	19716.657			19723.631			19723.779		
39	19716.790	0.012	6	19723.942			19724.094		
40	19716.926			19724.257			19724.413		
41	19717.068	0.004	6	19724.576			19724.736		
42	19717.213	-0.007	6	19724.899			19725.063		
43	19717.363	0.003	4	19725.227			19725.395		
44	19717.517	-0.005	4	19725.559			19725.730		
45	19717.675	0.004	4	19725.895			19726.071		
46	19717.838	-0.005	4	19726.236			19726.415		
47	19718.004	0.009	4	19726.580			19726.764		
48	19718.175	0.011	4	19726.929			19727.116		
49	19718.351			19727.283			19727.474		
50	19718.531	0.009	6	19727.640			19727.835		
51	19718.715	-0.004	4	19728.002			19728.201		
52	19718.903	0.004	6	19728.368			19728.571		
53	19719.095	0.005	6	19728.738			19728.945		

54	19719.292	0.022*	6	19729.113	19729.323
55	19719.493	0.004	6	19729.492	19729.706
56	19719.699	0.018*	6	19729.875	19730.093
57	19719.908	0.006	6	19730.262	19730.484
58	19720.122	0.006	6	19730.654	19730.880
59	19720.340	-0.006	6	19731.050	19731.279
60	19720.563	0.005	6	19731.450	19731.683
61	19720.790	0.001	6	19731.854	19732.092
62	19721.021	0.007	6	19732.263	19732.504
63	19721.256	0.009	6	19732.676	19732.921
64	19721.496	0.009	6	19733.093	19733.342
65	19721.740	0.012	6	19733.515	19733.767
66	19721.988			19733.940	19734.197
67	19722.241			19734.370	19734.631
68	19722.497			19734.804	19735.069
69	19722.759			19735.243	19735.511
70	19723.024			19735.686	19735.958

$^{172}\text{Yb}^{79}\text{Br}$

0 - 0 Band

N	P ₁			Q ₁			R ₁		
	CALC	DIFF	U	CALC	DIFF	U	CALC	DIFF	U
38	19693.973			19694.123			19701.042		
39	19693.993			19694.146			19701.248		
40	19694.017			19694.174			19701.458		
41	19694.045			19694.206			19701.672		
42	19694.078			19694.243			19701.891		
43	19694.115			19694.284			19702.115	-0.001	6
44	19694.156			19694.329			19702.342	-0.001	6
45	19694.202			19694.379			19702.574	0.001	6
46	19694.252			19694.433			19702.811	0.003	6
47	19694.307			19694.491			19703.052		
48	19694.366			19694.554			19703.297	0.001	6
49	19694.429			19694.622			19703.546		
50	19694.497			19694.693			19703.800	-0.004	6
51	19694.569			19694.769			19704.059	-0.004	6
52	19694.646			19694.850			19704.321	-0.001	6
53	19694.727			19694.935			19704.588	-0.002	6
54	19694.813			19695.024			19704.860	-0.005	6
55	19694.902			19695.118			19705.135	0.001	6
56	19694.997			19695.216			19705.416	-0.001	6
57	19695.095			19695.318			19705.700	0.002	6
58	19695.198			19695.425			19705.989	-0.002	6
59	19695.305			19695.536			19706.282	-0.002	6
60	19695.417			19695.652			19706.580	-0.002	6
61	19695.533			19695.772			19706.882	-0.004	6
62	19695.654			19695.897			19707.188	-0.007	6
63	19695.779			19696.025			19707.499	-0.002	6
64	19695.908			19696.159			19707.814	-0.007	6
65	19696.042			19696.296			19708.134	-0.006	6
66	19696.180			19696.438			19708.458	-0.003	6
67	19696.323			19696.585			19708.786	-0.007	6
68	19696.470			19696.736			19709.118	-0.009	6
69	19696.621			19696.891			19709.455	-0.003	6
70	19696.777			19697.051			19709.797		
71	19696.937	0.017	6	19697.215			19710.143		
72	19697.102	0.019*	6	19697.383			19710.493		
73	19697.271	0.020*	6	19697.556			19710.847		
74	19697.444	0.017	6	19697.734			19711.206		
75	19697.622	0.004	4	19697.915			19711.569		
76	19697.805	-0.004	4	19698.101			19711.937		
77	19697.991	-0.010	6	19698.292			19712.309		
78	19698.182	-0.004	6	19698.487	-0.009	6	19712.685	0.004	6
79	19698.378	-0.009	6	19698.686			19713.066	0.013	6
80	19698.578	-0.006	6	19698.890			19713.451	0.008	6
81	19698.782			19699.098	-0.002	6	19713.841	0.002	6
82	19698.991			19699.311	-0.005	6	19714.234	-0.001	6
83	19699.204			19699.528	-0.006	6	19714.633	0.004	6
84	19699.421			19699.749			19715.035	0.002	6
85	19699.643			19699.975			19715.442	0.005	6

86	19699.870			19700.205			19715.854	-0.003	4
87	19700.100			19700.440			19716.269	0.002	4
88	19700.335			19700.679			19716.690	-0.005	4
89	19700.575			19700.922			19717.114	0.001	4
90	19700.819	0.002	6	19701.170			19717.543	-0.001	4
91	19701.067			19701.423			19717.976	0.000	4
92	19701.320	0.008	6	19701.679			19718.414	-0.008	4
93	19701.578	0.010	6	19701.940			19718.856		
94	19701.839	-0.007	6	19702.206			19719.302		
95	19702.105	0.011	6	19702.476			19719.753		
96	19702.376			19702.750			19720.208		
97	19702.651			19703.029			19720.668		
98	19702.930			19703.312			19721.132		
99	19703.214			19703.600			19721.600		
100	19703.502			19703.892			19722.073		

	P ₂			Q ₂			R ₂		
N	CALC	DIFF	U	CALC	DIFF	U	CALC	DIFF	U
57	19701.638			19712.242			19712.466		
58	19701.856			19712.643			19712.870		
59	19702.079			19713.047			19713.278		
60	19702.306			19713.456			19713.691		
61	19702.537			19713.870			19714.108		
62	19702.773	-0.005	6	19714.287			19714.530		
63	19703.013	0.008	6	19714.709			19714.956		
64	19703.258	0.001	6	19715.136			19715.386		
65	19703.507	0.008	6	19715.567			19715.821		
66	19703.760	-0.005	6	19716.002			19716.260		
67	19704.018	0.005	6	19716.441			19716.703		
68	19704.280	-0.030*	6	19716.885			19717.151		
69	19704.546	0.006	6	19717.333			19717.603		
70	19704.817	-0.003	6	19717.786			19718.059		
71	19705.093	0.005	6	19718.242			19718.520		
72	19705.372	0.002	6	19718.704			19718.985		
73	19705.656	-0.002	6	19719.169			19719.454		
74	19705.945	0.009	6	19719.639			19719.928		
75	19706.237	0.001	6	19720.113			19720.406		
76	19706.534	0.001	6	19720.592			19720.889		
77	19706.836	0.003	6	19721.075			19721.376		
78	19707.142	-0.006	6	19721.562			19721.867		
79	19707.452	0.007	6	19722.054			19722.362		
80	19707.767	-0.004	6	19722.550			19722.862		
81	19708.086	-0.004	6	19723.050			19723.366		
82	19708.409	-0.003	6	19723.555			19723.875		
83	19708.737	-0.001	6	19724.064			19724.388		
84	19709.069	-0.003	6	19724.577			19724.905		
85	19709.406	-0.007	6	19725.095			19725.426		
86	19709.747			19725.617			19725.952		
87	19710.092			19726.143			19726.483		
88	19710.442			19726.674			19727.017		
89	19710.796			19727.209			19727.556		
90	19711.154			19727.748			19728.100		
91	19711.517			19728.292			19728.647		
92	19711.885	0.003	6	19728.840			19729.199		

93	19712.256	0.005	6	19729.393	19729.755
94	19712.632	0.009	6	19729.949	19730.316
95	19713.013	0.005	6	19730.511	19730.881
96	19713.397	0.008	6	19731.076	19731.450
97	19713.787	-0.003	6	19731.646	19732.024
98	19714.180	0.009	6	19732.220	19732.602
99	19714.578	0.004	6	19732.798	19733.185
100	19714.980	0.003	6	19733.381	19733.771
101	19715.387			19733.968	19734.362
102	19715.798			19734.560	19734.958
103	19716.214			19735.156	19735.557
104	19716.634			19735.756	19736.162
105	19717.058			19736.361	19736.770

0 - 1 Band

N	P ₁			Q ₁			R ₁		
	CALC	DIFF	U	CALC	DIFF	U	CALC	DIFF	U
28	19498.143			19498.256			19503.348		
29	19498.127			19498.243			19503.518		
30	19498.115			19498.235			19503.693		
31	19498.108			19498.232			19503.872		
32	19498.105			19498.233			19504.055		
33	19498.107			19498.239			19504.244	-0.001	6
34	19498.114			19498.249			19504.437	0.003	6
35	19498.125			19498.265			19504.634	0.003	6
36	19498.141			19498.284			19504.837	-0.007	6
37	19498.161			19498.309			19505.044	-0.004	6
38	19498.187			19498.338			19505.255		
39	19498.216			19498.372			19505.471	-0.002	6
40	19498.251			19498.411			19505.692	0.007	6
41	19498.290			19498.454			19505.918		
42	19498.334			19498.501			19506.148	-0.002	6
43	19498.383			19498.554			19506.383	0.000	6
44	19498.436			19498.611			19506.622	-0.006	6
45	19498.494			19498.673			19506.866		
46	19498.556			19498.739			19507.115	0.002	6
47	19498.623			19498.810			19507.368	-0.008	6
48	19498.695			19498.886			19507.626		
49	19498.772			19498.967			19507.888	0.017	6
50	19498.853			19499.052	0.003	4	19508.156	0.009	6
51	19498.938			19499.141	-0.003	4	19508.428	0.003	6
52	19499.029	0.006	6	19499.236			19508.704	0.001	6
53	19499.124	-0.002	6	19499.335	-0.010	6	19508.985	-0.003	6
54	19499.224	0.001	6	19499.439	0.000	6	19509.271	-0.012	6
55	19499.328	-0.003	6	19499.547	-0.005	6	19509.561		
56	19499.437	0.002	6	19499.660	-0.011	6	19509.856		
57	19499.551	-0.009	6	19499.778	-0.003	6	19510.156		
58	19499.670	0.012	4	19499.900	-0.001	4	19510.460		
59	19499.793	-0.004	4	19500.027	-0.001	4	19510.769		
60	19499.920	0.002	4	19500.159	0.000	6	19511.083		
61	19500.053	-0.001	6	19500.295	0.000	6	19511.401		

62	19500.190	0.015	6	19500.436	-0.011	6	19511.724	-0.006	4
63	19500.332	0.003	6	19500.582	0.003	6	19512.052	-0.001	4
64	19500.478	-0.006	6	19500.732	-0.006	6	19512.384	0.001	4
65	19500.629	-0.007	6	19500.887	-0.005	6	19512.721	0.004	4
66	19500.785			19501.047			19513.062	0.003	4
67	19500.945	-0.006	6	19501.211			19513.408	0.004	4
68	19501.111	0.008	6	19501.380			19513.759	0.000	4
69	19501.280			19501.554			19514.114	0.005	4
70	19501.455			19501.732			19514.474	-0.018*	4
71	19501.634			19501.916			19514.839	0.004	4
72	19501.818			19502.103			19515.208	0.002	4
73	19502.006			19502.296			19515.582	0.005	4
74	19502.199			19502.493			19515.961	0.009	4
75	19502.397			19502.694			19516.344	0.003	4
76	19502.600			19502.901			19516.732	-0.004	4
77	19502.807			19503.112			19517.124	0.004	4
78	19503.019			19503.328			19517.522		
79	19503.235			19503.548			19517.923		
80	19503.456			19503.773			19518.330		
81	19503.682			19504.003			19518.741		
82	19503.913			19504.238			19519.157		

	P ₂			Q ₂			R ₂		
N	CALC	DIFF	U	CALC	DIFF	U	CALC	DIFF	U
33	19501.878			19508.107			19508.239		
34	19502.001			19508.412			19508.548		
35	19502.128			19508.721			19508.861		
36	19502.259			19509.035			19509.179		
37	19502.396			19509.354			19509.502		
38	19502.537	0.004	4	19509.677			19509.829		
39	19502.682	0.015*	4	19510.005			19510.161		
40	19502.832	0.006	4	19510.338			19510.497		
41	19502.987	-0.006	4	19510.675			19510.838		
42	19503.147	-0.009	4	19511.017			19511.184		
43	19503.311			19511.363			19511.534		
44	19503.480			19511.714			19511.889		
45	19503.653			19512.070			19512.249		
46	19503.831			19512.430			19512.613		
47	19504.014			19512.795			19512.982		
48	19504.202	0.001	6	19513.165			19513.356		
49	19504.394	-0.001	6	19513.539			19513.734		
50	19504.590	0.000	6	19513.918			19514.116		
51	19504.792	-0.005	6	19514.301			19514.504		
52	19504.998	0.002	6	19514.689			19514.896		
53	19505.208	0.006	6	19515.082			19515.292		
54	19505.423	-0.004	6	19515.479			19515.694		
55	19505.643	0.003	6	19515.881			19516.099		
56	19505.868	0.001	6	19516.287			19516.510		
57	19506.097	-0.008	6	19516.698			19516.925		
58	19506.331	-0.002	6	19517.114			19517.345		
59	19506.569	-0.006	6	19517.535			19517.769		
60	19506.812	-0.006	6	19517.959			19518.198		
61	19507.060	-0.001	6	19518.389			19518.631		
62	19507.313			19518.823			19519.069		

63	19507.570			19519.262			19519.512		
64	19507.831			19519.706			19519.960		
65	19508.098	0.000	6	19520.154			19520.412		
66	19508.369	-0.001	6	19520.606			19520.868		
67	19508.644	-0.006	6	19521.064			19521.329		
68	19508.925	-0.007	6	19521.525			19521.795		
69	19509.209			19521.992			19522.266		
70	19509.499			19522.463			19522.741		
71	19509.793			19522.939			19523.221		
72	19510.092			19523.419			19523.705		
73	19510.396			19523.904			19524.194		

1 - 0 Band

N	P ₁			Q ₁			R ₁		
	CALC	DIFF	U	CALC	DIFF	U	CALC	DIFF	U
53	19909.007			19909.214			19918.839		
54	19909.078			19909.289			19919.096		
55	19909.153			19909.368			19919.356		
56	19909.232			19909.452			19919.621		
57	19909.316			19909.539			19919.890		
58	19909.404			19909.631			19920.163	0.007	4
59	19909.495			19909.726			19920.440	0.000	4
60	19909.591			19909.826			19920.721	-0.001	4
61	19909.691			19909.930			19921.006	0.007	4
62	19909.795			19910.038			19921.296	-0.002	4
63	19909.904			19910.150			19921.589	0.004	6
64	19910.016			19910.266			19921.887	0.000	4
65	19910.132			19910.387			19922.189	-0.002	4
66	19910.253			19910.511			19922.494	-0.003	4
67	19910.378			19910.640			19922.804	0.007	4
68	19910.507			19910.773			19923.118	0.027*	4
69	19910.640			19910.910			19923.436	0.002	4
70	19910.777			19911.051			19923.759	0.003	4
71	19910.918			19911.196			19924.085	0.001	4
72	19911.064			19911.345			19924.415	0.001	4
73	19911.213			19911.499			19924.750	-0.001	4
74	19911.367			19911.656			19925.089	0.003	4
75	19911.525			19911.818			19925.431	0.004	4
76	19911.687			19911.984			19925.778	-0.006	4
77	19911.853			19912.154			19926.129	0.002	4
78	19912.024			19912.328			19926.484	0.003	4
79	19912.198			19912.506			19926.843	0.001	4
80	19912.377			19912.689			19927.207	0.001	4
81	19912.559			19912.876			19927.574	-0.002	4
82	19912.746			19913.066			19927.945	-0.010	4
83	19912.937			19913.261			19928.321	0.004	4
84	19913.132			19913.460	-0.029*	6	19928.701	0.025*	4
85	19913.331	-0.030*	6	19913.663	-0.018*	6	19929.085	-0.003	4
86	19913.535	-0.021*	6	19913.871	0.001	6	19929.472	0.000	4
87	19913.742	-0.007	6	19914.082	-0.004	6	19929.864	-0.001	4
88	19913.954	-0.002	6	19914.298	0.001	6	19930.261	-0.001	4
89	19914.170	0.012	6	19914.517	0.015	6	19930.661	-0.007	4

90	19914.390	0.009	6	19914.741	0.015	6	19931.065	0.003	4
91	19914.614	0.021*	6	19914.969	0.017	6	19931.474	0.001	4
92	19914.842			19915.201	0.014*	4	19931.886	0.006	4
93	19915.075	0.011	4	19915.438	0.005	4	19932.303	-0.004	4
94	19915.311	0.008	4	19915.678	-0.005	4	19932.724	-0.002	4
95	19915.552	0.041*	4	19915.923			19933.148	-0.003	4
96	19915.797			19916.172			19933.577	-0.005	4
97	19916.046			19916.424			19934.010	-0.001	4
98	19916.299			19916.682			19934.448	0.001	4
99	19916.557			19916.943			19934.889	0.000	4
100	19916.818			19917.208			19935.334	0.002	4
101	19917.084			19917.478			19935.784	-0.001	4
102	19917.353			19917.751			19936.237		
103	19917.627			19918.029			19936.695	-0.008	4
104	19917.906			19918.311			19937.157	0.005	4
105	19918.188			19918.597			19937.623	0.007	4
106	19918.474			19918.887			19938.093	0.034*	4
107	19918.765			19919.182			19938.567	-0.010	4
108	19919.059			19919.481			19939.046	0.000	4
109	19919.358			19919.783			19939.528	0.013*	4
110	19919.661			19920.090			19940.014		
111	19919.969			19920.401			19940.505		
112	19920.280			19920.716			19941.000		
113	19920.595			19921.036			19941.499		
114	19920.915			19921.359			19942.002		

P_2				Q_2			R_2			
N	CALC	DIFF	U	CALC	DIFF	U	CALC	DIFF	U	
34	19912.324			19918.718			19918.852			
35	19912.433			19919.009			19919.147			
36	19912.545			19919.303			19919.445			
37	19912.662			19919.602			19919.748			
38	19912.783			19919.905			19920.054			
39	19912.908	-0.010	6	19920.212			19920.365			
40	19913.037	-0.003	6	19920.522			19920.680			
41	19913.170	0.008	6	19920.837			19920.998			
42	19913.307	-0.002	6	19921.156			19921.321			
43	19913.448	0.007	6	19921.480			19921.648			
44	19913.594			19921.807			19921.979			
45	19913.743			19922.138			19922.315			
46	19913.897	0.009	6	19922.473			19922.654			
47	19914.055	0.007	6	19922.813			19922.997			
48	19914.217			19923.156			19923.345			
49	19914.383	0.000	4	19923.504			19923.696			
50	19914.553	0.000	4	19923.856			19924.052			
51	19914.727	-0.011	6	19924.212			19924.411			
52	19914.905	0.001	4	19924.571			19924.775			
53	19915.088	-0.004	4	19924.935			19925.143			
54	19915.274	-0.003	4	19925.304			19925.515			
55	19915.465	-0.007	4	19925.676			19925.891			
56	19915.660	-0.005	4	19926.052			19926.271			
57	19915.858	-0.006	6	19926.432			19926.655			
58	19916.061	-0.005	6	19926.817			19927.044			
59	19916.268	0.001	6	19927.205			19927.436			

60	19916.480			19927.598			19927.832		
61	19916.695	-0.012	6	19927.994			19928.233		
62	19916.914	-0.008	6	19928.395			19928.637		
63	19917.138	0.009	6	19928.800			19929.046		
64	19917.365	0.004	6	19929.209			19929.459		
65	19917.597	0.004	4	19929.622			19929.876		
66	19917.833			19930.039			19930.297		
67	19918.073			19930.460			19930.722		
68	19918.317			19930.885			19931.151		
69	19918.565	-0.008	4	19931.314			19931.584		
70	19918.817	-0.007	4	19931.747			19932.021		
71	19919.074	-0.002	4	19932.185			19932.462		
72	19919.334			19932.626			19932.908		
73	19919.599	-0.006	4	19933.072			19933.357		
74	19919.867			19933.522			19933.811		
75	19920.140			19933.975			19934.268		
76	19920.417			19934.433			19934.730		
77	19920.698			19934.895			19935.196		
78	19920.983			19935.361			19935.666		

1 - 1 Band

N	P ₁			Q ₁			R ₁		
	CALC	DIFF	U	CALC	DIFF	U	CALC	DIFF	U
48	19713.065			19713.256			19721.970		
49	19713.129			19713.324			19722.219		
50	19713.197			19713.396			19722.472		
51	19713.269			19713.472			19722.730		
52	19713.346			19713.552			19722.992		
53	19713.427			19713.637			19723.259	-0.001	4
54	19713.512			19713.727			19723.530	0.005	4
55	19713.602			19713.821			19723.805	-0.001	4
56	19713.696			19713.919			19724.085	-0.003	4
57	19713.795			19714.021			19724.369	-0.004	4
58	19713.898			19714.128			19724.657	-0.005	4
59	19714.005			19714.240			19724.950	-0.004	4
60	19714.117			19714.356			19725.247	-0.005	4
61	19714.234			19714.476			19725.549	-0.006	4
62	19714.354			19714.600			19725.855	-0.005	4
63	19714.479			19714.729			19726.165	-0.002	4
64	19714.609			19714.863			19726.480	0.000	4
65	19714.743			19715.001			19726.799	0.005	4
66	19714.881	-0.011	6	19715.143			19727.122	-0.002	4
67	19715.023	-0.020	6	19715.289			19727.450	0.004	4
68	19715.170	-0.024*	6	19715.440			19727.782	0.006	4
69	19715.322	0.007	6	19715.596			19728.118	0.010	4
70	19715.478			19715.755			19728.459	0.016*	4
71	19715.638	0.012	6	19715.920			19728.804	0.000	4
72	19715.803	-0.010	6	19716.088			19729.154	0.005	4
73	19715.972	0.001	6	19716.261			19729.508	0.021*	4
74	19716.145	-0.005	6	19716.438			19729.866	-0.007	4
75	19716.323	0.004	6	19716.620			19730.229	0.000	4
76	19716.505	0.009	6	19716.806			19730.596	-0.007	4

77	19716.692	0.002	6	19716.997	19730.968	0.015*	4
78	19716.883	0.007	6	19717.192	19731.343	0.007	4
79	19717.078	-0.044*	6	19717.391	19731.724	0.016*	4
80	19717.278	0.016	6	19717.595	19732.108	-0.005	4
81	19717.482	0.011	6	19717.803	19732.497	-0.007	4
82	19717.691			19718.016	19732.890	-0.003	4
83	19717.904			19718.233	19733.288		
84	19718.122			19718.455	19733.690		
85	19718.344			19718.680	19734.097		
86	19718.570			19718.911	19734.507		
87	19718.801			19719.145	19734.923		

N	P ₂			Q ₂			R ₂		
	CALC	DIFF	U	CALC	DIFF	U	CALC	DIFF	U
41	19717.441			19725.106			19725.269		
42	19717.589			19725.436			19725.603		
43	19717.742			19725.770			19725.942		
44	19717.899			19726.109			19726.285		
45	19718.061			19726.453			19726.632		
46	19718.227	-0.001	6	19726.800			19726.983		
47	19718.397	-0.001	6	19727.152			19727.339		
48	19718.572			19727.509			19727.700		
49	19718.751	0.002	6	19727.869			19728.064		
50	19718.934	0.000	6	19728.234			19728.433		
51	19719.122	0.002	6	19728.604			19728.806		
52	19719.314	0.000	6	19728.977			19729.184		
53	19719.511	-0.014	6	19729.355			19729.566		
54	19719.712	0.005	6	19729.738			19729.953		
55	19719.917	-0.003	6	19730.125			19730.343		
56	19720.127	0.001	6	19730.516			19730.738		
57	19720.341	-0.007	6	19730.911			19731.138		
58	19720.559	0.009	6	19731.311			19731.541		
59	19720.782	0.009	6	19731.715			19731.950		
60	19721.009			19732.124			19732.362		
61	19721.241			19732.537			19732.779		
62	19721.477			19732.954			19733.200		
63	19721.717	-0.011	6	19733.375			19733.626		
64	19721.962			19733.801			19734.055		
65	19722.211	0.002	4	19734.232			19734.490		
66	19722.464	-0.001	4	19734.666			19734.928		
67	19722.722	0.001	4	19735.105			19735.371		
68	19722.984	0.009	4	19735.548			19735.818		
69	19723.251	0.002	4	19735.996			19736.270		
70	19723.522	0.008	4	19736.448			19736.726		
71	19723.797	0.000	4	19736.904			19737.186		
72	19724.077			19737.365			19737.651		
73	19724.361			19737.830			19738.120		
74	19724.649			19738.299			19738.593		
75	19724.942			19738.773			19739.070		
76	19725.239			19739.251			19739.552		

$^{172}\text{Yb}^{81}\text{Br}$

0 - 0 Band

N	P ₁			Q ₁			R ₁		
	CALC	DIFF	U	CALC	DIFF	U	CALC	DIFF	U
41	19694.000			19694.158			19701.498		
42	19694.032			19694.194			19701.714		
43	19694.068			19694.234			19701.933		
44	19694.109			19694.279			19702.157		
45	19694.154			19694.328			19702.385		
46	19694.204			19694.381			19702.617	0.000	4
47	19694.257			19694.438			19702.854	0.000	4
48	19694.315			19694.500			19703.095	0.002	4
49	19694.378			19694.566			19703.341	0.003	4
50	19694.444			19694.637			19703.590	0.001	4
51	19694.515			19694.712			19703.844	0.004	4
52	19694.591			19694.791			19704.102	0.000	4
53	19694.670			19694.874			19704.365	-0.007	4
54	19694.754			19694.962			19704.632	-0.003	4
55	19694.842			19695.054			19704.903	0.003	4
56	19694.935			19695.151			19705.178	0.001	4
57	19695.032			19695.251			19705.458	0.007	4
58	19695.133			19695.356			19705.742	0.002	4
59	19695.239			19695.466	-0.009	6	19706.030	-0.003	4
60	19695.349			19695.579	-0.008	6	19706.323		
61	19695.463			19695.697	0.001	6	19706.620	0.000	4
62	19695.581			19695.820	0.007	6	19706.921	0.003	4
63	19695.704			19695.947			19707.226	0.002	4
64	19695.831			19696.078	0.000	6	19707.536	0.003	4
65	19695.963			19696.213	-0.002	6	19707.850	-0.001	4
66	19696.099			19696.352	-0.004	6	19708.169	0.000	4
67	19696.239			19696.496	0.002	6	19708.491	-0.002	4
68	19696.383			19696.645	0.003	6	19708.818	0.005	4
69	19696.532			19696.797	-0.002	6	19709.150	0.000	4
70	19696.685	0.002	6	19696.954	-0.002	6	19709.485	0.002	4
71	19696.843	0.001	6	19697.116	0.002	6	19709.825	0.002	4
72	19697.005	0.002	6	19697.281	0.007	6	19710.169	-0.002	4
73	19697.171	0.000	6	19697.451	-0.003	4	19710.518	-0.001	4
74	19697.341	0.000	6	19697.626	-0.001	6	19710.871	0.003	4
75	19697.516	0.002	6	19697.804	-0.006	6	19711.228	0.000	4
76	19697.695	-0.001	6	19697.987	0.005	6	19711.589		
77	19697.879	0.005	6	19698.174	0.001	6	19711.955		
78	19698.067	-0.019	6	19698.366	0.003	6	19712.325		
79	19698.259			19698.562	0.003	6	19712.699	-0.010	6
80	19698.455			19698.762	-0.003	4	19713.078	0.001	6
81	19698.656			19698.967			19713.461	-0.002	6
82	19698.861			19699.176			19713.848	-0.005	6
83	19699.071			19699.389			19714.239	-0.006	6
84	19699.284	0.000	6	19699.607	0.007	6	19714.635	0.002	6
85	19699.503	-0.006	6	19699.829	-0.005	6	19715.035	0.002	6
86	19699.725	-0.008	6	19700.055	-0.001	6	19715.440	0.007	6
87	19699.952			19700.286	-0.002	6	19715.848	0.011	6
88	19700.183	-0.002	6	19700.521	-0.007	6	19716.261	0.011	6

89	19700.419	-0.008	6	19700.760	-0.002	6	19716.679
90	19700.658	-0.004	6	19701.004	-0.003	6	19717.100
91	19700.903			19701.252	0.003	6	19717.526
92	19701.151			19701.504	0.004	6	19717.957
93	19701.404			19701.761	0.008	6	19718.391
94	19701.661			19702.022			19718.830
95	19701.923			19702.287			19719.273
96	19702.189			19702.557			19719.720
97	19702.459			19702.831			19720.172
98	19702.733			19703.109			19720.628

P_2				Q_2			R_2		
N	CALC	DIFF	U	CALC	DIFF	U	CALC	DIFF	U
55	19701.048			19711.115			19711.327		
56	19701.254			19711.500			19711.716		
57	19701.464			19711.890			19712.109		
58	19701.679			19712.283			19712.506		
59	19701.898			19712.681			19712.908		
60	19702.121	-0.007	6	19713.083			19713.314		
61	19702.348	-0.007	6	19713.489			19713.724		
62	19702.580	-0.005	6	19713.900			19714.139		
63	19702.816	-0.002	6	19714.315			19714.557		
64	19703.057			19714.734			19714.980		
65	19703.301	-0.003	6	19715.158			19715.408		
66	19703.551			19715.585			19715.839		
67	19703.804	-0.008	6	19716.017			19716.275		
68	19704.062	-0.007	6	19716.454			19716.715		
69	19704.324	-0.004	6	19716.894			19717.159		
70	19704.590	-0.004	6	19717.339			19717.608		
71	19704.860	-0.005	6	19717.788			19718.061		
72	19705.135	0.001	6	19718.242			19718.518		
73	19705.414	0.001	6	19718.699			19718.980		
74	19705.698	0.004	6	19719.161			19719.446		
75	19705.986	0.001	6	19719.628			19719.916		
76	19706.278	0.002	6	19720.098			19720.390		
77	19706.574	0.004	6	19720.573			19720.869		
78	19706.875	0.003	6	19721.052			19721.351		
79	19707.180	0.005	6	19721.535			19721.839		
80	19707.489	0.010	6	19722.023			19722.330		
81	19707.803	0.006	6	19722.515			19722.826		
82	19708.121	0.005	6	19723.011			19723.326		
83	19708.443	0.013	6	19723.511			19723.830		
84	19708.770	0.009	6	19724.016			19724.338		
85	19709.101			19724.525			19724.851		
86	19709.436			19725.038			19725.368		
87	19709.775			19725.556			19725.889		
88	19710.119			19726.077			19726.415		
89	19710.467			19726.603			19726.945		
90	19710.820			19727.134			19727.479		
91	19711.176			19727.668			19728.017		
92	19711.537			19728.207			19728.560		
93	19711.903			19728.750			19729.107		
94	19712.272	-0.011	6	19729.298			19729.658		
95	19712.646	-0.005	6	19729.849			19730.214		

96	19713.025	-0.007	6	19730.405	19730.773
97	19713.407	-0.002	6	19730.965	19731.337
98	19713.794	-0.010	6	19731.530	19731.906
99	19714.185	0.004	6	19732.099	19732.478
100	19714.581	0.001	6	19732.672	19733.055
101	19714.981	0.002	6	19733.249	19733.636
102	19715.385			19733.830	19734.222
103	19715.793			19734.416	19734.811
104	19716.206			19735.006	19735.405
105	19716.623			19735.601	19736.003
106	19717.044			19736.199	19736.606

0 - 1 Band

N	P ₁			Q ₁			R ₁		
	CALC	DIFF	U	CALC	DIFF	U	CALC	DIFF	U
19	19500.110			19500.186			19503.577		
20	19500.053			19500.132			19503.703		
21	19500.000			19500.083			19503.834		
22	19499.952			19500.039			19503.969		
23	19499.908			19499.999			19504.108		
24	19499.869			19499.963			19504.252	-0.009	6
25	19499.834			19499.933			19504.401	0.009	6
26	19499.804			19499.906			19504.554	-0.014	6
27	19499.778			19499.885			19504.712	-0.005	6
28	19499.757			19499.868			19504.874	0.006	6
29	19499.741			19499.855			19505.041	-0.001	6
30	19499.729			19499.847			19505.212	0.002	6
31	19499.722			19499.844			19505.388	-0.011	6
32	19499.719			19499.845			19505.569	0.001	6
33	19499.721			19499.851			19505.754	0.007	6
34	19499.727			19499.861			19505.944	-0.003	6
35	19499.738			19499.876			19506.138	0.010	6
36	19499.754			19499.895			19506.337	0.004	6
37	19499.774			19499.919			19506.540	0.004	6
38	19499.799			19499.948			19506.748	-0.003	6
39	19499.828			19499.981			19506.960	0.001	6
40	19499.862			19500.019			19507.177	-0.002	6
41	19499.900			19500.061			19507.399		
42	19499.943			19500.108			19507.625		
43	19499.991			19500.159			19507.856		
44	19500.043			19500.215			19508.091		
45	19500.100			19500.276			19508.331		
46	19500.161			19500.341			19508.575		
47	19500.227			19500.411			19508.824		
48	19500.298			19500.485			19509.078	-0.007	6
49	19500.373			19500.564			19509.336	0.002	4
50	19500.452			19500.648			19509.598	0.008	6
51	19500.537			19500.736			19509.865	0.004	6
52	19500.625	0.014	6	19500.829			19510.137	-0.001	6
53	19500.719	0.017	6	19500.926			19510.413	0.010	6
54	19500.817	0.006	6	19501.028			19510.694	0.002	6

55	19500.919	0.001	6	19501.134	19510.979	0.001	6
56	19501.026	0.007	6	19501.245	19511.269	-0.009	6
57	19501.138	-0.002	6	19501.361	19511.564		
58	19501.254	-0.014	6	19501.481	19511.863	-0.002	6
59	19501.375			19501.606	19512.167	0.001	6
60	19501.501			19501.735	19512.475		
61	19501.631			19501.869	19512.787		
62	19501.765			19502.007	19513.105		
63	19501.905			19502.150	19513.427		
64	19502.048			19502.298	19513.753		

P_2				Q_2			R_2		
N	CALC	DIFF	U	CALC	DIFF	U	CALC	DIFF	U
32	19503.313			19509.257			19509.382		
33	19503.428			19509.552			19509.681		
34	19503.549			19509.851			19509.985		
35	19503.673			19510.155			19510.293		
36	19503.803			19510.464			19510.605		
37	19503.937	-0.002	6	19510.777			19510.922		
38	19504.075	0.000	6	19511.095			19511.244		
39	19504.218	0.007	6	19511.417			19511.570		
40	19504.366	-0.001	6	19511.744			19511.901		
41	19504.518	0.007	6	19512.076			19512.236		
42	19504.675	-0.006	6	19512.412			19512.576		
43	19504.836			19512.752			19512.920		
44	19505.002			19513.097			19513.269		
45	19505.172			19513.447			19513.623		
46	19505.347			19513.801			19513.981		
47	19505.527			19514.159			19514.343		
48	19505.711	-0.004	6	19514.523			19514.710		
49	19505.900	0.001	6	19514.890			19515.082		
50	19506.093	-0.002	6	19515.263			19515.458		
51	19506.291	0.000	6	19515.639			19515.839		
52	19506.493	-0.002	6	19516.021			19516.224		
53	19506.700	0.001	6	19516.407			19516.614		
54	19506.911	0.009	6	19516.797			19517.008		
55	19507.128	-0.004	6	19517.192			19517.407		
56	19507.348	-0.004	6	19517.592			19517.810		
57	19507.573	-0.006	6	19517.996			19518.218		
58	19507.803	-0.003	6	19518.404			19518.631		
59	19508.037	-0.003	6	19518.817			19519.048		
60	19508.276	-0.005	6	19519.235			19519.469		
61	19508.520	-0.006	6	19519.657			19519.895		
62	19508.768	0.000	6	19520.084			19520.326		
63	19509.020	-0.005	6	19520.515			19520.761		
64	19509.277			19520.951			19521.201		
65	19509.539	0.010	6	19521.391			19521.645		
66	19509.805	0.027*	6	19521.836			19522.094		
67	19510.076	-0.010	6	19522.286			19522.547		
68	19510.351	0.008	6	19522.740			19523.005		
69	19510.631	0.005	6	19523.198			19523.467		
70	19510.916	-0.013	6	19523.661			19523.934		
71	19511.205	-0.008	6	19524.129			19524.406		
72	19511.498			19524.601			19524.882		

73	19511.797	19525.077	19525.362
74	19512.099	19525.559	19525.847
75	19512.407	19526.044	19526.337
76	19512.719	19526.535	19526.831

1 - 0 Band

N	P ₁			Q ₁			R ₁		
	CALC	DIFF	U	CALC	DIFF	U	CALC	DIFF	U
61	19907.816			19908.050			19918.940		
62	19907.918			19908.156			19919.225		
63	19908.025			19908.267			19919.513		
64	19908.135			19908.381			19919.806		
65	19908.250			19908.500			19920.103		
66	19908.369			19908.622			19920.404	0.006	4
67	19908.491			19908.749			19920.708	0.011	4
68	19908.618			19908.880			19921.017	-0.004	4
69	19908.749			19909.014			19921.330	-0.004	4
70	19908.884			19909.153			19921.647	0.003	4
71	19909.023			19909.296			19921.968	-0.001	4
72	19909.166			19909.443			19922.293	0.001	4
73	19909.314			19909.594			19922.622	0.019*	4
74	19909.465			19909.749			19922.955	0.006	4
75	19909.620			19909.908			19923.292	-0.007	4
76	19909.780			19910.072			19923.633	-0.002	4
77	19909.943			19910.239			19923.979	-0.004	4
78	19910.111			19910.410			19924.328	0.004	4
79	19910.282			19910.586			19924.681	-0.002	4
80	19910.458			19910.765	0.004	4	19925.038	0.000	4
81	19910.638			19910.949	0.012	4	19925.400	-0.002	4
82	19910.822			19911.136	0.000	4	19925.765	0.007	4
83	19911.010			19911.328	-0.004	4	19926.134	-0.002	4
84	19911.202			19911.524			19926.508	0.005	4
85	19911.398			19911.724			19926.885	0.003	4
86	19911.598			19911.928			19927.267	0.004	4
87	19911.802	-0.015	6	19912.136	-0.006	4	19927.653	-0.001	4
88	19912.010	-0.006	6	19912.348	-0.001	4	19928.042	-0.003	4
89	19912.223	0.001	6	19912.564	0.000	4	19928.436	0.000	4
90	19912.439	-0.002	6	19912.784	0.004	4	19928.834	0.002	4
91	19912.660	0.027*	6	19913.009	0.009	6	19929.235	0.001	4
92	19912.884	0.010	6	19913.237	0.018*	6	19929.641	-0.005	4
93	19913.113	0.005	6	19913.470			19930.051	0.003	4
94	19913.346	0.008	6	19913.706			19930.465	0.002	4
95	19913.582	-0.001	6	19913.947			19930.883	0.005	4
96	19913.823			19914.192			19931.305	0.003	4
97	19914.068			19914.440			19931.730	0.001	4
98	19914.317			19914.693			19932.161	0.001	4
99	19914.571			19914.950			19932.595	-0.003	4
100	19914.828			19915.211			19933.033	-0.006	4
101	19915.089			19915.476			19933.475	0.020*	4
102	19915.355			19915.746			19933.921	0.004	4
103	19915.624			19916.019			19934.371	0.001	4
104	19915.898			19916.296			19934.825	-0.002	4

105	19916.175		19916.578		19935.284	-0.014*	4
106	19916.457		19916.863		19935.746	0.000	4
107	19916.743		19917.153		19936.213		
108	19917.033		19917.447		19936.683		
109	19917.327		19917.745		19937.157		
110	19917.625		19918.047		19937.636		
111	19917.927		19918.353		19938.118		

	P ₂			Q ₂			R ₂		
N	CALC	DIFF	U	CALC	DIFF	U	CALC	DIFF	U
24	19909.556			19914.053			19914.146		
25	19909.622			19914.298			19914.396		
26	19909.692			19914.548			19914.649		
27	19909.767			19914.801			19914.906		
28	19909.845			19915.059			19915.167		
29	19909.928			19915.320			19915.433	0.005	4
30	19910.015			19915.586	0.001	4	19915.702		
31	19910.105			19915.855			19915.975		
32	19910.200			19916.129	-0.002	4	19916.253	0.001	4
33	19910.298			19916.406			19916.534	0.004	4
34	19910.401			19916.688	-0.007	4	19916.819		
35	19910.508			19916.973	0.004	4	19917.109		
36	19910.619			19917.263			19917.402	-0.010	6
37	19910.734			19917.557	-0.021*	6	19917.700	-0.011	6
38	19910.852			19917.854	-0.008	6	19918.001	-0.004	6
39	19910.975			19918.156	-0.005	6	19918.307	-0.005	6
40	19911.102			19918.462	-0.002	6	19918.616	-0.002	6
41	19911.233			19918.771	0.004	6	19918.930	0.000	6
42	19911.368			19919.085	0.016	6	19919.247	0.002	6
43	19911.507			19919.403	0.024*	6	19919.569	0.008	6
44	19911.650			19919.725	0.021*	6	19919.894	-0.002	6
45	19911.798			19920.051			19920.224		
46	19911.949			19920.380			19920.558		
47	19912.104			19920.714			19920.895		
48	19912.263			19921.052			19921.237		
49	19912.426			19921.394			19921.583		
50	19912.594	0.008	4	19921.740			19921.932		
51	19912.765			19922.090			19922.286		
52	19912.941	0.001	4	19922.444			19922.644		
53	19913.120	0.002	4	19922.802			19923.006		
54	19913.304	0.000	4	19923.164			19923.371		
55	19913.491	0.000	4	19923.530			19923.741		
56	19913.683	-0.011	4	19923.900			19924.115		
57	19913.878	-0.002	4	19924.274			19924.493		
58	19914.078			19924.652			19924.875		
59	19914.281	-0.003	4	19925.034			19925.261		
60	19914.489	-0.001	4	19925.420			19925.650		
61	19914.701	-0.005	6	19925.810			19926.044		
62	19914.917	-0.005	6	19926.204			19926.442		
63	19915.137	-0.001	6	19926.602			19926.844		
64	19915.360	0.001	6	19927.004			19927.250		
65	19915.588	0.010	6	19927.410			19927.660		
66	19915.820	0.008	6	19927.820			19928.074		
67	19916.056			19928.234			19928.492		

68	19916.296			19928.653		19928.914
69	19916.541	-0.008	4	19929.075		19929.340
70	19916.789	-0.005	4	19929.501		19929.770
71	19917.041	-0.004	4	19929.931		19930.204
72	19917.297	-0.010	4	19930.365		19930.642
73	19917.557	0.004	4	19930.804		19931.084
74	19917.822			19931.246		19931.530
75	19918.090			19931.692		19931.980
76	19918.362			19932.142		19932.434
77	19918.639			19932.597		19932.892
78	19918.919			19933.055		19933.354

1 - 1 Band

N	P ₁			Q ₁			R ₁		
	CALC	DIFF	U	CALC	DIFF	U	CALC	DIFF	U
42	19712.572			19712.736			19720.231		
43	19712.608			19712.777			19720.450		
44	19712.649			19712.821			19720.674		
45	19712.694			19712.870			19720.901		
46	19712.744			19712.924			19721.133		
47	19712.798			19712.981			19721.369	-0.003	8
48	19712.856			19713.043			19721.610	0.003	8
49	19712.918			19713.110			19721.855	0.005	8
50	19712.985			19713.180			19722.104	0.003	8
51	19713.056			19713.255			19722.358	-0.004	8
52	19713.131			19713.335			19722.615	0.002	8
53	19713.211			19713.418			19722.877	-0.006	8
54	19713.295			19713.506			19723.144	0.003	8
55	19713.383			19713.598			19723.414	-0.003	8
56	19713.476			19713.695			19723.689	0.002	8
57	19713.573			19713.796			19723.969	-0.007	8
58	19713.674			19713.901			19724.252	-0.004	8
59	19713.780			19714.010			19724.540	-0.001	8
60	19713.890			19714.124			19724.832	0.000	8
61	19714.004			19714.242			19725.129	-0.004	8
62	19714.123			19714.365			19725.429	-0.006	8
63	19714.246			19714.491			19725.734	-0.001	8
64	19714.373			19714.623			19726.044	-0.001	8
65	19714.504			19714.758			19726.357	0.003	8
66	19714.640			19714.898			19726.675	-0.005	8
67	19714.780	-0.001	4	19715.042			19726.997	-0.007	8
68	19714.925	0.004	4	19715.190			19727.324	-0.007	8
69	19715.074	-0.008	4	19715.343			19727.655	-0.001	8
70	19715.227	-0.008	4	19715.500			19727.990	-0.002	8
71	19715.385	-0.005	4	19715.661			19728.329	0.002	8
72	19715.546	-0.010	4	19715.827			19728.673	0.002	8
73	19715.713	0.016*	4	19715.997			19729.021	-0.006	8
74	19715.883	0.017	6	19716.171			19729.373	0.006	8
75	19716.058	0.002	6	19716.350			19729.730	-0.011	8
76	19716.237	0.000	6	19716.533			19730.091	0.001	8
77	19716.420	-0.003	6	19716.720			19730.456	-0.003	8
78	19716.608	-0.008	6	19716.912			19730.825	0.005	8

79	19716.800	-0.016	6	19717.108	19731.199	0.004	8
80	19716.997	-0.010	6	19717.308	19731.577	0.000	8
81	19717.198	-0.007	6	19717.513	19731.959	0.003	8
82	19717.403	0.007	6	19717.722	19732.346	0.001	8
83	19717.612	-0.001	6	19717.935	19732.737	0.004	8
84	19717.826			19718.153	19733.132		
85	19718.044			19718.375	19733.532		
86	19718.267			19718.601	19733.936		
87	19718.493			19718.832	19734.344		
88	19718.725			19719.067	19734.756		

P_2				Q_2			R_2			
N	CALC	DIFF	U	CALC	DIFF	U	CALC	DIFF	U	
21	19715.140			19719.099			19719.183			
22	19715.200			19719.338			19719.425			
23	19715.265			19719.582			19719.673			
24	19715.333			19719.829			19719.924			
25	19715.406			19720.081			19720.180			
26	19715.483	-0.009	6	19720.337			19720.440			
27	19715.565	0.000	4	19720.597			19720.704			
28	19715.651	0.004	6	19720.862			19720.973			
29	19715.741	0.000	6	19721.131			19721.245			
30	19715.835	-0.007	6	19721.404			19721.522			
31	19715.934	0.004	6	19721.682			19721.804			
32	19716.037			19721.964			19722.090			
33	19716.144	0.001	6	19722.250			19722.380			
34	19716.256	-0.008	6	19722.540			19722.674			
35	19716.372	0.033*	6	19722.835			19722.972			
36	19716.492	0.026*	6	19723.134			19723.275			
37	19716.616	-0.004	6	19723.437			19723.582			
38	19716.745			19723.745			19723.894			
39	19716.878	0.011	6	19724.056			19724.209			
40	19717.015			19724.373			19724.529			
41	19717.157	-0.001	6	19724.693			19724.854			
42	19717.303	-0.001	6	19725.018			19725.182			
43	19717.453	-0.011	6	19725.346			19725.515			
44	19717.608	-0.012	6	19725.680			19725.852			
45	19717.767	-0.008	6	19726.017			19726.193			
46	19717.930	-0.007	4	19726.359			19726.539			
47	19718.097	0.003	4	19726.705			19726.889			
48	19718.269	0.001	4	19727.055			19727.243			
49	19718.445	0.005	4	19727.410			19727.601			
50	19718.625	0.005	4	19727.769			19727.964			
51	19718.810	0.004	4	19728.132			19728.331			
52	19718.999	0.005	6	19728.499			19728.702			
53	19719.192	0.002	4	19728.871			19729.078			
54	19719.390	0.017	6	19729.247			19729.458			
55	19719.592	0.025*	6	19729.627			19729.842			
56	19719.798	0.019*	6	19730.012			19730.230			
57	19720.008	0.003	4	19730.400			19730.623			
58	19720.223	0.012	6	19730.793			19731.020			
59	19720.442	0.006	6	19731.191			19731.421			
60	19720.665	0.003	6	19731.592			19731.827			
61	19720.893	0.012	6	19731.998			19732.236			

62	19721.125	0.007	6	19732.409	19732.651
63	19721.361	0.014	6	19732.823	19733.069
64	19721.602	0.010	6	19733.242	19733.491
65	19721.847	0.008	6	19733.665	19733.918
66	19722.096	0.016	6	19734.092	19734.349
67	19722.349			19734.523	19734.785
68	19722.607			19734.959	19735.225
69	19722.869			19735.399	19735.668
70	19723.135			19735.844	19736.117
71	19723.406			19736.292	19736.569

Appendix IV

YbBr Laser Excitation Line Positions - $A^2\Pi \leftarrow X^2\Sigma^+$ System

Calculated^a and observed line positions (cm^{-1}) in the 0 – 0 and 1 – 0 bands of the $A^2\Pi \leftarrow X^2\Sigma^+$ system of $^{174}\text{Yb}^{79}\text{Br}$ and $^{174}\text{Yb}^{81}\text{Br}$. Each band is labeled as $\nu' - \nu''$, while the symbol “*” indicates exclusion of the line from final fits; “J” indicates lines recorded using the laser ablation jet. The uncertainty of each line (U) is estimated based on the number of coincident lines (see text), and is given in units of 10^3 cm^{-1} .

^aUsing the parameters of Table 7.1

Page 220: $^{174}\text{Yb}^{79}\text{Br}$

Page 229: $^{174}\text{Yb}^{81}\text{Br}$

$^{174}\text{Yb}^{79}\text{Br}$

0 – 0 Band

J	$R_{11}(ee)$				$P_{12}(ff)$			
	OBS	CALC	DIFF	U	OBS	CALC	DIFF	U
5.5	-	17806.686			17804.411	17804.410	0.001	6
6.5	-	17806.898			17804.245	17804.243	0.002	6
7.5	-	17807.114			17804.081	17804.079	0.002	6
8.5	-	17807.333			17803.916	17803.919	-0.003	6
9.5	-	17807.556			17803.761	17803.762	-0.001	6
10.5	-	17807.781			17803.607	17803.608	-0.001	6
11.5	-	17808.011			17803.458	17803.458	0.000	6
12.5	-	17808.244			17803.313	17803.312	0.001	6
13.5	-	17808.480			17803.171	17803.169	0.002	6
14.5	-	17808.720			17803.028	17803.029	-0.001	6
15.5	-	17808.963			17802.898	17802.893	0.005	6
16.5	-	17809.209			17802.765	17802.760	0.005	6
17.5	-	17809.459			-	17802.631		
18.5	-	17809.713			-	17802.505		
19.5	-	17809.970			-	17802.383		
20.5	-	17810.230			-	17802.264		
21.5	-	17810.494			-	17802.149		
22.5	-	17810.761			-	17802.037		
23.5	-	17811.032			17801.924	17801.928	-0.004	6
24.5	-	17811.306			17801.821	17801.823	-0.002	6
25.5	-	17811.584			17801.721	17801.722	-0.001	6
26.5	17811.866	17811.865	0.001	4	17801.625	17801.624	0.001	6
27.5	17812.147	17812.149	-0.002	4	-	17801.529		
28.5	-	17812.437			-	17801.438		
29.5	17812.751	17812.729	0.022*	4	-	17801.351		
30.5	17813.022	17813.023	-0.001	4	-	17801.266		
31.5	17813.324	17813.322	0.002	4	-	17801.186		
32.5	17813.624	17813.623	0.001	4	-	17801.108		
33.5	17813.934	17813.929	0.005	4	-	17801.035		
34.5	17814.245	17814.237	0.008	4	-	17800.964		
35.5	17814.556	17814.549	0.007	4	-	17800.898		
36.5	17814.867	17814.865	0.002	4	-	17800.834		
37.5	17815.188	17815.184	0.004	4	-	17800.774		
38.5	17815.509	17815.506	0.003	4	-	17800.718		
39.5	-	17815.832			-	17800.665		
40.5	17816.160	17816.161	-0.001	4	-	17800.615		
41.5	17816.494	17816.494	0.000	4	-	17800.569		
42.5	17816.831	17816.830	0.001	4	-	17800.527		
43.5	17817.171	17817.169	0.002	4	-	17800.488		
44.5	17817.512	17817.512	0.000	4	-	17800.452		
45.5	-	17817.859			-	17800.420		
46.5	17818.205	17818.209	-0.004	4	-	17800.392		
47.5	17818.565	17818.562	0.003	4	-	17800.367		
48.5	17818.921	17818.919	0.002	4	-	17800.345		
49.5	17819.279	17819.279	0.000	4	-	17800.327		
50.5	17819.646	17819.642	0.004	4	-	17800.312		
51.5	-	17820.010			-	17800.301		
52.5	17820.381	17820.380	0.001	4	-	17800.293		

53.5	17820.755	17820.754	0.001	4	-	17800.289		
54.5	17821.131	17821.131	0.000	4	-	17800.288		
55.5	17821.511	17821.512	-0.001	4	-	17800.291		
56.5	17821.896	17821.896	0.000	4	-	17800.297		
57.5	17822.282	17822.284	-0.002	4	-	17800.307		
58.5	17822.673	17822.675	-0.002	4	-	17800.320		
59.5	17823.069	17823.070	-0.001	4	-	17800.337		
60.5	17823.468	17823.468	0.000	4	-	17800.357		
61.5	17823.865	17823.869	-0.004	4	-	17800.381		
62.5	17824.283	17824.274	0.009	4	-	17800.408		
63.5	17824.690	17824.683	0.007	4	-	17800.439		
64.5	17825.100	17825.094	0.006	4	-	17800.473		
65.5	17825.511	17825.510	0.001	4	-	17800.510		
66.5	17825.930	17825.928	0.002	4	-	17800.551		
67.5	17826.351	17826.350	0.001	4	-	17800.596		
68.5	17826.776	17826.776	0.000	4	-	17800.644		
69.5	17827.202	17827.205	-0.003	4	-	17800.696		
70.5	17827.633	17827.637	-0.004	4	-	17800.751		
71.5	17828.077	17828.073	0.004	4	-	17800.810		
72.5	17828.510	17828.513	-0.003	4	-	17800.872		
73.5	17828.954	17828.955	-0.001	4	-	17800.938		
74.5	17829.403	17829.401	0.002	4	-	17801.007		
75.5	17829.851	17829.851	0.000	4	-	17801.079		
76.5	17830.304	17830.304	0.000	4	-	17801.155		
77.5	17830.757	17830.761	-0.004	4	-	17801.235		
78.5	17831.218	17831.221	-0.003	4	-	17801.318		
79.5	-	17831.684			-	17801.405		
80.5	17832.151	17832.151	0.000	4	-	17801.495		
81.5	17832.618	17832.621	-0.003	4	-	17801.589		
82.5	17833.094	17833.095	-0.001	4	-	17801.686		
83.5	17833.572	17833.572	0.000	4	-	17801.787		
84.5	17834.050	17834.052	-0.002	4	-	17801.891		
85.5	17834.534	17834.536	-0.002	4	-	17801.999		
86.5	-	17835.024			-	17802.110		
87.5	17835.513	17835.515	-0.002	4	-	17802.225		
88.5	17836.008	17836.009	-0.001	4	-	17802.343		
89.5	17836.506	17836.507	-0.001	4	-	17802.465		
90.5	17837.007	17837.008	-0.001	4	-	17802.590		
91.5	-	17837.513			-	17802.719		
92.5	-	17838.021			-	17802.852		
93.5	-	17838.533			17802.979	17802.987	-0.008	6
94.5	-	17839.048			17803.128	17803.127	0.001	6
95.5	-	17839.566			17803.269	17803.270	-0.001	6
96.5	-	17840.088			17803.417	17803.416	0.001	6
97.5	-	17840.613			17803.567	17803.566	0.001	6
98.5	-	17841.142			17803.719	17803.720	-0.001	6
99.5	-	17841.674			17803.875	17803.877	-0.002	6
100.5	-	17842.210			17804.035	17804.037	-0.002	6
101.5	-	17842.749			17804.200	17804.202	-0.002	6
102.5	-	17843.292			17804.364	17804.369	-0.005	6
103.5	-	17843.838			17804.535	17804.540	-0.005	6
104.5	-	17844.387			17804.709	17804.715	-0.006	6
105.5	-	17844.940			17804.888	17804.893	-0.005	6
106.5	-	17845.496			17805.075	17805.075	0.000	6
107.5	-	17846.056			17805.242	17805.261	-0.019*	6

$P_{11}(ee)$

J	OBS	CALC	DIFF	U
52.5	17810.522	17810.521	0.001	4
53.5	-	17810.712		
54.5	17810.904	17810.906	-0.002	4
55.5	17811.105	17811.103	0.002	4
56.5	-	17811.304		
57.5	-	17811.508		
58.5	-	17811.716		
59.5	-	17811.927		
60.5	-	17812.142		
61.5	-	17812.360		
62.5	-	17812.582		
63.5	-	17812.807		
64.5	-	17813.035		
65.5	-	17813.267		
66.5	-	17813.503		
67.5	-	17813.742		
68.5	-	17813.984		
69.5	17814.230	17814.230	0.000	4
70.5	-	17814.479		
71.5	17814.729	17814.732	-0.003	4
72.5	17814.973	17814.988	-0.015*	4
73.5	-	17815.248		
74.5	17815.515	17815.511	0.004	4
75.5	-	17815.778		
76.5	-	17816.048		
77.5	-	17816.322		
78.5	-	17816.599		
79.5	-	17816.880		
80.5	-	17817.164		
81.5	-	17817.451		
82.5	17817.742	17817.742	0.000	4
83.5	17818.030	17818.037	-0.007	4
84.5	17818.330	17818.335	-0.005	4
85.5	17818.636	17818.636	0.000	4
86.5	17818.941	17818.941	0.000	4
87.5	17819.255	17819.250	0.005	4
88.5	17819.576	17819.562	0.014*	4
89.5	-	17819.877		
90.5	17820.184	17820.196	-0.012	4
91.5	17820.515	17820.518	-0.003	4
92.5	-	17820.844		
93.5	17821.170	17821.173	-0.003	4
94.5	17821.515	17821.506	0.009	4
95.5	-	17821.842		
96.5	-	17822.182		
97.5	-	17822.525		
98.5	17822.877	17822.872	0.005	4

$P_{22}(ff)$					$R_{21}(ee)$				
J	OBS	CALC	DIFF	U	OBS	CALC	DIFF	U	
3.5	19325.844	19325.844	0.000	J 4	-	19326.919			
4.5	19325.718	19325.725	-0.007	J 4	-	19327.069			
5.5	19325.601	19325.609	-0.008	J 4	-	19327.223			
6.5	19325.492	19325.497	-0.006	J 4	-	19327.379			
7.5	19325.386	19325.389	-0.003	J 4	-	19327.540			
8.5	19325.283	19325.284	-0.001	J 4	-	19327.704			
9.5	19325.175	19325.182	-0.007	J 4	-	19327.871			
10.5	19325.071	19325.084	-0.013*	J 4	-	19328.042			
11.5	19324.985	19324.989	-0.004	J 4	-	19328.216			
12.5	19324.898	19324.898	0.000	J 4	-	19328.393			
13.5	19324.809	19324.810	-0.001	J 4	-	19328.574			
14.5	19324.721	19324.726	-0.005	J 4	-	19328.759			
15.5	19324.640	19324.645	-0.005	J 4	-	19328.947			
16.5	19324.564	19324.568	-0.004	J 4	-	19329.138			
17.5	19324.491	19324.494	-0.003	J 4	-	19329.333			
18.5	19324.418	19324.424	-0.006	J 4	-	19329.532			
19.5	19324.346	19324.357	-0.011	J 4	-	19329.733			
20.5	19324.286	19324.293	-0.007	J 4	-	19329.939			
21.5	19324.224	19324.233	-0.009	J 4	19330.158	19330.147	0.011	4	
22.5	19324.183	19324.177	0.006	J 4	19330.374	19330.359	0.015*	4	
23.5	-	19324.123			19330.583	19330.575	0.008	4	
24.5	-	19324.074			-	19330.794			
25.5	-	19324.028			19331.022	19331.017	0.005	4	
26.5	-	19323.985			19331.249	19331.242	0.007	4	
27.5	-	19323.946			19331.476	19331.472	0.004	4	
28.5	-	19323.910			19331.709	19331.705	0.004	4	
29.5	-	19323.878			19331.944	19331.941	0.003	4	
30.5	-	19323.849			19332.183	19332.181	0.002	4	
31.5	-	19323.824			19332.426	19332.424	0.002	4	
32.5	-	19323.802			19332.682	19332.671	0.011	4	
33.5	-	19323.783			19332.922	19332.921	0.001	4	
34.5	-	19323.768			19333.172	19333.174	-0.002	4	
35.5	-	19323.757			19333.432	19333.431	0.001	4	
36.5	-	19323.749			19333.688	19333.692	-0.004	4	
37.5	-	19323.744			19333.956	19333.955	0.001	4	
38.5	-	19323.743			19334.223	19334.223	0.000	4	
39.5	-	19323.746			19334.496	19334.493	0.003	4	
40.5	-	19323.752			19334.771	19334.768	0.003	4	
41.5	-	19323.761			19335.045	19335.045	0.000	4	
42.5	-	19323.774			19335.331	19335.326	0.005	4	
43.5	-	19323.790			19335.611	19335.611	0.000	4	
44.5	-	19323.810			19335.901	19335.899	0.002	4	
45.5	-	19323.834			19336.193	19336.190	0.003	4	
46.5	-	19323.860			19336.485	19336.485	0.000	4	
47.5	-	19323.891			19336.788	19336.784	0.004	4	
48.5	-	19323.924			19337.088	19337.085	0.003	4	
49.5	-	19323.962			19337.392	19337.391	0.001	4	
50.5	-	19324.002			19337.701	19337.699	0.002	4	
51.5	-	19324.047			-	19338.012			
52.5	-	19324.094			-	19338.327			
53.5	-	19324.146			-	19338.646			
54.5	-	19324.200			-	19338.969			

55.5	19324.253	19324.258	-0.005	4	-	19339.295
56.5	19324.317	19324.320	-0.003	4	-	19339.624
57.5	19324.374	19324.385	-0.011	4	-	19339.957
58.5	19324.450	19324.454	-0.004	4	-	19340.293
59.5	19324.520	19324.526	-0.006	4	-	19340.633
60.5	19324.597	19324.602	-0.005	4	-	19340.976
61.5	19324.674	19324.681	-0.007	4	-	19341.323
62.5	19324.762	19324.763	-0.001	4	-	19341.673
63.5	19324.845	19324.849	-0.004	4	-	19342.026
64.5	19324.936	19324.939	-0.003	4	-	19342.383
65.5	19325.028	19325.032	-0.004	4	-	19342.743
66.5	19325.126	19325.129	-0.003	4	-	19343.107
67.5	19325.228	19325.229	-0.001	4	-	19343.475
68.5	19325.328	19325.332	-0.004	4	-	19343.845
69.5	19325.434	19325.439	-0.005	4	-	19344.220
70.5	19325.544	19325.550	-0.006	4	-	19344.597
71.5	19325.664	19325.664	0.000	4	-	19344.978
72.5	19325.781	19325.782	-0.001	4	-	19345.363
73.5	19325.901	19325.903	-0.002	4	-	19345.751
74.5	-	19326.027			-	19346.142
75.5	-	19326.156			-	19346.537
76.5	-	19326.287			-	19346.936
77.5	-	19326.422			-	19347.337
78.5	-	19326.561			-	19347.743
79.5	-	19326.703			-	19348.151
80.5	-	19326.849			-	19348.564
81.5	-	19326.998			-	19348.979
82.5	19327.155	19327.150	0.005	4	-	19349.398
83.5	19327.308	19327.307	0.001	4	-	19349.821
84.5	19327.468	19327.466	0.002	4	-	19350.247
85.5	19327.632	19327.630	0.002	4	-	19350.676
86.5	19327.795	19327.796	-0.001	4	-	19351.109
87.5	19327.965	19327.967	-0.002	4	-	19351.545
88.5	19328.142	19328.140	0.002	4	-	19351.985
89.5	19328.319	19328.318	0.001	4	-	19352.428
90.5	19328.499	19328.498	0.001	4	-	19352.875
91.5	19328.683	19328.683	0.000	4	-	19353.325
92.5	19328.869	19328.871	-0.002	4	-	19353.779

 $Q_{22}(ef)$ $P_{21}(ee)$

J	OBS	CALC	DIFF	U	OBS	CALC	DIFF	U
35.5	19327.027	19327.023	0.004	8	-	19326.805		
36.5	19327.111	19327.107	0.004	8	-	19326.882		
37.5	19327.196	19327.194	0.002	8	-	19326.962		
38.5	19327.289	19327.285	0.004	8	19327.067	19327.045	0.022*	8
39.5	19327.381	19327.379	0.002	8	19327.151	19327.132	0.019	8
40.5	19327.480	19327.477	0.003	8	19327.239	19327.223	0.016	8
41.5	19327.580	19327.578	0.002	8	19327.335	19327.317	0.018	8
42.5	19327.686	19327.683	0.003	8	19327.429	19327.414	0.015	8
43.5	19327.797	19327.791	0.006	8	19327.528	19327.515	0.013	8
44.5	19327.907	19327.903	0.004	8	19327.633	19327.619	0.014	8
45.5	19328.028	19328.018	0.010	8	19327.740	19327.727	0.013	8
46.5	19328.146	19328.137	0.009	8	19327.851	19327.838	0.013	8
47.5	19328.265	19328.259	0.006	8	19327.966	19327.953	0.013	8

48.5	19328.396	19328.384	0.012	8	19328.083	19328.071	0.012	8
49.5	19328.518	19328.513	0.005	8	19328.206	19328.193	0.013	8
50.5	-	19328.645			19328.331	19328.318	0.013	8

 $Q_{21}(fe)$

J	OBS	CALC	DIFF	U
42.5	19331.331	19331.326	0.005	6
43.5	19331.522	19331.518	0.004	6
44.5	19331.718	19331.715	0.003	6
45.5	19331.924	19331.914	0.010	6
46.5	19332.124	19332.117	0.007	6
47.5	19332.331	19332.324	0.007	6
48.5	19332.548	19332.534	0.014	6
49.5	19332.750	19332.748	0.002	6
50.5	19332.969	19332.965	0.004	6
51.5	-	19333.185		
52.5	-	19333.409		
53.5	-	19333.637		
54.5	-	19333.867		
55.5	19334.108	19334.102	0.006	6
56.5	19334.342	19334.340	0.002	6
57.5	19334.582	19334.581	0.001	6
58.5	19334.827	19334.825	0.002	6
59.5	19335.073	19335.074	-0.001	6
60.5	-	19335.325		
61.5	19335.581	19335.580	0.001	6
62.5	19335.831	19335.839	-0.008	6
63.5	19336.091	19336.101	-0.010	6
64.5	19336.356	19336.367	-0.011	6
65.5	19336.622	19336.636	-0.014*	6
66.5	19336.886	19336.908	-0.022*	6

1 - 0 Band

 $R_{11}(ee)$ $P_{12}(ff)$

J	OBS	CALC	DIFF	U	OBS	CALC	DIFF	U
39.5	18026.831	18026.834	-0.003	4	-	18011.708		
40.5	18027.147	18027.152	-0.005	4	-	18011.649		
41.5	18027.468	18027.474	-0.006	4	-	18011.593		
42.5	18027.792	18027.798	-0.006	4	-	18011.540		
43.5	18028.122	18028.126	-0.004	4	-	18011.490		
44.5	18028.454	18028.457	-0.003	4	-	18011.443		
45.5	18028.792	18028.791	0.001	4	-	18011.400		
46.5	18029.125	18029.128	-0.003	4	-	18011.360		
47.5	18029.468	18029.469	-0.001	4	-	18011.323		
48.5	18029.817	18029.813	0.004	4	-	18011.289		
49.5	18030.156	18030.159	-0.003	4	-	18011.259		
50.5	18030.507	18030.509	-0.002	4	-	18011.232		
51.5	18030.850	18030.863	-0.013*	4	-	18011.208		
52.5	18031.218	18031.219	-0.001	4	-	18011.187		
53.5	18031.580	18031.579	0.001	4	-	18011.169		

54.5	18031.939	18031.942	-0.003	4	-	18011.155		
55.5	18032.314	18032.307	0.007	4	-	18011.144		
56.5	18032.683	18032.677	0.006	4	-	18011.136		
57.5	-	18033.049			-	18011.132		
58.5	-	18033.424			-	18011.130		
59.5	18033.803	18033.803	0.000	4	-	18011.132		
60.5	18034.187	18034.185	0.002	4	-	18011.137		
61.5	18034.571	18034.570	0.001	4	-	18011.145		
62.5	-	18034.958			-	18011.157		
63.5	18035.346	18035.350	-0.004	4	-	18011.172		
64.5	18035.742	18035.744	-0.002	4	-	18011.190		
65.5	18036.145	18036.142	0.003	4	-	18011.211		
66.5	18036.545	18036.543	0.002	4	-	18011.235		
67.5	18036.951	18036.947	0.004	4	-	18011.263		
68.5	-	18037.354			-	18011.294		
69.5	18037.766	18037.765	0.001	4	-	18011.328		
70.5	18038.183	18038.178	0.005	4	-	18011.365		
71.5	18038.598	18038.595	0.003	4	-	18011.406		
72.5	18039.013	18039.015	-0.002	4	-	18011.450		
73.5	18039.442	18039.439	0.003	4	-	18011.497		
74.5	18039.869	18039.865	0.004	4	-	18011.548		
75.5	18040.284	18040.295	-0.011	4	-	18011.601		
76.5	18040.721	18040.727	-0.006	4	-	18011.658		
77.5	18041.162	18041.163	-0.001	4	-	18011.718		
78.5	18041.603	18041.602	0.001	4	-	18011.782		
79.5	18042.047	18042.045	0.002	4	-	18011.848		
80.5	18042.497	18042.490	0.007	4	-	18011.918		
81.5	-	18042.939			-	18011.991		
82.5	18043.392	18043.391	0.001	4	-	18012.068		
83.5	18043.845	18043.846	-0.001	4	-	18012.147		
84.5	18044.306	18044.304	0.002	4	-	18012.230		
85.5	18044.758	18044.765	-0.007	4	-	18012.316		
86.5	18045.226	18045.230	-0.004	4	-	18012.406		
87.5	18045.695	18045.698	-0.003	4	-	18012.498		
88.5	18046.174	18046.168	0.006	4	-	18012.594		
89.5	-	18046.643			-	18012.694		
90.5	-	18047.120			18012.803	18012.796	0.007	4
91.5	18047.599	18047.600	-0.001	4	18012.894	18012.902	-0.008	4
92.5	18048.087	18048.084	0.003	4	18012.993	18013.011	-0.018*	4
93.5	18048.573	18048.571	0.002	4	18013.122	18013.123	-0.001	4
94.5	18049.066	18049.061	0.005	4	18013.216	18013.238	-0.022*	4
95.5	18049.557	18049.554	0.003	4	18013.356	18013.357	-0.001	4
96.5	18050.053	18050.051	0.002	4	-	18013.479		
97.5	18050.550	18050.550	0.000	4	-	18013.604		
98.5	18051.054	18051.053	0.001	4	18013.737	18013.733	0.004	4
99.5	18051.560	18051.559	0.001	4	18013.875	18013.865	0.010	4
100.5	18052.070	18052.068	0.002	4	18014.012	18014.000	0.012	4
101.5	18052.579	18052.581	-0.002	4	18014.145	18014.138	0.007	4
102.5	18053.099	18053.096	0.003	4	18014.282	18014.280	0.002	4
103.5	18053.613	18053.615	-0.002	4	18014.421	18014.425	-0.004	4
104.5	18054.137	18054.137	0.000	4	18014.572	18014.573	-0.001	4
105.5	18054.659	18054.662	-0.003	4	18014.724	18014.725	-0.001	4
106.5	18055.191	18055.190	0.001	4	-	18014.879		
107.5	-	18055.722			-	18015.037		
108.5	-	18056.256			18015.186	18015.199	-0.013*	4
109.5	-	18056.794			18015.354	18015.363	-0.009	4
110.5	18057.333	18057.335	-0.002	4	-	18015.531		

111.5	18057.879	18057.879	0.000	4	-	18015.702
112.5	18058.430	18058.427	0.003	4	-	18015.877
113.5	18058.982	18058.977	0.005	4	-	18016.055
114.5	18059.549	18059.531	0.018*	4	-	18016.236

 $P_{22}(ff)$ $R_{21}(ee)$

J	OBS	CALC	DIFF	U	OBS	CALC	DIFF	U
18.5	-	19536.880			19541.982	19541.978	0.004	4
19.5	-	19536.808			19542.172	19542.175	-0.003	4
20.5	-	19536.740			-	19542.374		
21.5	-	19536.674			-	19542.577		
22.5	-	19536.612			-	19542.783		
23.5	19536.559	19536.553	0.006	J 4	19542.995	19542.993	0.002	4
24.5	-	19536.498			19543.209	19543.205	0.004	4
25.5	-	19536.445			19543.427	19543.421	0.006	4
26.5	19536.396	19536.396	0.000	J 4	19543.644	19543.639	0.005	4
27.5	19536.352	19536.350	0.002	J 6	19543.867	19543.861	0.006	4
28.5	-	19536.307			19544.088	19544.087	0.001	4
29.5	19536.267	19536.267	0.000	J 4	19544.313	19544.315	-0.002	4
30.5	19536.238	19536.231	0.007	J 6	19544.540	19544.547	-0.007	4
31.5	19536.204	19536.198	0.006	J 4	19544.778	19544.781	-0.003	4
32.5	-	19536.168			-	19545.019		
33.5	19536.140	19536.141	-0.001	J 4	-	19545.261		
34.5	-	19536.117			-	19545.505		
35.5	19536.098	19536.097	0.001	J 4	-	19545.752		
36.5	19536.081	19536.080	0.001	J 4	-	19546.003		
37.5	-	19536.066			-	19546.257		
38.5	-	19536.055			-	19546.514		
39.5	-	19536.047			-	19546.774		
40.5	-	19536.043			-	19547.038		
41.5	-	19536.042			-	19547.305		
42.5	-	19536.044			-	19547.574		
43.5	-	19536.050			-	19547.847		
44.5	-	19536.058			-	19548.124		
45.5	-	19536.070			-	19548.403		
46.5	-	19536.085			-	19548.686		
47.5	-	19536.103			-	19548.971		
48.5	-	19536.125			-	19549.260		
49.5	-	19536.149			-	19549.553		
50.5	-	19536.177			-	19549.848		
51.5	-	19536.209			19550.150	19550.147	0.003	4
52.5	-	19536.243			19550.452	19550.448	0.004	4
53.5	-	19536.281			19550.750	19550.753	-0.003	4
54.5	-	19536.321			19551.063	19551.061	0.002	4
55.5	-	19536.365			19551.372	19551.373	-0.001	4
56.5	-	19536.413			19551.694	19551.687	0.007	4
57.5	-	19536.463			19552.002	19552.005	-0.003	4
58.5	-	19536.517			19552.331	19552.326	0.005	4
59.5	-	19536.574			19552.649	19552.650	-0.001	4
60.5	-	19536.634			19552.982	19552.977	0.005	4
61.5	-	19536.698			19553.304	19553.308	-0.004	4
62.5	-	19536.764			19553.644	19553.641	0.003	4
63.5	-	19536.834			19553.973	19553.978	-0.005	4
64.5	-	19536.908			19554.312	19554.318	-0.006	4

65.5	-	19536.984			19554.656	19554.661	-0.005	4
66.5	-	19537.064			19555.012	19555.008	0.004	4

 $Q_{22}(ef)$ $P_{21}(ee)$

J	OBS	CALC	DIFF	U	OBS	CALC	DIFF	U
63.5	-	19542.651			19542.244	19542.245	-0.001	4
64.5	19542.812	19542.816	-0.004	4	-	19542.402		
65.5	19542.989	19542.983	0.006	4	19542.550	19542.563	-0.013*	4
66.5	19543.153	19543.154	-0.001	4	19542.724	19542.726	-0.002	4
67.5	19543.335	19543.328	0.007	4	-	19542.893		
68.5	19543.508	19543.505	0.003	4	19543.063	19543.063	0.000	4
69.5	19543.680	19543.686	-0.006	4	19543.239	19543.237	0.002	4
70.5	19543.859	19543.870	-0.011	4	19543.419	19543.413	0.006	4
71.5	-	19544.056			19543.588	19543.593	-0.005	4
72.5	-	19544.247			19543.764	19543.776	-0.012	4
73.5	-	19544.440			19543.953	19543.962	-0.009	4

 $R_{22}(ff)$ $Q_{21}(fe)$

J	OBS	CALC	DIFF	U	OBS	CALC	DIFF	U
47.5	19544.922	19544.909	0.013	6	-	19544.524		
48.5	19545.116	19545.114	0.002	6	-	19544.722		
49.5	19545.327	19545.322	0.005	6	19544.922	19544.923	-0.001	6
50.5	19545.543	19545.533	0.010	6	19545.116	19545.127	-0.011	6
51.5	19545.753	19545.747	0.006	6	19545.327	19545.334	-0.007	6
52.5	19545.973	19545.965	0.008	6	19545.543	19545.544	-0.001	6
53.5	19546.194	19546.185	0.009	6	19545.753	19545.758	-0.005	6
54.5	19546.422	19546.409	0.013	6	19545.973	19545.974	-0.001	6
55.5	19546.647	19546.636	0.011	6	19546.194	19546.194	0.000	6
56.5	19546.871	19546.866	0.005	6	19546.422	19546.418	0.004	6
57.5	19547.104	19547.100	0.004	6	19546.647	19546.644	0.003	6
58.5	19547.335	19547.336	-0.001	6	19546.871	19546.874	-0.003	6
59.5	19547.567	19547.576	-0.009	6	19547.104	19547.106	-0.002	6
60.5	19547.814	19547.819	-0.005	6	19547.335	19547.342	-0.007	6
61.5	19548.068	19548.066	0.002	6	19547.567	19547.582	-0.015	6
62.5	19548.307	19548.315	-0.008	6	19547.814	19547.824	-0.010	6
63.5	19548.567	19548.568	-0.001	6	19548.068	19548.070	-0.002	6
64.5	19548.823	19548.824	-0.001	6	19548.307	19548.319	-0.012	6
65.5	19549.082	19549.083	-0.001	6	19548.567	19548.571	-0.004	6
66.5	19549.343	19549.345	-0.002	6	19548.823	19548.826	-0.003	6
67.5	19549.602	19549.611	-0.009	6	19549.082	19549.084	-0.002	6
68.5	19549.880	19549.880	0.000	6	19549.343	19549.346	-0.003	6
69.5	19550.151	19550.152	-0.001	6	19549.602	19549.611	-0.009	6
70.5	19550.425	19550.427	-0.002	6	19549.880	19549.879	0.001	6
71.5	19550.669	19550.705	-0.036*	6	19550.151	19550.150	0.001	6
72.5	19550.983	19550.987	-0.004	6	19550.425	19550.425	0.000	6
73.5	19551.265	19551.272	-0.007	6	19550.669	19550.703	-0.034*	6
74.5	19551.553	19551.560	-0.007	6	19550.983	19550.984	-0.001	6
75.5	19551.847	19551.851	-0.004	6	19551.265	19551.268	-0.003	6
76.5	19552.143	19552.145	-0.002	6	19551.553	19551.555	-0.002	6
77.5	19552.435	19552.443	-0.008	6	19551.847	19551.846	0.001	6
78.5	-	19552.744			19552.143	19552.140	0.003	6
79.5	-	19553.048			19552.435	19552.437	-0.002	6

$^{174}\text{Yb}^{81}\text{Br}$

0-0 Band

J	$R_{11}(ee)$				$P_{12}(ff)$			
	OBS	CALC	DIFF	U	OBS	CALC	DIFF	U
5.5	-	17806.597			17804.353	17804.360	-0.007	6
6.5	-	17806.806			17804.199	17804.195	0.004	6
7.5	-	17807.018			17804.038	17804.034	0.004	6
8.5	-	17807.233			17803.879	17803.877	0.002	6
9.5	-	17807.452			17803.725	17803.722	0.003	6
10.5	-	17807.674			17803.571	17803.572	-0.001	6
11.5	-	17807.900			17803.422	17803.424	-0.002	6
12.5	-	17808.128			17803.283	17803.280	0.003	6
13.5	-	17808.361			17803.130	17803.140	-0.010	6
14.5	-	17808.596			17803.003	17803.002	0.001	6
15.5	-	17808.835			17802.868	17802.868	0.000	6
16.5	-	17809.078			17802.737	17802.738	-0.001	6
17.5	-	17809.324			17802.601	17802.611	-0.010	6
18.5	17809.577	17809.573	0.004	4	17802.489	17802.487	0.002	6
19.5	17809.820	17809.825	-0.005	4	17802.358	17802.367	-0.009	6
20.5	17810.082	17810.081	0.001	4	17802.253	17802.250	0.003	6
21.5	-	17810.341			17802.140	17802.137	0.003	6
22.5	17810.606	17810.603	0.003	4	17802.028	17802.027	0.001	6
23.5	17810.867	17810.870	-0.003	4	17801.924	17801.920	0.004	6
24.5	17811.117	17811.139	-0.022**	4	17801.821	17801.817	0.004	6
25.5	-	17811.412			17801.721	17801.717	0.004	6
26.5	-	17811.688			17801.625	17801.621	0.004	6
27.5	17811.963	17811.968	-0.005	4	17801.529	17801.528	0.001	6
28.5	17812.250	17812.251	-0.001	4	17801.440	17801.438	0.002	6
29.5	17812.534	17812.537	-0.003	4	17801.350	17801.352	-0.002	6
30.5	17812.819	17812.827	-0.008	4	17801.270	17801.269	0.001	6
31.5	17813.124	17813.120	0.004	4	17801.189	17801.190	-0.001	6
32.5	17813.419	17813.417	0.002	4	-	17801.114		
33.5	17813.721	17813.717	0.004	4	-	17801.042		
34.5	-	17814.020			-	17800.972		
35.5	17814.323	17814.327	-0.004	4	-	17800.907		
36.5	17814.632	17814.637	-0.005	4	-	17800.844		
37.5	17814.945	17814.951	-0.006	4	-	17800.786		
38.5	17815.267	17815.268	-0.001	4	-	17800.730		
39.5	17815.589	17815.588	0.001	4	-	17800.678		
40.5	-	17815.912			-	17800.629		
41.5	17816.240	17816.239	0.001	4	-	17800.584		
42.5	17816.572	17816.569	0.003	4	-	17800.542		
43.5	17816.909	17816.903	0.006	4	-	17800.504		
44.5	17817.248	17817.240	0.008	4	-	17800.469		
45.5	17817.588	17817.581	0.007	4	-	17800.437		
46.5	-	17817.924			-	17800.409		
47.5	17818.279	17818.272	0.007	4	-	17800.385		
48.5	17818.626	17818.623	0.003	4	-	17800.363		
49.5	17818.974	17818.977	-0.003	4	-	17800.345		
50.5	17819.335	17819.334	0.001	4	-	17800.331		
51.5	17819.695	17819.695	0.000	4	-	17800.320		
52.5	17820.059	17820.059	0.000	4	-	17800.312		

53.5	17820.427	17820.427	0.000	4	-	17800.308		
54.5	17820.797	17820.798	-0.001	4	-	17800.307		
55.5	17821.173	17821.172	0.001	4	-	17800.310		
56.5	17821.547	17821.550	-0.003	4	-	17800.316		
57.5	17821.930	17821.931	-0.001	4	-	17800.326		
58.5	17822.312	17822.316	-0.004	4	-	17800.339		
59.5	17822.697	17822.703	-0.006	4	-	17800.355		
60.5	17823.094	17823.095	-0.001	4	-	17800.375		
61.5	17823.490	17823.489	0.001	4	-	17800.398		
62.5	17823.886	17823.887	-0.001	4	-	17800.425		
63.5	17824.283	17824.289	-0.006	4	-	17800.455		
64.5	17824.690	17824.694	-0.004	4	-	17800.489		
65.5	-	17825.102			-	17800.526		
66.5	17825.511	17825.513	-0.002	4	-	17800.566		
67.5	17825.930	17825.928	0.002	4	-	17800.610		
68.5	17826.351	17826.347	0.004	4	-	17800.657		
69.5	17826.776	17826.768	0.008	4	-	17800.708		
70.5	17827.202	17827.193	0.009	4	-	17800.762		
71.5	-	17827.622			-	17800.820		
72.5	17828.058	17828.054	0.004	4	-	17800.881		
73.5	17828.493	17828.489	0.004	4	-	17800.945		
74.5	17828.926	17828.928	-0.002	4	-	17801.013		
75.5	17829.366	17829.370	-0.004	4	-	17801.085		
76.5	17829.815	17829.815	0.000	4	-	17801.159		
77.5	17830.263	17830.264	-0.001	4	-	17801.238		
78.5	17830.712	17830.716	-0.004	4	-	17801.319		
79.5	17831.171	17831.171	0.000	4	-	17801.405		
80.5	17831.631	17831.630	0.001	4	-	17801.493		
81.5	-	17832.093			-	17801.585		
82.5	17832.557	17832.558	-0.001	4	-	17801.681		
83.5	17833.027	17833.027	0.000	4	-	17801.780		
84.5	-	17833.500			-	17801.882		
85.5	17833.972	17833.976	-0.004	4	-	17801.988		
86.5	17834.454	17834.455	-0.001	4	-	17802.097		
87.5	17834.933	17834.937	-0.004	4	-	17802.210		
88.5	17835.422	17835.423	-0.001	4	-	17802.326		
89.5	17835.912	17835.913	-0.001	4	-	17802.446		
90.5	17836.405	17836.406	-0.001	4	-	17802.569		
91.5	17836.900	17836.902	-0.002	4	-	17802.696		
92.5	-	17837.401			-	17802.826		
93.5	-	17837.904			17802.956	17802.960	-0.004	6
94.5	-	17838.410			17803.095	17803.097	-0.002	6
95.5	-	17838.920			17803.237	17803.237	0.000	6
96.5	-	17839.433			17803.382	17803.381	0.001	6
97.5	-	17839.950			17803.535	17803.528	0.007	6
98.5	-	17840.469			17803.680	17803.679	0.001	6
99.5	-	17840.993			17803.836	17803.834	0.002	6
100.5	-	17841.519			17803.995	17803.991	0.004	6
101.5	-	17842.049			17804.156	17804.153	0.003	6
102.5	-	17842.583			17804.320	17804.317	0.003	6
103.5	-	17843.119			17804.487	17804.486	0.001	6
104.5	-	17843.659			17804.659	17804.657	0.002	6
105.5	-	17844.203			17804.833	17804.833	0.000	6
106.5	-	17844.750			17805.012	17805.011	0.001	6
107.5	-	17845.300			17805.196	17805.193	0.003	6

$P_{22}(ff)$					$R_{21}(ee)$				
J	OBS	CALC	DIFF	U	OBS	CALC	DIFF	U	
3.5	19325.780	19325.781	-0.001	J 4	-	19326.838			
4.5	19325.665	19325.664	0.001	J 4	-	19326.986			
5.5	19325.548	19325.551	-0.002	J 4	-	19327.136			
6.5	19325.435	19325.440	-0.006	J 4	-	19327.291			
7.5	19325.326	19325.334	-0.008	J 4	-	19327.448			
8.5	19325.227	19325.231	-0.004	J 4	-	19327.609			
9.5	19325.125	19325.131	-0.006	J 4	-	19327.774			
10.5	19325.028	19325.034	-0.006	J 4	-	19327.942			
11.5	19324.940	19324.941	-0.001	J 4	-	19328.113			
12.5	19324.847	19324.851	-0.004	J 4	-	19328.287			
13.5	19324.761	19324.765	-0.004	J 4	-	19328.465			
14.5	19324.681	19324.682	-0.001	J 4	-	19328.647			
15.5	19324.608	19324.603	0.005	J 4	-	19328.832			
16.5	19324.526	19324.527	-0.001	J 4	-	19329.020			
17.5	19324.452	19324.454	-0.002	J 4	-	19329.211			
18.5	19324.384	19324.385	-0.001	J 4	-	19329.406			
19.5	19324.316	19324.319	-0.003	J 4	-	19329.605			
20.5	19324.253	19324.257	-0.004	J 4	-	19329.806			
21.5	-	19324.198			-	19330.012			
22.5	-	19324.142			19330.216	19330.220	-0.004	4	
23.5	-	19324.090			19330.434	19330.432	0.002	4	
24.5	-	19324.041			19330.640	19330.647	-0.007	4	
25.5	-	19323.996			-	19330.866			
26.5	-	19323.954			19331.089	19331.088	0.001	4	
27.5	-	19323.915			19331.313	19331.314	-0.001	4	
28.5	-	19323.880			19331.541	19331.542	-0.001	4	
29.5	-	19323.848			19331.774	19331.775	-0.001	4	
30.5	-	19323.820			19332.008	19332.010	-0.002	4	
31.5	-	19323.795			19332.247	19332.249	-0.002	4	
32.5	-	19323.773			19332.492	19332.492	0.000	4	
33.5	-	19323.755			19332.740	19332.738	0.002	4	
34.5	-	19323.741			19332.989	19332.987	0.002	4	
35.5	-	19323.729			19333.239	19333.240	-0.001	4	
36.5	-	19323.722			19333.496	19333.496	0.000	4	
37.5	-	19323.717			19333.755	19333.755	0.000	4	
38.5	-	19323.716			19334.019	19334.018	0.001	4	
39.5	-	19323.719			19334.291	19334.284	0.007	4	
40.5	-	19323.724			19334.558	19334.553	0.005	4	
41.5	-	19323.734			19334.833	19334.826	0.007	4	
42.5	-	19323.746			19335.112	19335.103	0.009	4	
43.5	-	19323.762			19335.398	19335.382	0.016*	4	
44.5	-	19323.782			19335.680	19335.666	0.014*	4	
45.5	-	19323.805			19335.965	19335.952	0.013*	4	
46.5	-	19323.831			19336.239	19336.242	-0.003	4	
47.5	-	19323.861			19336.535	19336.535	0.000	4	
48.5	-	19323.894			19336.833	19336.832	0.001	4	
49.5	-	19323.931			19337.133	19337.132	0.001	4	
50.5	-	19323.971			19337.437	19337.435	0.002	4	
51.5	-	19324.014			19337.743	19337.742	0.001	4	
52.5	-	19324.061			19338.054	19338.053	0.001	4	
53.5	-	19324.111			19338.363	19338.366	-0.003	4	
54.5	-	19324.165			19338.680	19338.683	-0.003	4	

55.5	-	19324.222			19339.009	19339.004	0.005	4
56.5	-	19324.283			19339.333	19339.327	0.006	4
57.5	-	19324.347			19339.657	19339.654	0.003	4
58.5	19324.411	19324.414	-0.003	4	19339.986	19339.985	0.001	4
59.5	19324.486	19324.485	0.001	4	19340.316	19340.319	-0.003	4
60.5	19324.561	19324.559	0.002	4	-	19340.656		
61.5	19324.638	19324.637	0.001	4	-	19340.997		
62.5	19324.721	19324.718	0.003	4	-	19341.341		
63.5	19324.805	19324.803	0.002	4	-	19341.689		
64.5	19324.892	19324.891	0.001	4	-	19342.040		
65.5	19324.981	19324.982	-0.001	4	-	19342.394		
66.5	19325.077	19325.077	0.000	4	-	19342.752		
67.5	19325.167	19325.176	-0.009	4	-	19343.113		
68.5	-	19325.278			-	19343.477		
69.5	-	19325.383			-	19343.845		
70.5	-	19325.491			-	19344.216		
71.5	-	19325.604			-	19344.591		
72.5	-	19325.719			-	19344.969		
73.5	-	19325.838			-	19345.350		
74.5	-	19325.961			-	19345.735		
75.5	-	19326.086			-	19346.123		
76.5	19326.216	19326.216	0.000	4	-	19346.515		
77.5	19326.350	19326.349	0.001	4	-	19346.910		
78.5	19326.490	19326.485	0.005	4	-	19347.308		
79.5	19326.631	19326.625	0.006	4	-	19347.710		
80.5	19326.774	19326.768	0.006	4	-	19348.115		
81.5	19326.925	19326.914	0.011	4	-	19348.524		
82.5	19327.070	19327.064	0.006	4	-	19348.936		
83.5	19327.227	19327.218	0.009	4	-	19349.351		
84.5	19327.380	19327.375	0.005	4	-	19349.770		
85.5	19327.544	19327.535	0.009	4	-	19350.192		
86.5	19327.707	19327.699	0.008	4	-	19350.617		

 $Q_{22}(ef)$ $P_{21}(ee)$

J	OBS	CALC	DIFF	U	OBS	CALC	DIFF	U
36.5	19327.027	19327.023	0.004	8	-	19326.802		
37.5	19327.111	19327.109	0.002	8	-	19326.880		
38.5	19327.196	19327.198	-0.002	8	-	19326.962		
39.5	19327.289	19327.291	-0.002	8	19327.067	19327.048	0.019**	8
40.5	19327.381	19327.387	-0.006	8	19327.151	19327.137	0.014	8
41.5	19327.480	19327.486	-0.006	8	19327.239	19327.229	0.010	8
42.5	19327.580	19327.589	-0.009	8	19327.335	19327.325	0.010	8
43.5	19327.686	19327.695	-0.009	8	19327.429	19327.424	0.005	8
44.5	19327.797	19327.805	-0.008	8	19327.528	19327.526	0.002	8
45.5	19327.907	19327.918	-0.011	8	19327.633	19327.632	0.001	8
46.5	19328.028	19328.035	-0.007	8	19327.740	19327.741	-0.001	8
47.5	19328.146	19328.155	-0.009	8	19327.851	19327.854	-0.003	8
48.5	19328.265	19328.278	-0.013	8	19327.966	19327.970	-0.004	8
49.5	19328.396	19328.405	-0.009	8	19328.083	19328.090	-0.007	8
50.5	19328.518	19328.535	-0.017	8	19328.206	19328.213	-0.007	8
51.5	-	19328.669			19328.331	19328.339	-0.008	8

$R_{22}(ff)$					$Q_{21}(fe)$			
J	OBS	CALC	DIFF	U	OBS	CALC	DIFF	U
41.5	19331.331	19331.331	0.000	6	-	19330.984		
42.5	19331.522	19331.525	-0.003	6	-	19331.170		
43.5	19331.718	19331.721	-0.003	6	-	19331.359		
44.5	19331.924	19331.921	0.003	6	19331.545	19331.552	-0.007	6
45.5	19332.124	19332.125	-0.001	6	19331.749	19331.748	0.001	6
46.5	19332.331	19332.332	-0.001	6	19331.949	19331.948	0.001	6
47.5	19332.548	19332.542	0.006	6	19332.149	19332.151	-0.002	6
48.5	19332.750	19332.756	-0.006	6	19332.355	19332.358	-0.003	6
49.5	19332.969	19332.973	-0.004	6	19332.567	19332.568	-0.001	6
50.5	-	19333.193			19332.785	19332.781	0.004	6
51.5	-	19333.417			-	19332.998		
52.5	-	19333.645			-	19333.218		
53.5	-	19333.875			-	19333.441		
54.5	19334.108	19334.110	-0.002	6	-	19333.668		
55.5	19334.342	19334.347	-0.005	6	-	19333.899		
56.5	19334.582	19334.588	-0.006	6	19334.135	19334.132	0.003	6
57.5	19334.827	19334.832	-0.005	6	19334.373	19334.370	0.003	6
58.5	19335.073	19335.080	-0.007	6	19334.612	19334.610	0.002	6
59.5	-	19335.331			19334.855	19334.854	0.001	6
60.5	19335.581	19335.586	-0.005	6	19335.108	19335.101	0.007	6
61.5	-	19335.844			-	19335.352		
62.5	-	19336.105			19335.608	19335.606	0.002	6
63.5	-	19336.370			19335.854	19335.864	-0.010	6
64.5	-	19336.638			19336.113	19336.125	-0.012	6
65.5	-	19336.910			19336.382	19336.389	-0.007	6
66.5	-	19337.185			19336.655	19336.657	-0.002	6
67.5	-	19337.463			19336.918	19336.928	-0.010	6

1 - 0 Band

$R_{11}(ee)$					$P_{12}(ff)$			
J	OBS	CALC	DIFF	U	OBS	CALC	DIFF	U
37.5	18024.180	18024.185	-0.005	4	-	18010.058		
38.5	18024.490	18024.492	-0.002	4	-	18009.993		
39.5	18024.796	18024.801	-0.005	4	-	18009.932		
40.5	18025.106	18025.114	-0.008	4	-	18009.873		
41.5	-	18025.430			-	18009.818		
42.5	18025.750	18025.750	0.000	4	-	18009.766		
43.5	18026.068	18026.072	-0.004	4	-	18009.717		
44.5	18026.391	18026.397	-0.006	4	-	18009.672		
45.5	18026.723	18026.726	-0.003	4	-	18009.629		
46.5	18027.056	18027.058	-0.002	4	-	18009.590		
47.5	18027.393	18027.393	0.000	4	-	18009.554		
48.5	18027.727	18027.730	-0.003	4	-	18009.521		
49.5	18028.072	18028.072	0.000	4	-	18009.491		
50.5	18028.411	18028.416	-0.005	4	-	18009.464		
51.5	18028.763	18028.763	0.000	4	-	18009.441		
52.5	18029.099	18029.114	-0.015*	4	-	18009.420		
53.5	18029.468	18029.467	0.001	4	-	18009.403		
54.5	18029.817	18029.824	-0.007	4	-	18009.389		
55.5	18030.188	18030.184	0.004	4	-	18009.378		

56.5	18030.545	18030.547	-0.002	4	-	18009.371		
57.5	18030.915	18030.913	0.002	4	-	18009.366		
58.5	18031.281	18031.282	-0.001	4	-	18009.365		
59.5	18031.658	18031.655	0.003	4	-	18009.367		
60.5	18032.033	18032.030	0.003	4	-	18009.372		
61.5	18032.412	18032.409	0.003	4	-	18009.380		
62.5	18032.791	18032.791	0.000	4	-	18009.392		
63.5	18033.173	18033.176	-0.003	4	-	18009.406		
64.5	-	18033.564			-	18009.424		
65.5	18033.953	18033.955	-0.002	4	-	18009.445		
66.5	18034.352	18034.349	0.003	4	-	18009.469		
67.5	18034.745	18034.747	-0.002	4	-	18009.496		
68.5	18035.149	18035.147	0.002	4	-	18009.527		
69.5	18035.553	18035.551	0.002	4	-	18009.561		
70.5	18035.959	18035.958	0.001	4	-	18009.598		
71.5	18036.366	18036.368	-0.002	4	-	18009.638		
72.5	18036.783	18036.781	0.002	4	-	18009.681		
73.5	18037.202	18037.197	0.005	4	-	18009.728		
74.5	18037.620	18037.616	0.004	4	-	18009.777		
75.5	18038.041	18038.039	0.002	4	-	18009.830		
76.5	18038.464	18038.464	0.000	4	-	18009.886		
77.5	18038.894	18038.893	0.001	4	-	18009.945		
78.5	18039.328	18039.325	0.003	4	-	18010.008		
79.5	18039.759	18039.760	-0.001	4	-	18010.073		
80.5	18040.201	18040.198	0.003	4	18010.141	18010.142	-0.001	4
81.5	18040.643	18040.639	0.004	4	18010.222	18010.214	0.008	4
82.5	-	18041.083			18010.293	18010.289	0.004	4
83.5	-	18041.531			18010.381	18010.368	0.013*	4
84.5	-	18041.982			18010.446	18010.450	-0.004	4
85.5	18042.436	18042.435	0.001	4	18010.543	18010.534	0.009	4
86.5	18042.893	18042.892	0.001	4	18010.624	18010.622	0.002	4
87.5	18043.346	18043.352	-0.006	4	18010.711	18010.714	-0.003	4
88.5	18043.812	18043.815	-0.003	4	18010.800	18010.808	-0.008	4
89.5	18044.282	18044.282	0.000	4	18010.917	18010.906	0.011	4
90.5	18044.758	18044.751	0.007	4	18011.021	18011.007	0.014*	4
91.5	18045.226	18045.224	0.002	4	-	18011.111		
92.5	18045.695	18045.699	-0.004	4	-	18011.218		
93.5	18046.174	18046.178	-0.004	4	-	18011.328		
94.5	-	18046.660			18011.441	18011.442	-0.001	4
95.5	-	18047.145			18011.550	18011.559	-0.009	4
96.5	-	18047.634			18011.671	18011.679	-0.008	4
97.5	18048.130	18048.125	0.005	4	-	18011.802		
98.5	18048.618	18048.619	-0.001	4	-	18011.929		
99.5	18049.112	18049.117	-0.005	4	18012.054	18012.059	-0.005	4
100.5	18049.618	18049.618	0.000	4	18012.198	18012.192	0.006	4
101.5	18050.125	18050.122	0.003	4	18012.330	18012.328	0.002	4
102.5	18050.629	18050.629	0.000	4	-	18012.467		
103.5	18051.139	18051.139	0.000	4	-	18012.610		
104.5	18051.654	18051.652	0.002	4	18012.747	18012.756	-0.009	4
105.5	18052.170	18052.169	0.001	4	18012.898	18012.905	-0.007	4
106.5	-	18052.688			18013.050	18013.057	-0.007	4
107.5	18053.211	18053.211	0.000	4	18013.216	18013.213	0.003	4
108.5	18053.739	18053.737	0.002	4	18013.356	18013.371	-0.015*	4
109.5	18054.264	18054.266	-0.002	4	-	18013.533		
110.5	18054.798	18054.798	0.000	4	-	18013.699		
111.5	18055.330	18055.333	-0.003	4	-	18013.867		
112.5	18055.873	18055.871	0.002	4	-	18014.039		

113.5	-	18056.413			-	18014.214		
114.5	-	18056.958			-	18014.392		
115.5	18057.506	18057.505	0.001	4	-	18014.573		
116.5	18058.054	18058.056	-0.002	4	-	18014.758		
117.5	18058.610	18058.610	0.000	4	-	18014.945		
118.5	18059.165	18059.168	-0.003	4	-	18015.137		
119.5	18059.725	18059.728	-0.003	4	-	18015.331		
120.5	-	18060.292			-	18015.528		
121.5	-	18060.858			-	18015.729		
122.5	-	18061.428			-	18015.933		
123.5	-	18062.001			18016.151	18016.141	0.010	4
124.5	-	18062.577			18016.353	18016.351	0.002	4

 $P_{22}(ff)$ $R_{21}(ee)$

<i>J</i>	OBS	CALC	DIFF	U	OBS	CALC	DIFF	U
4.5	19536.352	19536.355	-0.003	J 6	-	19537.674		
5.5	19536.238	19536.240	-0.002	J 6	-	19537.823		
6.5	19536.140	19536.129	0.011	J 6	-	19537.976		
7.5	-	19536.021			-	19538.131		
8.5	19535.909	19535.916	-0.007	J 4	-	19538.290		
9.5	19535.816	19535.814	0.002	J 4	-	19538.452		
10.5	-	19535.715			-	19538.617		
11.5	-	19535.619			-	19538.785		
12.5	19535.535	19535.526	0.009	J 4	-	19538.956		
13.5	19535.439	19535.437	0.002	J 4	-	19539.130		
14.5	19535.354	19535.351	0.003	J 4	-	19539.308		
15.5	-	19535.268			-	19539.488		
16.5	19535.190	19535.188	0.002	J 4	-	19539.672		
17.5	19535.111	19535.111	0.000	J 4	-	19539.859		
18.5	19535.035	19535.037	-0.002	J 4	-	19540.049		
19.5	-	19534.967			-	19540.242		
20.5	19534.898	19534.899	-0.001	J 4	-	19540.438		
21.5	19534.834	19534.835	-0.001	J 4	-	19540.638		
22.5	19534.772	19534.774	-0.002	J 4	-	19540.841		
23.5	19534.712	19534.716	-0.004	J 4	-	19541.046		
24.5	19534.663	19534.662	0.001	J 4	-	19541.255		
25.5	-	19534.610			-	19541.467		
26.5	19534.560	19534.562	-0.002	J 4	-	19541.682		
27.5	19534.516	19534.516	0.000	J 4	-	19541.901		
28.5	-	19534.474			-	19542.122		
29.5	19534.432	19534.435	-0.003	J 4	-	19542.347		
30.5	19534.407	19534.400	0.007	J 4	-	19542.574		
31.5	19534.366	19534.367	-0.001	J 4	-	19542.805		
32.5	19534.338	19534.337	0.001	J 4	-	19543.039		
33.5	19534.313	19534.311	0.002	J 4	-	19543.276		
34.5	-	19534.288			-	19543.517		
35.5	-	19534.268			-	19543.760		
36.5	-	19534.251			-	19544.007		
37.5	-	19534.238			-	19544.256		
38.5	-	19534.227			-	19544.509		
39.5	-	19534.220			-	19544.765		
40.5	-	19534.216			-	19545.024		
41.5	-	19534.215			-	19545.286		
42.5	-	19534.217			-	19545.552		

43.5	-	19534.222	-	19545.820		
44.5	-	19534.231	19546.093	19546.092	0.001	4
45.5	-	19534.242	19546.361	19546.367	-0.006	4
46.5	-	19534.257	19546.644	19546.645	-0.001	4
47.5	-	19534.275	19546.928	19546.926	0.002	4
48.5	-	19534.297	19547.219	19547.210	0.009	4
49.5	-	19534.321	19547.498	19547.497	0.001	4
50.5	-	19534.349	19547.809	19547.788	0.021*	4
51.5	-	19534.379	19548.082	19548.081	0.001	4
52.5	-	19534.413	19548.374	19548.378	-0.004	4
53.5	-	19534.450	19548.682	19548.678	0.004	4
54.5	-	19534.490	19548.982	19548.981	0.001	4
55.5	-	19534.534	19549.286	19549.287	-0.001	4
56.5	-	19534.580	-	19549.596		
57.5	-	19534.630	19549.909	19549.909	0.000	4
58.5	-	19534.683	19550.228	19550.224	0.004	4
59.5	-	19534.739	19550.541	19550.543	-0.002	4
60.5	-	19534.799	19550.870	19550.865	0.005	4
61.5	-	19534.861	19551.195	19551.190	0.005	4
62.5	-	19534.927	19551.533	19551.518	0.015*	4
63.5	-	19534.996	19551.853	19551.849	0.004	4
64.5	-	19535.068	19552.177	19552.184	-0.007	4
65.5	-	19535.143	19552.515	19552.521	-0.006	4
66.5	-	19535.221	19552.863	19552.862	0.001	4

 $P_{21}(ee)$

J	OBS	CALC	DIFF	U
57.5	19539.446	19539.453	-0.007	4
58.5	19539.588	19539.588	0.000	4
59.5	19539.730	19539.727	0.003	4
60.5	19539.868	19539.869	-0.001	4
61.5	19540.027	19540.015	0.012	4
62.5	19540.165	19540.163	0.002	4
63.5	19540.313	19540.315	-0.002	4
64.5	19540.459	19540.469	-0.010	4
65.5	19540.617	19540.627	-0.010	4

 $R_{22}(ff)$

J	OBS	CALC	DIFF	U
46.5	19542.740	19542.734	0.006	6
47.5	19542.938	19542.932	0.006	6
48.5	19543.146	19543.134	0.012	6
49.5	19543.340	19543.338	0.002	6
50.5	19543.553	19543.546	0.007	6
51.5	19543.764	19543.756	0.008	6
52.5	19543.974	19543.970	0.004	6
53.5	19544.198	19544.187	0.011	6
54.5	19544.415	19544.407	0.008	6
55.5	19544.639	19544.631	0.008	6
56.5	19544.869	19544.857	0.012	6
57.5	19545.093	19545.087	0.006	6

 $Q_{21}(fe)$

J	OBS	CALC	DIFF	U
46.5	-	19542.363		
47.5	-	19542.554		
48.5	19542.740	19542.748	-0.008	6
49.5	19542.938	19542.946	-0.008	6
50.5	19543.146	19543.146	0.000	6
51.5	19543.340	19543.350	-0.010	6
52.5	19543.553	19543.557	-0.004	6
53.5	19543.764	19543.767	-0.003	6
54.5	19543.974	19543.980	-0.006	6
55.5	19544.198	19544.196	0.002	6
56.5	19544.415	19544.416	-0.001	6
57.5	19544.639	19544.638	0.001	6

58.5	19545.330	19545.319	0.011	6	19544.869	19544.864	0.005	6
59.5	19545.557	19545.555	0.002	6	19545.093	19545.093	0.000	6
60.5	19545.795	19545.794	0.001	6	19545.330	19545.325	0.005	6
61.5	19546.030	19546.037	-0.007	6	19545.557	19545.561	-0.004	6
62.5	19546.261	19546.282	-0.021**	6	19545.795	19545.799	-0.004	6
63.5	19546.510	19546.531	-0.021**	6	19546.030	19546.041	-0.011	6
64.5	19546.781	19546.782	-0.001	6	19546.261	19546.285	-0.024**	6
65.5	19547.040	19547.037	0.003	6	19546.510	19546.533	-0.023**	6
66.5	19547.300	19547.295	0.005	6	19546.781	19546.784	-0.003	6
67.5	19547.563	19547.556	0.007	6	19547.040	19547.039	0.001	6
68.5	-	19547.821			19547.300	19547.296	0.004	6
69.5	-	19548.088			19547.563	19547.557	0.006	6
70.5	-	19548.359			-	19547.820		
71.5	-	19548.633			-	19548.087		
72.5	-	19548.910			-	19548.357		
73.5	-	19549.190			-	19548.630		
74.5	-	19549.473			-	19548.907		
75.5	19549.759	19549.760	-0.001	6	-	19549.186		
76.5	19550.064	19550.049	0.015	6	-	19549.469		
77.5	19550.330	19550.342	-0.012	6	19549.759	19549.755	0.004	6
78.5	19550.626	19550.638	-0.012	6	19550.064	19550.044	0.020**	6
79.5	19550.922	19550.937	-0.015	6	19550.330	19550.336	-0.006	6
80.5	19551.227	19551.239	-0.012	6	19550.626	19550.631	-0.005	6
81.5	19551.540	19551.545	-0.005	6	19550.922	19550.929	-0.007	6
82.5	19551.851	19551.853	-0.002	6	19551.227	19551.231	-0.004	6
83.5	19552.162	19552.165	-0.003	6	19551.540	19551.536	0.004	6
84.5	19552.480	19552.480	0.000	6	19551.851	19551.844	0.007	6
85.5	-	19552.798			19552.162	19552.155	0.007	6
86.5	-	19553.119			19552.480	19552.469	0.011	6

References

1. R. W. Field, *Disc. Faraday Soc.* **71**, 111 (1981).
2. J. O. Schröder and W. E. Ernst, *J. Mol. Spectrosc.* **112**, 413 (1985).
3. W. E. Ernst and J. O. Schröder, *J. Mol. Spectrosc.* **117**, 444 (1986).
4. J. A. Coxon and C. S. Dickinson, *J. Mol. Spectrosc.* **190**, 150 (1998).
5. L. A. Kaledin, J. C. Bloch, M. C. McCarthy and R. W. Field, *J. Mol. Spectrosc.* **197**, 289 (1999).
6. A. R. Allouche, G. Wannous and M. Aubert-Frécon, *Chem. Phys.* **170**, 11 (1993).
7. T. Törring, K. Zimmerman, J. Hoefft, *Chem. Phys. Lett.* **151**, 520 (1988).
8. P.F. Bernath, B. Pinchemel and R. W. Field, *J. Chem. Phys.* **74**, 5508 (1981).
9. W. J. Childs, D. R. Cok and L. S. Goodman, *J. Chem. Phys.* **76**, 3993 (1982).
10. Y. Ohshima and Y. Endo, *Chem. Phys. Lett.* **213**, 95 (1993).
11. K. A. Walker and M. C. L. Gerry, *J. Chem. Phys.* **107**, 9835 (1997).
12. J. Schlembach and E. Tiemann, *Chem. Phys.* **68**, 21 (1982).
13. H. Knöckel and E. Tiemann, *Chem. Phys. Lett.* **104**, 83 (1984).
14. H. Knöckel, T. Kröckertskothén and E. Tiemann, *Chem. Phys.* **93**, 349 (1985).
15. J. G. McCaffrey, R. R. Bennett, M. D. Morse and W. H. Breckenridge, *J. Chem. Phys.* **91**, 92 (1989).
16. G. Herzberg, "Molecular Spectra and Molecular Structure, I. Spectra of Diatomic Molecules," D. Van Nostrand, Inc. New York (1950).
17. H. Lefebvre-Brion and R. W. Field, "Perturbations in the Spectra of Diatomic Molecules," Academic Press, Orlando (1986).

18. P. F. Bernath, "Spectra of Atoms and Molecules," Oxford University Press, New York (1995).
19. W. Gordy and R. L. Cook, "Microwave Molecular Spectra," 3rd Ed., John Wiley & Sons, New York (1984).
20. R. N. Zare, A. L. Schmeltekopf, W. J. Harrop, and D. L. Albritton, *J. Mol. Spectrosc.* **46**, 37 (1973).
21. R. A. Frosh and H. M. Foley, *Phys. Rev.* **88**, 1337 (1952).
22. H. E. Radford, *Phys. Rev.* **136**, 1571 (1964).
23. T. A. Dixon and R. C. Woods, *J. Chem. Phys.* **67**, 3956 (1977).
24. R. N. Zare, "Angular Momentum," John Wiley & Sons, New York (1988).
25. W.H. Press, B. P. Flannery, S. A. Teukolsky and W. T. Vetterling, "Numerical Recipes," Cambridge University Press, New York (1986).
26. B. J. Drouin, C. E. Miller, E. A. Cohen, G. Wagner and M. Birk, *J. Mol. Spectrosc.* **207**, 4 (2001).
27. J. B. West, R. S. Bradford Jr., J. D. Eversole and C. R. Jones, *Rev. Scien. Instr.* **46**, 164 (1975).
28. K. Walker, Ph.D. Thesis, University of British Columbia (1998).
29. T. F. Johnston, Jr., R. H. Brady and W. Proffitt, *Appl. Opt.*, **21**, 2307 (1982).
30. S. Gerstenkorn and P. Luc, *Atlas du Spectre d'Absorption de la Molécule d'Iodide*, Laboratoire Aimé-Cotton, CRNS II, 91405 Orsay, France (1978).
31. S. Gerstenkorn and P. Luc, *Rev. Phys. Appl.* **14**, 791 (1979).
32. D. E. Reisner, P. F. Bernath and R. W. Field, *J. Mol. Spectrosc.* **89**, 107 (1981).

33. B. A. Palmer, R. A. Keller, R. S. Engleman, Jr., "An Atlas of Uranium Emission Intensities in a Hollow Cathode Discharge" Los Alamos Sci. Rep. LA-8521-MS (1980).
34. A. E. Derome, "Modern NMR Techniques for Chemistry Research," Pergamon, Oxford (1987).
35. L. Klynning and H. Martin, *Phys. Scripta*, **24**, 24 (1981).
36. W. E. Ernst, J. O. Schröder and B. Zeller, *J. Mol. Spectrosc.* **135**, 161 (1989).
37. K. Hedfeld, *Z. Phys.* **68**, 610 (1931).
38. R. E. Harrington, Dissertation, University of California, Berkeley (1942).
39. K. P. Huber and G. Herzberg, *Molecular Spectra and Molecular Structure Vol. IV. Constants of Diatomic Molecules*, Van Nostrand Reinhold, New York (1979).
40. T. Törring, K. Doehl, and G. Weiler, *Chem. Phys. Lett.* **117**, 539 (1985).
41. A. J. Kotlar, R. W. Field, J. I. Steinfeld and J. A. Coxon, *J. Mol. Spectrosc.* **80**, 86 (1980).
42. J. A. Coxon, *J. Quant. Spectrosc. Radiat. Transfer* **11**, 443 (1971).
43. J. A. Coxon and S. C. Foster, *J. Mol. Spectrosc.* **91**, 243 (1982).
44. J. A. Coxon, *J. Quant. Spectrosc. Radiat. Transfer* **11**, 1355 (1971).
45. C. E. Moore, *Atomic Energy Levels Vol. II*, National Bureau of Standards (US), Washington D.C. (1971).
46. B. E. Sauer, J. Wang and E.A. Hinds, *Phys. Rev. Lett.* **74**, 1554 (1995).
47. K. L. Dunfield, C. Linton, T. E. Clarke, J. McBride, A. G. Adam and J. R. D. Peers, *J. Mol. Spectrosc.* **174**, 433 (1995).
48. B. E. Sauer, J. Wang and E.A. Hinds, *J. Chem. Phys.* **105**, 7412 (1996).

49. R. J. Van Zee, *J. Phys. Chem.* **82**, 1192 (1978).
50. T. C. Melville, J. A. Coxon and C. Linton, *J. Mol. Spectrosc.* **200**, 229 (2000).
51. C. Linton and A. G. Adam, *J. Mol. Spectrosc.* **206**, 161 (2001).
52. J. Kramer, *J. Chem. Phys.* **68**, 5370 (1978).
53. I. Mills, T. Cvitaš, K. Homann, N. Kallay and K. Kuchitsu, "Quantities, Units and Symbols in Physical Chemistry," Blackwell Science, Oxford (1993).
54. W. J. Childs, D. R. Cok, G. L. Goodman and L. S. Goodman, *J. Chem. Phys.* **75**, 501 (1981).
55. Ch. Ryzlewicz and T. Törring, *Chem. Phys.* **51**, 329 (1980).
56. Ch. Ryzlewicz, H. -U. Schütze-Pahlmann, J. Hoefft and T. Törring, *Chem. Phys.* **71**, 389 (1982).
57. W. E. Ernst, G. Weiler and T. Törring, *Chem Phys. Lett.* **121**, 494 (1985).
58. J. R. Morton and K. F. Preston, *J. Magn. Reson.* **30**, 577 (1978).
59. S. A. Beaton and M. C. L. Gerry, *J. Chem. Phys.* **110**, 10715 (1999).
60. W. Lin, S. A. Beaton, C. J. Evans and M. C. L. Gerry, *J. Mol. Spectrosc.* **199**, 275 (2000).
61. K. A. Walker and M. C. L. Gerry, *J. Chem. Phys.* **109**, 5439 (1998).
62. J. K. G. Watson, *J. Mol. Spectrosc.* **45**, 99 (1973).
63. J. L. Dunham, *Phys. Rev.* **41**, 721 (1932).
64. H. U. Lee and R. N. Zare, *J. Mol. Spectrosc.* **64**, 233 (1977).
65. P. J. Mohr and B. N. Taylor, *Rev. Mod. Phys.* **72**, 351 (2000).
66. R. J. Le Roy, Version 7.1 of Program LEVEL, University of Waterloo Chemical Physics Research Report No. CP-555R (1996).

67. G. Audi and A. H. Wapstra, *Nucl. Phys. A.* **565**, 1 (1993).
68. L. A. Kaledin, M. G. Erickson and M.C. J. Heaven, *J. Mol. Spectrosc.* **165**, 323 (1994).
69. J. C. Block, M. C. McCarthy, R. W. Field and L. A. Kaledin, *J. Mol. Spectrosc.* **177**, 251 (1996).
70. A. L. Kaledin, M. C. Heaven, R. W. Field and L. A. Kaledin, *J. Mol. Spectrosc.* **179**, 310 (1996).
71. L.A. Kaledin, J. C. Bloch, M. C. McCarthy, E. A. Shenyavskaya and R. W. Field, *J. Mol. Spectrosc.* **176**, 148 (1996).
72. M. C. McCarthy, J. C. Bloch, R. W. Field and L. A. Kaledin, *J. Mol. Spectrosc.* **179**, 253 (1996).
73. K. N. Uttam, R. Gopal and M. M. Joshi, *J. Mol. Spectrosc.* **185**, 8 (1997).
74. B. E. Sauer, S. B. Cahn, M. G. Kozlov, G. D. Redgrave and E. A. Hinds, *J. Chem. Phys.* **110**, 8424 (1999).
75. R. S. Ram, A. G. Adam, A. Tsouli, J. Liévin and P. F. Bernath, *J. Mol. Spectrosc.* **202**, 116 (2000).
76. C. S. Dickinson, J. A. Coxon, N. R. Walker and M. C. L. Gerry, *J. Chem. Phys.* **115**, 6979 (2001).
77. S. A. McDonald, S. F. Rice and R. W. Field, *J. Chem. Phys.* **93**, 7676 (1990).
78. A. Gatterer, G. Piccardi and F. Vincenzi, *Ricerche Spettroscopiche*, **1**, 181 (1942).
79. R. F. Barrow and A. H. Chojnicki, *J. Chem. Soc. Far. Trans.*, **71**, 728 (1975).
80. H. U. Lee and R. N. Zare, *J. Mol. Spectrosc.*, **64**, 233 (1977).
81. K. N. Uttam and M. M. Joshi, *J. Mol. Spectrosc.*, **174**, 290 (1995).

82. K. N. Uttam, R. Gopal and M. M. Joshi, *J. Mol. Spectrosc.*, **185**, 8 (1997).
83. K. N. Uttam and M.M. Joshi, *Indian J. Phys. B*, **69**, 261 (1995).
84. A-M. Mårtensson-Pendrill, D. S. Gough and P. Hannaford, *Phys. Rev. A.*, **49**, 3351 (1994).
85. H. G. Kuhn, "Atomic Spectra," Longmans, Green & Co. Ltd., London (1962).
86. J. A. Coxon and P. G. Hajigeorgiou, *J. Mol. Spectrosc.*, **203**, 49 (2000).
87. T. C. Melville and J. A. Coxon, *J. Chem. Phys.*, **115**, 6974 (2001).
88. M. Dolg, H. Stoll and H. Preuss, *Chem. Phys.*, **165**, 21 (1992).